Fakultät für Medizin

Hämatologische Forschung

The Functional Role of Zeta-Chain-Associated Protein 70 in the Pathogenesis of B-Cell Chronic Lymphocytic Leukemia

Constanze Anneliese Jakwerth

Vollständiger Abdruck der von der Fakultät für Medizin der Technischen Universität München zur Erlangung des akademischen Grades eines

Doktors der Naturwissenschaften

genehmigten Dissertation.

Vorsitzender: Prof. Dr. Jürgen Ruland

Prüfer der Dissertation:

1. Priv.-Doz. Dr. Ingo Ringshausen
2. Prof. Dr. Bernhard Küster

Die Dissertation wurde am 04.02.2016 bei der Technischen Universität München eingereicht und durch die Fakultät der Medizin der Technischen Universität München am 03.08.2016 angenommen.

meinem Mann Marvin

Table of Contents

Register of Abbreviations

ADAP	adhesion- and degranulation-promoting adaptor protein
AP-MS	affinity purification-mass spectrometry
AID	activation-induced deaminase
AP-1	activator protein 1
APC	antigen-presenting cell
ATAC-Seq	assay for transposase-accessible chromatin with high throughput sequencing
ATM	ataxia teleangiectasia mutated
Bak	Bcl-2 homologous antagonist killer
Bax	Bcl-2 associated X
Bcl-2	B-cell lymphoma 2
Bcl-XL	B-cell lymphoma-extra large
BCL6	B-cell lymphoma 6 protein
BCR	B-cell receptor
BH3	Bcl-2 homology domain 3
BLNK = SLP-65	B cell linker protein
BrdU	Bromodeoxyuridine
BSA	bovine serum albumin
Btk	Bruton's tyrosine kinase
C-terminus/al	carboxy-terminus/al
CD	cluster of differentiation
Cdk	cyclin-dependent kinase
CDKN1C	inhibitor of cyclin-dependent kinases 1C
ChIP	chromatin immunoprecipitation
CLL	B-cell chronic lymphocytic leukemia
cNLS	classical nuclear location signal

CpG	CpG dinucleotide
CRAPome	contaminant repository for affinity purification-mass spectrometry data
CrkII	CT10 regulator of kinase II
CXCR4	C-X-C chemokine receptor type 4
D	diversity gene segments
DAG	diacylglycerol
DLEU2	deleted in lymphocytic leukemia 2
DNA	desoxyribonucleic acid
DTT	DL-dithiothreitol
EDTA	ethylene diamine tetraacetic acid
EGFR	epidermal growth factor receptor
EGTA	ethylene glycol tetraacetic acid
FA	formic acid
FACS	fluorescence-activated cell sorting
Fbw7	F-box and WD repeat domain-containing 7
FITC	fluorescein-isothiocyanate
FRAP	fluorescence recovery after photobleaching
FRET	fluorescence resonance energy transfer
GRB2	growth factor receptor-bound protein 2
GSK3β	glycogen synthase kinase 3β
H1	histone H1
H2A	histone H2A
H2B	histone H2B
H_2SO_4	sulfuric acid
H3	histone H3
H4	histone H4
H4K16	lysine 16 of histone H4

H4K16ac	histone H4 acetylated on lysine 16
H4K20	lysine 20 of histone H4
H4K20me3	histone H4 trimethylated on lysine 20
H4Y72	tyrosine 72 of histone H4
HAT	histone acetyltransferase
HCl	hydrochloric acid
HDAC	histone deacetylase
HEPES	4-(2-hydroxyethyl)-1-piperazineethanesulfonic acid
HP1α	heterochromatin protein 1α
HSCT	hematopoietic stem cell transplantation
Ig/IG	immunoglobuline
IgA	immunoglobuline A
IgD	immunoglobuline D
IgE	immunoglobuline E
IgG	immunoglobuline G
IGHV	variable region of the immunoglobulin heavy chain
IgM	immunoglobuline M
INHAT	inhibitor of acetyltransferases
ITAM	immunoreceptor tyrosine-based activation motifs
ITK	interleukin-2-inducible T cell kinase
J	joining gene segments
JAK2	Janus kinase 2
K	lysine
KCl	potassium chloride
LAB	linker for activation of B cells
LAT	linker for activation of T cells
Lck	lymphocyte-specific protein tyrosine kinase
MAPK	mitogen-activated protein kinase

MBL	monoclonal B-cell lymphocytosis
Mcl-1	myeloid cell leukemia 1
Mdm2	murine double minute 2 homologue
$MgCl_2$	magnesium chloride
MHC	major histocompatibility complex
miR	micro-RNA
MOPS	3-(N-Morpholino)propanesulfonic acid
mRNA	messenger RNA
MULE	Mcl-1 ubiquitin ligase E3
MYD88	myeloid differentiation primary response 88
N-terminus/al	amino-terminus/al
NaCl	sodium chloride
NAP1L1/hNRP	nucleosome assembly protein 1 like 1
NAP1L2	nucleosome assembly protein 1 like 2
NFAT	nuclear factor of activated T cells
NF-κB	nuclear factor 'kappa-light-chain-enhancer' of activated B-cells
NK cells	natural killer cells
NP-40	IPEGAL CA-630
NPM1	nucleophosmin
ORR	overall response rate
OS	overall survival
PBS	phosphate-buffered saline
PC5	R-phycoerathrincyanin 5.1
PCR	polymerase chain reaction
PE	R-phycoerythrin
PFS	progression-free survival
PI3K	phosphatidylinositol 3-kinase

PKC	protein kinase C
PLC	phospholipase C
PMSF	phenylmethylsulfonyl fluoride
PP2A	protein phosphatase 2A
PPP2R1B	65 kDa regulatory subunit A β isoform of PP2A
qPCR	quantitative PCR
RAG	recombinant activating genes
Rb	tumor suppressor retinoblastoma
RNA	ribonucleic acid
RT-PCR	real-time PCR
SDS	sodium dodecyl sulfate
SF3B1	splicing factor 3b, subunit 1, 155 kDa
SH2	src homology domain
SLL	small lymphocytic leukemia
SLP-76	SH2 domain-containing leukocyte protein of 76 kDa
SLR	Signal Log Ratio
SOS	sevenless homologue
Suv4-20H1	suv4-20 homologue 1
Suv4-20H2	suv4-20 homologue 2
Syk	spleen tyrosine kinase
TCA	trichloroacetic acid
TCR	T-cell receptor
TP53/p53	tumor protein p53
Usp9x	ubiquitin specific peptidase 9, X-linked
V	variable gene segments
Y	tyrosine
ZAP70	zeta-chain associated protein of 70 kDa

Register of Tables

Register of Figures

1 Introduction

1.1 Chronic Lymphocytic Leukemia (CLL)

1.1.1 Definition and Clinical Course of CLL

B-cell chronic lymphocytic leukemia (CLL) is the most common leukemia in Central Europe. By the World Health Organization, CLL is defined as indolent non-Hodgkin lymphoma caused by an oncogenic transformation of B cells (Harris et al., 1999). Despite several promising therapy approaches, CLL remains incurable to date. CLL is a neoplastic disease of elderly patients. In Germany, CLL is the most common leukemia with about 5,000 newly diagnosed cases and more than 1,900 cases of death per year (Katalinic, 2015). Males are rather affected than females with a ratio of 1.7:1. In 2011, the incidence of CLL was at about 4.9 per 100,000 male inhabitants per year and at 2.5 per 100,000 female inhabitants per year.

Chronic lymphocytic leukemia is defined by the accumulation of mature but immunologically dysfunctional B cell lymphocytes (Zenz et al., 2010). Its immunological phenotype is characterized by a weak surface expression of immunoglobulins, the expression of B cell antigens CD19, CD20 (weak) and CD23, as well as the T cell antigen CD5, and κ or λ B cell receptor (BCR) light chain restriction (Campo et al., 2011; Matutes et al., 1994). CLL is the leukemic counterpart of small lymphocytic leukemia (SLL), which differs from CLL only in the extent of peripheral blood lymphocytosis (Kumar, 2004). The two disease entities are otherwise identical in genotype and phenotype. In most cases, an undiagnosed, clinically asymptomatic preliminary stage with proliferation of monoclonal or oligoclonal B cells precedes the CLL stage. This phenomenon is called Monoclonal B cell Lymphocytosis (MBL) (Landgren et al., 2009). One criterion by which CLL is distinguished from MBL is the presence of more than 5,000 clonal B lymphocytes per microliter in the peripheral blood (Hallek et al., 2008). The risk for MBL to transform into CLL is at about 1% per year (Rawstron et al., 2008).

Most CLL cases are discovered accidentally because of a present lymphocytosis during a routine blood panel. Patients often do not show any clinical signs of the disease. CLL cells are mainly found in the peripheral blood and in lymphatic organs, such as lymph nodes, spleen and bone marrow, where they eventually expel and outgrow healthy blood cells. This extrusion mechanism can subsequently result in bone marrow failure characterized by anemia and thrombocytopenia. Therefore, with progressing disease, patients often present with lymphadenopathy, splenomegaly, and hepatomegaly as well as B symptoms, like night sweats, fever and weight loss, and finally, signs of bone marrow failure, like excessive bruising and bleeding or recurrent infections. Approximately 5 to 10% of CLL patients develop an aggressive form of Non-Hodgkin lymphoma, mostly a diffuse-large B cell lymphoma (Jain and O'Brien, 2012). This process is called the Richter's transformation. Clinically, Richter's transformation is characterized by a very aggressive course of disease with rapidly worsening lymphadenopathy and hepatosplenomegaly. Patients have a poor prognosis with a median survival time of 10 months.

The cell-of-origin of the transformed CLL cell is still an intensely debated issue (Zhang and Kipps, 2014). Regarding the differences in the mutational status of the IGHV locus, it was suggested that the two CLL cell subsets derive from B cells from different developmental stages (Forconi et al., 2010). However, gene-expression studies revealed a common gene-expression profile for mutated and unmutated patient samples (Klein et al., 2001; Rosenwald et al., 2001), which showed a high similarity with the profile of peripheral blood $CD5^+$ B cells. IGHV mutation analyses revealed that $CD5^+$ blood B cells are clonally expanded and include a small number of post–germinal center B cells expressing CD27, which is known as a surface marker for memory B cells (Tangye and Good, 2007). More recent data suggest that CLL cells with an unmutated IGHV region derive from unmutated mature $CD5^+CD27^-$ B cells and that CLL cells with mutated IGHVs derive from the newly discovered $CD5^+IgM^+CD27^+$ post-germinal center B cell subset (Seifert et al., 2012).

1.1.2 Molecular Pathogenesis of CLL

1.1.2.1 Genetic Aspects

In about 55% of CLL patients 13q14.3 is deleted, which encodes a non-transcribed gene and two micro-RNAs, miR-15a and miR-16, encoded in the intron of the *DLEU2* gene (Calin et al., 2002; Chiorazzi et al., 2005; Migliazza et al., 2001). This deletion is associated with a rather favorable prognosis (Caporaso et al., 2007; Dohner et al., 2000). Other common genetic abnormalities in CLL are the deletion of 11q22–23 with a frequency of 18%; 16% of CLL patients carry a trisomy 12 and another genetic deletion occurs at the site 17p13 in 7% of the cases. The *ataxia-teleangiectasia (ATM)* gene is involved in cases with 11q22–23 deletion and an inactivation of the tumor suppressor gene *TP53* occurs in patients with 17p13 deletions (Stilgenbauer et al., 1997). Both *TP53* and *ATM* genes regulate apoptosis and confer resistance to chemotherapy (Chiorazzi et al., 2005). Those alterations are correlated significantly with adverse clinical outcomes (Dohner et al., 2000).

In recent years, massive progress in next generation sequencing techniques has revealed further genetic lesions in CLL cells. In 2011, mutations in *MYD88, SF3B1, NOTCH1*, and other genes were identified (Puente et al., 2011), which are all associated with a less favorable prognosis. An L265P amino acid exchange in *MYD88* leads to potential constitutive NF-κB signaling. Mutations in *SF3B1* are localized in conserved regions of its carboxy-terminal (C-terminal) HEAT domain – with the most common mutation being K700E (Quesada et al., 2012; Wang et al., 2011b). Finally, *NOTCH1* is mostly mutated in its PEST domain, leading to its constitutive activation (Fabbri et al., 2011). Thus, current research revolves around the functional role of the important component of the U2 spliceosome *SF3B1* and the ligand-activated transcription factor *NOTCH1* in the CLL context. The presence of these and other mutations identified by high throughput sequencing were associated with advanced clinical stages and poor prognostic markers like ZAP70 expression (Vollbrecht et al., 2015).

With the tremendous expansion of our knowledge about the heterogeneity of genetic lesions among cancer patients, but also within an individual patient malignancy, a new paradigm among oncologic researchers is currently evolving,

called clonal evolution. Clonal evolution is defined by the accumulation of genetic changes in cancer cells over time, which gives rise to new tumor subclones (Guieze and Wu, 2015). It is called evolution, because the mechanism is in line with the Darwinian theory of species evolution and his claim of the “Survival of the fittest”. Treatment with chemotherapy propels clonal evolution, which contributes to the high diversity of clinical outcomes among CLL patients. The three clonal lesions driving early evolution in CLL were identified as mutations in *MYD88*, trisomy 12 and deletion of the long arm of chromosome 13 (Landau et al., 2013). The expansion of subclones carrying aberrations in *SF3B1* and *TP53* were involved in clonal evolution following chemotherapy and hence described as later events during CLL pathogenesis. As data from several recent publications demonstrate, the frequency of *MYD88* mutations does not change across the course of disease (Baliakas et al., 2015; Clifford et al., 2014; Cortese et al., 2014; Dreger et al., 2013; Jeromin et al., 2014; Oscier et al., 2013; Rossi et al., 2013; Schnaiter et al., 2013; Skowronska et al., 2012; Stilgenbauer et al., 2014). *SF3B1* mutations were associated with early disease progression, as their frequency increases between diagnosis and time of first therapy. *NOTCH1* aberrations, on the other hand, were shown to increase between time of first therapy and relapse and mutations in *ATM* and *TP53* rise continuously throughout the evolution of CLL (Guieze et al., 2015). Transformation to Richter’s syndrome presumably occurs following further genetic lesions in the predominant CLL clone, including lesions characteristically appearing in later stages of CLL clonal evolution, like *NOTCH1* and *TP53* mutations, and the predominant mutation in cell cycle regulator gene *CDKN2A/B* in 30% of transformed cases (Fabbri et al., 2013; Fabbri et al., 2011). Notably, similar genetic aberrations to those involved in clonal evolution of CLL occur many years before disease onset in MBL cases, including *SF3B1* and *NOTCH1* (Ojha et al., 2014). As those genetic lesions seem to have a significant impact on the clinical course of CLL patients, further research will focus on the involved pathogenic biologic mechanisms they are involved in. Hence, those mutations may serve as additional genetic prognostic biomarkers or even as potential therapeutic targets in the future.

1.1.2.2 Molecular Aspects

An intrinsic defect of apoptosis and a deregulated proliferation seem to be the main factors driving the pathogenesis of all cancer entities. Studies have demonstrated a profound defect of apoptosis for CLL cells, which is believed to be attributed to the overexpression of anti-apoptotic proteins of the *bcl2* family, like B-cell lymphoma 2 (Bcl-2) and myeloid cell leukemia 1 (Mcl-1) (Gandhi et al., 2008; Kitada et al., 1998).

Several circumstances can lead to the initiation of the programmed cell death, also called apoptosis. The final steps are initiated following activation of a proteolytic cascade involving the cysteine proteases called caspases (Adams, 2003; Shi, 2006). The activation of caspases further leads to the degradation of cellular organelles and a global degradation of messenger RNA (mRNA) (Thomas et al., 2015). The main characteristics of the final steps are chromatin condensation, the so called pyknosis, disruption of the nuclear membrane followed by DNA fragmentation, appearance of irregular buds on the surface of the cell called “blebbing”, cell shrinkage due to the degradation of the cytoskeleton, and finally, decompensation of the cell in small apoptotic bodies, which are then phagocytosed by other cells (Nagata, 2000).

There are two pathways leading to the activation of the caspase cascade, the extrinsic and the intrinsic pathway (see *Figure 1*). The extrinsic apoptosis pathway is initiated by the ligation of certain death receptor molecules on the surface of a cell, such as CD95/Fas and TRAIL (tumor-necrosis factor–related apoptosis-inducing ligand) in CLL (Burger et al., 1999). Specialized immune cells carry the according ligands and can thereby force an affected cell to undergo apoptosis in order to protect integrity of the microenvironment, e.g. in case of a preceding viral infection of the cell (Adams and Cory, 2007b). The intrinsic pathway is initialized due to cell-intrinsic and environmental changes, like a lack of survival signals. It is mediated by the release of cytochrome c from the mitochondria, which subsequently activates the caspase cascade. The mitochondrial release of cytochrome C is controlled by proteins of the *bcl2* family (Adams and Cory, 2007a): In its anti-apoptotic function, Mcl-1 – together with its homologues Bcl-2 and B-cell lymphoma-extra large (Bcl-X_L) – inhibits the formation of the pore in the mitochondrial membrane by binding and sequestering the pore-forming pro-

apoptotic proteins Bcl-2 associated X (Bax) and Bcl-2 homologous antagonist killer (Bak). Another important pro-apoptotic group of regulators contain only one Bcl-2 homology domain and are therefore called BH3-only proteins. There are BH3-only activators and sensitizers (Adams and Cory, 2007b). The activators interact directly with Bax and Bak to promote their activation and subsequently the release of cytochrome c, whereas the sensitizers inhibit anti-apoptotic members of the *bcl2* family like Mcl-1 and Bcl-2. High levels of Mcl-1 are known to prolong cell survival by facilitating the resistance to programmed cell death of CLL cells (Reed and Pellecchia, 2005). Notably, its expression is significantly associated with failure to achieve complete remission following cytotoxic therapy, suggesting its predominant role for the pathogenesis of CLL (Kitada et al., 1998; Saxena et al., 2004).

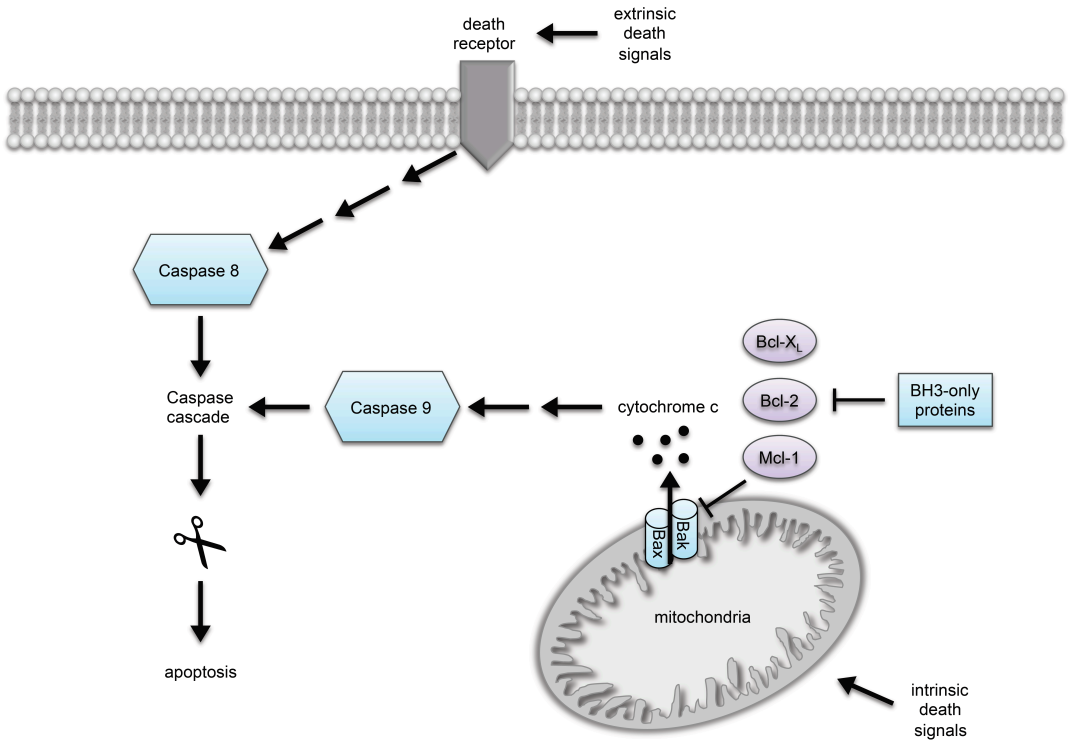

Figure 1 The apoptotic machinery

The majority of CLL cells in the peripheral blood are arrested in the G0/G1 phase of the cell cycle. In contrast, recent studies revealed evidence for a proliferative pool of CLL cells in patients with a high rate of turnover (Plander et al., 2009). Astonishingly, a rather stable course of disease in these patients suggests that a high rate of spontaneous apoptosis is counterbalanced by proliferation. In addition, CLL cells carry shorter telomeres compared to healthy B cells (Bechter et

al., 1998). CLL cells with unmutated IGHV have much shorter telomeres and higher telomerase activity than CLL cells with a mutated IGHV region (Damle et al., 2004). These findings object the concept of slowly accumulating neoplastic cells but promote the idea of extensive proliferative capacity of – especially unmutated – CLL cells prior to oncogenic transformation. A subset of CLL cases expresses the cyclic ADP ribose hydrolase CD38 on their surface. CD38 expression is associated with a significantly more aggressive course of disease due to an active proliferation of $CD38^+$ CLL cells (Damle et al., 2007; Ibrahim et al., 2001). The interaction of CD38 with the platelet endothelial cell adhesion molecule CD31 expressed by the CLL microenvironment might be a reason for the strong activation of their proliferation (Deaglio et al., 2010).

1.1.2.3 Immunological Aspects

B cells are the key regulators of the humoral immune response. They are responsible for recognizing pathogens with their surface BCR molecules and producing antibodies to protect the organism from the threat. The BCR consists of two heavy and two light immunoglobulin chains. In fact, each B cell only uses two of its six antibody loci – one of the two maternal and paternal heavy chain loci and one of the four maternal and paternal κ and λ light chain loci (Alberts, 2008). This first step to diversity of the immunoglobulin repertoire is called allelic exclusion. Each immunoglobulin chain consists of a constant (C) and a variable (V) region, whereby the variable region is important to create a diverse repertoire of monospecific antigen receptors to defend the organism against all sorts of pathogens. Each heavy-chain locus contains sets of C-region coding sequences and sets of V-regions encoding sequences, long variable (*IGHV*) gene segments, diversity (D) gene segments and short joining (J) gene segments. In contrast, the light chain variable (*IGLV*) loci lack D gene segments. During the B cell development in the bone marrow, the variable gene segments are joined by site-specific recombination through the RAG complex (recombinant activating genes) – during a process called the V(D)J recombination. The RAG complex induces double-strand breaks precisely between the gene segments to be joined and their recombination signal sequences. Then, the rejoining process is initiated by enzymes involved in DNA double-strand repair. This second step to diversity is called junctional diversification.

Each of the assembled V-region coding sequences is then co-transcribed with the appropriate C-region sequence and spliced to generate RNA molecules with adjoining V, D, J and C sequences. These initial antibodies are low-affinity IgM and IgD antibodies, which further diversify following antigen stimulation by the process of class-switch recombination and somatic hypermutation in the germinal centers of the lymph nodes. Somatic hypermutation arises during affinity maturation from accumulated point mutations in both the *IGHV* and *IGLV* genes. One key enzyme in this process is called activation-induced deaminase (AID), which deaminates cytosine to uracil in transcribed V-region loci and thereby produces U:G mismatches in the sequence. Finally, high-affinity IgG, IgA and IgE antibodies are selected by these modifications.

CLL is a highly heterogeneous disease with differential outcomes ranging from a disease which may not require to be treated for a decade to an aggressive form with fatal outcome in a couple of years. This heterogeneity is reflected in the biologic differences between CLL cases. Two subsets of patients can be distinguished by the mutational status of the *IGHV* gene. Those patients without somatic hypermutations in the *IGHV* locus tend to have a more aggressive course of disease. CLL cells are likely to express certain IGHVs, such as *IGHV1-69*, *IGHV3-7*, *IGHV3-23* and *IGHV4-34* (Chiorazzi and Ferrarini, 2003; Kipps, 1993). Only *IGHV3-7*, *IGHV3-23*, and *IGHV4-34* are commonly somatically hypermutated, but *IGHV1-69* has usually few or no mutations (Fais et al., 1998). This restricted BCR repertoire is thought to arise from a selection mechanism driven by auto-antigens that may promote the expansion of the CLL clone (Ghia et al., 2008; Stevenson et al., 2011). In 2012, Dühren-von Minden et al. suggested that the complementarity-determining region 3 of a CLL BCR heavy chain interacts with a cell-autonomous internal epitope of the BCR, leading to an antigen-independent, autonomous signaling, which provides a survival benefit for CLL cells (Duhren-von Minden et al., 2012).

1.1.3 Therapy of CLL

1.1.3.1 State of the Art

There are two staging systems based on physical examination and blood counts – the Rai staging system and the Binet classification. In Germany, the Binet classification is predominantly used (Binet et al., 1981):

Stage	Definition	Median Survival
A	hemoglobin ≥ 10 g/dL	> 10 years
	thrombocytes ≥ 100,000 / µL	
	< 3 regions affected (lymph nodes, liver or spleen)	
B	hemoglobin ≥ 10 g/dL	5 years
	thrombocytes ≥ 100,000 / µL	
	≥ 3 regions affected (lymph nodes, liver or spleen)	
C	hemoglobin < 10 g/dL	2 - 3 years
	thrombocytes < 100,000 / µL	

Table 1 The Binet classification

As efforts to improve the clinical course of CLL in patients with early stages were unsuccessful (Dighiero et al., 1998), the standard of care for those patients without significant symptoms is a watch-and-wait strategy (Cramer et al., 2015). Intent to treat is generally given at Binet stage C or at stage A or B, if symptoms worsen and impair the patient's quality of life. At more advanced stages, patients have to undergo chemoimmunotherapy (Nabhan and Rosen, 2014) with a combination therapy of fludarabine, cyclophosphamide and rituximab being the standard regime (Eichhorst et al., 2006; Eichhorst et al., 2009; Hallek et al., 2010).

1.1.3.1 B cell receptor inhibitors as novel therapeutics for CLL

To date, more promising new therapeutic options have been approved for the treatment of CLL. These are small molecule inhibitors, which target different components of the BCR signaling pathway: The phosphatidylinositol 3-kinase (PI3K) inhibitor idelalisib (formerly GS-1101 or CAL-101) and the Bruton's tyrosine kinase (Btk) inhibitor ibrutinib (formerly PCI32765) (Byrd et al., 2013; Nabhan et al., 2011; Ponader et al., 2012). Early lymphocytosis and reduction in lymph nodes and organomegaly are acknowledged as class effects of BCR antagonists. The overall response rate (ORR) according to 2008 International Workshop on CLL (IWCLL) criteria was 71% in a phase IB/II study (Byrd et al., 2014). The most recent phase III study was ended by the data safety and monitoring committee because of the significant benefit seen in both progression-free survival (PFS) and

overall survival (OS). The Food and Drug Administration (FDA) approved ibrutinib in February 2014 for the treatment of patients with CLL who had received at least one previous treatment (Dangi-Garimella, 2014). Current clinical trials concentrate on the combinatory therapy of ibrutinib with monoclonal antibodies, chemotherapy and immunomodulators. In addition, strong preclinical and clinical data support idelalisib, a reversible inhibitor of PI3Kδ, as a new therapeutic for CLL (Coutre et al., 2015; Herman et al., 2010; Lannutti et al., 2011). It has been published that idelalisib promotes apoptosis in CLL cells and impedes their survival. Combination therapies with anti-CD20 antibody rituximab or the chemotherapeutic bendamustine or both showed a response rate of > 80% and therefore a better rate than rituximab alone (Friedberg et al., 2010; Furman et al., 2014). In addition, spleen tyrosine kinase (Syk) inhibitors like fostamatinib and bcl-2 inhibitors like ABT-263 and ABT-199 are currently in clinical trials and may follow idelalisib and ibrutinib in their success (Hallek, 2013).

Because of the high heterogeneity among CLL patients, there was an urge for strong prognostic factors to predict the clinical course for each individual patient (Nabhan et al., 2015). Hundreds of prognostic markers proofed to be clinically irrelevant. Besides genetic lesions, the mutational status of the *IGHV* locus and CD38 surface expression described above, another strong prognostic biomarker in CLL was identified in 2001 – the expression of zeta-chain-associated protein of 70 kDa (ZAP70) (Rosenwald et al., 2001). The comparison of gene expression profiles of IGHV-mutated and IGHV-unmutated CLL patient samples led to the discovery that high expression of ZAP70 correlates with absence of IGHV mutations and poor outcomes of CLL patients (see *Figure 2*) (Rassenti et al., 2004). It has been proven to have an even better predictive value than the mutational status of the IGHV.

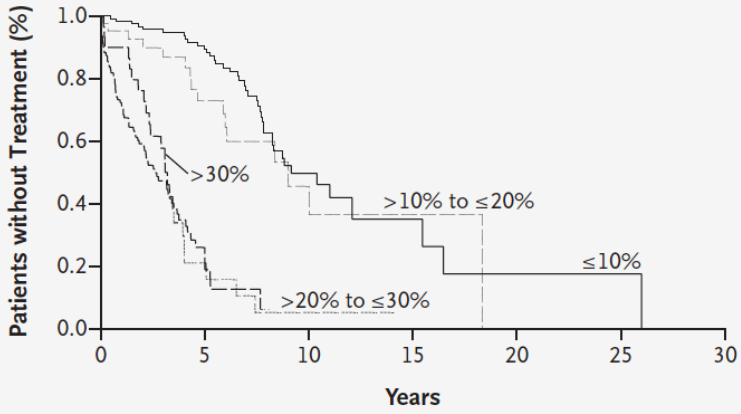

No./No. at Risk						
ZAP-70 level, ≤10%	11/123	24/79	3/15	2/4	0/1	1/1
ZAP-70 level, >10% to ≤20%	9/43	6/20	0/4	1/1	0/0	0/0
ZAP-70 level, >20% to ≤30%	21/30	3/4	0/1	0/0	0/0	0/0
ZAP-70 level, >30%	67/111	4/9	0/0	0/0	0/0	0/0

Figure 2 Relationship between ZAP70 expression level and the time from diagnosis to initial therapy (Rassenti et al., 2004).

1.2 The Zeta-chain-associated Protein of 70 kDa (ZAP70)

The zeta(ζ)-chain-associated protein of 70 kDa (ZAP70) (Chan et al., 1991) is a protein tyrosine kinase, which is primarily expressed in T cells and NK cells (Chan et al., 1992). Several B cell lines were tested negative for ZAP70 expression. ZAP70 has the greatest homology to porcine Syk (Taniguchi et al., 1991) and was therefore defined as member of the Syk/ZAP70 kinase family.

1.2.1 The Discovery of ZAP70

In 1994, ZAP70 was discovered to play a key role in human T cell activation and development. Mutations in the *ZAP70* gene were reported in patients of different families to lead to severe T cell deficiencies. Arpaia et al. reported a severe splicing defect of the *ZAP70* gene resulting in the insertion of three amino acids in the kinase domain (Arpaia et al., 1994). Chan et al. discovered a point mutation and a 9-base pair (bp) insertion, again both changing the amino acid sequence of the catalytic domain of ZAP70 (Chan et al., 1994). Finally, Elder et al. reported a 13-bp deletion resulting in a frame-shift after amino acid 503 and therefore in premature termination of translation (Elder et al., 1994). Most of further identified mutations that lead to a severe immunodeficiency occur in the catalytic domain of ZAP70 (Meinl et al., 2000; Noraz et al., 2000; Turul et al., 2009). Mice lacking ZAP70 cannot develop CD4- or CD8-single positive T cells (Negishi et al., 1995). During T cell development the αβ T-cell receptor (TCR) encounters a self-major histocompatibility complex (MHC) molecule bearing a self-peptide (Au-Yeung et al., 2009). For further propagation, T cells have to respond to antigens (positive selection) but not as strongly as to be autoreactive (negative selection). This checkpoint is blocked in ZAP70-deficient mice (Kadlecek et al., 1998; Negishi et al., 1995). Therefore, the proposed pathogenic mechanism for severe immunodeficiency in men is that a complete lack of ZAP70 protein results in deficient TCR signaling capacity during early T cell development, leading to low numbers or total absence of $CD8^+$ cytotoxic T cells and normal numbers of non-functional $CD4^+$ helper T cells (Fischer et al., 2010; Perlmutter, 1994).

1.2.2 The Structure of the Tyrosine Kinase ZAP70

The *ZAP70* gene is located on chromosome 2q11.2 (Chan et al., 1994). It encodes a 70 kDa protein composed of two tandem src homology domains (SH2), linked by a so called interdomain A (see *Figure 3*). Another linker region, the interdomain B, links the second SH2 domain to the carboxy-terminal (C-terminal) catalytic region maintaining the kinase function (Brdicka et al., 2005; Chan et al., 1992).

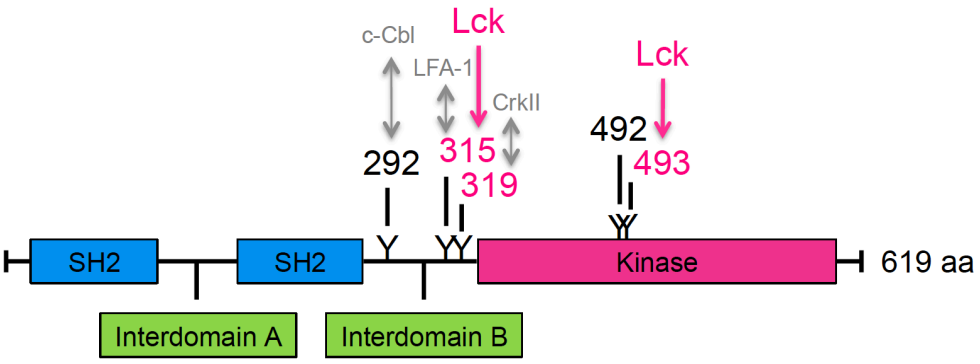

Figure 3 The domain structure of ZAP70
pink – processes involved in ZAP70 activation during TCR signaling; *grey* – protein-protein interactions

The tandem SH2 domains of ZAP70 are essential for the interaction with double-phosphorylated immunoreceptor tyrosine-based activation motifs (ITAMs) of the T cell receptor (TCR) ζ chain (Bu et al., 1995). The more amino-terminal (N-terminal) SH2 domain has an incomplete phosphotyrosine binding pocket (Au-Yeung et al., 2009; Hatada et al., 1995). One wall of this binding pocket is completed by the surface of the more C-terminal and more typical SH2 domain. In the current model, the C-terminal SH2 domain first binds to the N-terminal phosphotyrosine of an ITAM. Then, binding of the C-terminal phosphotyrosine occurs, when C- and N-terminal SH2 domains are properly aligned. This conformational change might be mediated by interdomain A. The most important regulatory substructure of ZAP70 is the interdomain B, containing three tyrosine residues, Y292, Y315 and Y319, phosphorylated by the lymphocyte-specific protein tyrosine kinase (Lck) following TCR stimulation (Zhao et al., 1999).

In the inactive state, ZAP70 is maintained in an auto-inhibited confirmation. This state of ZAP70 is maintained by an intimate association between the distal surface of the kinase domain and the interdomains A and B, leading to a distorted

constitution of the tandem SH2 domains in a manner that is inconsistent with ITAM binding (Deindl et al., 2007). The catalytic domain of auto-inhibited ZAP70 is similar to a Cdk/Src-like inactive confirmation (De Bondt et al., 1993). Helix αC is displaced from the active site, a short helix locks the displaced helix in its position and the catalytically crucial salt bridge between Q386 and K369 is disrupted (Au-Yeung et al., 2009). The key residues that have an impact on this auto-inhibitory switch are Y315 and Y319 inside interdomain B. Another important residue is proline P147 due to the fact that this residue interacts with Y597 and Y598 in the C-lobe of the kinase domain. The two tyrosine residues form a cleft on the surface of the catalytic domain into which the inter-SH2 linker residue P147 is docked in the auto-inhibited conformation (Deindl et al., 2007).

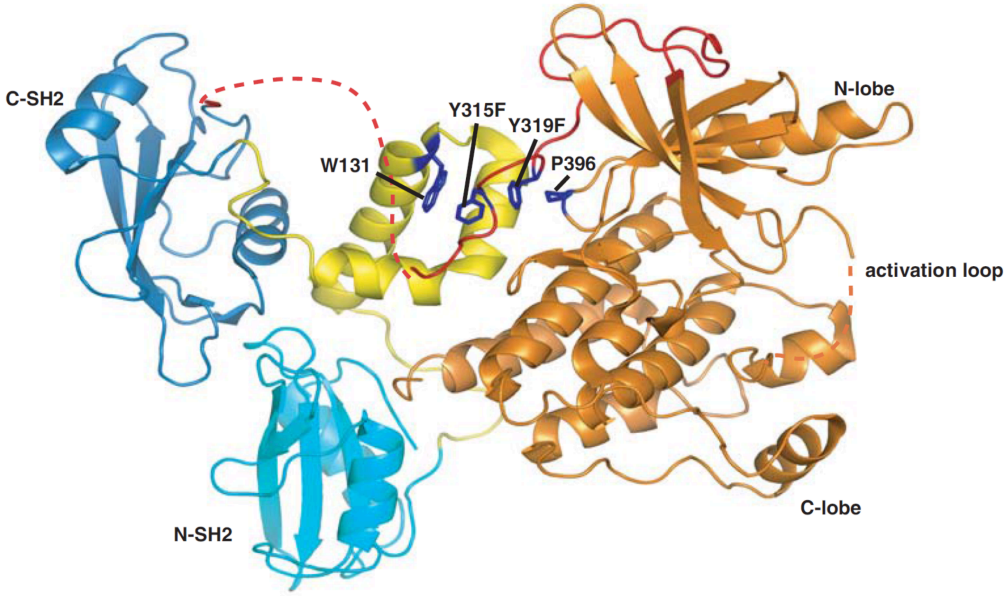

Figure 4 Crystal structure of auto-inhibited ZAP70 (Wang et al., 2010)

1.2.3 The Physiological Function of ZAP70 in the TCR Pathway

T cells are the key players in the cell-mediated adaptive immune response. They are mainly responsible for antigen recognition and cytotoxic reaction towards infected cells. The TCR recognizes pathogenic peptides, which are bound to MHC complexes on antigen-presenting cells (APCs) (Garcia et al., 1999; Hennecke and Wiley, 2001; Weiss, 1991). Upon antigen encounter, Lck is recruited to the cytoplasmic tails of the CD3 complex and phosphorylates tyrosines in the ITAMs of the CD3 and ζ chain of the TCR complex (see *Figure 5*) (Horejsi et al., 2004; Irving and Weiss, 1991; Letourneur and Klausner, 1991; Lovatt et al., 2006; Straus and Weiss, 1992). Once the ITAMs are double-phosphorylated, ZAP70 is recruited

to the plasma membrane and can interact with these phosphotyrosines (Chan et al., 1991; Iwashima et al., 1994), leading to the release from its auto-inhibited confirmation (see *Figure 4*). Y315 and Y319 inside the interdomain B are both phosphorylated by Lck or by ZAP70 itself upon ITAM encounter (Brdicka et al., 2005; Di Bartolo et al., 1999; Williams et al., 1999), thus serving as a SH2 docking site and subsequently destabilizing the auto-inhibited conformation of ZAP70 (Deindl et al., 2007). Then, Y493 inside the activation loop of the kinase domain of ZAP70 is phosphorylated by Lck, leading to subsequent auto-phosphorylation of Y492 by ZAP70 itself (Chan et al., 1995; Neumeister et al., 1995). The phosphorylation of the two tyrosine residues leads to a conformational change and displaces the activation loop from the catalytic site, thereby activating the tyrosine kinase function of ZAP70 (Hatada et al., 1995; Wange et al., 1995). Activated ZAP70 further phosphorylates the transmembrane adapter protein linker of activated T cells (LAT) on four key tyrosine residues (Zhang et al., 1999a; Zhang et al., 1998; Zhang et al., 1999b; Zhang et al., 2000), which recruits several further signaling molecules to form a complex called the LAT signalosome (Werlen et al., 2000; Zhang et al., 1998). The LAT signalosome is involved in three major downstream pathways, the calcium mobilization pathway, the mitogen-activated protein kinase (MAPK) pathway and the NF-κB pathway (Zhang et al., 1999a). Important factors of the LAT signalosome are adhesion- and degranulation-promoting adaptor protein (ADAP), NCK1 and the proto-oncogene Vav1. Also, the growth factor receptor-bound protein 2 (GRB2) associates with LAT and son of sevenless homologue (SOS) to recruit and activate the G protein Ras (Egan et al., 1993), which leads to a downstream activation of the kinase Raf and altered gene expression through the activation of the transcription factor activator protein 1 (AP-1) via the MAPK signaling cascade. GRB2-related adaptor protein GADS, SH2 domain-containing leukocyte protein of 76 kDa (SLP-76) (Jackman et al., 1995) and interleukin-2-inducible T cell kinase (ITK) (Liu et al., 1998) are involved in the activation of phospholipase Cγ1 (PLCγ1) (Finco et al., 1998; Weiss, 1991; Zhang et al., 2000), producing inositol trisphosphate (IP_3) and diacylglycerol (DAG). Inositol triphosphate initiates the release of Ca^{2+} ions from the endoplasmatic reticulum into the cytoplasm and Ca^{2+} subsequently activates the transcription factor NFAT through calcineurin (Zhang et al., 1999a). Diacylglycerol, however, is an activator of protein kinase C (PKC), which is involved in NF-κB activation

(Schulze-Luehrmann and Ghosh, 2006). The downstream transcription factors NFAT (Motto et al., 1996), AP-1 and NF-κB change gene expression to promote T cell proliferation and differentiation (Dolmetsch et al., 1997; Dolmetsch et al., 1998; Feske et al., 2001). Furthermore signaling through the TCR leads to actin reorganization and the activation of integrins by inside-out signaling (Brownlie and Zamoyska, 2013; Horejsi et al., 2004; Samelson, 2002).

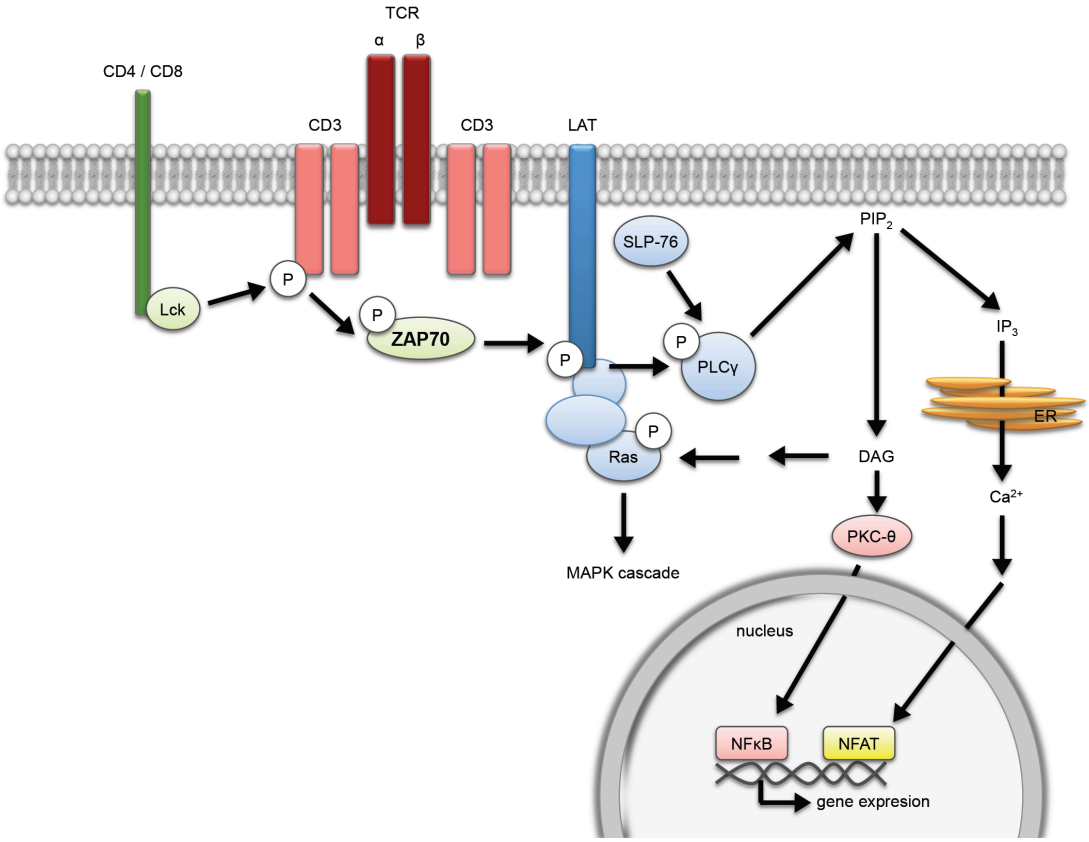

Figure 5 The T-cell receptor signaling pathway

ZAP70 is a key protein in the T cell receptor signaling pathway. Mutational studies of the tyrosine residue Y292 in interdomain B of ZAP70 have discovered that it plays a negative regulatory role for ZAP70 activation (Zhao and Weiss, 1996). ζ chain ubiquitination and TCR downmodulation is mediated by the interaction of ζ chain bound ZAP70 with the E3 ubiquitin ligase c-Cbl via its phosphorylated Y292 (Lupher et al., 1997; Magnan et al., 2001; Wang et al., 2001). How this phosphorylation alters ZAP70 activity is not completely understood to date. Y319 is involved in the Ca^{2+} mobilization and subsequent IL-2 secretion in T cells following antigen recognition by the TCR (Di Bartolo et al., 1999; Williams et al., 1999). Phosphorylated Y315, on the other hand, was shown to interact with CT10 regulator of kinase II (CrkII) adapter protein and therefore

plays a regulatory role for the remodeling of the actin cytoskeleton (Gelkop and Isakov, 1999). Y315 has also been reported to participate in T cell adhesion via TCR-induced activation of the integrin LFA-1 (Epler et al., 2000; Goda et al., 2004). Through both mechanisms, ZAP70 controls the formation of the immunological synapse between T cells and APCs (Blanchard et al., 2002). It reorganizes the polarization of the microtubule organization center toward the APC. However, ZAP70 has also been shown to be involved in TCR down-regulation following antigen encounter. ZAP70 activity is required for the internalization and degradation of TCR-CD3 complexes (Dumont et al., 2002). The key residue involved in this homeostatic system is the formerly described negative regulatory Y292 (Davanture et al., 2005). Conclusively, ZAP70 is a tyrosine kinase with a crucial role in T cell activation and early T cell development.

1.3 The Role of ZAP70 in CLL

The expression of the T-lineage specific gene *ZAP70* in the B-lineage background of CLL is an unexpected finding and warrants further investigations (Wang et al., 2010). Its strong correlation with poor clinical outcome suggests a functional role of ZAP70 in CLL pathogenesis (Au-Yeung et al., 2009; Rassenti et al., 2004; Rosenwald et al., 2001). Arbitrarily defined, patients carrying more than 20% of ZAP70-expressing CLL cells are standardly referred to as ZAP70-positive CLL cases and patients with less than 20% as ZAP70-negative CLL cases, indicating that expression levels vary over a broad range.

1.3.1 Genetic and Epigenetic Aspects

The expression of ZAP70 in CLL cells seems to be epigenetically regulated, as recent studies showed that the ZAP70 promoter is associated with active histone modifications and with reduced DNA methylation leading to transcriptional de-repression of ZAP70 (Amin et al., 2012). Higher levels of global acetylation of histone H3 as well as significant enrichment of di- and trimethylation of lysine 4 of histone H3 are associated with the ZAP70 promoter regions in ZAP70-positive primary CLL cells. Additionally, treatment with histone deacetylase (HDAC) and DNA methylation inhibitors leads to recovery of ZAP70 expression in ZAP70-negative patients. Other studies described that the loss of methylation of a single CpG dinucleotide in a 5' regulatory sequence mediates ZAP70 overexpression in CLL cells and is associated with poor prognosis (Claus et al., 2014; Claus et al., 2012). Global DNA methylation analysis of CLL cells using high-resolution arrays revealed differential methylation of several genes. Differential methylation profiles were described for IGHV-mutated and IGHV-unmutated CLL cells (Cahill et al., 2013). Notably, these methylation profiles remain rather unchanged over the time course of disease, implying that the changes occur early in disease development and are maintained throughout the clonal evolution.

1.3.2 Function of ZAP70 in the BCR Signaling of CLL cells

In 2002, it has been suggested that ZAP70 is engaged in the BCR signaling in CLL cells (Chen et al., 2002). To understand the possible involvement of ZAP70 in the BCR signaling, the pathway will be briefly reviewed.

1.3.1.1 The Physiological BCR Signaling Pathway

Upon antigen encounter, Src family kinases Lyn, Fyn, and Blk, phosphorylate the immunoreceptor tyrosine-based activation motifs (ITAMs) of CD79 in healthy B cells (Del Porto et al., 1995; Reth, 1989; Saijo et al., 2003; Slupsky, 2014; Yao et al., 1995; Zhang and Kipps, 2014). Subsequently, Syk is able to bind to the phosphorylated ITAMs via its SH2 domain (Kurosaki et al., 1995), is activated and subsequently phosphorylates itself (Rowley et al., 1995). Then, the adaptor proteins B cell linker protein (BLNK or SLP-65), linker for activation of B cells (LAB), and Nck are recruited to phosphotyrosine residues in CD79 outside the ITAMs (Castello et al., 2013; Kabak et al., 2002; Malhotra et al., 2009). BLNK is subsequently phosphorylated by Syk, which allows the recruitment and activation of other kinases to the BCR adaptor protein complex like Btk and PI3K (Slupsky, 2014). The signal leads to a downstream activation of AKT/mTor (mammalian target of rapamycin) and NF-κB (nuclear factor 'kappa-light-chain-enhancer' of activated B-cells) (Hers et al., 2011). Once the complex of Syk, Btk, BLNK, and PLCγ2 has formed, PLCγ2 is activated through phosphorylation by Btk and Syk. Activated PLCγ2 then hydrolyzes phosphatidylinositol 4,5-bisphosphate (PIP_2) to DAG and IP_3, which leads to a Ca^{2+} release from the endoplasmic reticulum (Kim et al., 2004). The combination of free Ca^{2+} ions and DAG subsequently activates PKCβ (Newton, 2010). PKCβ activation regulates the inhibitor of κB kinase (IKK) and thereby leads to the downstream activation of NF-κB (Guo et al., 2004). Furthermore, Ca^{2+} release directly activates further transcription factors Jun and nuclear factor of activated T cells (NFAT) (Dolmetsch et al., 1997; Dolmetsch et al., 1998). NF-κB, NFAT and Jun migrate to the nucleus and activate genes, which support B cell survival, proliferation and migration (see *Figure 6*).

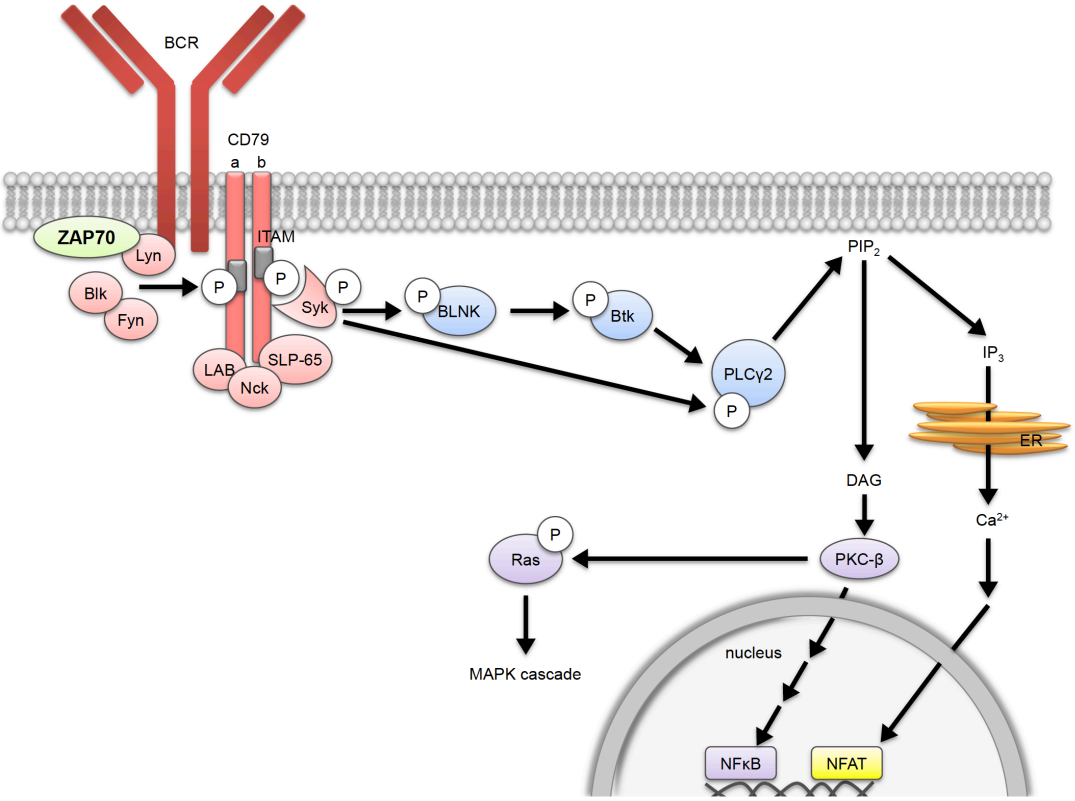

Figure 6 The B-cell receptor signaling pathway in CLL

CLL cells express low levels of surface immunoglobulins and CD79b, but respond variably to antigen stimulation. Syk, Lyn and Btk expression as well as PI3K activity is elevated compared to normal B cells and – as mentioned above – anti-apoptotic signaling pathways are tonically activated in CLL cells (Woyach et al., 2014). CLL cells exhibit an activated state that is more advanced than that of normal circulating $CD5^+$ B cells from age-matched controls and share many features with antigen-activated mature B cells, suggesting an important role for BCR signaling in the pathogenesis of CLL (Damle et al., 2007). This assumption is supported by the promising therapeutic effects of early BCR signaling antagonists (see *Introduction p.9*).

1.3.1.2 Involvement of ZAP70 in the BCR Signaling of CLL cells

As described above, ZAP70 shows a high structural homology to the tyrosine kinase Syk, which is essentially involved in the B-cell receptor signaling of healthy B cells. Hence, the involvement of aberrantly expressed ZAP70 in BCR signaling of leukemic B cells is widely discussed in the research community. This theory is supported by the discovery that ZAP70 is able to reconstitute BCR signaling in

Syk-deficient B cells and vice versa (Kong et al., 1995; Toyabe et al., 2001). Chen et al. published two studies investigating this mechanism in CLL cells. In 2005, the group presented data showing that ZAP70 becomes phosphorylated upon BCR engagement, associates with surface immunoglobulin and CD79b and subsequently enhances phosphorylation of Syk, BLNK and PLCγ (Chen et al., 2005a). Furthermore, ZAP70-positive CLL cells exhibit stronger calcium mobilization upon BCR ligation than ZAP70-negative cells. Still, the functional mechanism remained elusive. Then, in 2008, Chen et al. further postulated that ZAP70 functions as adapter protein independently of its enzymatic kinase activity (Chen et al., 2008). In addition, truncation studies revealed that the C-terminal SH2 domain of ZAP70 is required to enhance intracellular calcium flux following BCR ligation. Still, a conflicting publication by Deglesne et al. postulated that ZAP70 expression was neither mandatory nor sufficient to generate a survival response through the BCR in CLL cells (Deglesne et al., 2006). In addition, Gobessi et al. showed that ZAP70 is not sufficiently phosphorylated and subsequently activated following BCR engagement in CLL cells (Gobessi et al., 2007). Comparison to Syk activation indicates a much stronger role for Syk than for ZAP70 in the downstream BCR signaling in CLL cells. This fact supports a hypothesis that ZAP70 may function by recruiting downstream signaling factors and thereby enhancing the activation of several BCR-associated kinases, like Syk, MAPK and AKT. The inhibition of the anti-apoptotic response to BCR stimulation leads to a decrease in Mcl-1 protein levels and the subsequent induction of apoptosis. As previous studies showed, ZAP70-positive CLL cases express higher amounts of anti-apoptotic Mcl-1 (Pepper et al., 2008). In conclusion, the current concept of the mechanism of ZAP70 in CLL suggests it may primarily act as a scaffolding protein, required to enhance signaling through the BCR. However, its function in malignant B cells is ill-defined.

1.4 Aim of this study

This study intends to characterize the functional role of ZAP70 in CLL using an inducible protein expression system as well as primary leukemic B cells extracted from the peripheral blood of CLL patients.

2 Material and Methods

2.1 Material

2.1.1 Devices

Table 2 *Laboratory devices*

Device	Name	Manufacturer
Icemaker	SPR 80 L	NordCap, Bremen, Germany
Steam sterilizer	Varioklav®	HP Medizintechnik, Oberschleißheim, Germany
Precision balance	EG-2200-2NM	KERN & Sohn GmbH,
Hotplate stirrer	MONOTHERM VarioMag	HP Medizintechnik, Oberschleißheim, Germany
pH meter	SevenEasy™ pH	Mettler-Toledo, Gießen, Germany
Chemical hood	Chemical Hood 7597	Köttermann, Uetze/Hänigsen, Germany
Flow cytometer	CyAn™ ADP Analyzer	Beckman Coulter, Brea, CA, USA
Power supply	Power Pack P25	Biometra, Göttingen, Germany
SDS-PAGE system	Maxigel	Biometra, Göttingen, Germany
Transfer chamber	Trans-Blot® Electrophoretic Transfer Cell	Bio-Rad Laboratories, Berkeley, CA, USA
Tumbling table	WT12 tumbling table	Biometra, Göttingen, Germany
Rotating wheel	L 28 28000	CAT Scientific, Paso Robles, CA, USA
Power Supply	PowerPac™ 300 Basic Power Supply	Bio-Rad Laboratories, Berkeley, CA, USA
Gel Electrophoresis Apparatus	Horizon 11-14	Life Technologies, Carlsbad, CA, USA
UV transilluminator	Universal Hood II	Bio-Rad Laboratories, Berkeley, CA, USA
Geldryer	Geldryer MidiDry D62	Biometra, Göttingen, Germany
Vortexer	REAX Top	Heidolph Instruments, Schwabach, Germany
	MS1 shaker	IKA®-Werke, Staufen, Germany
Thermomixer	Thermomixer Compact	Eppendorf, Hamburg, Germany
	Thermomixer Comfort	Eppendorf, Hamburg, Germany

Device	Name	Manufacturer
Spectrophotometer	NanoDrop 2000c UV-Vis Spectrophotometer	Thermo Fisher Scientific, Waltham, MA, USA
DNA quantification with high sensitivity	Qubit® Fluorometer	Life Technologies, Carlsbad, CA, USA
PCR cycler	MyCycler™ Thermal Cycler	Bio-Rad Laboratories, Berkeley, CA, USA
Real-Time PCR System	StepOnePlus™ System	Life Technologies, Carlsbad, CA, USA
Immunoblot developer machine	Protex Optimax	Röntgen Bender, Baden Baden, Germany

Table 3 *Cell culture devices*

Device	Name	Manufacturer
Sterile hood for cell culture	Herasafe™, Biological Safety Cabinet	Heraeus, Hanau, Germany
CO_2 Incubators	Heracell™ 150i Tri-Gas Incubator	Thermo Fisher Scientific, Waltham, MA, USA
Safety-vacuum-system	EcoVac	Schuett-biotec, Göttingen, Germany
Water bath	Incubation/Inactivation Water Bath 1008	GFL, Burgwedel, Germany
Inverted Transmitted Light Micropscope	Axiovert 25	Zeiss, Oberkochen, Germany
Amaxa™ transfection device	Nucleofector™ II Device	Lonza, Basel, Switzerland

Table 4 *Centrifuges*

Device	Name	Manufacturer
Bench top centrifuge	Qualitron DW-41 Microcentrifuge	Artisan Technology Group, Champaign, IL, USA
Small bench centrifuges	Microcentrifuge 5415C	Eppendorf, Hamburg, Germany
	Microcentrifuge 5415D	Eppendorf, Hamburg, Germany
	Mikro 22R	Hettich, Tuttlingen, Germany
	MC 6 Centrifuge	Sarstedt, Nümbrecht, Germany
Mid bench centrifuges	Megafuge 1.0R	Heraeus, Hanau, Germany

Table 5 *Cooling devices*

Device	Name	Manufacturer
Freezing container	Nalgene® Mr. Frosty® Cryo 1°C	Nalge Nunc International, Thermo Fisher Scientific, Waltham, MA, USA
Refrigerator +4°C	Profi Line	Liebherr, Bulle, Switzerland
Freezer -20°C	Premium	Liebherr, Bulle, Switzerland
Freezer -80°C	MDF-U52V V.I.P.™	Sanyo, Moriguchi, Ōsaka, Japan
Liquid nitrogen tank	Biosafe®MD	Messer Austria, Gumpoldskirchen, Austria
	Apollo®	Messer Austria, Gumpoldskirchen, Austria

Table 6 *Pipets*

Name	Volume range [µl]	Manufacturer
Eppendorf Research	0.5 – 10	Eppendorf, Hamburg, Germany
Eppendorf Research	10 – 100	Eppendorf, Hamburg, Germany
Eppendorf Research	100 – 1000	Eppendorf, Hamburg, Germany
Eppendorf Reference	0.5 – 10	Eppendorf, Hamburg, Germany
Eppendorf Reference	10 – 100	Eppendorf, Hamburg, Germany
Eppendorf Reference	100 – 1000	Eppendorf, Hamburg, Germany
Pipetman Classic™ P10	1 – 10	Gilson, Middletown, WI, USA
Pipetman Classic™ P100	20 – 100	Gilson, Middletown, WI, USA
Pipetman Classic™ P200	20 – 200	Gilson, Middletown, WI, USA
Pipetman Classic™ P1000	100 – 1000	Gilson, Middletown, WI, USA
Finnpipette™ F1	0.5 – 3	Thermo Fisher Scientific, Waltham, MA, USA
Finnpipette™ F1	10	Thermo Fisher Scientific, Waltham, MA, USA
Finnpipette™ F1	10 – 50	Thermo Fisher Scientific, Waltham, MA, USA
Finnpipette™ F1	10 – 100	Thermo Fisher Scientific, Waltham, MA, USA
Transferpette®	100 – 1000	Brand, Wertheim, Germany
ErgoOne® Single Channel Pipet	100 – 1000	Starlab, Hamburg, Germany
Pipetboy acu		Ibs | tecnomara, Fernwald, Germany

Table 7 *Pipet tips*

Name	Volume	Manufacturer
Pipette Tip	10 µl	Sarstedt, Nümbrecht, Germany
Pipette Tip	200 µl	Sarstedt, Nümbrecht, Germany
Pipette Tip	1000 µl	Sarstedt, Nümbrecht, Germany
Filter Tip	10 µl	Sarstedt, Nümbrecht, Germany
Filter Tip	100 µl	Sarstedt, Nümbrecht, Germany
Filter Tip	1000 µl	Sarstedt, Nümbrecht, Germany
Falcon™ Disposable Aspirating Pipet	2 ml	Fisher Scientific International, Hampton, NH, USA
Serological Pipettes, single packed	5 ml	Greiner Bio-One, Kremsmünster, Austria
Serological Pipettes, single packed	10 ml	Greiner Bio-One, Kremsmünster, Austria
Serological Pipettes, single packed	25 ml	Greiner Bio-One, Kremsmünster, Austria
Serological Pipettes, single packed	50 ml	Greiner Bio-One, Kremsmünster, Austria

2.1.2 Plasticware

Table 8 *Filtration systems*

Description	Name	Filter Capacity	Manufacturer
Vacuum Driven Sterile Filer System	Stericup®	500 ml	Merck Millipore, Billerica, MA, USA
	Steritop™	500 ml	Merck Millipore, Billerica, MA, USA
Description	Name	Size	Manufacturer
Single Cell Suspension Filter	Filcon, Syringe-Type	30 µm	BD™ Medimachine, BD Biosciences, Franklin Lakes, NJ, USA

Table 9 *Cell culture dishes*

Name	Number of wells	Area	Working Volume	Manufacturer
CELLSTAR® 96 Well Polystyrene Cell Culture Microplates, F-Bottom / Standard (ST)	96	32 mm^2	340 µl	Greiner Bio-One, Kremsmünster, Austria
CELLSTAR® Cell Culture Multiwell Plates	48	1.0 cm^2	1 ml	Greiner Bio-One, Kremsmünster, Austria
CELLSTAR® Cell Culture Multiwell Plates	24	1.9 cm^2	1.5 ml	Greiner Bio-One, Kremsmünster, Austria
CELLSTAR® Cell Culture Multiwell Plates	12	3.9 cm^2	4 ml	Greiner Bio-One, Kremsmünster, Austria
CELLSTAR® Cell Culture Multiwell Plates	6	9.6 cm^2	5 ml	Greiner Bio-One, Kremsmünster, Austria

Table 10 *Cell culture flasks*

Name	Area	Working Volume	Manufacturer
Tissue Culture Dish	60.1 cm^2	25 ml	TPP Techno Plastic Products, Trasadingen, Switzerland
CELLSTAR® Filter Cap Cell Culture Flask, TC-treated, sterile	25 cm^2	50 ml	Greiner Bio-One, Kremsmünster, Austria
CELLSTAR® Filter Cap Cell Culture Flask, TC-treated, sterile	75 cm^2	250 ml	Greiner Bio-One, Kremsmünster, Austria
CELLSTAR® Filter Cap Cell Culture Flask, TC-treated, sterile	175 cm^2	550 ml	Greiner Bio-One, Kremsmünster, Austria

Table 11 *Reaction tubes*

Name	Volume	Manufacturer
PCR Tube Strips, Full-Height, PP thin-wall	0.2 ml	Bio-Rad Laboratories, Berkeley, CA, USA
Micro tube SafeSeal	1.5 ml	Sarstedt, Nümbrecht, Germany
Micro tube SafeSeal	2.0 ml	Sarstedt, Nümbrecht, Germany
Cryo.s™, PP, Round Bottom, External Thread, Natural Screw Cap, Starfoot, natural, sterile	2.0 ml	Greiner Bio-One, Kremsmünster, Austria
Falcon™ Round-Bottom Polypropylene Tubes	14 ml	Fisher Scientific International, Hampton, NH, USA
CELLSTAR® Centrifuge Tube, Polypropylene, sterile	15 ml	Greiner Bio-One, Kremsmünster, Austria
CELLSTAR® Centrifuge Tube, Polypropylene, sterile	50 ml	Greiner Bio-One, Kremsmünster, Austria

2.1.3 Reagents

Table 12 *Chemicals*

Item	Manufacturer
TRIS	Carl Roth, Karlsruhe, Germany
3-(N-Morpholino)propanesulfonic acid (MOPS)	Sigma-Aldrich, St. Louis, MO, USA
Hydrochloric acid (HCl) fuming 37%	Carl Roth, Karlsruhe, Germany
Glycine	Carl Roth, Karlsruhe, Germany
Sodium chloride (NaCl)	Carl Roth, Karlsruhe, Germany
Ethylene diamine tetraacetic acid (EDTA)	Sigma-Aldrich, St. Louis, MO, USA
Ethylene glycol tetraacetic acid (EGTA)	Sigma-Aldrich, St. Louis, MO, USA
Sodium phosphate	Sigma-Aldrich, St. Louis, MO, USA
Sodium pyrophosphate	Sigma-Aldrich, St. Louis, MO, USA
Sodium fluoride	Sigma-Aldrich, St. Louis, MO, USA
Benzamidine	Sigma-Aldrich, St. Louis, MO, USA
Phenylmethylsulfonyl fluoride (PMSF)	Sigma-Aldrich, St. Louis, MO, USA
Sodium orthovanadate	Sigma-Aldrich, St. Louis, MO, USA
Sodium dodecyl sulfate (SDS)	Serva Electrophoresis, Heidelberg Germany
Sodium carbonate	Sigma-Aldrich, St. Louis, MO, USA
Sodium azide	Sigma-Aldrich, St. Louis, MO, USA
Potassium chloride (KCl)	Sigma-Aldrich, St. Louis, MO, USA
Magnesium chloride ($MgCl_2$)	Sigma-Aldrich, St. Louis, MO, USA
β-Glycerophosphate	Sigma-Aldrich, St. Louis, MO, USA
DL-Dithiothreitol (DTT)	Fluka, Sigma-Aldrich, St. Louis, MO, USA
Bromophenol blue	Sigma-Aldrich, St. Louis, MO, USA
Brillant blue	Sigma-Aldrich, St. Louis, MO, USA

Item	Manufacturer
Acetone	Sigma-Aldrich, St. Louis, MO, USA
Acetic acid	Sigma-Aldrich, St. Louis, MO, USA
Trichloroacetic acid (TCA)	Sigma-Aldrich, St. Louis, MO, USA
Sulfuric acid (H_2SO_4)	Sigma-Aldrich, St. Louis, MO, USA
Glycerol	Sigma-Aldrich, St. Louis, MO, USA
Sucrose	Sigma-Aldrich, St. Louis, MO, USA
IPEGAL® CA-630 (NP-40)	Sigma-Aldrich, St. Louis, MO, USA
Triton™ X-100	Sigma-Aldrich, St. Louis, MO, USA
Chloroform	Sigma-Aldrich, St. Louis, MO, USA
Methanol	J.T.Baker® Chemicals, Center Valley, PA, USA
Ethanol	Sigma-Aldrich, St. Louis, MO, USA

Table 13 *Cell culture reagents*

Description	Name	Manufacturer
Media supplements	4-(2-hydroxyethyl)-1-piperazineethanesulfonic acid (HEPES) Buffer Solution (1 M)	Gibco™, Life Technologies, Carlsbad, CA, USA
	L-Glutamine (200 mM)	Gibco™, Life Technologies, Carlsbad, CA, USA
	Penicillin-Streptomycin (10,000 U/ml)	Gibco™, Life Technologies, Carlsbad, CA, USA
	Antibiotic-Antimycotic (100X)	Gibco™, Life Technologies, Carlsbad, CA, USA
	Sodium Pyruvate (100 mM)	Gibco™, Life Technologies, Carlsbad, CA, USA
	Minimum Essential Medium Non-Essential Amino Acids (100X)	Gibco™, Life Technologies, Carlsbad, CA, USA
	2-Mercaptoethanol (50 mM)	Gibco™, Life Technologies, Carlsbad, CA, USA
	Fetal calf serum	PAA, Thermo Fisher Scientific, Waltham, MA, USA
	Horse serum	PAA, Thermo Fisher Scientific, Waltham, MA, USA

Description	Name	Manufacturer
Media	RPMI Medium 1640	Gibco™, Life Technologies, Carlsbad, CA, USA
	MEM alpha, GlutaMAX™	Gibco™, Life Technologies, Carlsbad, CA, USA
	Dulbecco's Phosphate Buffered Saline DPBS (1X)	Gibco™, Life Technologies, Carlsbad, CA, USA
Gelatin	Gelatin from bovine skin	Sigma-Aldrich, St. Louis, MO, USA
Trypsin	Trypsin-EDTA (0.5%), no phenol red (10X)	Gibco™, Life Technologies, Carlsbad, CA, USA
Ficoll separating solution	Biocoll	Merck Millipore, Billerica, MA, USA
Viability staining	Trypan Blue Solution, 0.4%	Gibco™, Life Technologies, Carlsbad, CA, USA
Erythrocyte lysis	EasyLyse™	Dako, Agilent Technologies, Santa Clara, CA, USA
Cell lines	HELA	DSMZ, Braunschweig, Germany
	MEC-1	DSMZ, Braunschweig, Germany
CLL cell purging	Dynabeads® CD2	Invitrogen™, Life Technologies, Carlsbad, CA, USA
	Dynabeads® CD14	Invitrogen™, Life Technologies, Carlsbad, CA, USA
Amaxa Nucleofector® Technology	Amaxa Human B Cell Nucleofector® Kit V	Lonza, Basel, Switzerland
Selection antibiotics	Geneticin® Selective Antibiotic (G418 Sulfate), Powder	Gibco™, Life Technologies, Carlsbad, CA, USA
	Blasticidin S HCl, powder	Gibco™, Life Technologies, Carlsbad, CA, USA
	Zeocin™ Selection Reagent	Gibco™, Life Technologies, Carlsbad, CA, USA
	Tetracycline	Invitrogen™, Life Technologies, Carlsbad, CA, USA
Inhibitors	Cycloheximide	Sigma-Aldrich, St. Louis, MO, USA
	Lactacystin, Synthetic	Calbiochem, Merck Millipore, Billerica, MA, USA
Cytostatic compounds	ABT-737 (M1002)	MediMol, Centereach, NY, USA
	Doxorubicine	Sigma-Aldrich, St. Louis, MO, USA

Table 14 *Reagents for bacterial cultures*

Description	Item	Manufacturer
Bacterial culture	LB Agar (Luria/Miller)	Carl Roth, Karlsruhe, Germany
	Peptone ex casein	Carl Roth, Karlsruhe, Germany
	Yeast Extract	Carl Roth, Karlsruhe, Germany
Bacterial selection antibiotics	Ampicillin sodium salt	Sigma-Aldrich, St. Louis, MO, USA
	Kanamycin sulfate from Streptomyces kanamyceticus	Sigma-Aldrich, St. Louis, MO, USA

Table 15 *Reagents for agarose gel electrophoresis*

Description	Item	Manufacturer
Agarose electrophoresis	Agarose NEEO ultra-quality	Carl Roth, Karlsruhe, Germany
	Ethidium bromide solution 1%	Carl Roth, Karlsruhe, Germany
	DNA Gel Loading Dye (6X)	Thermo Scientific™, Life Technologies, Carlsbad, CA, USA
	100 bp DNA Ladder	Invitrogen™, Life Technologies, Carlsbad, CA, USA
	1 Kb Plus DNA Ladder	Invitrogen™, Life Technologies, Carlsbad, CA, USA
	Ethyl alcohol, Pure, 200 proof, for molecular biology	Sigma-Aldrich, St. Louis, MO, USA

Table 16 *Reagents for vector subcloning*

Description	Item	Manufacturer
Vector subcloning	AmpliTaq Gold Fast PCR Master Mix	Applied Biosystems™, Life Technologies, Carlsbad, CA, USA
	Restriction enzymes	Thermo Fisher Scientific, Waltham, MA, USA
	QIAquick Gel Extraction Kit	Qiagen, Venlo, Netherlands
	Rapid DNA Ligation Kit	Roche, Basel, Switzerland
	One Shot TOP10 Chemically Competent E. coli	Invitrogen™, Life Technologies, Carlsbad, CA, USA
Vector subcloning	peqGOLD Plasmid Miniprep Kit I	Peqlab, VWR International, Radnor, PA, USA
	Sequencing	Eurofins, MWG-Biotech, Ebersberg, Germany

Table 17 *DNA vectors*

Description	Item	Manufacturer
DNA vectors	T-REx™ System	Invitrogen™, Life Technologies, Carlsbad, CA, USA
	pEGFP-C3	Clontech Laboratories, Mountain View, CA, USA
	pcDNA3 - modified construct with string containing N-terminal *Strep*-tags kindly provided by Prof. Bassermann and colleagues (Klinikum rechts der Isar, TU Munich, Germany)	Invitrogen™, Life Technologies, Carlsbad, CA, USA

Vector cards

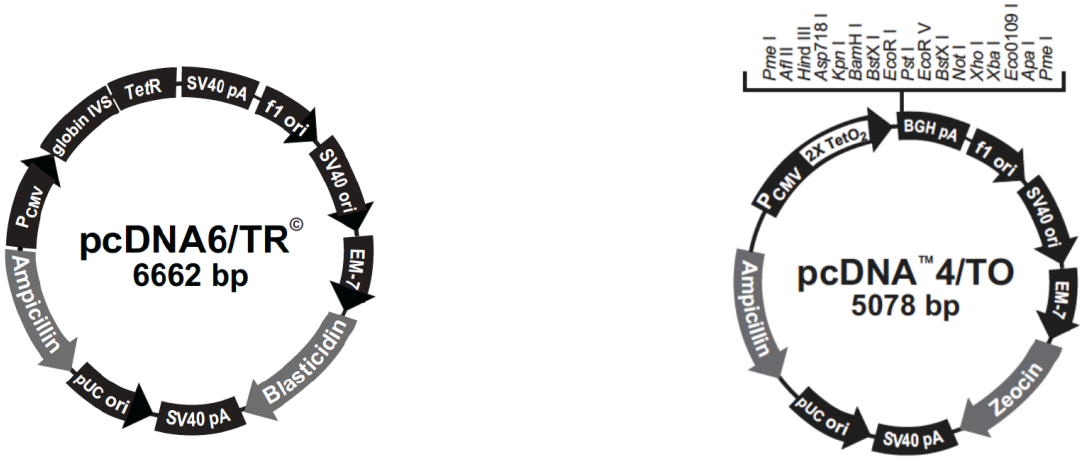

Figure 7 Vector cards of the T-REx™ System

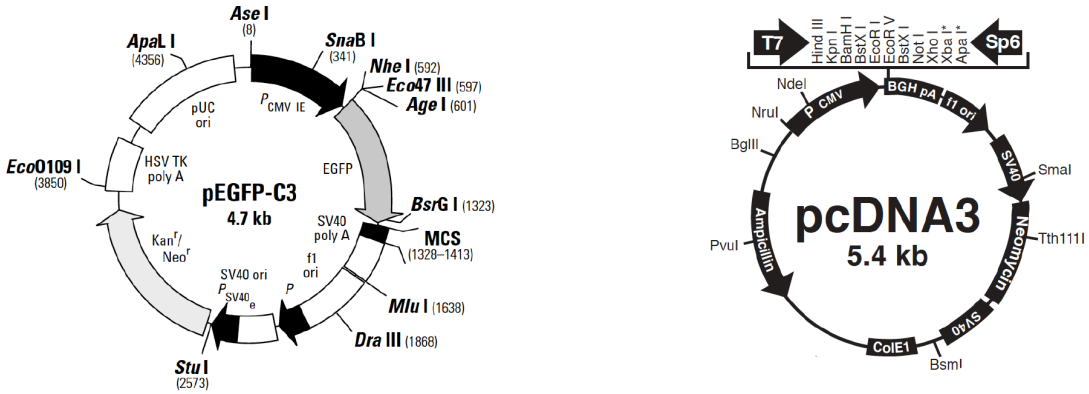

Figure 8 Vector cards of the pEGFP-C3 and pcDNA3

pcDNA3 vector constructs containing N-terminal Strep-tags were kindly provided by Prof. Dr. Florian Bassermann (Klinikum rechts der Isar, TU Munich, Germany).

Table 18 *Primer sequences for vector subcloning*

Final construct	Name	Sequence 3'-5'
GFP-ZAP70 fusion constructs	GFP3_ZAP70 F	GTCAGAATTCTGATGCCAGACC CCGCG
	C3_GFP_Ztrunc1 F	GTCAGAATTCTGATGAACCGGC CGTC
	C3_GFP_Ztrunc2 F	GTCAGAATTCTGATGCCCAACA GCAG
	C3_GFP_Ztrunc3 F	GTCAGAATTCTGATGCTCATAG CTGA
	GFP3_ZAP70 R	GTCAGGATCCTCAGGCACAGGC AGC
	C3_GFP_Z(NLS) R	GTCAGGATCCTCAATAGCTCCA GAC
Strep-tags ZAP70 fusion constructs	NheI ZAP70 F 2	ATATGCTAGCCCAGACCCCGCG GC
	XhoI pcDNA3 R 2	ATATCTCGAGCACTGTGCTGGA TATCTGCA
	XhoI ZAP70 R	ATATCTCGAGTCAGGCACAGGC AGCCTCAG

Table 19 *Reagents for gene expression analysis*

Description	Name	Manufacturer
RNA extraction	2-Mercaptoethanol	Sigma-Aldrich, St. Louis, MO, USA
	RNAprotect Cell Reagent	Qiagen, Venlo, Netherlands
	QIAshredder	Qiagen, Venlo, Netherlands
	RNeasy Mini Kit	Qiagen, Venlo, Netherlands
	RNase-Free DNase Set	Qiagen, Venlo, Netherlands
	Nuclease-Free Water	Qiagen, Venlo, Netherlands
Reverse transcription	Transcriptor High Fidelity cDNA Synthesis Kit	Roche, Basel, Switzerland
Quantitative PCR	Platinum® SYBR® Green qPCR SuperMix-UDG with ROX	Invitrogen™, Life Technologies, Carlsbad, CA, USA

Table 20 *Primer sequences for quantitative Real-Time PCR*

Gene	Sense primer 3'-5'	Antisense primer 3'-5'
ZAP70	TATGGGAAGACGGTGTACCA	AGAGCGTGTCAAACTTGGTG
Mcl-1	TTGCACCCTAGCAACCTAGC	CAATCAATGGGGAGCACTCT
GSK3β	GAGACAAGGACGGCAGC	AGCTGACTTCTTGTGGCCTG
hMOF	GGAGAAGCCACTGTCTGACC	AGGATCTCTAGCAGCACCCA
SIRT1	TCCAGCCATCTCTCTGTCAC	CAGCGTGTCTATGTTCTGGGT
PrSet7	TGGAATGCGTTTCCCCCTTC	TGGTTTCCCCTGGCATTTGA
Suv4-20H1	TGGTAACTCGGGATTTGAAGGA	TTCACAGAGTTCCTTGGCGG
Suv4-20H2	ACTTTCCTGAGGCAGCGG	GGCTCTGGAAGTAGCGGG
GAPDH	GTGAAGGTCGGAGTCAACG	TGAGGTCAATGAAGGGGTC

Table 21 *Reagents for flow cytometry analysis*

Assay	Item	Manufacturer
BSA	Albumin Fraction V	Carl Roth, Karlsruhe, Germany
AnnexinV / PI apoptosis assay	FITC AnnexinV	BioLegend, San Diego, CA, USA
	APC AnnexinV	BD Pharmingen™, BD Biosciences, Franklin Lakes, NJ, USA
	Propidium iodide (PI)	Sigma-Aldrich, St. Louis, MO, USA
Intracellular antigen staining	Fix & Perm® Cell Fixation & Permeabilization Kit	Invitrogen™, Life Technologies, Carlsbad, CA, USA
BrdU proliferation assay	FITC BrdU Flow Kit	BD Pharmingen™, BD Biosciences, Franklin Lakes, NJ, USA

Fluorochromes:

FITC	Fluorescein-isothiocyanate
PE	R-Phycoerythrin
PC5	R Phycoerathrincyanin 5.1
APC	Allophyocyanin

Table 22 *Antibodies for flow cytometry analysis of human samples*

Antigen	Fluorochrome	Clone	Isotype	Manufacturer
CD2	PE	S5.2	Mouse IgG_{2a}	BD Biosciences, Franklin Lakes, NJ, USA
CD5	FITC	L17F12	Mouse IgG_{2a}	BD Biosciences, Franklin Lakes, NJ, USA
CD14	FITC	M5E2	Mouse IgG_{2a}	BD Pharmingen™, BD Biosciences, Franklin Lakes, NJ, USA
Antigen	Fluorochrome	Clone	Isotype	Manufacturer
CD19	PC5	J3-119	Mouse IgG_1	Beckman Coulter, Brea, CA, USA
CD20	PE-Cy7	2H7	Mouse IgG_{2b}	BD Biosciences, Franklin Lakes, NJ, USA
CD38	PC5	LS198-4-3	Mouse IgG_1	Beckman Coulter, Brea, CA, USA
ZAP70	R-PE	1E7.2	Mouse IgG_1	Invitrogen™, Life Technologies, Carlsbad, CA, USA

Table 23 *Isotype control antibodies for flow cytometry analysis*

Isotype	Fluorochrome	Manufacturer
Mouse IgG_1	PE	Beckman Coulter, Brea, CA, USA
Mouse IgG_1	R-PE	Invitrogen™, Life Technologies, Carlsbad, CA, USA
Mouse IgG_1	PC5	Beckman Coulter, Brea, CA, USA
Mouse IgG_{2a}	FITC	Beckman Coulter, Brea, CA, USA
Mouse IgG_{2a}	PE	Immunotech, Vaudreuil-Dorion, Canada
Mouse IgG_{2b}	PE-Cy7	BD Pharmingen™, BD Biosciences, Franklin Lakes, NJ, USA

Table 24 *Reagents for lysis buffers*

Description	Name	Manufacturer
Protease inhibitors	cOmplete™, Mini	Roche, Basel, Switzerland
	cOmplete™, EDTA-free	Roche, Basel, Switzerland

Table 25 *Reagents for immunoblotting*

Description	Name	Manufacturer
Protein concentration measurement	DC™ Protein Assay	Bio-Rad Laboratories, Berkeley, CA, USA
SDS-PAGE	Rotiphorese® Gel 30 (37,5:1)	Carl Roth, Karlsruhe, Germany
SDS-PAGE Immunoblotting	N,N,N',N′-Tetramethylethylenediamine	Sigma-Aldrich, St. Louis, MO, USA
	Bromophenol Blue solution	Fluka, Sigma-Aldrich, St. Louis, MO, USA
	Skim Milk Powder	Fluka, Sigma-Aldrich, St. Louis, MO, USA
Immunoblotting	Phosphate buffered saline (PBS)	Sigma-Aldrich, St. Louis, MO, USA
	TWEEN® 20	Sigma-Aldrich, St. Louis, MO, USA
	Amersham ECL Rabbit IgG, HRP-linked whole Ab (from donkey)	GE Healthcare Life Sciences, München, Germany
	Amersham ECL Mouse IgG, HRP-linked whole Ab (from donkey)	GE Healthcare Life Sciences, München, Germany
	SuperSignal™ West Pico Chemiluminescent Substrate	Thermo Fisher Scientific, Waltham, MA, USA
	SuperSignal™ West Dura Extended Duration Substrate	Thermo Fisher Scientific, Waltham, MA, USA
	SuperSignal™ West Femto Maximum Sensitivity Substrate	Thermo Fisher Scientific, Waltham, MA, USA
	CL-XPosure™ Film 18 x 24 cm	Thermo Fisher Scientific, Waltham, MA, USA

Table 26 *Polyclonal antibodies for immunoblotting of human samples*

Antigen	Host	Dilution	Manufacturer
Fbw7	Rabbit	1:2000	Bethyl Laboratories, Montgomery, TX, USA
Acetyl-Histone H4 (Lys16)	Rabbit	1:1000	Cell Signaling Technology, Cambridge, UK
HUWE-1 (MULE)	Rabbit	1:2000	LSBio, Seattle, WA, USA
Mcl-1	Mouse	1:2000	Santa Cruz Biotechnology, Dallas, TX, USA
Usp9x	Rabbit	1:2000	Bethyl Laboratories, Montgomery, TX, USA

Table 27 *Monoclonal antibodies for immunoblotting of human samples*

Antigen	Clone	Isotype	Dilution	Manufacturer
Bcl-2	7/Bcl-2	Mouse IgG_1	1:2000	BD Transduction Laboratories™, BD Biosciences, Franklin Lakes, NJ, USA
Bcl-X_L	54H6	Rabbit IgG	1:2000	Cell Signaling Technology, Cambridge, UK
β actin	AC-15	Mouse IgG_1	1:8000	Thermo Fisher Scientific, Waltham, MA, USA
GSK3β	27C10	Rabbit IgG	1:2000	Cell Signaling Technology, Cambridge, UK
Histone H3	96C10	Mouse IgG_1	1:1000	Cell Signaling Technology, Cambridge, UK
Histone H4	L64C1	Mouse IgG	1:500	Cell Signaling Technology, Cambridge, UK
Tri-Methyl-Histone H4 (Lys20)	D84D2	Rabbit IgG	1:4000	Cell Signaling Technology, Cambridge, UK
ZAP70	29/ZAP70 Kinase	Mouse IgG_{2a}	1:2000	BD Transduction Laboratories™, BD Biosciences, Franklin

Table 28 *Reagents for Strep-affinity purification*

Description	Name	Manufacturer
Protease inhibitor	cOmplete™ Protease Inhibitor Cocktail Tablets	Roche, Basel, Switzerland
Phosphatase inhibitor	Phosphatase Inhibitor Cocktail 2	Sigma-Aldrich, St. Louis, MO, USA
	Phosphatase Inhibitor Cocktail 3	Sigma-Aldrich, St. Louis, MO, USA
Reaction columns	MicroSpin Columns	GE Healthcare Life Sciences, München, Germany
Strep-Tactin resin	Strep-Tactin® Sepharose® 50% suspension	IBA Lifesciences, Göttingen, Germany
Elution buffer	D-Desthiobiotin 10x Buffer E	IBA Lifesciences, Göttingen, Germany

Table 29 *Reagents for chromatin fractionation and native chromatin immunoprecipitation (ChIP)*

Description	Name	Manufacturer
Benzonase	Benzonase® Nuclease	Sigma-Aldrich, St. Louis, MO, USA
ChIP	TRIzol® Reagent	Ambion™, Life Technologies, Carlsbad, CA, USA
	Chloroform:Isoamyl alcohol 24:1	Sigma-Aldrich, St. Louis, MO, USA
	Nuclease micrococcal from Staphylococcus aureus	Sigma-Aldrich, St. Louis, MO, USA
	MaXtract High Density	Qiagen, Venlo, Netherlands
	UltraPure™ Glycogen	Invitrogen™, Life Technologies, Carlsbad, CA, USA
	Low Binding Tubes	Biozym Scientific, Hessisch Oldendorf, Germany
DNA quantification with high sensitivity	Qubit dsDNA HS Assay Kit	Life Technologies, Carlsbad, CA, USA

Table 30 *Reagents for immunofluorescence staining for confocal imaging*

Item	Manufacturer
Lipofectamine®	Invitrogen™, Life Technologies, Carlsbad, CA, USA
SlowFade® Gold Antifade Mountant with DAPI	Molecular Probes™, Life Technologies, Carlsbad, CA, USA
Hoechst 33342, Trihydrochloride, Trihydrate	Molecular Probes™, Life Technologies, Carlsbad, CA, USA
Alexa Fluor® 647 Phalloidin	Molecular Probes™, Life Technologies, Carlsbad, CA, USA

Table 31 *Reagents for radioactive kinase assay*

Description	Item	Manufacturer
Nonradioactive ATP	ATP Solution (100 mM)	Thermo Fisher Scientific, Waltham, MA, USA
Radioactive ATP (hot ATP)	[gamma-P32]Adenosine 5'-triphosphate (hot ATP)	Hartmann Analytic, Braunschweig, Germany
Positive control substrate	Purified bovine brain Tubulin	Alpha Diagnostics Intl, San Antonio, TX, USA
Active ZAP70 kinase	Recombinant Human Active ZAP70	R&D Systems, Minneapolis, MN, USA

2.1.4 Buffers and media

2.1.4.1 Cell culture

CLL medium

10%	fetal calf serum
50 IU/ml	penicillin/streptomycin
1mM	sodium pyruvate
2mM	L-glutamine
0.05mM	2-mercaptoethanol
10mM	HEPES
0.7X	non-essential amino-acids
1X	RPMI 1640 medium

2.1.4.2 Vector Subcloning

TAE Buffer

40 mM	Tris
0.1%	Acetic acid
1 mM	EDTA pH 8.0

LB medium

1%	Peptone ex casein
0.5%	Yeast extract
1%	NaCl
autoclaved	

LB agar

1%	Peptone ex casein
0.5%	Yeast extract
1%	NaCl
1.5%	LB agar
autoclaved	

2.1.4.3 Flow cytometry

FACS Buffer

0.5%	BSA
1 X	PBS

AnnexinV Binding Buffer

10 mM	HEPES pH 7.4
140 mM	NaCl
160 mM	$CaCl_2$

2.1.4.4 Proteomics

Immunoblotting

Regular Lysis Buffer

10 mM	Tris/HCl pH 7.5
130 mM	NaCl
5 mM	EDTA pH 8.0
1%	Triton X-100
20 mM	Sodium phosphate pH 7.0
10 mM	Sodium pyrophosphate pH 7.0-7.5
50 mM	Sodium fluoride (NaF)
0.05 mM	Benzamidine
1mM	PMSF
1 mM	Sodium orthovanadate
1X	cOmplete™, Mini protease inhibitor

Stacking Gel Buffer

0.5 M	Tris-HCl pH = 6.8
0.4%	SDS

Separating Gel Buffer

1.5 M	Tris-HCl pH = 8.8
0.4%	SDS

2X Loading Buffer

100 mM	Tris-HCl pH= 6.8
0.05%	Bromophenol blue
20%	glycerol
200 mM	DTT
4%	SDS

SDS-PAGE Running Buffer

25 mM	TRIS
200 mM	Glycine
0.1%	SDS

Transfer Buffer

25 mM	TRIS
200 mM	Glycine
0.1%	SDS
20%	Methanol

PBS-T

0.1%	Tween-20
1X	PBS

PBS-T/milk

5 %	non-fat dried milk powder
1X	PBS-T

PBS-T/milk + azid

0.02%	Sodium azide
1X	PBS-T/milk

Subcellular nuclear fractionation

Nuclear extraction buffer A

10 mM	HEPES pH 7.9
10 mM	KCl
300 mM	Sucrose
1.5 mM	MgCl2
0.5 mM	DTT
0.1%	NP-40
0.5 mM	PMSF
1X	cOmplete™, Mini protease inhibitor

Nuclear extraction buffer B

20mM	HEPES pH 7.9
100 mM	KCl
100 mM	NaCl
0.5 mM	DTT
20%	Glycerol
0.5 mM	PMSF
1X	cOmplete™, Mini protease inhibitor

2.1.4.6 Protein visualization on SDS-PAGE

Silver Staining

Silver Staining Fixation Buffer

50%	Methanol
12%	Acetic acid
0.037%	Formaldehyde

Silver Staining Wash Buffer

50%	Ethanol

Silver Staining Sensitizing Solution

1.3 mM	Sodium thiosulfate

Silver Staining Staining Solution

11.8 mM	Silver nitrate
0.028%	Formaldehyde

Silver Staining Developing Solution

566 mM	Sodium carbonate
32.5 µM	Sodium thiosulfate
0.0185%	Formaldehyde

Silver Staining Stopping Buffer

50%	Methanol
12%	Acetic acid

Coomassie Staining

Coomassie Staining Solution

50%	Methanol
10%	Acetic acid
0,1%	Brilliant Blue

Coomassie Destain Solution

30%	Methanol
10%	Acetic Acid

2.1.4.7 Chromatin Immunoprecipitation (ChIP)

EX-100 (10 mL)

10 mM	HEPES pH 7.6
100 mM	NaCl
1.5 mM	MgCl2
0.5 mM	EGTA
10 %	Glycerol
10 mM	β-Glycerol phosphate
1 mM	DTT
1X	cOmplete™, Mini protease inhibitor

ChIP Wash Buffer 1

10 mM	Tris pH 7.5
150 mM	NaCl
0.1%	NP-40
1 mM	DTT
1X	cOmplete™, Mini protease inhibitor

ChIP Wash Buffer 2

10 mM	Tris-HCl pH 7.5
150 mM	NaCl
1 mM	DTT
1X	cOmplete™, Mini protease inhibitor

TE buffer

10 mM	Tris-HCl pH 7.5
1 mM	EDTA

Chromatin Fractionation Buffer A

10 mM	HEPES pH = 7.9
10 mM	KCl
1.5 mM	MgCl2
0.34 M	Sucrose
10%	Glycerol
1 mM	DTT
1X	cOmplete™, EDTA-free protease inhibitor

Chromatin Fractionation No Salt Buffer

3 mM	EDTA
0.2 mM	EGTA
1X	cOmplete™, EDTA-free protease inhibitor

2.1.4.8 Strep-affinity purification

10X TBS for Strep-Affinity Purification

300 mM	Tris-HCl pH 7.4
1.5 M	NaCl

Strep-Affinity Purification Lysis Buffer

1%	NP-40
1%	Phosphatase Inhibitor Cocktail 2
1%	Phosphatase Inhibitor Cocktail 3
1X	cOmplete™ Protease Inhibitor Cocktail
1X	TBS pH 7.4

Strep-Affinity Purification Wash Buffer

0.25%	NP-40
1%	Phosphatase Inhibitor Cocktail 2
1%	Phosphatase Inhibitor Cocktail 3
1X	TBS pH 7.4

2.1.4.9 Histone extraction

Hypotonic Lysis Buffer

10 mM	Tris-HCl pH 8.0
1 mM	KCl
1.5 mM	MgCl2
0.4 mM	PMSF
1 mM	orthovanadate
1 mM	DTT
1X	cOmplete™, EDTA-free protease inhibitor

2.1.4.10 Confocal imaging

Immunofluorescence Staining Buffer

0,2%	TritonX-100
1%	BSA
1X	PBS

2.1.4.11 Radioactive ZAP70 kinase assay

Kinase Assay Buffer

25 mM	MOPS pH 7.2
12.5 mM	β-Glycerophosphate
25 mM	MgCl2
5 mM	EGTA
2 mM	EDTA
0.25 mM	DTT
50 µM	nonradioactive ATP
5 µCi	hot ATP

2.2 Methods

2.2.1 Vector Subcloning

Subcloning of the *ZAP70* gene onto different vector backbones was performed using specific restriction enzymes from Thermo Fisher Scientific's Fermentas. If necessary, a polymerase chain reaction (PCR) using AmpliTaq Gold Fast PCR Master Mix according to manufacturer's instructions was performed to amplify *ZAP70* with specific primers containing the appropriate restriction sites and possibly spacer nucleotides for in-frame subcloning. DNA fragments were separated using agarose gel electrophoresis performed in a Tris-acetate-EDTA (TAE) buffer system and extracted from the gel using QIAquick Gel Extraction Kit according to manufacturer's instructions. The inserts were then ligated with the vector backbone using Rapid DNA Ligation Kit over-night at 16°C according to manufacturer's instructions. One Shot TOP10 Chemically Competent *E. coli* were transformed with 5 µl of the ligation mixtures for 30 seconds at 42°C according to manufacturer's instructions and selected on lysogeny broth (LB) agar containing the appropriate antibiotics. Colonies were picked and grown in LB medium at 37°C shaking at 225 rpm over-night. DNA vectors were purified from bacterial culture using the peqGold Plasmid Miniprep Kit I according to manufacturer's instructions and subsequently analyzed by control restriction digest with Fermentas enzymes. Plasmid DNA from bacterial clones showing the right DNA band pattern was sent to MWG Eurofins for sequencing using specific DNA oligomers according to manufacturer's suggestions to check the correct insertion of the gene of interest.

2.2.2 Cell Culture

Culture conditions

CLL cell lines and primary CLL cells were cultured in RPMI 1640 medium supplemented with 10% fetal calf serum, 50 IU/ml penicillin/streptomycin, 1 mM Na-pyruvate, 2 mM L-glutamine, 0.05 mM 2-mercaptoethanol, 10 mM HEPES and 0.7X non-essential amino acids at 37°C and 5% CO_2 in a fully humidified atmosphere.

Primary human CLL cells

After informed patients' consent and in accordance with the Helsinki declaration, peripheral blood was obtained from patients with a diagnosis of CLL. Whole blood samples were obtained from patients seen at the Klinikum rechts der Isar, Munich, Germany. ZAP70 status information was obtained from the routine diagnostic laboratories of the IIIrd Medical Department of the Klinikum rechts der Isar, Munich, Germany. PBMCs were isolated from heparinized whole blood by centrifugation over a Ficoll-Hypaque layer of 1.077 g/ml density. T cells and monocytes were removed using anti-CD2 and anti-CD14 magnetic beads. CLLs were >98% pure as assessed by flow cytometry.

Creation of stable cell lines

The sensitivity to antibiotics was assessed for each cell line and each antibiotic separately. Cells were incubated with different antibiotic concentrations and apoptosis was assessed after three days by AnnexinV/PI flow cytometry staining (see below). The lowest concentration lethal for the cell line was determined as the selective antibiotic concentration.

DNA purity of vector constructs was assessed by UV absorption measurement at 260 and 280 nm. Only vector DNA with a 260/280 ratio of more than 1.8 was used for transfection. 2 million MEC-1 cells were nucleofected using the Amaxa Nucleofector Technology with 2 µg of plasmid using the Amaxa Human B Cell Nucleofector® Kit V and the Amaxa program X-001 according to manufacturer's instructions. Batch cultures were incubated for two weeks at 37°C and 5% CO_2 in a humidified incubator and selective medium containing the appropriate antibiotic concentration was changed every three days. The batch culture was diluted to a single cell solution, which was spread onto several 96-well plates and again incubated for two to three weeks until clones started to grow. Clones were picked by eye and expanded to then be analyzed by PCR, immunoblotting or flow cytometry for expression of the gene of interest.

Establishment of MEC-1 tetracycline-regulated inducible ZAP70 expression system

To create an inducible ZAP70 expression system, Life Technologies' T-REx™ system was used according to manufacturer's instructions. The *ZAP70* gene was cloned into the pcDNA4/TO vector backbone (see above). MEC-1 cells were transfected by Amaxa nucleofection according to manufacturer's instructions with pcDNA6/TR vector containing the tet repressor gene (see *Figure 7*). Clones were selected by single cell dilution using 5 µg/ml blasticidin. A positive clone containing the pcDNA6/TR vector was subsequently transfected with the pcDNA4TO_ZAP70 construct (MEC-$1^{ZAP70\text{-}tet\text{-}ON}$) or the unmodified pcDNA4/TO mock control vector (MEC-1^{mock}) as described above. Following single cell dilution under double selection with 5 µg/ml blasticidin and 200 µg/ml zeocin clones were selected by flow cytometry analysis of ZAP70 expression after treatment with 500 ng/ml tetracycline for 24 hours.

Induction of apoptosis using chemotherapeutics

ZAP70 expression was switched on in the inducible MEC-$1^{ZAP70\text{-}tet\text{-}ON}$ cell line and the MEC-1^{mock} control by adding 500 ng/ml tetracycline for 72 hours prior to treatment with 10 to 30 µg/ml doxorubicin or 1 nM to 10 nM ABT-737. After 48 hours of treatment, cells were objected to AnnexinV/PI apoptosis assay.

Half-life analysis of Mcl-1

Half-life of the Mcl-1 protein was analyzed by the addition of 50 µg/ml cycloheximid to the culture and incubating the cells using time kinetics of 15 to 120 minutes. In some cases, the proteasome was inhibited in its activity beforehand for 30 minutes with 2.5 µg/ml lactacystin. Cell pellets were harvested at certain time points, washed once with PBS and snap-frozen using liquid nitrogen for further processing for immunoblot analyses.

2.2.3 Flow Cytometry

Staining of surface antigens

Cells were stained in 500 µl of FACS buffer containing specific antibodies or matching isotype control antibodies for 10 minutes at 4°C. Cells were washed

once with FACS buffer prior to flow cytometry analysis using a Beckman Coulter CyAn ADP Analyzer.

ZAP70 expression analysis by flow cytometry

ZAP70 expression was quantified in MEC-1$^{ZAP70\text{-}tet\text{-}ON}$ cells and purified CLL cells. To this end, leukemic cells were fixed and permeabilized using Fix & Perm Cell Fixation & Permeabilization Kit according to manufacturer's instructions. Cells were incubated with R-PE-conjugated monoclonal antibody (mAb) against ZAP70 (clone 1E7.2) or an irrelevant isotype control Ab for 30 min, then washed with FACS buffer and analyzed by flow cytometry using a Beckman Coulter CyAn ADP Analyzer.

Apoptosis assay using AnnexinV/PI staining

The AnnexinV/PI assay was used to determine the phosphatidylserine exposure on the outer plasma membrane during apoptosis. Cells to be examined for apoptosis were washed with phosphate-buffered saline and resuspended with 500 µl AnnexinV Binding Buffer containing 2 µl of the AnnexinV-fluorescein isothiocyanate stock and 5 µl of a 20 mg/ml propidium iodide (PI) solution. After incubation for 10 min at 4°C in a light protected area, the specimens were quantified by flow cytometry using a Beckman Coulter CyAn ADP Analyzer.

Proliferation assay

ZAP70 expression was switched on in MEC-1$^{ZAP70\text{-}tet\text{-}ON}$ and in its mock control by adding 500 ng/ml tetracycline for 48 hours. Bromodeoxyuridine (BrdU) was added at a concentration of 10 µM for 3 and 6 hours to either untreated or treated cells. Uptake of BrdU was quantified using flow cytometry using the FITC BrdU Flow Kit according to manufacturer's instructions.

2.2.4 Proteomics

Regular cell lysis for immunoblotting

Cell pellets were washed once with 1X PBS and lysed on ice in regular lysis buffer for 15 minutes with repeated vortexing. Depending on the goal of the experiment, the solution was sonicated for 20 seconds to include nuclear proteins.

The debris was centrifuged for 20 minutes at 14,000 rpm and 4°C. Protein concentration of the cell lysates was determined using a DC Protein Assay according to manufacturer's instructions. Cell lysates were diluted in deionized water (H_2O) and a new standard curve was assessed each time. The absorption was measured at 750 nm with an ELx800 Absorbance Reader.

Immunoprecipitation (IP)

All steps were conducted on a rotating table at 4°C. To pre-clear the lysate, 2 µg of rabbit-anti-mouse antibody were added to 300 µg of protein and the mixture was incubated rotating for 20 minutes. 30 µl of pre-washed Protein A sepharose beads were added to each sample and incubated for 20 minutes. Beads were discarded after centrifugation for 2 minutes at 1,400 rpm. This step was repeated once. 2 µg of specific antibody or 2 µg of appropriate isotype control antibody respectively were added to the supernatant and the mixture was incubated over-night on the rotating table. 3 µg rabbit-anti-mouse antibody were added and incubated for 20 minutes, if the primary antibody was characterized by a mouse isotype. 25 µl pre-washed Protein A sepharose beads were added to each sample and incubated for 1 hour. After centrifugation for 2 minutes at 1,400 rpm and 4°C, supernatant was discarded and beads were washed four times by adding 500 µl regular lysis buffer and incubating for 2 minutes. 25 µl of loading buffer were added to the beads and heated for 10 minutes at 96°C. After one last centrifugation step for 2 minutes at 1,400 rpm and 4°C, total sample was loaded onto appropriate sodium dodecyl sulfate polyacrylamide gel electrophoresis (SDS-PAGE) for immunoblotting.

Nuclear Fractionation

Cell pellets were washed once with PBS and lysed on ice for 5 minutes in Nuclear Fractionation Buffer A. The nuclear pellet was centrifuged for 5 seconds at 13,200 rpm. The supernatant was kept as cytosolic fraction. Subsequently, the nuclear pellet was washed once in Nuclear Fractionation Buffer A and centrifuged for 5 seconds at 13,200 rpm. The nuclear pellet was resuspended in Nuclear Fractionation Buffer B and sonicated for 30 sec. The debris was centrifuged for 5 seconds at 13,200 rpm and the supernatant contained the nuclear fraction of the assay. Protein concentration of the different fractions was determined using a DC

Protein Assay according to manufacturer's instructions. Cell lysates were diluted in H_2O and a new standard curve was assessed each time. The absorption was measured at 795 nm with an ELx800 Absorbance Reader.

Chromatin Fractionation

Cell pellets were washed once with PBS and lysed on ice for 10 minutes in Chromatin Fractionation Buffer A + 0.1% nonyl phenoxypolyethoxylethanol (NP-40) and occasional vortexing. The nuclear pellet was centrifuged for 5 minutes at 4°C and 3,200 g. Then, the nuclear pellet was washed once in Chromatin Fractionation Buffer A and centrifuged centrifuged for 5 minutes at 4°C and 3,200 g. Subsequently, the nuclear pellet was resuspended in No-Salt Buffer, incubated on ice for 30 minutes with occasional vortexing, and then centrifuged for 5 minutes at 4°C and 3,200 g. The remaining chromatin pellet was washed twice with Chromatin Fractionation Buffer A, and, again, centrifuged for 5 minutes at 4°C and 3,200 g. All supernatants were combined to represent the non-chromatin fraction. The chromatin pellet was solubilized by adding 200 µl 1X SDS loading buffer, homogenizing it with a 27 G x ¾ " needle and incubating it shaking for 10 minutes at 95°C. 500 U of benzonase were added and incubated for 2 hours at room temperature (RT). Then the mixture was cooked again shaking for 10 minutes at 95°C. Protein concentration of the different fractions was determined using a DC Protein Assay according to manufacturer's instructions. Cell lysates were diluted in H_2O and a new standard curve was assessed each time. The absorption was measured at 795 nm with an ELx800 Absorbance Reader.

Histone extraction

Cell lysis was performed in hypotonic lysis buffer for 30 minutes at 4°C rotating. After centrifugation for 10 minutes at 10,000 rpm at 4°C, the cell pellet was resuspended in 400 µl of 0.2 M sulfuric acid (H_2SO_4) and incubated at 4°C rotating over-night. After centrifugation for 10 minutes at full-speed and 4°C, the supernatant was mixed with 132 µl of trichloric acid (TCA) to obtain a final concentration of 33% TCA. The mixture was incubated on ice for 30 minutes and then spun down for 10 minutes at full-speed and 4°C. The histone pellet was washed twice with ice-cold acetone, air dried and reconstituted in H_2O. Subsequently, the histone extract was mixed 1:1 with 2X SDS loading buffer and

10 µl were loaded onto a 15% SDS-PAGE. Proteins were visualized by silver stain and analyzed by ImageJ to calculate the ratios of the wanted histone signals and therefore balance the protein loading for immunoblotting (Rasband, 1997; Schneider et al., 2012).

Mononucleosome preparation

Cell pellets were washed once with PBS and lysed in PBS + 0.3 % Triton X-100 + EDTA-free complete protease inhibitors for 10 minutes at 4°C rotating. Nuclear pellet was centrifuged for 10 minutes at 3,000 rpm and 4°C. The pellet was washed once with PBS + EDTA-free complete protease inhibitors and centrifuged for 5 minutes at 3,000 rpm at 4°C. The nuclear pellet was resuspended in 500 µl EX-100 buffer. $CaCl_2$ concentration was adjusted to 2 mM. 5 SIGMA units of MNase were added and samples were incubated for 35 minutes at 26°C. The reaction was stopped by adjusting the EGTA concentration to 10 mM. The samples were centrifuged for 30 minutes at full-speed and 4°C to separate the early chromatin fraction from the chromatin which was not accessible for the MNase. The supernatant S1 contains only mononucleosomes. The completion of the MNase digest was checked by agarose gel electrophoresis.

Native chromatin immunoprecipitation (ChIP)

Native ChIP was performed with mononucleosmes from differentially modified MEC-1 cells. All steps were conducted on a rotating table at 4°C. To pre-clear the mononucleosome preparation, 2 µg of rabbit-anti-mouse antibody were added to 500 µl of early chromatin fraction and the mixture was incubated rotating for 20 minutes. 30 µl of pre-washed Protein A sepharose beads were added to each sample and incubated for 20 minutes. Beads were discarded after centrifugation for 2 minutes at 1,400 rpm. This step was repeated once. 2 µg specific antibody or 2 µg isotype control antibodies were added to the supernatant and the mixture was incubated over-night. 3 µg rabbit-anti-mouse antibodies were added to mixtures containing mouse anti-human antibodies and incubated for 20 minutes. 25 µl pre-washed Protein A sepharose beads were added to each sample and incubated for 1 hour. After centrifugation for 2 minutes at 1,400 rpm and 4°C, the supernatant was discarded and the beads were washed twice with 1 ml ChIP Wash Buffer 1 and twice with 1 ml ChIP Wash Buffer 2, incubating for 5 minutes rotating and

centrifuging beads at 1,400 rpm and 4°C. With the last washing step, the samples were split in half, one part being objected to immunoblot analysis and the other to DNA precipitation.

For immunoblotting, 12.5 µl of 2X SDS loading buffer were added to the beads and heated for 10 minutes at 96°C. After one last centrifugation step for 2 minutes at 1,400 rpm and 4°C, same volumes of the samples were loaded onto the appropriate SDS-PAGE. For DNA precipitation, the beads were centrifuged for 2 minutes at 1,400 rpm and 4°C and then resuspended in 100 µl Tris-EDTA buffer (TE). 0.3% SDS and 100 µg proteinase K was added and the mixture was incubated for 1 hour at 65°C. The beads were centrifuged for 2 minutes at 1,400 rpm and 4°C, washed once with TE + 0.5 M NaCl and centrifuged again. The supernatants were combined and objected to subsequent phenol/chloroform DNA precipitation.

Phenol/chloroform DNA precipitation

200 µl of phenol were mixed with 200 µl of DNA solution. Then, 200 µl of chloroform:isoamylalcohol (24:1) were added and vortexed. The mixture was transferred to prepared maXtract tubes and centrifuged for 1 minute at 11,000 rpm to separate the organic solvent and the nucleic acid-containing aqueous phase. The upper aqueous phase was transferred to a new tube, 40 µg of glycogen was added, and the sodium acetate concentration was adjusted to 0.3 M. 500 µl of 100% ethanol was added, mixture was vortexed vigorously, and then incubated at -20°C for at least 20 minutes. DNA was centrifuged at full-speed and 4°C for 20 minutes, washed once with ice-cold 70% ethanol and centrifuged again at full-speed and 4°C for 5 minutes. Supernatant was carefully removed and pellet was allowed to dry from remaining ethanol. The DNA pellet was then reconstituted with H_2O and DNA concentration was determined with UV absorption measurement at the NanoDrop.

Methanol/chloroform protein precipitation

800 µl of 100% methanol were mixed with 200 µl of protein solution, vortexed and centrifuged at 9,000 g for 30 seconds at RT. 200 µl of chloroform were added, vortexed and centrifuged at 9,000 g for 30 seconds at RT. Then, 600 µl H_2O were added, vortexed and the mixture was centrifuged at 9,000 g for 2 minutes at RT.

Supernatant was removed just until 2 mm above the interphase, which contains the proteins. 600 µl 100% methanol were added, vortexed and the mixture was centrifuged at 15,000 g for 2 minutes at RT. Supernatant was carefully removed and the white protein precipitate was allowed to dry from remaining methanol. The precipitate was reconstituted in 1X SDS loading buffer, cooked at 95°C for 5 minutes and objected to SDS-PAGE.

Sodium dodecyl sulfate polyacrylamide gel electrophoresis (SDS-PAGE)

The separating gel was prepared on a Tris/Glycine-buffered basis at different acrylamide percentages according to the molecular weight of the protein of interest. The gel solution was covered with 1 ml of 100% isopropanol and incubated for 35 minutes at RT to polymerize. The isopropanol was removed and polymerization of the stacking gel was started by the addition of APS. Again, the stacking gel was incubated for 25 minutes at RT to complete polymerization. Dependent on gel size 7-10 µg or 30-50 µg protein of each sample were subjected to SDS-PAGE and gel electrophoresis was started at 60 V until samples slowly moved into the gel and subsequent 150 V to complete the run.

Coomassie staining

Coomassie staining was performed to visualize protein bands separated by polyacrylamide gel electrophoresis, e.g. for assessment of protein integrity for recombinant histone molecules or to visualize proteins in SDS-PAGEs of kinase assays to identify the correct bands on the autoradiography film. The gel was stained with Coomassie staining solution for 2 hours at RT, shaking and subsequently destained using Coomassie destain solution at 4°C over-night.

Silver staining

Silver staining of SDS-PAGEs is another method I performed to visualize protein bands, especially to verify the efficiency of Strep-affinity purifications. In addition, I detected histone molecules from histone extractions as those very positively charged proteins cannot be easily determined by conventional protein detection assays, like the DC Protein Assay. Subsequently, I balanced the histone bands using ImageJ software for further analysis using an appropriate immunoblot assay (Rasband, 1997; Schneider et al., 2012). The staining was performed on an

orbital shaker at RT. The gel was fixed in silver staining fixation buffer for 40 minutes, followed by three washes à 10 minutes with silver staining wash buffer. The gel was incubated with silver staining sensitizing solution for 1 minute and then shortly washed twice with de-ionized water. SDS-PAGES were stained with silver staining staining solution for 20 minutes and shortly washed twice with de-ionized water. Bands were developed in silver staining developing solution for about 10 minutes, until bands became visible, and then development was stopped using silver staining stopping buffer.

Immunoblotting

Cell pellets were lysed in regular lysis buffer, sometimes followed by sonication, if not only cytosolic, but also nuclear proteins were of interest. The debris was removed by centrifugation and protein concentration was determined using a DC Protein Assay according to manufacturer's instructions. 2X Bromphenolblue protein electrophoresis buffer (= SDS loading buffer) was added to the cell lysate at a 1:1 ratio and the solutions were heated to 95°C for 5 minutes. Protein solutions were loaded onto gels, separated by SDS-PAGE, and blotted onto PVDF membranes. Blocking was performed in PBS containing 0.1% Tween 20 (PBS-T) and 5% skim milk. Primary antibodies were diluted in PBS-T containing 5% skim milk at an antibody-specific dilution ratio and were allowed to bind their antigen while and over-night incubation at 4°C on a shaking table. The membranes were washed with PBS-T three times shaking for 5 minutes at RT. Then, the according horse-radish peroxidase (HRP)-conjugated secondary antibody were diluted in PBS-T containing 5% skim milk at a 1:10,000 dilution and added to the membrane for 30 minutes at RT, shaking. After two washes with PBS-T and one wash with PBS for 5 minutes each, protein bands were visualized using ECL developing solution. Densitometric quantification was performed using ImageJ Software (Rasband, 1997; Schneider et al., 2012). Certain antibodies required immunoblotting to be performed in a tris-buffered saline (TBS) buffer system.

2.2.5 Gene Expression Analysis

Quantitative expression analysis by Real Time PCR (qPCR)

Cell pellets were washed once with 1X phosphate-buffered saline (PBS) and stored in 300 µl RNAprotect Cell Reagent at -80°C. Total RNA was extracted using the RNeasy Mini Kit following the manufacturer's instructions. cDNA was prepared using the Transcriptor High Fidelity cDNA Synthesis Kit following the manufacturer's protocol. Quantitative PCR was performed using primers specific for the coding sequence of the gene of interest and Platinum SYBR Green qPCR SuperMix-UDG according to manufacturer's instructions. Following normalization to housekeeping gene GAPDH, fold changes were calculated using the ΔΔCT method (Livak and Schmittgen, 2001).

Microarray profiling – partly performed and edited by PD Dr. Klein-Hitpaß (Universitätsklinikum Essen, Germany)

The MEC-1 cell line carrying inducible ZAP70 and the mock control cell line were treated for 72 hours with 500 ng/mL tetracycline or medium. The induction was performed in biological replicates. Total RNA was extracted using the RNeasy Mini Kit including an on-column digest of contamination DNA using the RNase-Free DNAse Set according to manufacturer's instructions.

Microarray profiling was performed by PD Dr. Klein-Hitpaß (Universitätsklinikum Essen, Germany): for microarray analyses, the group used the Affymetrix GeneChip platform employing the Express Kit protocol for sample preparation and microarray hybridization. Total RNA (200 ng) was converted into biotinylated cRNA, purified, fragmented and hybridized HG-U133Plus_2.0 microarrays (Affymetrix). The arrays were washed and stained according to the manufacturer's recommendation and finally scanned in a GeneChip scanner 3000 (Affymetrix) with G7 update.

Array images were processed to determine signals and detection calls (Present, Absent, Marginal) for each probeset using the Affymetrix MAS 5.0 statistical algorithm Arrays were scaled across all probesets to an average intensity of 1000 to compensate for variations in the amount and quality of the cRNA samples and other experimental variables of non-biological origin. Pairwise

comparisons of treated versus control samples were carried out with GCOS1.4, which calculates the significance (change p-value) of each change in gene expression based on a Wilcoxon ranking test. To limit the number of false positives, we restricted further target identification to those probesets, which received at least one present detection call in the treated/control pair. Only probesets exhibiting a significant increase or decrease in the comparison analysis and at least one Present detection call per pair were considered as potentially regulated targets.

2.2.6 Immunofluorescence

To identify potential classical nuclear localization signal in the ZAP70 amino acid sequence, I performed an *in silico* analysis using the online tool *cNLS Mapper*. The analysis was performed on the ZAP70 NCBI Reference Sequence: NP_001070.2. “cNLS Mapper extracts putative NLS sequences with a score equal to or more than the selected cut-off score. Higher scores indicate stronger NLS activities. Briefly, a GUS-GFP reporter protein fused to an NLS with a score of 8, 9, or 10 is exclusively localized to the nucleus, that with a score of 7 or 8 partially localized to the nucleus, that with a score of 3, 4, or 5 localized to both the nucleus and the cytoplasm, and that with a score of 1 or 2 localized to the cytoplasm.” (Kosugi et al., 2008; Kosugi et al., 2009a; Kosugi et al., 2009b)

Confocal microscopy

HELA cells were seeded onto glass cover slips and then transfected with GFP_ZAP70 or GFP mock control constructs using Lipofectamine 2000 transfection reagent according to manufacturer’s instructions. After 24 hours of gene expression, HELA cells were washed with PBS and fixed with 4% formaldehyde in PBS for 15 minutes at RT. Slides were protected from light at all steps. Cells were permeabilized and blocked with Immunofluorescence Blocking/Staining Buffer for 20 minutes at RT. Samples were rinsed three times with PBS prior to the addition of phalloidin diluted 1:40 in PBS + 1% BSA. After rinsing with PBS, cover slips were mounted on microscope slides in the Slow Fade Gold antifade reagent containing DAPI nuclear staining. Confocal laser scanning microscopy was carried out using a Leica TCS SP5 microscope.

Stable CLL cell line cells were plated on Superfrost Plus Adhesion slides, previously coated with Poly-L-Lysine. After attachment for 4 hours at 4°C, slides were rinsed three times for 5 minutes with PBS. Slides were kept protected from light. Samples were blocked in Immunofluorescence Blocking/Staining Buffer for 1 hour at RT and subsequently stained with antigen specific primary antibodies diluted 1:50 in Immunofluorescence Blocking/Staining Buffer at 4°C over-night. Rinsing the slides three times with PBS stopped the staining. Secondary antibodies were added in a 1:1,000 dilution in Immunofluorescence Blocking/Staining Buffer and incubated for 1 hour at RT. Samples were rinsed three times with PBS prior to the addition of phalloidin diluted 1:40 in PBS + 1% BSA. After rinsing with PBS cover slips were mounted on microscope slides in the Slow Fade Gold antifade reagent containing DAPI nuclear staining. Confocal laser scanning microscopy was carried out using a Leica TCS SP5 microscope.

Fluorescence Recovery After Photobleaching (FRAP)

FRAP analyses were performed by my collaborators Dr. Yolanda Markaki and Susanne Lena Kathrin Leidescher (Leonhardt Group, LMU, Munich, Germany) essentially as described in Schneider et al., 2013. Following transfection of HELA cells with the GFP-fusion constructs indicated, live cell imaging and FRAP experiments were typically performed on an UltraVIEW VoX spinning disc microscope with integrated FRAP PhotoKinesis accessory (PerkinElmer) assembled to an Axio Observer D1 inverted stand (Zeiss) and using a 100X / 1.4 NA Plan-Apochromat oil immersion objective. The microscope was equipped with a heated environmental chamber set to 37°C. Fluorophores were excited with 488 nm solid-state diode laser line. Confocal image series were typically recorded with 14-bit image depth, a frame size of 512 × 512 pixels, a pixel size of 68.5 nm and with time intervals of 154 ms. For photobleaching experiments, the bleach regions, typically with a length of 8–10 µm, were chosen to cover the anterior half of the oval-shaped nucleus. Photobleaching was performed using two iterations with the acousto-optical tunable filter (AOTF) of the 488 nm laser line set to 100% transmission. Typically, 20 prebleach and 330 postbleach frames were recorded for each series. Data correction, normalization and quantitative evaluations were performed by automated processing with ImageJ using a set of self-developed macros followed by calculations in Excel (Rasband, 1997; Schneider et al., 2012).

2.2.7 Strep-affinity purifications analyzed using mass spectrometry (AP-MS)

Clone establishment

The *ZAP70* gene was cloned in frame with a DNA string containing one Flag Tag and two Strep II tags onto a pcDNA3 vector backbone for further expression of a N-terminal tagged ZAP70 protein (see *Figure 8*). pcDNA3 vectors containing tags were kindly provided by Prof. Florian Bassermann (Klinikum rechts der Isar, TU Munich, Germany). MEC-1 cells were transfected by Amaxa nucleofection according to manufacturer's instructions with pcDNA3_N-SF-TAP_ZAP70 vector containing the tagged ZAP70 ($ZAP70^{high}$) and pcDNA3_N-SF-TAP only containing the tags ($ZAP70^{low}$), respectively. Clones were selected by single cell dilution under 600 µg/ml G418 selection.

Stable isotope labeling by amino acids in cell culture (SILAC)

The SILAC technique is commonly used for a direct quantitative analysis of two samples in the same mass spectrometry run. Hereby, one sample is labeled with light and one with heavy amino acids for an internal discrimination and therefore direct comparison. To perform stable isotope labeling by amino acids in cell culture (SILAC), passage-matched MEC-1 $ZAP70^{low}$ cells and MEC-1 $ZAP70^{high}$ cells were grown according to manufacturer's instructions in medium containing light (Lys-0, Arg-0) versus medium (Lys-4, Arg-6) amino acids, respectively (Silantes). Analysis of complete labeling was assessed after nine passages using ESI-LC-MS/MS. Cells were exposed to phorbol 10 ng/ml myristate acetate (PMA) and 500 ng/ml ionomycine for 24 hours prior to lysis and subsequent Strep-tag based affinity purification. The experiment was performed in triplicates.

Strep affinity purification and sample preparation for LC-MS/MS analysis – partly performed and edited by Dr. Juliane Merl (Core Facility, Helmholtz Center, Munich, Germany)

Cell pellets were lysed for 30 minutes at 4°C in lysis buffer (Protease Inhibitor Cocktail (Roche), Phosphatase Inhibitor Cocktail 2 and 3 (Sigma), 1% NP40 in Tris-buffered Saline) and cell debris was removed by centrifugation for 10 minutes at 4°C. The protein content was measured using the DC Protein Assay (BioRad) according to manufacturer's instructions. 50 µl Strep-Tactin beads (IBA) per

sample were washed three times with TBS. Lysates (diluted 1:4 with TBS) were combined with the beads and incubated at 4°C rotating for two hours. After brief centrifugation, beads of one AP of ZAP70^{high} (light condition) and one ZAP70^{low} control (medium condition) were combined, loaded onto MicroSpin Columns (GE Healthcare) and washed three times with wash buffer (Phosphatase Inhibitor Cocktail 2 and 3 (Sigma), 0,25% NP40 in Tris-buffered Saline). The experiment was carried out in triplicates. Elution was performed using Strep-Tag elution buffer (IBA) diluted in TBS/ 0.25% NP40. Combined eluates were precipitated using methanol/chloroform. After methanol/chloroform precipitation, the samples were further treated by Dr. Juliane Merl (Core Facility, Helmholtz Center, Munich, Germany). The proteins were separated on a 4-12% SDS-PAGE. Each lane was cut in 5 pieces and an in-gel digest was performed as published in (Merl et al., 2012). Proteins were reduced with DTT and alkylated using iodoacetamide and subjected to tryptic in-solution digest.

Air-dried digestion samples were dissolved in 45 µl of 2% ACN / 0.5% TFA by incubation for 30 minutes at RT under agitation. Before loading, the samples were centrifuged for 5 minutes at 4°C. LC-MS/MS analysis of 20µl of each sample was performed as described in Merl et al., 2012. For separation of the peptides on the analytical column a 170 min gradient was used.

Every sample was automatically injected and loaded onto the trap column at a flow rate of 30 µl/min in 5% buffer B (98% ACN / 0.1% formic acid (FA) in HPLC-grade water) and 95% buffer A (2% ACN / 0.1% FA in HPLC-grade water). After 5 minutes, the peptides were eluted from the trap column and separated on the analytical column by a 120 min gradient from 5% to 31% of buffer B at 300 nl/min flow rate followed by a short gradient from 31% to 95% buffer in 5 minutes. Between each sample, the gradient was set back to 5% buffer B and left to equilibrate for 20 minutes. From the MS prescan, the ten most abundant peptide ions were selected for fragmentation in the linear ion trap if they exceeded an intensity of at least 200 counts and if they were at least doubly charged. During fragment analysis, a high-resolution (60,000 full-width half maximum) MS spectrum was acquired in the Orbitrap with a mass range from 200 to 1500 Da.

2.2.8 Radioactive ZAP70 Kinase Assay

The radioactive ZAP70 kinase assay was performed using between 75 and 300 ng recombinant human active ZAP70 and different recombinant human histone molecules as substrates. Recombinant histone proteins H1.1, H2A, H3.1 and H4 were kindly provided from PD Dr. Sandra Hake (LMU, Munich). I also included a commercially available recombinant H4 protein. The kinase reaction was carried out in 20 µl total reaction volume at 30°C for 15 minutes in kinase assay buffer. The reaction was initiated by the addition of the enzyme and stopped by cooking the samples at 95°C for 5 minutes with 5 µl of 5X SDS loading buffer. Proteins were separated on an 18% SDS-PAGE as described above and ^{32}P-labeled proteins were visualized by autoradiography of the dried gel.

2.2.9 Statistical Analysis

The mean value ± standard error of the mean (SEM) of biologic replicates are illustrated in the diagrams of this thesis. Statistical significances were determined using the unpaired Student's t-test as appropriate. A p-value < 0.05 was considered to be statistically significant.

3 Results

3.1 The functional Role of ZAP70 in the Cytosol of CLL cells

3.1.1 Introduction of the Inducible ZAP70 Expression System

To study the functional role of ZAP70 in CLL, I established a tetracycline-regulated inducible protein expression system using the human CLL cell line MEC-1 (see *Figure 9A*). The switch system is based on the Tet-On tetracycline-controlled transcriptional activation of the target gene *ZAP70* using the *E. coli* Tn*10*-encoded tetracycline resistance operon. In the static "OFF" state, two homodimers of tet-repressor molecules are bound to the two tet-operator 2 ($TetO_2$) sequences, thereby inhibiting the transcription of the target gene, *ZAP70* (Hillen and Berens, 1994; Hillen et al., 1983; Hillen and Schollmeier, 1983). Once tetracycline is added to switch "ON" expression of ZAP70, it binds to the tet-repressor provoking a conformational change and thereby releasing it from the operon. The dissociation of the tet repressor-tetracycline complex allows the transcription of *ZAP70*. Tetracycline treatment led to the overexpression of ZAP70 specifically in the inducible MEC-$1^{ZAP70\text{-}tet\text{-}ON}$ cell line containing the gene of interest (see *Figure 9B*). Endogenous ZAP70 expression was detected at very low levels in the control cell line treated the same way, which contains the pcDNA6/TR and the pcDNA4/TO vector backbones without the *ZAP70* gene. This control cell line will be called the mock control throughout this thesis (MEC-1^{mock}). The up-regulation of ZAP70 expression was observed as early as after 24 hours (see *Figure 9C*). ZAP70 protein levels continuously increased over a tetracycline treatment course of four days. In addition, induced expression of ZAP70 could be switched off by a thorough washout of tetracycline (see *Figure 9D*). Once tetracycline is removed and ZAP70 expression is therefore switched off after 24 hours, ZAP70 protein expression declines to baseline levels within 24 hours.

In this dissertation, the inducible ZAP70 expression system in the CLL cell line MEC-1 was used as a cell culture model to study causal relations between ZAP70 overexpression and deregulated oncogenic pathways. Even though multiple biochemical studies are feasible on primary leukemic cells, they have been very difficult to modify *ex vivo*. Hence, I sought to create a cell line model to scrutinize

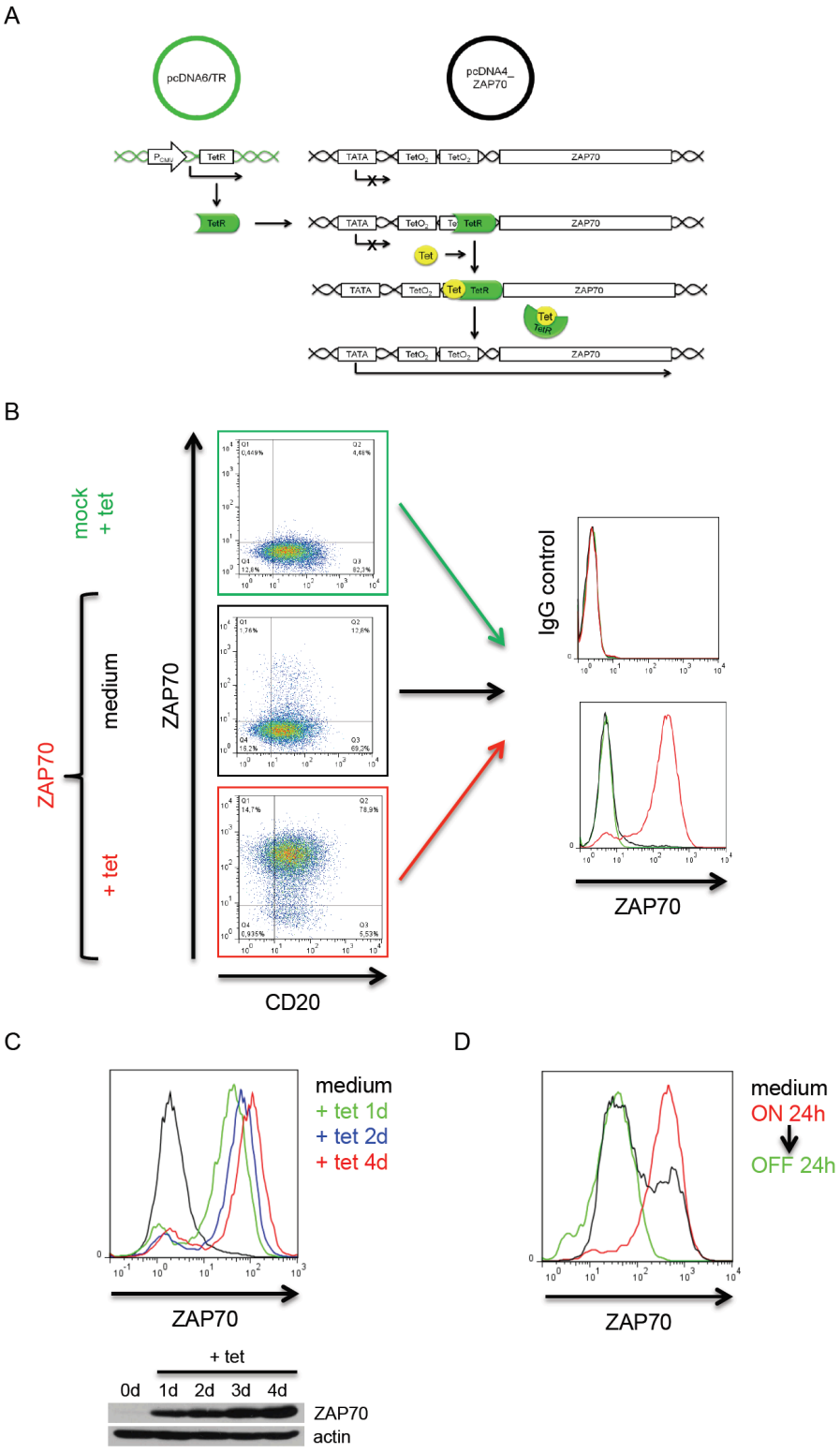

Figure 9 Introduction of the ZAP70 switch expression system in the MEC-1 cell line

(A) A stable MEC-1 cell line carrying a tetracycline-regulated inducible ZAP70 expression system was established by nucleofection and subsequent single cell dilution. Clone populations overexpressing ZAP70 protein after induction with tetracycline were identified by flow cytometry staining with specific antibodies for ZAP70. (B) ZAP70 gene expression was induced by treatment of MEC-1$^{ZAP70\text{-}tet\text{-}ON}$ with tetracycline for 96 hours and analyzed by flow cytometry. Cells were counterstained for the B-cell surface marker CD20. (C) MEC-1$^{ZAP70\text{-}tet\text{-}ON}$ cells were treated with tetracycline over a time course of 1, 2, and 4 days. ZAP70 protein expression was detected by antibody staining for flow cytometry and immunoblotting. (D) ZAP70 gene expression was switched on by tetracycline treatment for 24 hours and subsequently switched off through a thorough washout of tetracycline with medium. Protein expression was analyzed by flow cytometry.

the functional role of ZAP70 in the CLL background. However, as cancer cell lines are generally derived from the tumor of only one patient, immortalized and then propagated in culture over innumerous passages, it is often difficult to extrapolate these findings to primary cells and a more *in vivo* scenario. Therefore, I included primary CLL samples in this study to verify hypothetic mechanisms discovered in the cell line model. However, the switchable system, by which ZAP70 expression can be toggled on and off at specific time points, is a useful tool to study immediate effects of ZAP70 and circumvents the difficulties arising from inter-patient variability, inherent to the work with primary cells.

3.1.2 Characterization of CLL Features in the Inducible Cell Line Model

A characteristic feature of CLL cells is a profound defect of the apoptotic machinery, which is partly explained by the overexpression of anti-apoptotic proteins of the *bcl2* family (see *Introduction p.5*). As CD38 expression on CLL cells is associated with unmutated IGHV and ZAP70 expression in CLL cells (Huttmann et al., 2006), I analyzed CD38 expression before and after ZAP70 induction in comparison with unmodified MEC-1 cells (see *Figure 10A*). CD38 expression was significantly increased upon ZAP70 induction (see *Figure 10B*), similar to the increased expression of CD38 in ZAP70-positive CLL cells (see *Figure 10C*). The increased baseline expression of CD38 in untreated MEC-$1^{ZAP70\text{-}tet\text{-}ON}$ cells compared to MEC-1^{mock} cells suggested a low level of leakiness of the system (see *Figure 10C*). As CD38 and ZAP70 expression have been associated with enhanced BCR signaling capacity (Cutrona et al., 2008), I analyzed the phosphorylation of CD79a, an upstream component of the BCR signaling pathway (see *Figure 6*). Upon ZAP70 induction, CD79a was upregulated and BCR signaling was constitutively activated by phosphorylation (see *Figure 10D*). Since CD38 expression was reported to be associated with a more active proliferation (Damle et al., 2007), a BrdU proliferation assay was used to analyze the proliferative capacity of the cell line model. Induced (MEC-$1^{ZAP70\text{-}tet\text{-}ON}$) and non-induced (MEC-$1^{ZAP70\text{-}tet\text{-}OFF}$) MEC-1 cells were labeled with BrdU for three and six hours and BrdU incorporation was analyzed using flow cytometry (see *Figure 10E*). No significant differences in proliferative capacity were detected. However, I found that ZAP70 upregulation mediated higher resistance to chemotherapy-induced apoptosis.

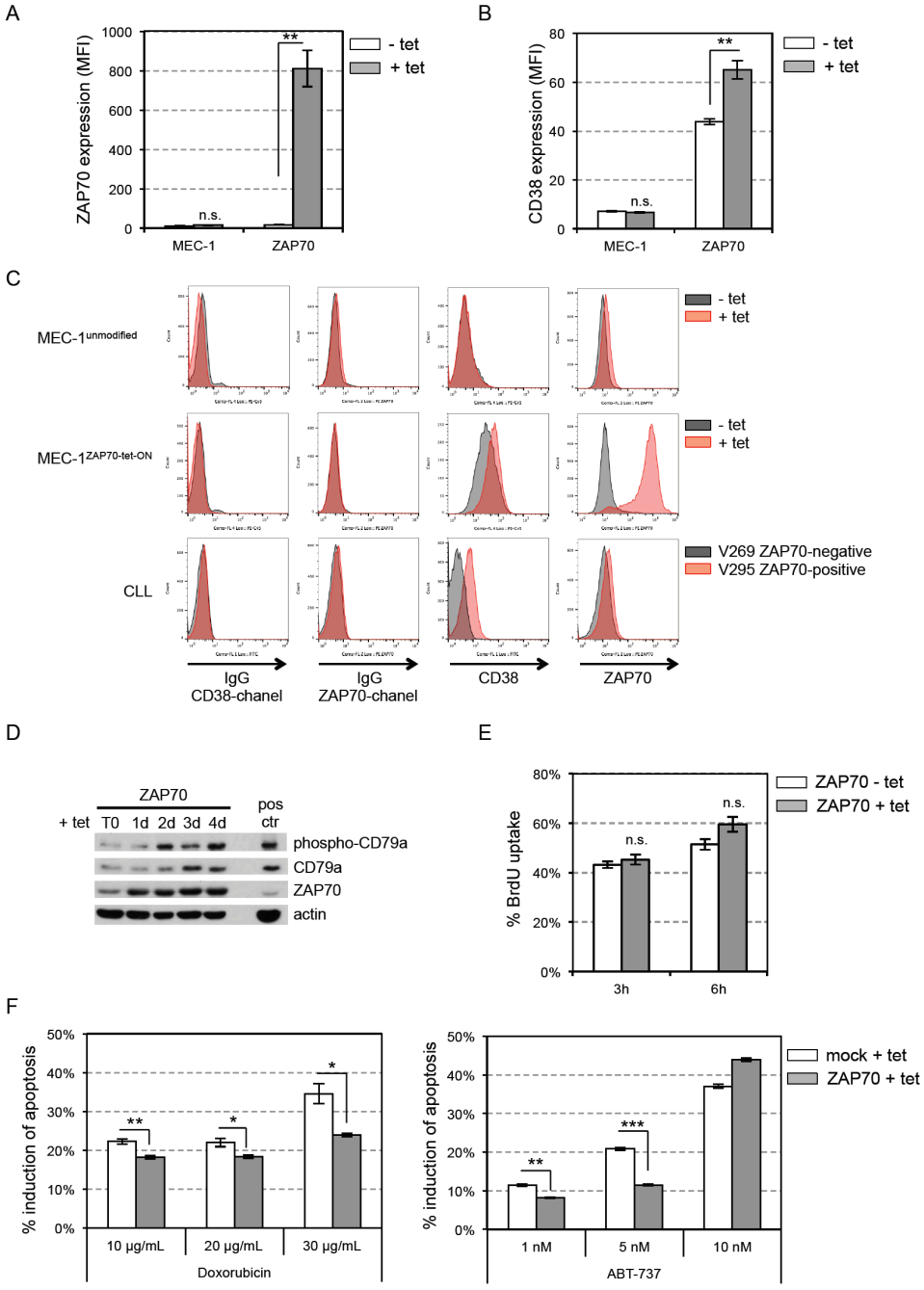

Figure 10 Characterization of CLL features in the inducible cell line model

ZAP70 expression was induced with tetracycline for 72 hours and, subsequently, expression of (A) CD38 and (B) ZAP70 was analyzed using flow cytometry. Unmodified MEC-1 cells were used as negative control. Error bars show mean ± SEM from one representative experiment carried out in triplicates. (C) Comparison of CD38 and ZAP70 expression levels in unmodified MEC-1 cells (MEC-$1^{unmodified}$), the inducible cell line (MEC-$1^{ZAP70\text{-}tet\text{-}ON}$) and primary CLL samples using flow cytometry. (D) Tetracycline was added for up to 4 days to MEC-$1^{ZAP70\text{-}tet\text{-}ON}$ cells to induce ZAP70 overexpression. Phosphorylation and basic expression levels of the BCR component CD79a was analyzed using immunoblotting. Positive control = primary CLL sample stimulated with anti-IgM for 12 hours. One representative experiment out of three is shown. (E) ZAP70 expression was switched on in MEC-$1^{ZAP70\text{-}tet\text{-}ON}$ by adding tetracycline for 48 hours. BrdU was added at a concentration of 10 µM for 3 and 6 hours to either untreated or treated cells. Uptake of BrdU was quantified using flow cytometry. Error bars show mean ± SEM from three different inducible cell lines. (F) MEC-$1^{ZAP70\text{-}tet\text{-}ON}$ and mock control cell line (MEC-1^{mock}) were treated with tetracycline for 72 hours. Cells were then exposed to doxorubicin or ABT-737 at varying doses for 48 hours. Apoptotic cells were detected by AnnexinV/PI staining. Error bars show mean ± SEM of the percentage of AnnexinV-positive cells normalized to the values in medium control samples to depict induction of apoptosis upon treatment. Results are shown from one representative experiment carried out in triplicates.

** $p < 0.01$, * $p < 0.05$, n.s. $p > 0.05$.

The inducible system was treated with tetracycline for 72 hours prior to induction of apoptosis using increasing concentrations of the anthracycline doxorubicin as well as with the Bcl-2 antagonist ABT-737. After 48 hours of cytotoxic treatment, I assessed apoptosis levels by AnnexinV staining using flow cytometry and referred apoptosis induction to basic apoptosis levels in untreated cells. I found that MEC-1$^{ZAP70\text{-}tet\text{-}ON}$ cells were significantly protected from the induction of programmed cell death following treatment with the anthracycline doxorubicin as well as with the Bcl-2 antagonist ABT-737 (see *Figure 10F*).

3.1.3 Upregulation of Anti-apoptotic Factors

As MEC-1$^{ZAP70\text{-}tet\text{-}ON}$ cells showed a relative resistance to apoptosis induction by ABT-737, I analyzed several anti-apoptotic proteins, likely to be involved in this phenotype, using immunoblotting. Strikingly, I found an increase in Mcl-1 protein levels following ZAP70 induction (see *Figure 11A & B*). When ZAP70 expression was switched on, Mcl-1 levels increased, and, subsequently, decreased again once ZAP70 expression was switched off (see *Figure 11C*). Mcl-1 levels did not change upon tetracycline treatment of MEC-1^{mock} cells, indicating that the upregulation of Mcl-1 was not a direct tetracycline effect, but indeed related to the expression of ZAP70 (see *Figure 11D*).

Importantly, analyses of primary CLL cells indicated higher expression levels of Mcl-1 in ZAP70-positive cells as compared to ZAP70-negative cells, in keeping with previously published data (Michels et al., 2004; Pepper et al., 2008; Petlickovski et al., 2005; Saxena et al., 2004). It is known to increase CLL cell survival by enhancing resistance to apoptosis (Reed and Pellecchia, 2005). Hence, I assessed the protein expression of Mcl-1 by immunoblotting comparing ZAP70-negative with ZAP70-positive primary CLL samples (see *Figure 11E*). Comparing a total of 22 patient samples, I was able to validate the data proposed by Pepper et al. I could show that ZAP70-positive CLL cells express significantly higher levels of Mcl-1 compared to ZAP70-negative CLL cells (see *Figure 11F*).

In conclusion, the MEC-1$^{ZAP70\text{-}tet\text{-}ON}$ system recapitulated important features of primary CLL cells with regard to the expression of anti-apoptotic proteins and CD38 expression. Therefore, in spite of limited conclusions, which can be drawn from experiments with immortalized cells, the MEC-1$^{ZAP70\text{-}tet\text{-}ON}$ system allowed me to study the function of ZAP70 in a B cell related context.

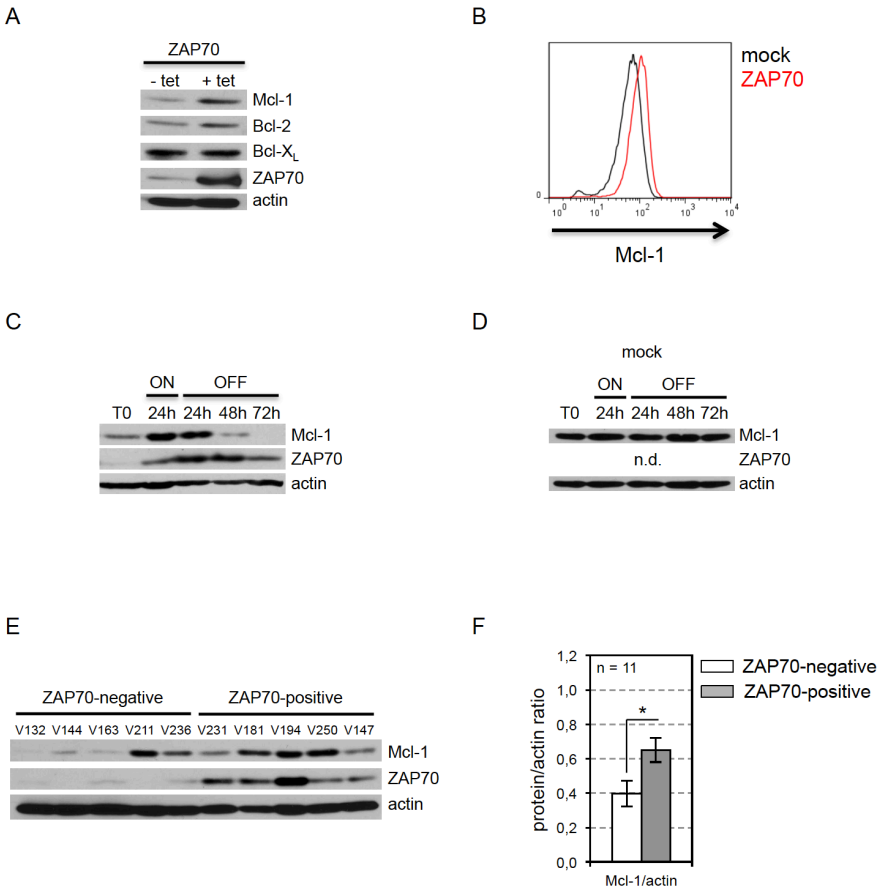

Figure 11 Regulation of anti-apoptotic factors upon ZAP70 overexpression

(A) MEC-1$^{ZAP70\text{-}tet\text{-}ON}$ cells were treated with tetracycline or medium for 96 hours. Protein expression of the anti-apoptotic key players Mcl-1, Bcl-2 and Bcl-XL was analyzed. One representative immunoblot out of three individual experiments is shown. (B) Mcl-1 protein levels were analyzed by flow cytometry after 72 hours of tetracycline treatment. MEC-1$^{ZAP70\text{-}tet\text{-}ON}$ cells were compared to MEC-1^{mock} control cells. One representative experiment out of three individual experiments is shown. (C) MEC-1$^{ZAP70\text{-}tet\text{-}ON}$ cells were treated with tetracycline for 24 hours. Cells were washed three times with media to switch ZAP70 gene expression off. Mcl-1 protein levels were analyzed by immunoblotting. One representative experiment out of five individual experiments is shown. (D) MEC-1^{mock} control cells were treated as in (C). n.d. – not detectable. (E) Mcl-1 protein expression was analyzed by immunoblotting comparing five ZAP70-negative with five ZAP70-positive primary CLL samples. (F) Results from three individual Mcl-1 immunoblot experiments with different primary CLL cells were quantified using ImageJ software. Eleven ZAP70-negative CLL samples were compared to eleven ZAP70-positive CLL samples.

* $p < 0.05$.

3.1.4 Regulation of the Degradation of Mcl-1

The data presented in *Figure 11* indicated that ZAP70 actively contributes to the expression of anti-apoptotic proteins in CLL.

Quantitative gene expression analysis using specific primers for the human *MCL1* coding region revealed no significant change of Mcl-1 mRNA levels

following ZAP70 induction (see *Figure 12A*), suggesting that Mcl-1 levels were post-transcriptionally regulated by ZAP70. To test this hypothesis, I analyzed the protein stability of Mcl-1 by blocking its translation with cycloheximide. I found the half-life of Mcl-1 to be markedly prolonged in MEC-1$^{ZAP70\text{-}tet\text{-}ON}$ cells (see *Figure 12B*). In non-induced MEC-1$^{ZAP70\text{-}tet\text{-}OFF}$ cells, Mcl-1 was detectable until 30 minutes of treatment with cycloheximide by immunoblotting, whereas it remained detectable for 45 minutes of treatment in ZAP70-expressing MEC-1$^{ZAP70\text{-}tet\text{-}ON}$ cells (see *Figure 12C*). To rule out that this change in Mcl-1 regulation was due to the tetracycline effect alone, I also performed Mcl-1 half-life analysis in the mock cell line and did not see a change upon tetracycline treatment (see *Figure 12D*).

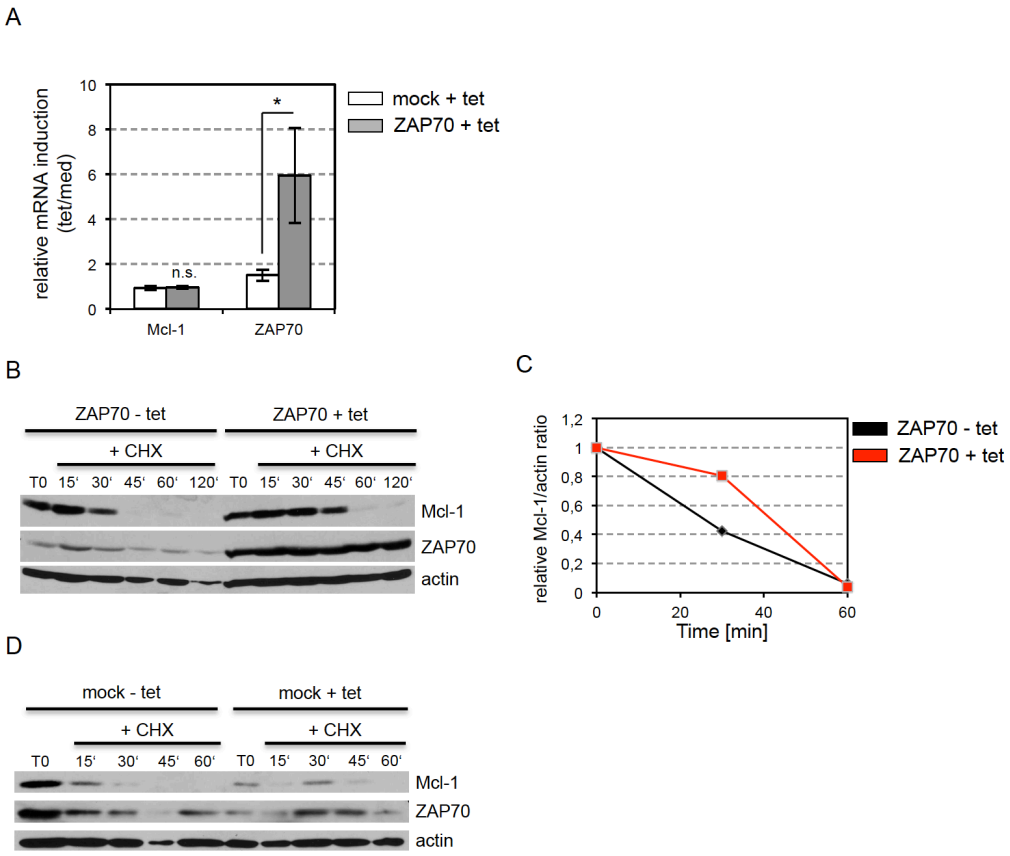

Figure 12 Regulation of the degradation of Mcl-1 in MEC-1$^{ZAP70\text{-}tet\text{-}ON}$

(A) Transcriptional regulation of Mcl-1 in MEC-1^{mock} versus MEC-1$^{ZAP70\text{-}tet\text{-}ON}$ was analyzed by quantitative RT-PCR using specific primers for the human *mcl-1* coding region. The relative induction of gene expression after ZAP70 overexpression was normalized to the expression of GAPDH and compared to the expression in the non-treated inducible clone (depicted as fold induction). Results are calculated by the delta delta Ct ± SEM from three experiments. (B) ZAP70 gene expression was induced by treatment with tetracycline or medium as negative control for 72 hours. Cells were subsequently treated with cycloheximide (50 µg/ml) for 15, 30, 45, 60, and 120 minutes to analyze the half-life of the Mcl-1 protein by immunoblotting. One representative blot out of three individual experiments is shown. (C) Results from three individual experiments were quantified using ImageJ software and mean values from three Mcl-1 half-life experiments are depicted. (D) MEC-1^{mock} control cells were treated with tetracycline for 72 hours. Cells were subsequently treated with cycloheximide (50 µg/ml) for 15, 30, 45, and 60 minutes to analyze the half-life of the Mcl-1 protein by immunoblotting. One representative blot is shown.

* $p < 0.05$, n.s. $p > 0.05$.

In primary leukemic B cells, I observed the same effect as in the cell line: the stability of the Mcl-1 protein was distinctly increased in the ZAP70-positive subgroup (see *Figure 13A & B*). These findings provide evidence that ZAP70 controls Mcl-1 expression levels primarily by a post-transcriptional mechanism affecting the half-life of Mcl-1.

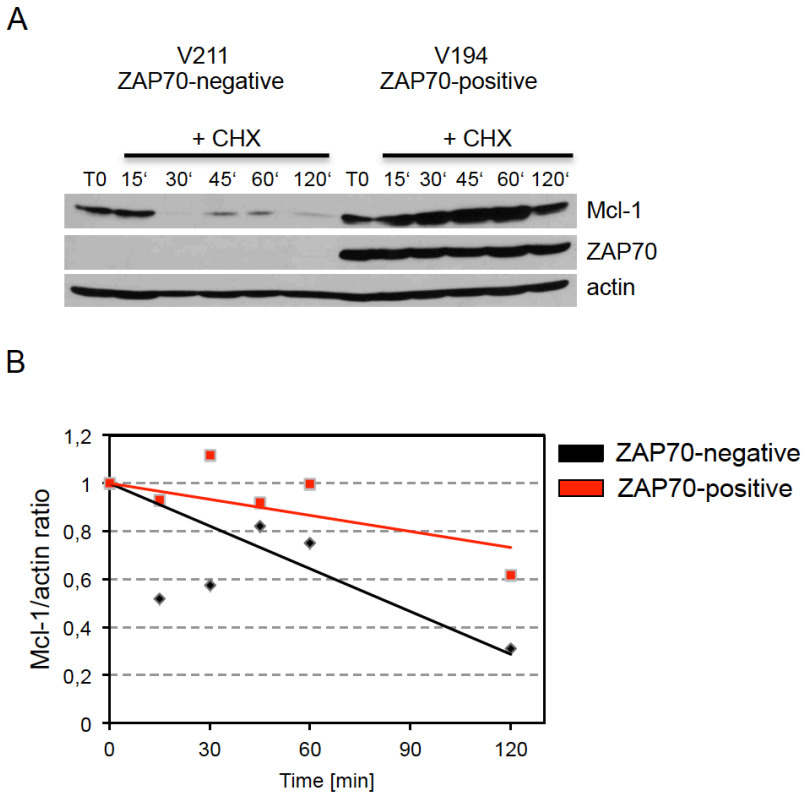

Figure 13 Regulation of the degradation of Mcl-1 in ZAP70-positive CLL cells

(A) Half-life of Mcl-1 protein in primary CLL samples was assessed by treatment with cycloheximide (50 µg/ml) for 15, 30, 45, 60 and 120 minutes and subsequent immunoblot analysis. ZAP70-negative CLL patient samples were compared to ZAP70-positive primary samples. One representative immunoblot out of three individual experiments is shown. (B) Results from three individual experiments were quantified using ImageJ software.

The two PEST domains in Mcl-1 contain mainly proline, glutamic acid, serine, and threonine residues, and lead to a tight regulation of Mcl-1 expression by its degradation via the proteasome (Akgul et al., 2000; Chen et al., 2005a). Inhibition of this pathway by pretreatment with lactacystin stopped the degradation of Mcl-1, proving evidence that this pathway is also relevant to Mcl-1 expression in the MEC-1$^{ZAP70\text{-}tet\text{-}ON}$ system (see *Figure 14A*). Three important regulators of proteasomal degradation of Mcl-1 are the ubiquitin ligases Fbw7 (Inuzuka et al., 2011), MULE (Zhong et al., 2005), and the ubiquitin specific peptidase USP9X

(Schwickart et al., 2010). Fbw7 and MULE target Mcl-1 for ubiquitination, whereas USP9X removes the lysine 48-linked polyubiquitin chains and thereby saves Mcl-1 from destruction. Immunoblot analyses revealed no significant differences in the baseline protein expression of Fbw7, MULE or USP9X between the ZAP70-negative and the ZAP70-positive subgroup (see *Figure 14B & C*). This result suggests that these factors are not accountable for the different half-lives of Mcl-1 observed between ZAP70-positive and ZAP70-negative samples.

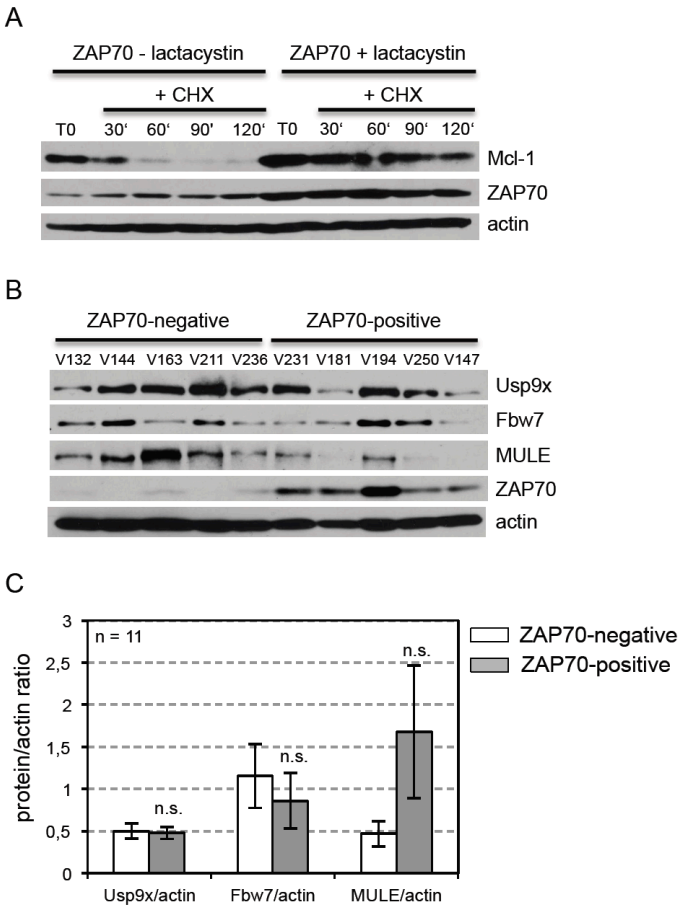

Figure 14 The proteasomal degradation of Mcl-1 in CLL cells

(A) MEC-1$^{ZAP70\text{-}tet\text{-}ON}$ were pre-treated with medium or proteasome inhibitor lactacystin (2.5 µM) for 30 minutes and subsequently treated with cycloheximide (50 µg/ml) for 30, 60, 90 and 120 minutes. Mcl-1 protein was analyzed by immunoblotting. One representative blot out of three individual experiments is shown. (B) E3 ubiquitin ligases Fbw7 and MULE, and ubiquitin specific peptidase USP9X were analyzed by immunoblotting, comparing five individual primary CLL samples from each ZAP70 patient subset. One out of three experiments with different primary CLL cells is shown. (C) Results from three individual experiments with 22 different primary CLL cells were quantified using ImageJ software.

n.s. $p > 0.05$.

3.1.5 The role of GSK3β in Apoptosis Regulation

Upstream of the proteasome, Mcl-1 is marked for destruction by phosphorylation of serine 159 through glycogen synthase kinase 3β (GSK3β) (Ding et al., 2007). Comparison of primary CLL samples using immunoblot experiments revealed that GSK3β protein levels were significantly reduced in ZAP70-positive CLL cells. Representative immunoblot is shown in *Figure 15A*. 22 primary samples were analyzed (see *Figure 15B)*. In addition to the low levels of GSK3β in ZAP70-positive CLL cells, the expressed GSK3β was significantly more phosphorylated at serine 9 and therefore inactivated (see *Figure 15C)*. Quantitative RT-PCR demonstrated that the low levels of GSK3β were related to decreased transcription of the gene (see *Figure 15D)*. This result illustrates that ZAP70 is associated with a downregulation of *GSK3B* gene expression. I propose the subsequent post-transcriptional stabilization of the anti-apoptotic factor Mcl-1 as a possible mechanism, of how ZAP70 expression enables CLL cells to evade programmed cell death.

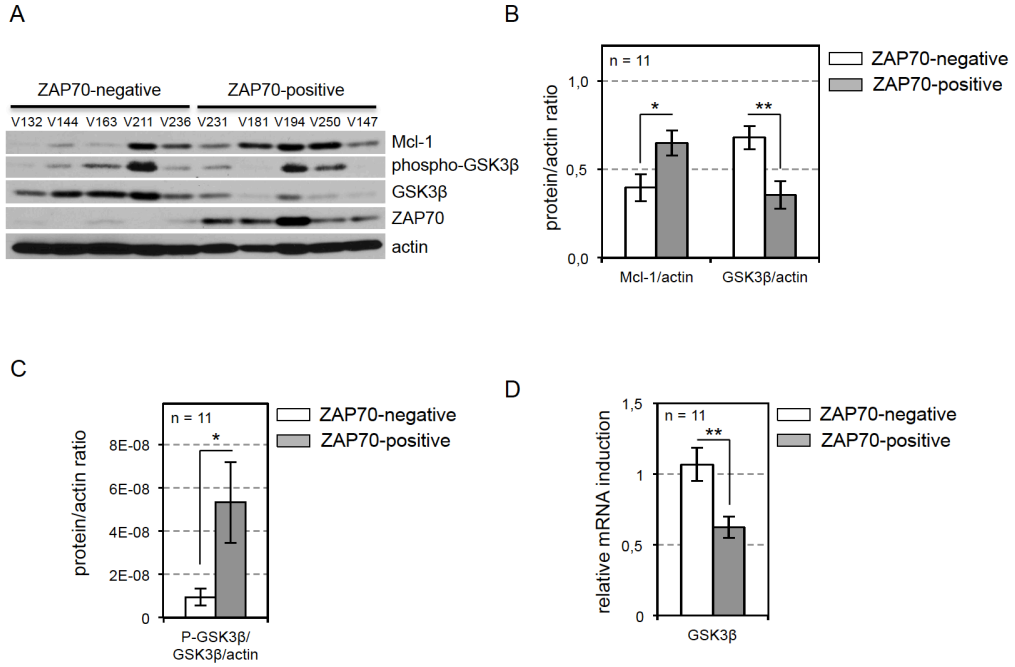

Figure 15 **Analysis of GSK3β expression in respect to ZAP70 expression**

(A) GSK3β phosphorylation at serine 9 and basic expression levels were analyzed by immunoblotting. Five ZAP70-negative were compared to five ZAP70-positive primary CLL samples. One out of three experiments is shown. (B) and (C) Results from three individual experiments with 22 different primary CLL cells were quantified using ImageJ software. (D) Transcriptional levels of GSK3β were analyzed by quantitative RT-PCR using specific primers for the human *gsk3b* coding region. mRNA expression was normalized to the expression of GAPDH and gene expression levels were compared between ZAP70-positive and ZAP70-negative CLL samples and normalized to the mean expression level of the ZAP70-negative subset (depicted as fold induction). Results are calculated by the mean delta delta Ct ± SEM from eleven individual primary CLL samples from each subgroup.

** $p < 0.01$, * $p < 0.05$, n.s. $p > 0.05$.

3.2 The Functional Role of ZAP70 in the Nucleus of CLL cells

In 1997, Sloan-Lancaster et al. described that ZAP70 not only localizes near the plasma membrane in the cytosol of T cells as expected from its original function in the T cell receptor pathway, but that it also appears in the nucleus of activated and resting T cells (Sloan-Lancaster et al., 1997). As this study showed that ZAP70 expression in CLL cells is associated with a differential regulation of the gene *GSK3B* and as another non-receptor tyrosine kinase has been implicated to regulate transcription via the phosphorylation of histones in the nucleus of leukemic cells (see *Discussion p.93*), ZAP70 might influence gene expression in a similar way. Epigenetic mechanisms play an important role in the pathogenesis of CLL (Amin et al., 2012; Kn et al., 2004; Smith et al., 2015) and other tyrosine kinases originally described to function in the cytosol, have been implicated to translocate to the nucleus and play a role in epigenetic regulation of gene expression (Dawson et al., 2009).

To address this question, a global gene expression study was performed to identify, which genes are regulated by ZAP70. I switched on ZAP70 expression in the MEC-1$^{ZAP70\text{-}tet\text{-}ON}$ cell line by tetracycline stimulation for 72 hours and treated the MEC-1^{mock} cell line the same way. I performed this experiment in biological duplicates and extracted total RNA. The subsequent gene expression analysis using a Human Genome U133 Plus 2.0 Array was carried out and analyzed by PD Dr. Klein-Hitpaß (Universitätsklinikum Essen, Germany). 136 genes were significantly upregulated and 291 were significantly downregulated upon ZAP70 overexpression (see *Appendix*). Of these genes, about 93 genes were involved in the regulation of apoptosis, 123 genes in lymphocyte activation, 79 genes in regulation of humoral immune responses, as well as 69 genes involved in B cell differentiation were differentially regulated upon ZAP70 induction (see *Appendix*).

A subset of 54 genes, which significantly differed and were reported to contribute to the pathogenesis of CLL, is displayed in *Figure 16*. Strikingly, these data indicate that ZAP70 overexpression in a B cell background directly alters gene expression. Therefore, the second part of my thesis focuses on the potential role of nuclear localized ZAP70 for gene expression.

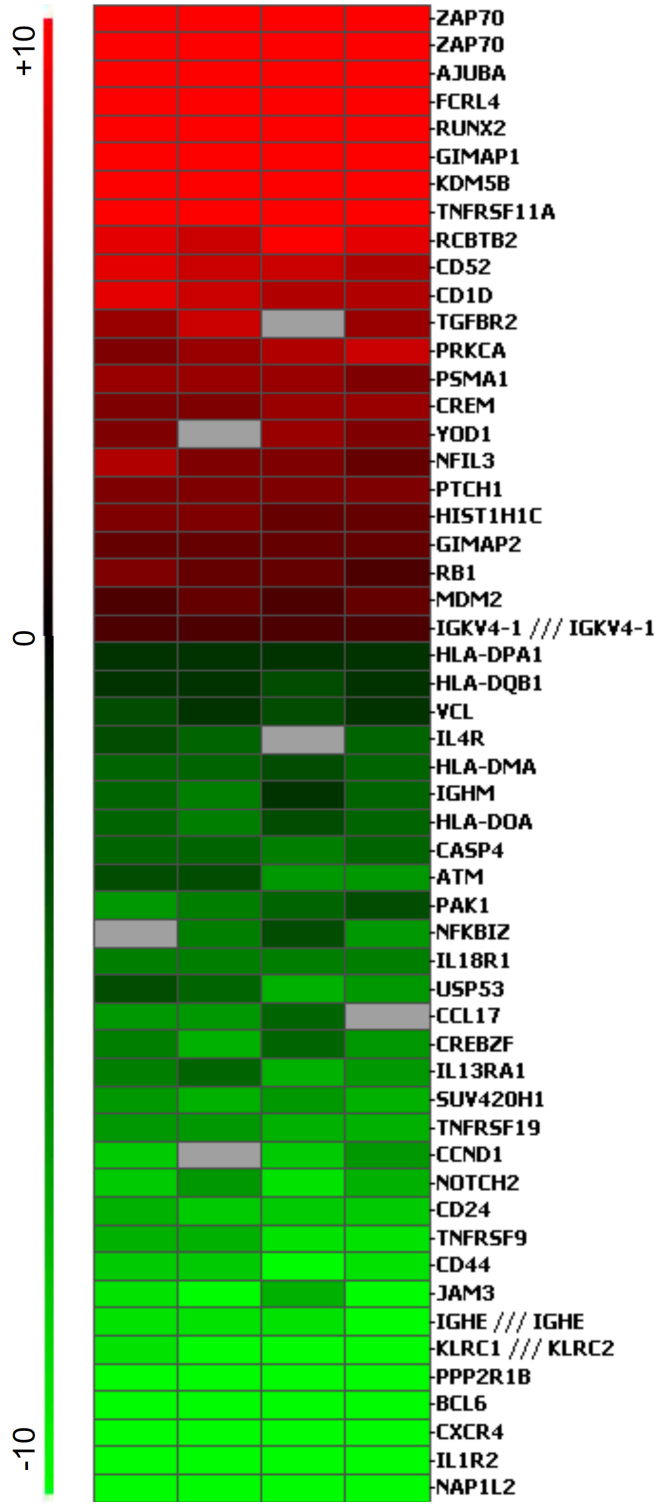

Figure 16 Microarray profiling of the inducible system

MEC-1$^{ZAP70\text{-}tet\text{-}ON}$ and MEC-1^{mock} were treated with tetracycline or medium for 72 hours and mRNA levels were analyzed using an HG-U133Plus_2.0 microarray. Pairwise comparisons of treated versus control samples were carried out with GCOS1.4, which calculates the significance (change p-value) of each change in gene expression based on a Wilcoxon ranking test. Results are depicted as a heat map of significant signal log ratios comparing MEC-1$^{ZAP70\text{-}tet\text{-}ON}$ and MEC-1^{mock}. The experiment was carried out in biological and technical replicates – all four samples are shown. Green represents downregulation of gene expression, red represents upregulation of gene expression. Results were reduced to genes of interest for improved representability. Heat maps including all results can be found in the *Appendix*. All heat maps were created in collaboration with PD Dr. Ludger Klein-Hitpaß (Universitätsklinikum Essen, Germany).

3.2.1 Subcellular Distribution of ZAP70 in CLL cells

The study of Sloan-Lancaster et al. discovered translocation of ZAP70 to the nucleus of T cells (Sloan-Lancaster et al., 1997). To further study the potential nuclear function of ZAP70, I analyzed the cellular distribution of ZAP70 in CLL cells. I was able to validate these published data in the B-cell derived CLL background. The human cervical cancer cell line HELA is widely used as research model for differential questions as it is easily propagated and modified in culture. Furthermore, as polyploid and rather big cells, HELA cells provided a good model to study subcellular ZAP70 distribution by confocal imaging. I used HELA cells as a non-hematopoietic cell line system for ZAP70 diffusion throughout the cell body. First transfection experiments with HELA cells showed that an enhanced green fluorescent protein (eGFP)-ZAP70 fusion protein localizes to the cytosol and the nucleus using confocal immunofluorescence imaging (see *Figure 17A*). Hoechst staining was used to depict the nucleus of the cells, and phalloidin to counterstain the cytoskeleton. In addition, ZAP70 also translocated to the nucleus of the inducible CLL cell line upon ZAP70 induction using tetracycline (see *Figure 17B*). Subcellular nuclear fractionation assays with subsequent immunoblot analyses confirmed this result in primary ZAP70-positive CLL cells (see *Figure 17C*). The nuclear localization of ZAP70 appears further to be independent of signals through the BCR of a CLL cell, as BCR ligation using anti-IgM antibodies did not have an effect on the amount of ZAP70 detected in the nuclear fraction of three primary ZAP70-positive patient samples (see *Figure 17D*).

The nuclear lamina contains pores assembled by nucleoporins, through which ions and small proteins with a molecular mass from <40 kDa can passively diffuse, whereas larger proteins are restricted by their appropriate localization signal (Bonner, 1975; Lange et al., 2007; Paine et al., 1975). ZAP70, as its name implies, has a molecular weight of 70 kDa and needs to be actively transported through the nuclear lamina by import proteins, which only interact with proteins carrying a nuclear localization signal (NLS). The classical NLS (cNLS) consists of either one or two characteristic stretches of amino acids and is therefore called either monopartite or bipartite cNLS (Dingwall and Laskey, 1991; Schmidt-Zachmann et al., 1993; Schmidt-Zachmann and Nigg, 1993).

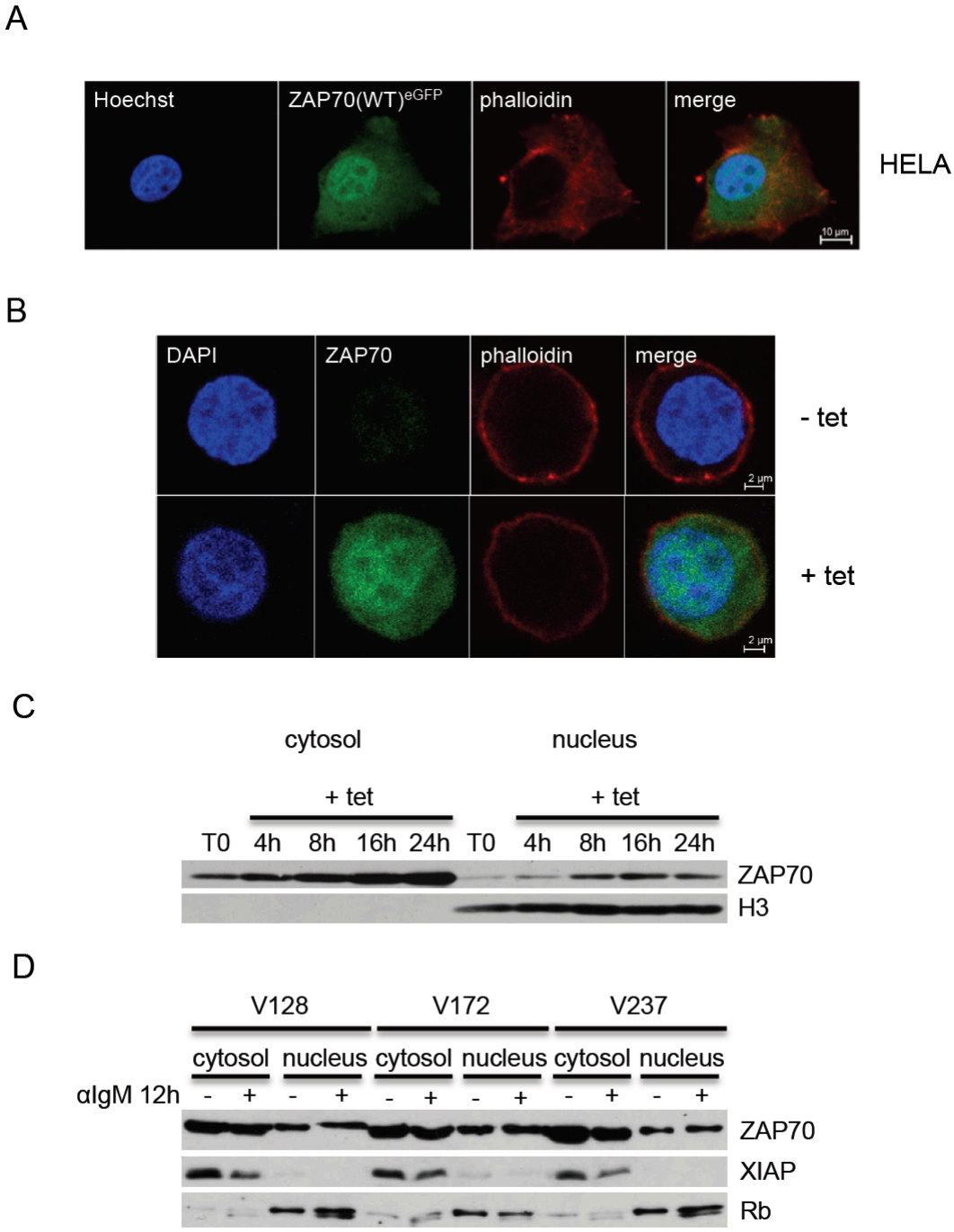

Figure 17 The subcellular distribution of ZAP70 in CLL cells

(A) HELA cells were transfected with the GFP_ZAP70 wild-type fusion construct using lipofectamin and analyzed for ZAP70 localization by confocal laser scanning microscopy. Cells were counterstained with phalloidin for visualization of the cytoskeleton and with Hoechst for nuclear depiction. (B) Representative images of MEC-1$^{ZAP70\text{-}tet\text{-}ON}$, analyzed for the localization of ZAP70 by confocal laser scanning microscopy. MEC-1$^{ZAP70\text{-}tet\text{-}ON}$ were treated with tetracycline for 72 hours and compared to an untreated MEC-1$^{ZAP70\text{-}tet\text{-}OFF}$ population. Cells were counterstained with phalloidin for visualization of the cytoskeleton and with DAPI for nuclear depiction. (C) ZAP70 expression was switched on by the addition of tetracycline for 4, 8, 16, and 24 hours and MEC-1$^{ZAP70\text{-}tet\text{-}ON}$ were subsequently subjected to nuclear fractionation. ZAP70 expression was analyzed by immunoblotting comparing the cytosolic and the nuclear fraction. (D) Three ZAP70-positive CLL patient samples were treated with anti-IgM (10 µg/ml) for 12 hours and, subsequently, subjected to nuclear fractionation. ZAP70 localization in the different cell compartments was evaluated using immunoblotting. XIAP was used as loading control for the cytosolic fraction, whereas Rb served as nuclear loading control.

An *in silico* analysis using the online tool *cNLS Mapper* revealed that ZAP70 carries three potential classical NLS, two bipartite cNLS, and one potential monopartite cNLS. Recent studies revealed, that a monopartite cNLS requires a lysine in position 1 followed by basic amino acid residues in positions 2 and 4 (Conti and Kuriyan, 2000; Fontes et al., 2000; Hodel et al., 2001). The nuclear accumulation of a protein can further be predicted by its affinity to importin α (Hodel et al., 2006; Hodel et al., 2001). The first potential bipartite cNLS of ZAP70 starts at position 71, which is localized inside the N-terminal SH2 domain, the second starts at position 298 in the interdomain B. The potential monopartite cNLS is localized at position 536 at the C-terminal part of the ZAP70 kinase domain (see *Figure 18*). The localization score of 5 indicates that the protein localizes to both the cytoplasm and the nucleus.

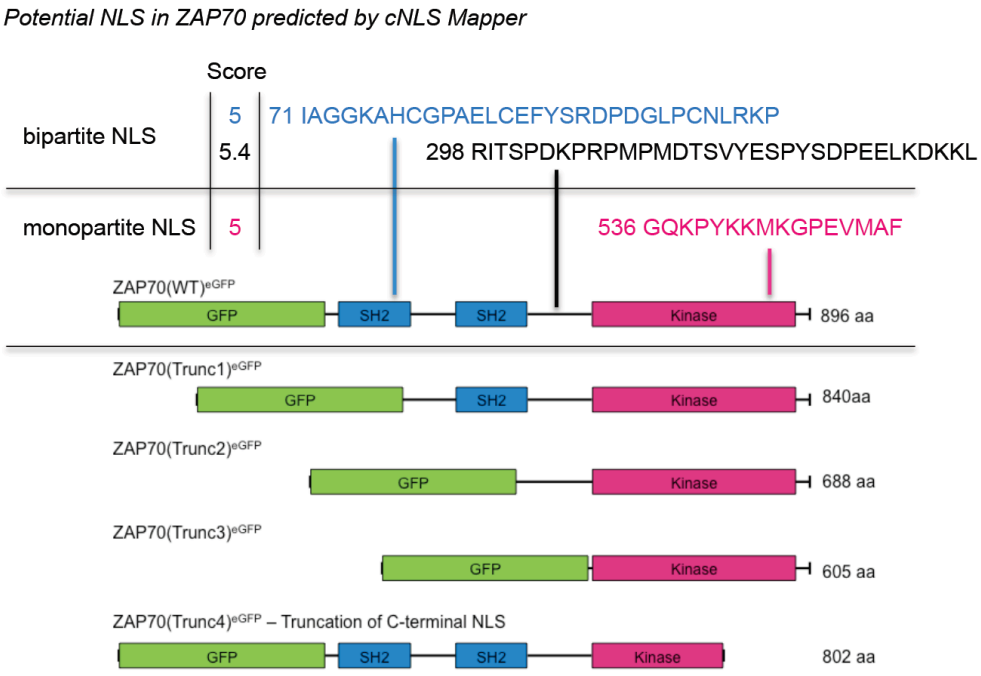

Figure 18 Potential NLS in ZAP70 predicted by cNLS Mapper

In silico analysis of potential nuclear localization sequences (NLS) in the amino acid sequence of ZAP70 was performed using the cNLS Mapper according to manufacturer's instructions (http://nls-mapper.iab.keio.ac.jp/cgi-bin/NLS_Mapper_form.cgi). Three N-terminal truncation constructs (Trunc1 – Trunc3) and one C-terminal truncation of the predicted monopartite NLS of ZAP70 (Trunc4) were established.

To investigate the role of these potential cNLS and of the ZAP70 kinase function in subcellular distribution, I established several N-terminal eGFP-ZAP70 fusion constructs. First, I cloned the full-length wild-type (WT) string *in frame* with the upstream eGFP coding region. I also included a kinase-deficient mutant, which

carries a point mutation from lysine (K) to alanine (A) at position 369 – the so-called KA mutant. In wild-type ZAP70, K369 is located within the kinase domain of ZAP70 near the ATP binding site at position 345 to 352 and is essential for the building of a salt bridge with glutamate residue E386 during catalytical activation of the kinase (see *Introduction p.13*). In addition, I created three N-terminal and one C-terminal truncation constructs, still N-terminally linked to eGFP. The first truncation (Trunc1) removes the N-terminal string including the whole N-terminal SH2 domain of ZAP70 and thereby the first putative bipartite cNLS starting at position 71. Secondly, I deleted the N-terminal amino acid sequence of ZAP70 including the second C-terminal SH2 domain (Trunc2). The third N-terminal truncation (Trunc3) excludes the whole N-terminal part of ZAP70 except the kinase domain and thereby removes not only the N-terminal bipartite cNLS, but also the C-terminal bipartite cNLS starting at position 298. Last, I included one C-terminal truncation construct (Trunc4), which lacks part of the ZAP70 kinase domain including the whole monopartite cNLS.

HELA cells were transfected with the six different GFP-ZAP70 fusion constructs described above using lipofectamine. I conducted confocal imaging experiments using DAPI as nuclear counterstain (see *Figure 19A*) and subsequent quantification of eGFP fluorescence in the cytosol or the nucleus using the ImageJ software revealed several important findings (Rasband, 1997; Schneider et al., 2012). I compared three areas of the same size of the cytoplasm and of the nucleus of the same cell and analyzed a total of five cells of each cell type (see *Figure 19B*). The results revealed that ZAP70 lacking the N-terminal bipartite cNLS still localized to the nucleus (Trunc1 and Trunc2 in *Figure 19*). However, removal of both predicted N-terminal cNLS from the ZAP70 fusion construct significantly decreased the green fluorescence levels in the nucleus compared to the cytosol of the HELA cells (Trunc3 in *Figure 19*). Furthermore, ZAP70 without the C-terminal monopartite NLS showed the fewest abundance of localization to the nucleus and thereby a significant reduction compared to wild-type ZAP70. This observation could be explained by the fact that not only the relevant cNLS was removed, but also part of the ZAP70 kinase domain and this most probably affected its catalytic function. Indeed, nuclear expression of ZAP70 depends on its kinase function as the kinase-deficient mutant localized significantly less to the nucleus compared to wild-type ZAP70.

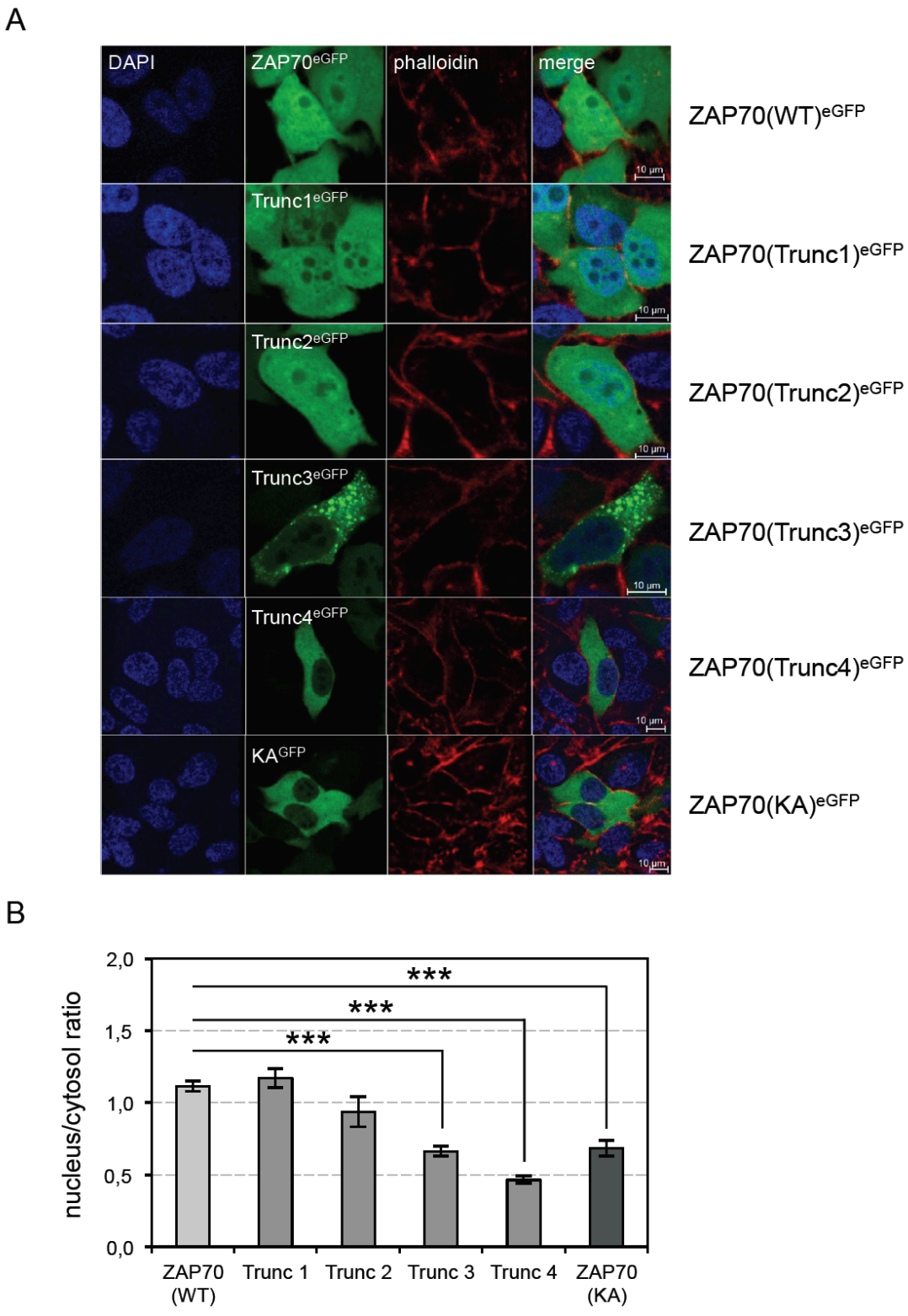

Figure 19 Functional analysis of the nuclear translocation of ZAP70

(A) Representative pictures of HELA cells, which were transfected with 6 different GFP_ZAP70 fusion constructs using lipofectamine. Wild-type ZAP70, three N-terminal truncation products (Trunc1 – Trunc3), one C-terminal truncation of ZAP70 (Trunc4) and a kinase-deficient mutant (KA) were compared in regard to their subcellular distribution. Cells were counterstained with phalloidin for visualization of the cytoskeleton and with DAPI for nuclear depiction. (B) ImageJ analysis of confocal microscopy pictures was performed. Three areas of the same size of the cytoplasm and of the nucleus of the same cell were compared. Five cells of each cell type were analyzed calculating the ratio of the mean values of nucleus/cytosol and results are depicted as mean ± SEM.

** $p < 0.01$, * $p < 0.05$.

Consequently, I focused on the activation of ZAP70 by analyzing activating phosphorylations on tyrosine residues Y315/319 and Y493. As mentioned above, Y315 and Y319 are both located in the interdomain B and initially phosphorylated during the ZAP70 activation process – known from its physiologic expression in T cells (see *Introduction p.13*).

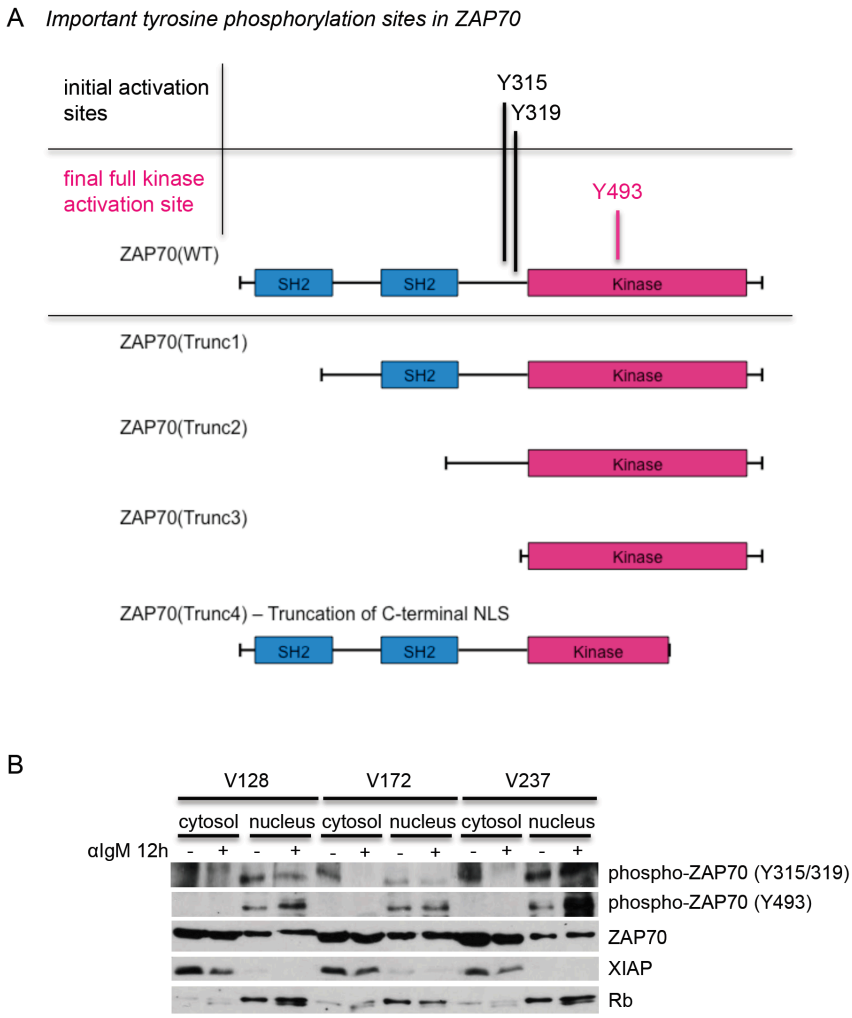

Figure 20 Phosphorylation of ZAP70 upon BCR signals in CLL cells

(A) Location of tyrosine phosphorylation sites in the ZAP70 sequence in relation to the truncation studies. (B) Three ZAP70-positive CLL patient samples were purged and treated with anti-IgM (10 µg/ml) for 12 hours and subsequently subjected to nuclear fractionation. ZAP70 activation was analyzed in the nuclear cell compartment by immunoblotting using antibodies specific to different phosphorylated forms of the protein. XIAP was used as loading control for the cytosolic fraction, whereas Rb served as nuclear loading control.

Y493 is located in the activation loop of ZAP70. Phosphorylation of Y493 is required for the full kinase activity of ZAP70 (see *Figure 20A*). Comparing the cytosolic and the nuclear fractions of ZAP70-positive primary CLL cells treated with either BCR ligating anti-IgM or medium, I discovered that nuclear ZAP70 was phosphorylated on both Y315/319 and Y493 residues (see *Figure 20B*).

Phosphorylation of Y493 was upregulated upon anti-IgM stimulation after 12 hours, whereas, phosphorylation of the residues Y315/319 was steadily detected in the nucleus of ZAP70-positive primary CLL cells, independently of exogenous BCR signals. Strikingly, only nuclear ZAP70 is phosphorylated on Y493, suggesting an active functional role for the tyrosine kinase rather in the nucleus of CLL cells than – as assumed so far – in the cytosol.

3.2.2 The Interaction of ZAP70 with Chromatin Structures

To further characterize the function of ZAP70 in the nucleus and to address the question whether ZAP70 is tightly bound to chromatin in CLL cells, the mobility of ZAP70 in the nucleus of HELA cells was analyzed by fluorescence recovery after photobleaching (FRAP) analysis. HELA cells were transfected with GFP fusion constructs, then spots with a diameter of 8 to 10 µm inside the nucleus of the cell were photo-destroyed using an intensed focused laser beam (Schneider et al., 2013). The fluorescent proteins are irreversibly converted to a non-fluorescent state and a black spot remains (Axelrod et al., 1976; Meyvis et al., 1999; Sprague et al., 2004). Slowly, unimpaired fluorescent molecules diffuse into the black spot and recover the fluorescence. The fluorescence recovery is measured over time, thereby predicting the mobility of the protein of interest in the nucleus. Immobilized proteins show slower fractional fluorescence recovery than unbound, mobile proteins.

Using my previously cloned eGFP_ZAP70 fusion constructs, Dr. Markaki and Ms. Leidescher at the LMU Munich performed the FRAP experiments of wild-type eGFP_ZAP70 compared to unfused eGFP (see *Figure 21A*). No significant difference in the fractional fluorescence recovery in the nucleus of HELA cells was detected, implicating that ZAP70 is very mobile in the nucleus of CLL cells. In addition, following mononucleosome preparations, I performed native chromatin immunoprecipitation studies using specific antibodies to the ZAP70 protein itself or to its eGFP tag. I established reaction conditions for the native ChIP in several experiments using special buffer systems to keep the mononucleosome particles stable. These experiments confirmed the FRAP results, as no clear difference could be detected neither in the pull-down of histone molecules like histone H3 nor in the amount of purified DNA (see *Figure 21B* and data not shown).

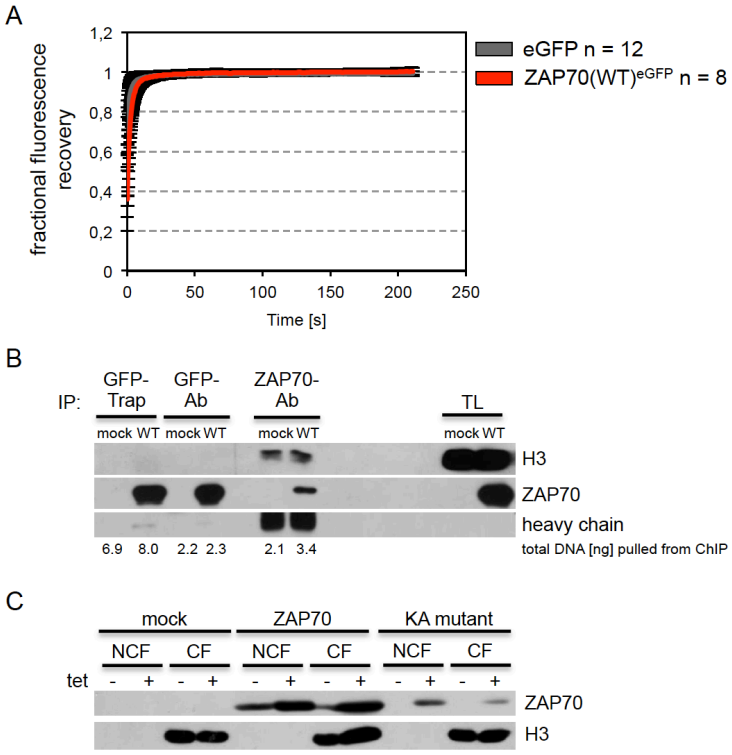

Figure 21 Analysis of the interaction of ZAP70 with chromatin structures

(A) The mobility of ZAP70 was analyzed in the nucleus of HELA cells using the FRAP technique performed by Dr. Yolanda Markaki and Susanne Leidescher (Leonhardt Group, LMU, Munich, Germany). GFP_ZAP70 wild-type fusion protein was compared to unfused GFP protein. (B) Native chromatin immunoprecipitation of ZAP70 was performed from MEC-1 stably expressing either wild-type GFP or GFP_ZAP70 fusion proteins. The pull-down was performed with three different methods: using 1) GFP trap, 2) antibodies specific to GFP and 3) antibodies specific to ZAP70. ZAP70 and associated histone H3 were detected by immunoblotting. Numbers beneath the blot indicate total amount of DNA isolated from the ChIP beads. (C) Chromatin fractionation studies were performed using the inducible ZAP70 expression system. ZAP70 expression was analyzed by immunoblotting comparing the induction of wild-type and kinase-deficient mutant (KA) between the chromatin and the non-chromatin fraction. One representative experiment out of two is shown.

On the other hand, chromatin fractionation experiments using the inducible *ZAP70* expression system showed that ZAP70 appears in the chromatin fraction of MEC-1$^{ZAP70\text{-}tet\text{-}ON}$ (see *Figure 21C*). These results implicate that nuclear ZAP70 is characterized by a high mobility when localized in the nucleus and therefore does not tightly bind to nucleosomes or DNA. The exclusive expression of activated ZAP70 in the nucleus and within the chromatin fraction strongly suggests that its function in this cellular compartment is related to gene expression (see *Figure 16*), potentially through an epigenetic mechanism.

3.2.3 Differential Expression of Histone Modifiers in CLL cells

To further address this hypothesis, I used a rather global approach to identify potential protein binding partners. Stable MEC-1 cell lines constitutively overexpressing ZAP70 containing two N-terminal *Strep*-tags (ZAP70^{high} MEC-1) or carrying the control vector containing the tags without the gene of interest (ZAP70^{low} MEC-1) were established. Both cell lines were subjected to stable isotope labeling by amino acids in cell culture (SILAC) (see *Material and Methods p.63*), whereby proteins of the different cell lines were labeled with amino acids containing stable non-radioactive isotopes. In this study, control ZAP70^{low} MEC-1 cells were labeled with medium heavy amino acids (M) by ingesting lysine (Lys-4) and arginine (Arg-6) with incorporated hydrogen-2 isotopes ^{2}H and carbon-13 isotopes ^{13}C, whereas ZAP70-overexpressing ZAP70^{high} MEC-1 cells remained unlabeled and its proteins were therefore considered as light (L). The completion of the labeling process was analyzed by mass spectrometry by Dr. Merl (Helmholtz Center Munich, Germany), whereby a rate of >95% of labeling was considered as enough. To ensure the completion of the labeling process, labeling was continued for two more passages, before subjecting the cells to Strep-affinity purification. The affinity purification samples of the different cell lines are combined during the purification process and subsequently analyzed in the core facility of the Helmholtz Center Munich by Dr. Merl using mass spectrometry (AP-MS). The differential labeling allowed us to quantify the identified proteins in one mass spectrometry run by directly comparing the peptide peaks produced by the slightly heavier proteins from ZAP70^{low} MEC-1 cells to the light peptide peaks from ZAP70^{high} MEC-1 cells.

As the affinity purification showed a high purity with very low background levels in the control purification, barely any protein with a ratio L/M below 1 was detected (see *Figure 22A*). For the same reason we found only eleven proteins to be significantly enriched in the ZAP70 affinity purification (L) compared to the tags only control (M) (see *Figure 22B*). For my analyses, I took all proteins into account which were enriched more than 2.5-fold in the ZAP70 purification compared to the control.

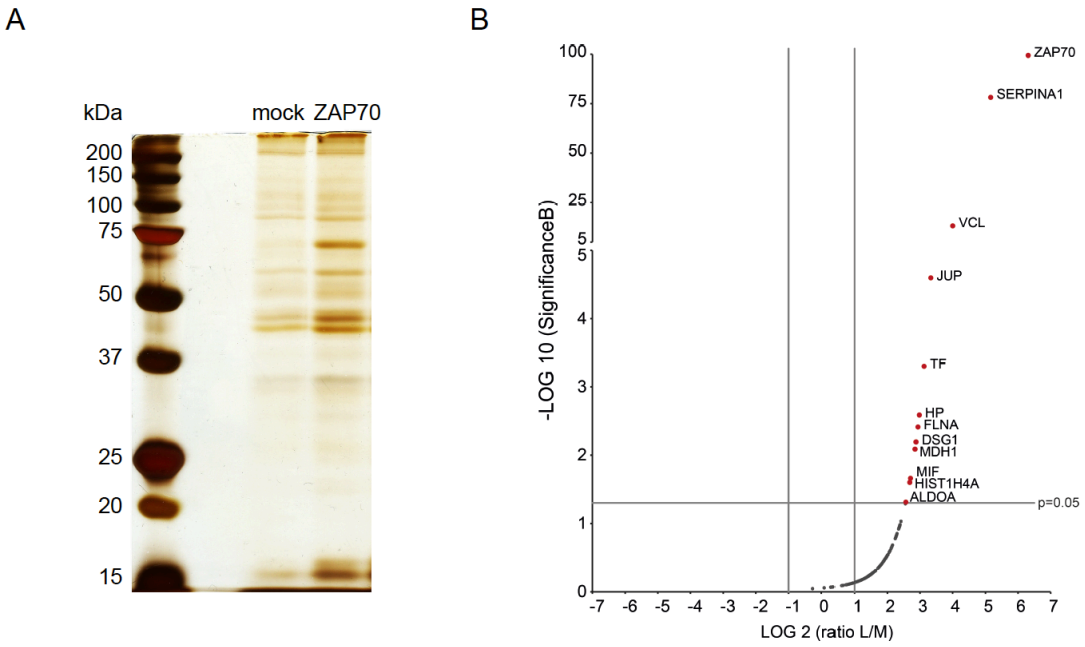

Figure 22 Potential binding partners of ZAP70

Passage-matched MEC-1 cells overexpressing tagged ZAP70 or mock control were grown labeled with medium heavy (Lys-8, Arg-10) versus light (Lys-0, Arg-0) amino acids, respectively (SILAC). Cells were exposed to with PMA (10 ng/ml) and ionomycine for 24 hours before lysis and subsequent Strep-tag based affinity purification. (A) Silver staining of affinity purifications before mass spectrometry analysis. ZAP70 can be assumed as the band appearing only in the ZAP70 affinity purification at 70 kDa. (B) Binding partners of ZAP70 were analyzed using ESI-LC-MS/MS and depicted in a volcano plot by Dr. Juliane Merl (Helmholtz Center, Munich, Germany). Experiment was performed in triplicates.

As mentioned above, ZAP70 is a macromolecule of a size of more than 40 kDa, and therefore, to shuttle to the nucleus, it needs to associate with translocation factors, such as importins and their associated GTPases. The potential cNLS regions inside the ZAP70 amino acid sequence described earlier hint to classical import mechanism. Indeed, I found KPNB1, the importin subunit β-1 to be 3.4-fold enriched with four unique peptides in the protein fraction extracted from the ZAP70 affinity purification (see *Table 32*). In addition, the GTP-binding nuclear protein Ran was found to be enriched 2.5-fold with three unique peptides in the ZAP70 affinity purification compared to control. Besides the shuttling molecules, several nuclear molecules were enriched in the affinity purification of ZAP70 compared to tags only control. As I assumed a potential epigenetic role of ZAP70 in the nucleus of CLL cells, I found it to be a highly interesting that several histone proteins and histone metabolism regulators were associated with ZAP70. I discovered the following histone modulators to be associated with ZAP70: the two prohibitin molecules *PHB* and *PHB2* with an enrichment ratio of 4.1 and 4.9,

respectively, are nuclear factors that are involved in several pathways (Coates et al., 2001; Montano et al., 1999); another example is NAP1L1, the nucleosome

Gene	Protein ID	Unique peptides	Ratio L/M	Ratio L/M variability [%]	Ratio L/M count	p value	Significance
ZAP70	zeta-chain (TCR) associated protein kinase 70kDa	43.00	**78.20**	145.23	172.00	**0.0000**	significant
SERPINA1	Alpha-1-antitrypsin	3.00	**35.37**	27.31	2.00	**0.0000**	significant
VCL	Vinculin	19.00	**15.84**	160.63	16.00	**0.0000**	significant
JUP	Junction plakoglobin	8.00	**10.05**	148.08	7.00	**0.0000**	significant
TF	Serotransferrin	3.00	**8.74**	110.14	3.00	**0.0005**	significant
HP	Haptoglobin	3.00	**7.89**	126.26	3.00	**0.0026**	significant
FLNA	Filamin-A	8.00	**7.66**	116.03	10.00	**0.0039**	significant
DSG1	Desmoglein 1	7.00	**7.36**	47.83	6.00	**0.0064**	significant
MDH1	Malate dehydrogenase, cytoplasmic	2.00	**7.21**	106.13	4.00	**0.0082**	significant
MIF	Macrophage migration inhibitory factor	2.00	**6.55**	40.82	5.00	**0.0218**	significant
HIST1H4A	Histone H4	3.00	**6.45**	107.65	8.00	**0.0250**	significant
ALDOA	Fructose-bisphosphate aldolase A	11.00	**5.93**	114.56	20.00	**0.0488**	significant
GAPDH	Glyceraldehyde-3-phosphate dehydrogenase	11.00	**5.88**	72.43	34.00	0.0518	
DCD	Dermcidin	2.00	**5.35**	35.82	3.00	0.0935	
DSP	Desmoplakin	14.00	**5.15**	101.13	14.00	0.1144	
ENO1	Alpha-enolase	11.00	**5.14**	63.56	31.00	0.1155	
LDHB	L-lactate dehydrogenase B chain	6.00	**5.09**	41.44	14.00	0.1213	
FABP5	Fatty acid-binding protein, epidermal	4.00	**4.93**	139.99	6.00	0.1411	
PRDX1	Peroxiredoxin-1	7.00	**4.92**	67.35	16.00	0.1424	
PHB2	Prohibitin-2	3.00	**4.87**	51.52	7.00	0.1490	
FKBP1A	Peptidyl-prolyl cis-trans isomerase FKBP1A	2.00	**4.82**	202.90	2.00	0.1559	
NAP1L1	Nucleosome assembly protein 1-like 1	3.00	**4.76**	39.75	7.00	0.1643	
NPM1	Nucleophosmin	6.00	**4.74**	66.00	12.00	0.1672	
LDHA	L-lactate dehydrogenase A chain	4.00	**4.41**	47.85	9.00	0.2197	
PKM	Pyruvate kinase PKM	14.00	**4.34**	90.22	33.00	0.2319	
PDIA6	Protein disulfide-isomerase A6	3.00	**4.16**	53.80	7.00	0.2650	
PHB	Prohibitin	4.00	**4.05**	24.11	8.00	0.2864	
HIST1H1C	Histone H1.2	2.00	**3.95**	31.62	5.00	0.3065	
PSMA8	Proteasome (prosome, macropain) subunit, alpha type, 8	2.00	**3.88**	8.06	2.00	0.3209	
LSM12	Protein LSM12 homolog	2.00	**3.72**	120.10	3.00	0.3549	
CCT2	T-complex protein 1 subunit beta	2.00	**3.54**	73.23	3.00	0.3946	
ATXN2L	Ataxin-2-like protein	6.00	**3.49**	37.47	11.00	0.4058	
SET	SET nuclear oncogene	4.00	**3.49**	44.52	12.00	0.4058	
CD74	HLA class II histocompatibility antigen gamma chain	7.00	**3.46**	47.23	20.00	0.4126	
TUBB	Tubulin beta chain	3.00	**3.45**	29.07	7.00	0.4148	
VCP	Transitional endoplasmic reticulum ATPase	7.00	**3.38**	56.89	11.00	0.4308	
KPNB1	Importin subunit beta-1	4.00	**3.37**	32.30	6.00	0.4331	
HIST2H2BE	Histone H2B type 2-E	2.00	**3.34**	92.98	2.00	0.4399	
HIST1H2AH	Histone H2A type 1-H	2.00	**3.29**	53.32	5.00	0.4514	
TKT	Transketolase	4.00	**3.09**	20.11	6.00	0.4977	
LCP1	Plastin-2	20.00	**3.07**	41.04	35.00	0.5023	
CANX	Calnexin	3.00	**3.06**	57.52	7.00	0.5046	
SLC25A5	Solute carrier family 25	2.00	**2.96**	22.30	6.00	0.5278	
NCL	Nucleolin	7.00	**2.92**	79.09	9.00	0.5371	
SLC25A6	Solute carrier family 25 member 6	2.00	**2.82**	23.41	7.00	0.5601	
SFPQ	Splicing factor proline/glutamine-rich	6.00	**2.80**	52.91	8.00	0.5647	
FASN	Fatty acid synthase	11.00	**2.78**	41.05	10.00	0.5692	
DDX5	Probable ATP-dependent RNA helicase DDX5	4.00	**2.78**	32.99	6.00	0.5692	
PABPC1	Polyadenylate-binding protein 1	3.00	**2.67**	31.24	3.00	0.5942	
GNB2L1	Guanine nucleotide-binding protein subunit beta-2-like 1	3.00	**2.64**	41.68	5.00	0.6010	
PGK1	Phosphoglycerate kinase 1	6.00	**2.63**	32.84	8.00	0.6032	
IGHM	immunoglobulin heavy mu constant region	3.00	**2.59**	41.11	9.00	0.6121	
TPI1	Triosephosphate isomerase	10.00	**2.54**	103.58	20.00	0.6232	
RAN	GTP-binding nuclear protein Ran	3.00	**2.53**	72.82	4.00	0.6254	
RBBP4	Histone-binding protein RBBP4	2.00	**2.53**	38.45	2.00	0.6254	
XRCC6	X-ray repair cross-complementing protein 6	6.00	**2.51**	87.90	8.00	0.6298	

Table 32 List of potential binding partners of ZAP70

Results were focused on proteins with more than 2 unique peptides. Common unspecific results, like chaperones and ribosomal proteins, members of the cytoskeleton, heterogeneous nuclear ribonucleoproteins were excluded.

assembly protein 1-like 1, with an enrichment of 4.8-fold; I also found NPM1 with a L/M ratio of 4.7, which is known as nucleophosmin; the SET nuclear oncogene, a histone chaperone, was enriched 3.5-fold compared to control; the RBBP4 protein was enriched 2.5-fold (Balboula et al., 2015; Liu et al., 2015). In addition, ZAP70 is

also associated at a L/M ratio of 2.9 with NCL, nucleolin, which is the main protein in the nucleolus of a cell (Lapeyre et al., 1987). It induces chromatin decondensation by binding to histone H1 (Erard et al., 1988). Assuming an involvement of ZAP70 in epigenetic changes, it is even more exciting, that histone molecules were enriched in the ZAP70 affinity purification. Histone H1 showed a 4.0-fold enrichment, histone H2A a 3.3-fold enrichment, and histone H2B also a 3.3-fold enrichment compared to control purifications. However, the only significant protein that sticks out in this context is histone H4 with a 6.5-fold enrichment in the ZAP70 affinity purification compared to control and a significant p value of 0.025.

3.2.4 Modification of Histone Molecules by ZAP70

The DNA of a eukaryotic cell is wrapped around protein complexes, called nucleosomes (Luger et al., 1997). Histone H4 is part of the nucleosome core particles, which consists of a histone octamer (Davey et al., 2002). Two H2A-H2B dimers encompass a $(H3\text{-}H4)_2$ tetramer in the center of the complex (Arents et al., 1991). Histone H1 interacts with the DNA outside of the nucleosomes near the exits or entries, where it regulates the conformation of the linker DNA between the nucleosomes and subsequently chromatin condensation (Happel and Doenecke, 2009). Nucleosomal core particles are frequently post-transcriptionally modified by acetylation or methylation (Jenuwein and Allis, 2001). These modifications are part of the epigenetic regulation machinery of gene expression as they differentially interfere with DNA accessibility and therefore transcriptional activation or repression (Hake et al., 2004).

Considering that the kinase function of nuclear ZAP70 is constitutively activated independent of BCR signals in the nucleus of CLL cells, that ZAP70 is associated with a changed gene expression profile, and that ZAP70 is significantly associated with histone H4, my next approach was to investigate whether ZAP70 is able to phosphorylate histone H4. For that reason, I established a suitable buffer system to perform a radioactive ZAP70 kinase assays using recombinant histone molecules as substrates and bovine brain tubulin as positive control. The auto-phosphorylation of ZAP70 served as internal positive control. As shown in the autoradiography display of the first experiment, I was able to prove that ZAP70 can phosphorylate histone molecules H2A, H3.1 and, predominantly, H4 *in vitro* (see *Figure 23A*).

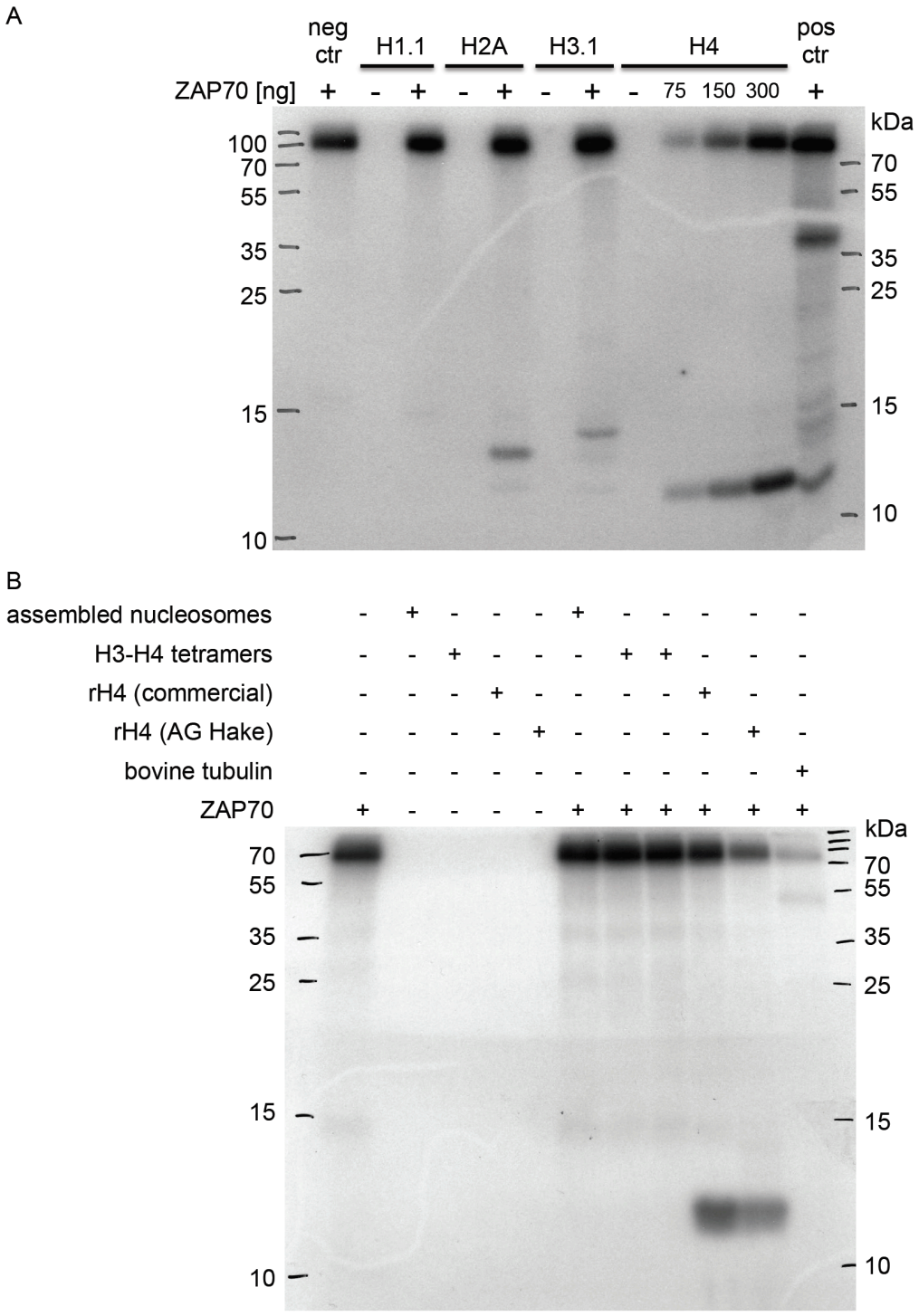

Figure 23 Radioactive ZAP70 kinase assays targeting histone molecules

(A) Radioactive kinase assay was used to analyze the phosphorylation of histone molecules H1.1, H2A, H3.1 and H4 by ZAP70. Samples were analyzed for kinase activity by SDS-PAGE followed by autoradiography. Band pattern were compared to histone only and enzyme only negative controls. Purified bovine brain tubulin at 55 kDa and the auto-phosphorylation of recombinant GST-tagged ZAP70 at 96 kDa served as positive control. One representative experiment out of three is shown. (B) Radioactive ZAP70 kinase assay was used to analyze the phosphorylation of histone H4 in differently complexed nucleosomal particles. Assembled nucleosomes, H3-H4 tetramers and two different recombinant histone H4 proteins were used as substrate and subjected to phosphorylation by recombinant ZAP70 (300 ng). Samples were analyzed for kinase activity by SDS-PAGE followed by autoradiography. Band pattern were compared to histone only and enzyme only negative controls. Purified bovine brain tubulin at 55 kDa and the auto-phosphorylation of recombinant GST-tagged ZAP70 at 96 kDa served as positive control.

I discovered that H4 is only phosphorylated by ZAP70, if it is not associated with other histone molecules, since assembled nucleosomes or H3-H4 tetramers are not subject to phosphorylation by ZAP70 (see *Figure 23B*).

Two modifications of histone H4 play an important role in cancerogenesis, the acetylation of lysine 16 (H4K16ac) and the trimethylation of lysine 20 (H4K20me3) (Fraga et al., 2005). These two modifications were reported to be lost in the process of malignant transformation in different neoplastic disorders. Therefore, I examined the acetylation and the methylation status of H4 in primary CLL samples comparing the ZAP70-positive with the ZAP70-negative subgroup. Contrary to my assumption, ZAP70-positive CLL samples revealed higher acetylation levels of lysine K16 and higher trimethylation levels of lysine K20 of histone H4 than ZAP70-negative CLL cells (see *Figure 24*).

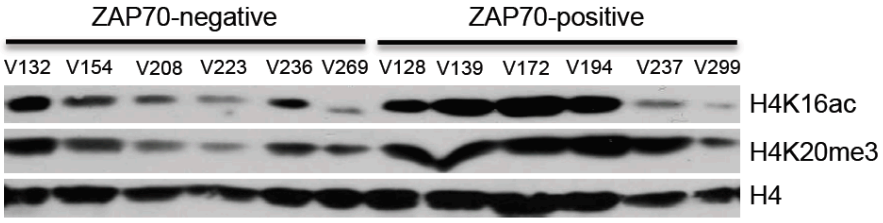

Figure 24 Lysine modifications of histone H4 in primary CLL cells

Histone H4 modifications were analyzed by immunoblotting using antibodies specific for H4 acetylated on lysine 16 (H4K16ac), for H4 tri-methylated on lysine 20 (H4K20me3) and for total H4 protein. Six individual primary CLL samples from each ZAP70 subgroup were compared.

Consecutively, I analyzed the alterations in the transcriptional expression levels of the upstream key regulators by quantitative RT-PCR – the histone H4 acetylase hMOF, the key histone H4 deacetylase SIRT1 and the histone H4 methyl transferases PrSert7, and Suv4-20 homologues 1 and 2 (see *Figure 25A*). ZAP70 induction by tetracycline treatment led to a significant reduction of Suv4-20H2 mRNA level in the inducible cell line (see *Figure 25B*). Analysis of this important histone H4 methyl transferase in primary CLL cells confirmed these results. Suv4-20H2 mRNA transcript levels were significantly lower in ZAP70-positive CLL cells compared to ZAP70-negative (see *Figure 25C*).

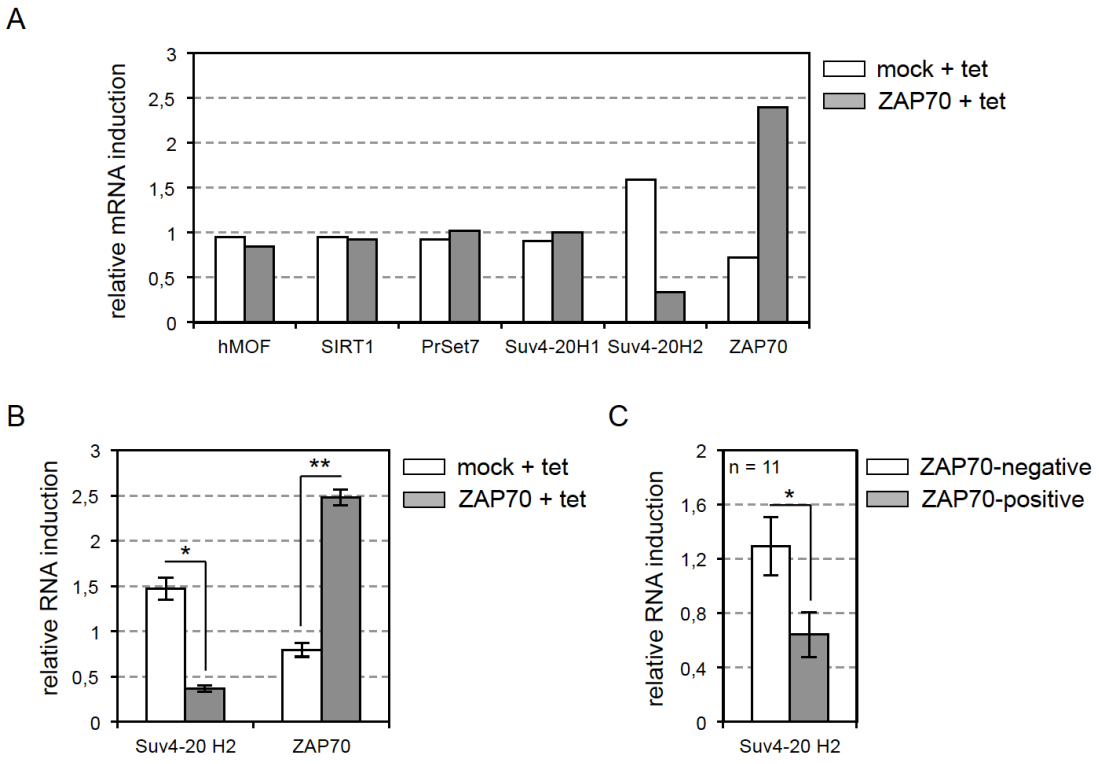

Figure 25 Differential expression of histone modifiers in CLL cells

(A) Transcriptional regulation of histone acetyl transferase hMOF, histone deacetylase SIRT1 and histone methyltransferases PrSet7, Suv4-20 homologues 1 and 2 were analyzed by quantitative RT-PCR using specific primers for the appropriate human coding region. The relative induction of gene expression after ZAP70 induction over 72 hours with tetracycline in MEC-1$^{ZAP70\text{-}tet\text{-}ON}$ was normalized to the expression of GAPDH and compared to the expression in tetracycline-treated MEC-1^{mock} control (depicted as fold induction). Results are depicted as delta delta Ct ± SEM. (B) Transcriptional regulation of the histone methyltransferase Suv4-20 homologue 2 was analyzed by quantitative RT-PCR using specific primers for the appropriate human coding region. The relative induction of gene expression after ZAP70 induction over 72 hours with tetracycline in MEC-1$^{ZAP70\text{-}tet\text{-}ON}$ was normalized to the expression of GAPDH and compared to the expression in tetracycline-treated MEC-1^{mock} control (depicted as fold induction). Results are depicted as the mean delta delta Ct ± SEM calculated from two experiments. (C) Transcriptional regulation of the histone methyltransferase Suv4-20 homologue 2 was analyzed by quantitative RT-PCR using specific primers for the appropriate human coding region. Suv4-20h2 mRNA expression in ZAP70-positive CLL samples was normalized to the expression of GAPDH and compared to the mean expression levels in ZAP70-negative CLL cells (depicted as fold induction). Results are depicted as mean delta delta Ct ± SEM from eleven individual primary CLL samples from each subgroup.

Concluding, the data presented in this thesis suggest a functional role of ZAP70 in the differential epigenetic regulation of gene expression in CLL cells, leading to a higher resistance to apoptosis.

4 Discussion

4.1 The Involvement of ZAP70 in Apoptosis Regulation in CLL

Despite the promising cutting-edge progresses in developing new targeted therapies for CLL, still, the medical research community faces the challenge of scientifically explaining the very differential clinical outcomes of CLL patients (Woyach et al., 2012). Even though we can be confident that the new compounds targeting the BCR signaling pathway will be applicable to a high number of CLL patients, current medical developments focus on personalized treatment approaches to possibly cure cancer in the future. As published and widely discussed, one might ask the question why IGHV-unmutated and IGHV-mutated CLL cases are currently diagnosed with the same disease, even though we suspect a different type of cell-of-origin for the two entities and the clinical courses differ vastly (Forconi et al., 2010).

In this study, I attempted to contribute to a better understanding of the underlying pathogenic mechanisms that lead to the differential behavior of CLL cells of different subtypes based on the expression of ZAP70. The expression of ZAP70 in CLL cells is associated with an unmutated IGHV mutational status and is a strong predictor of a dismal clinical course (Rassenti et al., 2004). Patients carrying a ZAP70-positive leukemia require treatment far earlier than patients with a ZAP70-negative leukemia. In addition, ZAP70-positive CLL cases develop resistance to chemotherapy more often than those not expressing the kinase (Danilov et al., 2005; Tam and Keating, 2010; zum Buschenfelde et al., 2010). Primary leukemic B cells are very difficult to maintain in culture (Collins et al., 1989). It has been impossible to propagate primary CLL cells *ex vivo* for a longer time period and to transfect them with DNA constructs. Hence, I used an inducible ZAP70 expression system that proved to be a suitable cell line model to study the differential behavior of the cell line upon ZAP70 expression. Firstly, the ZAP70-induced increase of CD38 expression in MEC-1 cells fits previous reports on ZAP70-positive primary CLL cells (Huttmann et al., 2006; Pepper et al., 2006). Secondly, the BCR signaling pathway appeared to become more active upon ZAP70 induction in MEC-1$^{ZAP70\text{-}tet\text{-}ON}$, in accordance with previous reports, where ZAP70 has been implicated to participate and thereby enhance autologous BCR

signaling in CLL cells (Chen et al., 2005a; Chen et al., 2008; Cutrona et al., 2008; Duhren-von Minden et al., 2012). Finally, I showed that the inducible cell line was rather characterized by a deregulated apoptosis than proliferation, which again falls in line with previous work regarding the increased resistance to apoptosis of ZAP70-positive CLL cells (Lorand-Metze et al., 2015).

In 2008, Pepper et al. described an association of increased anti-apoptotic Mcl-1 protein levels and ZAP70 levels in primary CLL cells (Pepper et al., 2008). However, these data were descriptive in nature and no causal relation was assumed. The findings in this study provide evidence for the first time that ZAP70 expression in CLL cells indeed causes the upregulation of Mcl-1 protein levels. When ZAP70 expression was switched on, Mcl-1 levels increased, and they decreased again once ZAP70 expression was switched off. As an off-target tetracycline effect could be excluded, I postulate that ZAP70 is partly causative for the higher resistance to chemotherapeutics mediated by a downstream upregulation of Mcl-1. Especially, the BH3 mimetic ABT-737 is known to specifically inhibit Bcl-2, Bcl-X_L and Bcl-w, but not Mcl-1, and high levels of Mcl-1 protect cells from ABT-737-induced apoptosis (van Delft et al., 2006; Vaux, 2008). Mcl-1 protein levels are regulated with a rapid turnover rate, which gives the cell the opportunity to adapt immediately to environmental changes and switch from cell survival to apoptosis (Binsky-Ehrenreich et al., 2014; Pedersen et al., 2002). The proteasome was reported as the main degradation pathway of Mcl-1 and also proved to be the responsible degradation mechanism in this study (Ding et al., 2007; Nijhawan et al., 2003). The post-transcriptional stabilization of Mcl-1 can either be due to an increase in downstream regulatory factors of the proteasomal machinery or due to differences in the expression and activity of molecules, which function upstream to mark Mcl-1 for polyubiquitination and therefore for destruction by the proteasome.

As previously published, MULE is the main E3 ubiquitin ligase responsible for Mcl-1 polyubiquitination (Zhong et al., 2005). Another E3 ubiquitin ligase, the tumor suppressor Fbw7, has been implicated to counteract Mcl-1 stability in a GSK3β-dependent manner in acute lymphocytic leukemia (Inuzuka et al., 2011). Fbw7 is frequently mutated in human malignancies and its loss of function disturbs the turnover of several oncoproteins like Myc, cyclin E and Notch (Welcker and

Clurman, 2008). Even though I discovered a tendency of lower Fbw7 expression in ZAP70-positive CLL cells, however, the slightly higher expression of MULE could compensate for this reduction. Recent discoveries revealed a counter mechanism of the proteasomal degradation of Mcl-1, caused by the de-ubiquitination of lysine 48 of Mcl-1 by Usp9x (Schwickart et al., 2010). Overexpression of Usp9x was correlated with higher Mcl-1 levels in colon and lung carcinoma as well as in B-cell lymphoma. The results of this study suggest that this oncogenic mechanism is not enhanced in ZAP70-positive CLL cells. Still, one needs to consider that protein levels and deubiquitinase activity of Usp9x might fluctuate depending on the location and the state of the CLL cell. Basic protein expression levels do not sufficiently prove differences in the activity of these regulators. Further investigations like polyubiquitination assays and knock-down experiments of Usp9x are needed to provide deeper insight into the Mcl-1 regulation in CLL cells.

The main axis by which Mcl-1 is subjected to degradation in CLL cells has been described by Gandhi et al. in 2008 (Gandhi et al., 2008). Before Mcl-1 is degraded by the proteasome, it is marked for polyubiquitination through phosphorylation by GSK3β at serine residue 159 (Maurer et al., 2006). GSK3β phosphorylates and thereby destabilizes Mcl-1 in response to external growth factors. Maurer et al. postulated that Mcl-1 phosphorylated at serine 159 is recognized and subsequently polyubiquitinated by MULE. In this study, I report a highly significant reduction of baseline expression and enhanced inactivation of GSK3β in ZAP70-positive CLL cells compared to ZAP70-negative CLL cells. Notably, loss of GSK3β activity by missense splicing has been associated with chronic myeloid leukemogenesis (Abrahamsson et al., 2009). In flow cytometry analyses, the group could show that GSK3β protein levels decrease during the transition from chronic phase to blast crisis in CML patient samples. In addition, misspliced GSK3β-expressing leukemic progenitor cells showed enhanced engraftment in mice compared to cells expressing full-length GSK3β. In addition, GSK3β is highly inactivated in epithelial cancers (Kao et al., 2014) and breast cancer (Wang et al., 2006). In these types of cancer, loss of GSK3β function leads to oncogenic events and hence, GSK3β functions as tumor suppressor.

GSK3β is a central signaling molecule, which is involved in multiple signaling pathways and needed for cell survival. Its silencing mediates resistance to

radiotherapy and overexpression of cyclin D1 (Plate, 2004; Shimura, 2011; Watson et al., 2010). In this study, a significant reduction of *CCND1*, which encodes cyclin D1, was observed following ZAP70 induction in the microarray. Cyclin D1 is synthesized during G1 phase regulating cyclin-dependent kinases 4 and 6 and is rapidly degraded, once the cell enters the S phase (Baldin et al., 1993). Indeed, former studies have shown that high levels of cyclin D1 are associated with a better overall survival of CLL patients (Paul et al., 2005). Furthermore, the group around Ougolkov described GSK3β to translocate to the nucleus of CLL cells (Ougolkov et al., 2007). Its inhibition leads to epigenetic silencing of NFκB-mediated transcription of Bcl-2 and XIAP and induction of apoptosis through an increase of methylation of H3K9, H3K27 and, most importantly, H4K20 at the promoter sites of these gene.

Most probably, there are multiple pathways involved in the GSK3β-dependent stabilization of Mcl-1 in CLL cells: it is known that the protein kinase AKT phosphorylates GSK3β at serine 9 and thereby causes the inhibition of its kinase function (Cross et al., 1995; Frame et al., 2001). It has also been established, that sustained BCR signaling in CLL cells is responsible for a higher activity of AKT (Castello et al., 2013; Donahue and Fruman, 2003) and that the AKT pathway is more important for the survival of ZAP70-positive compared to ZAP70-negative CLL cells (Schrader et al., 2014). Hence, the AKT-mediated inhibition of GSK3β is facilitated in ZAP70-positive CLL cells, which my data confirm by showing that the inhibitory phosphorylation of GSK3β is significantly enhanced in ZAP70-positive primary leukemic cells. Therefore, I postulate that the lower basic protein levels and the lower activity of GSK3β in ZAP70-positive CLL cells entail a higher stability of Mcl-1 protein levels.

Another possible impact might be the overexpression of the oncogene SET in CLL cells (Christensen et al., 2011). I identified SET as potential binding partner of ZAP70 by AP-MS as seen in *Table 32*, but I was not able to validate it as strong binder by immunoprecipitation, because of low antibody affinity presumably due to of a low antigenicity of the SET protein. In general, SET proved difficult to be detected in protein analyses. Recently, SET has been described to be associated with shorter time to treatment and overall survival (Christensen et al., 2011). SET overexpression was also significantly associated with an unmutated IGHV status

and therefore, one can assume that SET protein levels might be increased in ZAP70-positve CLL cases. SET is also known as I2PP2A, which describes its cytosolic function to inhibit the serine/threonine protein phosphatase 2A (PP2A) (Li et al., 1996; Switzer et al., 2011). PP2A itself is involved in multiple cellular pathways, one being the regulation of AKT and GSK3β (Eichhorn et al., 2009; Schonthal, 2001; Wera and Hemmings, 1995). PP2A may activate GSK3β by direct dephosphorylation at serine 9 as some reports suggest (Wang et al., 2015), but more probably through dephosphorylation and subsequent inhibition of AKT, which usually inhibits GSK3β (Ivaska et al., 2002; Kim and Kimmel, 2000; Millward et al., 1999). A higher expression of SET might therefore inhibit PP2A, thereby adding to the effect of AKT-dependent inhibition of GSK3β. These hypotheses are further supported by the microarray analysis. The gene *PPP2R1B* was significantly downregulated in MEC-1 cells overexpressing ZAP70. *PPP2R1B* encodes the 65 kDa regulatory subunit A β isoform of PP2A, which functions as a scaffold for the heterotrimerization with a regulatory B subunit and a catalytic C subunit to form the functional holoenzyme PP2A. *PPP2R1B* has been proposed as potential tumor suppressor gene, as *PPP2R1B* somatic aberrations, including deletions and missense mutations in human lung, colon and ovarian cancer probably disrupt the PP2A holoenzyme structure and thereby impair its function (Campbell and Manolitsas, 1999; Wang et al., 1998). The downregulation of the tumor suppressor gene *PPP2R1B* following ZAP70 induction might therefore hint to an impaired function of PP2A in ZAP70-positive CLL cells, a subsequent increase in AKT kinase activity and hence the inactivation of GSK3β by phosphorylation at serine 9. These data add to the conjecture that ZAP70 entails stabilization of the anti-apoptotic Mcl-1 via the inhibition of its determination to destruction via the PP2A/AKT/GSK3β cascade and thereby enhance resistance to apoptotic stimuli (see *Figure 26*). SET has been studied intensely in immunoblot analyses in the inducible cell line system, were one initial experiment showed a correlating increase in SET protein levels upon ZAP70 induction and also a reduction upon switch-off (data not shown), but as discussed below, the immunoblot conditions were not sufficient to provide valid data. To address this issue in the future, overexpression studies of SET in the inducible ZAP70 cell line combined with fluorescence resonance energy transfer (FRET) can be used to prove that ZAP70 and SET interact and that the protein levels of SET increase upon ZAP70

induction. Further research is needed to complete the complex picture of the cytosolic mechanisms taking place in ZAP70-positive CLL cells.

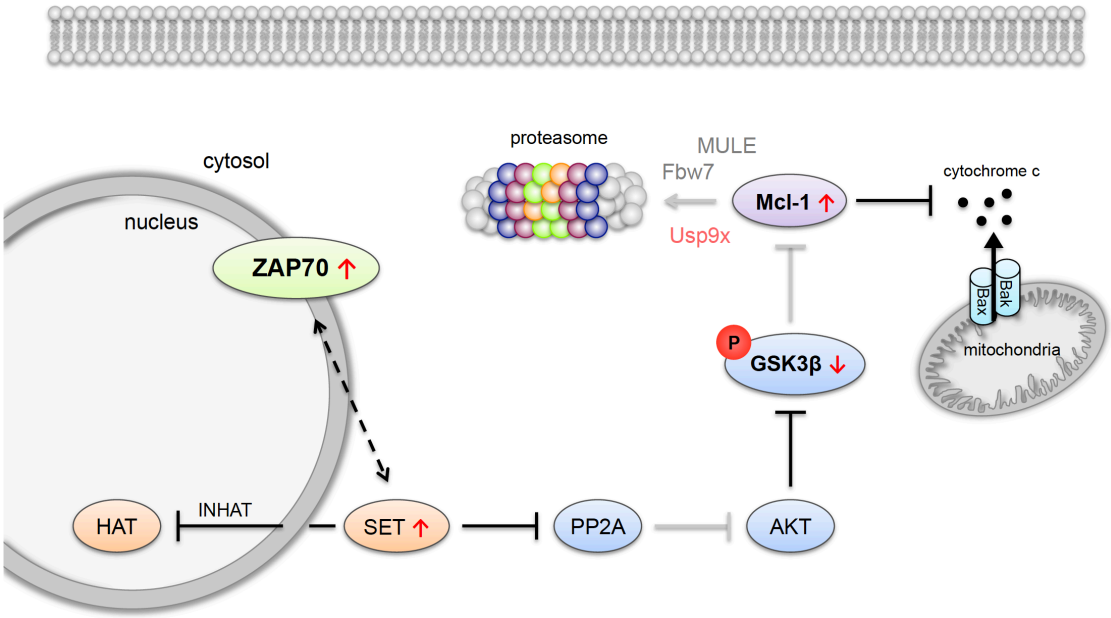

Figure 26 Proposed model

To functionally prove the involvement of SET in the pathogenic anti-apoptotic processes, knock-down experiments using siRNA in primary CLL cells were attempted, but failed due to three obstacles (data not shown): As mentioned above, the lack in specificity of commercially available antibodies impaired the read-out. Second, primary CLL cells are generally transfected with a low efficiency using traditional methods. And lastly, the long half-life of SET of 72 hours is problematic, as CLL cells cannot be obtain in culture *ex vivo* without certain stimulation regimes or stromal support. Under stromal support, however, the CLL cells change phenotypically, become very resistant to apoptosis and hence, apoptosis-related studies are not comparable to the conditions used for my studies (Lutzny et al., 2013). In future, the new clustered interspaced short palindromic repeats (CRISPR) knock-out method could be valuable to perform such functional studies, as it has similar features as RNA interference and shows a high efficiency in primary cells (Ledford, 2015). One could also use SET-inhibiting peptides and GSK3β inhibitors to further functionally characterize the Mcl-1 degradation pathway in ZAP70-positive CLL cells. Furthermore, I suggest performing CRISPR for Usp9x in ZAP70-positive CLL cells to study the potential functional differences

and effects on the ubiquitination and degradation of Mcl-1 using an *in vitro* ubiquitination assay and half-life analyses.

Notably, ZAP70 is also characterized by a very long half-life in CLL cells, as it has been shown that it is protected from degradation by the interaction with heat shock proteins (Castro et al., 2005). In this study, even though I was able to successfully knock down ZAP70 in primary CLL cells on stromal support and subsequently performed microarray analyses, the data were not shown, as the stromal support changes intrinsic features of the primary leukemic cells. The CRISPR method will be used in future studies to knock down ZAP70 in CLL cells without stromal support and, therefore, to extend the functional analysis of the ZAP70 kinase function in CLL cells.

4.2 Implications for ZAP70 in Epigenetic Mechanisms in CLL

My data provide evidence that the overexpression of ZAP70 is associated with a significantly altered expression of GSK3β in CLL cells. Notably, even though one would assume to find ZAP70 solely near the plasma membrane in the cytosol, I could show that ZAP70 is also located to the nucleus of CLL cells independently of external BCR signals, where it is constitutively activated. With its molecular mass of 70 kDa, ZAP70 is too big to passively diffuse through nuclear pores and therefore needs a nuclear localization sequence to be actively transported to the nucleus by shuttling molecules (Lange et al., 2007). Through deletion of predicted cNLS in different truncation constructs, I discovered that, in order to localize to the nucleus, ZAP70 needs its kinase activity as well as the C-terminal monopartite cNLS. In the classical nuclear import mechanism, cNLS are recognized by a trafficking molecule, importin α. Importin α on its end forms a heterodimer with importin β, which mediates the interaction with the nuclear pore during translocation of the protein (Gorlich et al., 1995). Once inside the nucleus, the Ras family GTPase Ran binds the complex provoking the release of importin β from importin α, which again interacts with its export receptor and a nucleoporin to release the cNLS-carrying cargo into the nuclear lumen (Bonner, 1975; Lee et al., 2005; Paine et al., 1975). Notably, I identified importin β as well as Ran as binding partners of ZAP70 by AP-MS. Furthermore, the implication that ZAP70 needs its kinase function to translocate to the nucleus, provoke the idea that ZAP70 phosphorylates yet unknown target molecules involved in the intracytoplasmatic transport of ZAP70 towards the nuclear lamina or the nuclear import. These findings provide evidence that the functional ZAP70 kinase is actively transported via the nuclear lamina by the classical import machinery.

My data suggest that ZAP70 is very mobile inside the nucleus of CLL cells. Although it is probably not a strong binder of chromatin components, however, the subcellular fractionation assays proved that ZAP70 is associated with chromatin structures. Notably, the AP-MS analyses revealed several nuclear and, even more important, chromatin-associated interaction partners of ZAP70. Four histone molecules seem to associate with ZAP70. Histone H4 revealed as the only nuclear interacting partner of ZAP70 with a significant p value and ZAP70 was also associated with several histone-remodeling factors. In addition, I co-purified

histone H1.2, histone 2A and 2B with an enrichment of more than 3-fold compared to control and I found a significant upregulation of the gene *HIST1H1C* upon ZAP70 overexpression, which encodes the histone molecule H1.2. Histone H1.2 is the most abundant nuclear histone in most cell types. It is part of the linker histone H1 family, but shows – together with H1.1 – the lowest affinity to chromatin compared to the other isoforms (Th'ng et al., 2005). It is known to bind chromatin at regions with low GC content and associates with low gene expression (Millan-Arino et al., 2014). H1.2 is differentially phosphorylated in different stages of human breast cancer (Harshman et al., 2014). Notably, it was also reported to participate in apoptosis induction, however the exact mechanism is not clear (Garg et al., 2014). Żołnierczyk *et al.* recently proposed that histone H1.2 is translocated from the nucleus to the cytoplasm of CLL cells following treatment with cytostatic purine analogs and alkylating agents (Zolnierczyk et al., 2013). The group postulated this translocation as a hallmark of apoptosis induction. However, this translocation could not be linked to a higher potential to undergo apoptosis. Hence, I postulate that the upregulation of H1.2 upon ZAP70 overexpression may enable the cell to react faster to apoptotic stress by recognition of DNA double-strand breaks.

Still, one might wonder, why I chose to pursue a possible involvement of ZAP70 in chromatin remodeling, as chromatin immunoprecipitations could not validate a tight binding of ZAP70 to histone molecules. The ChIP experiments performed in this study were carried out under native conditions following mononucleosome preparation. For follow-up studies, I suggest to cross-link proteins to chromatin structures using formaldehyde conditions, which have to be titrated to an optimum before subjecting the samples to ZAP70-specific ChIP followed by sequencing. Additionally, the positively charged histones are generally described as “sticky”, as they easily interact with negatively charged components, e.g. with matrix particles or tags in an affinity purification. Recently, a consortium of researchers composed the so-called contaminant repository for affinity purification-mass spectrometry data, short the CRAPome, and described histone molecules as ubiquitous contaminants (Mellacheruvu et al., 2013).

However, a high number of hits in the AP-MS were identified as chromatin-associated factors and these factors present more reliable results than histones.

Furthermore, ZAP70 expression in CLL cells leads to a distinct change in the gene expression signature. Notably, recent evidence suggested a histone-modifying role for other non-receptor tyrosine kinases in the nucleus of human leukemic cells (Dawson et al., 2009). The group showed that the Janus kinase 2 (JAK2) phosphorylates histone H3 molecules on a particular tyrosine residue, Y41. ChIP experiments revealed that JAK2 hereby directly regulates the expression of the oncogene *LMO2* by the exclusion of the heterochromatin protein alpha (HP1α) from its promoters, which is involved in gene repression by heterochromatin formation. Due to these data, I chose to pursue the potential chromatin-associated function of ZAP70 in the nucleus of CLL cells and suggest further studies on this subject.

DNA accessibility for transcriptional activation is regulated by several epigenetic mechanisms, one being the covalent modifications of amino acid residues in the histone tails, e.g. by acetylation or methylation. Acetyl groups carry rather negatively charged atoms, whereas methyl groups are rather positively charged. As the DNA is negatively charged due to its phosphate groups in the backbone of the helix, the chromatin is more tightly packed, when the histone molecules the DNA is wrapped around are methylated. And vice versa, the DNA becomes more accessible upon histone acetylation. However, one has to keep in mind that there are several amino acid residues in the histone molecules H2A, H2B, H3 and H4, which are frequently modified (Strahl and Allis, 2000) and only a few modifications of histone H3 and H4 have been described as contingent with transcriptional repression. DNA strings carrying silent genes are primarily associated with di- or trimethylated histone H3 on lysine residues K9 and K27, or trimethylated lysine 20 in histone H4 (Mikkelsen et al., 2007; Rosenfeld et al., 2009). Low levels of methylation of H4K20 and acetylation of H4K16 have been associated with areas of high gene expression. Still, a comprehensive understanding of the histone code theory and its different combinatory possibilities of the individual histone modifications remains broadly elusive (Jenuwein and Allis, 2001). Several studies have investigated accessory molecules, which interact with histone molecules and influence the epigenetic regulation of gene expression. For instance, there are so called histone chaperones that act as scaffold to facilitate the approximation of histone modifying enzymes, like histone acetylases (HAT) and deacetylases (HDAC), and histone methyltransferases (HMT) to the histones

molecules and therefore support covalent histone modifications (Burgess and Zhang, 2013). Other factors help the nucleosome assembly or disassembly and chromatin compaction. We are just beginning to comprehend the multiple regulatory patterns involved. Interestingly, I identified several histone- or nucleosome-associated molecules by AP-MS as ZAP70-interacting proteins. Prohibitin molecules, for example, are involved in cell cycle regulation as response to exogenous growth signals (Gamble et al., 2007; Rossi et al., 2014) and the nucleosome assembly protein 1 like 1 (NAP1L1), short hNRP, is potentially involved in regulating chromatin formation and the modulation of cell proliferation. In addition, I found that the *NAP1L2* gene, whose gene product is involved in transcriptional regulation of the cell cycle, was significantly downregulated upon ZAP70 induction in the gene expression array (Attia et al., 2007; Simon et al., 1994). Finally, ZAP70 also interacts with the histone chaperones nucleophosmin (NPM1) (Swaminathan et al., 2005) and RBBP4, which target chromatin remodeling factors and histone deacetylases to their substrates (Liu et al., 2015). The epigenetic regulation of gene expression is composed of highly complex mechanisms that include multiple combinations of histone modifications. Although, ZAP70 appeared to be very mobile in the nucleus of CLL cells, still, it can be assumed that future CHIPSeq experiments using formaldehyde cross-linking as proposed above will identify specific DNA binding sites. The interaction of ZAP70 with several histone-remodeling molecules further nurtures the idea that ZAP70 engages in an epigenetic mechanism. In addition, the enzymatic activity of HDACs has recently been proposed as an independent prognostic marker in CLL (Van Damme et al., 2014). Higher HDAC activity is associated with ZAP70 overexpression, shorter treatment-free survival and overall survival (Wang et al., 2011a). Hence, results from my work underscore that ZAP70 is associated with histone molecules and histone-modulating factors and hence might influence DNA accessibility for transcriptional activation or repression in the nucleus of CLL cells.

For future experiments, I propose a new technology called assay for transposase-accessible chromatin with high throughput sequencing (ATAC-Seq), which is used to study the accessibility of the chromatin for transcription-regulating factors (Buenrostro et al., 2013). In this assay, the activity of the enzyme Tn5 transposase is used to map chromatin structures accessible to transcription genome-wide. The transposase inserts sequencing adapters into these accessible

regions, which are subsequently subjected to high throughput sequencing. One major advantage of ATAC-Seq is the low number of 500 to 50,000 cells needed for a proper readout. I propose to use this new technique to examine the influence of ZAP70 expression on the accessibility of the chromatin of primary CLL cells and in the inducible MEC-1$^{ZAP70\text{-}tet\text{-}ON}$ system, and compare the sequencing results to regions associated with genes, which were identified in the microarray from this study. This experiment will start from a rather global perspective without the need of immunoprecipitation under aggravated buffer conditions and will focus on the change of epigenetic regulation of transcription in respect to ZAP70 expression.

Notably, ZAP70 was associated with a significant change in the expression of 427 genes, including proto-oncogenes and tumor suppressor genes. One tumor suppressor gene, which was found to be significantly downregulated upon ZAP70 induction, is the *ATM* gene mentioned in the introduction (Stilgenbauer et al., 1997). It encodes a serine/threonine protein kinase, which acts as a central regulator of cell cycle arrest and apoptosis induction following DNA damage (Banin et al., 1998; Canman and Lim, 1998). In this process, ATM phosphorylates the tumor suppressor p53 and the oncogene Mouse double minute 2 homolog (Mdm2), which was found to be significantly upregulated in MEC-1$^{ZAP70\text{-}tet\text{-}ON}$. Mdm2 functions as an E3 ubiquitin ligase, which marks tumor suppressor p53 and itself for destruction by polyubiquitination (Chen et al., 1995; Honda et al., 1997; Oliner et al., 1992). Its overexpression has been reported for several cancer types, including solid tumors as well as leukemia (Rayburn et al., 2005). The underrepresentation of ATM combined with the overexpression of Mdm2 might enable ZAP70-positive CLL cells to evade apoptosis following DNA damage. It also might have an impact on cell cycle regulation. Lastly, it is important to note for future therapy regimes for ZAP70-positive CLL cells that *CD52* was significantly overexpressed of in MEC-1$^{ZAP70\text{-}tet\text{-}ON}$ cells. As current therapeutics include the monoclonal anti-CD52-antibody alemtuzumab, this therapy approach may be especially applicable for patients with a ZAP70-positive CLL cases relapsing from chemotherapy (Hu et al., 2009; Nabhan, 2005). Therefore, I postulate that ZAP70 overexpression increases the malignancy of the CLL clone by suppressing tumor suppressor genes and enhancing the expression of proto-oncogenes.

One particular molecule already mentioned in the first part of this discussion is the SET nuclear oncogene, which is known as a multitasking protein (Seo et al., 2001). Besides its cytosolic function to inhibit PP2A, it is predominantly localized in the nucleus and here it acts as histone chaperone. It is part of the inhibitor of acetyltransferases (INHAT) complex, which modulates epigenetic histone modifications by inhibiting the transfer of acetyl residues onto histone molecules by masking their lysine residues. Notably, its most sensitive target is histone H4. So, if SET is overexpressed or somehow stabilized, acetylation of H4 should presumably be reduced. Also, Fraga et al. postulated the oncogenic decrease of histone H4 modifications, like the acetylation of H4K16 (H4K16ac) and the trimethylation of H4K20 (H4K20me3). Contrary to assumptions, I did not detect a global reduction in H4K16ac or H4K20me3 in the ZAP70-positive CLL subgroup. Still, one has to keep in mind that only one specific time point in the life of the CLL cells was analyzed and histone modification patterns usually follow a certain fluctuation dependent on their upstream regulation. Therefore, expression analyses of upstream key regulators of these histone modifications present as more reliable results. In this study, I detected a significantly lower gene expression of the H4K20-specific HMTs Suv4-20 homologue 1 (Suv4-20H1) and Suv4-20 homologue 2 (Suv4-20H2) in MEC-1$^{ZAP70\text{-}tet\text{-}ON}$ and primary CLL cells, respectively. Hence, one can hypothesize, that even if immunoblot analyses did not show the assumed effect of less H4K20me3 in ZAP70-positive CLL cells, that the ZAP70-associated downregulation of the histone H4-specific Suv4-20 methyltransferases subsequently leads to a reduction of trimethylated H4K20 at specific transcription-regulatory sites and therefore to a change in gene expression as seen in the microarray analysis by modulating the accessibility of the DNA.

Already in the late 70ies, it has been postulated that tyrosine residues in histones maybe involved in the assembly of the histone core complex (Eickbush and Moudrianakis, 1978). The histone H4 molecule contains four conserved tyrosine residues at positions 51, 72, 88 and 98 (Singh and Gunjan, 2011). The resolution of the crystal structure of nucleosomal particles revealed that H4 and H2B are responsible for the nucleosome assembly through their interaction by formation of a hydrophobic cluster (Luger et al., 1997). Santisteban et al. described the H4 residues Y72, Y88 and Y98 to be essential for the interaction of H3-H4 tetramers with H2A-H2B dimers inside the nucleosome (Santisteban et al.,

1997). In 1981, using iodination studies it has been discovered that H4Y72 is physically protected within the native nucleosome (Burch and Martinson, 1981). In mutational studies in *Saccharomyces cerevisiae*, the residue Y72 was discovered to be essential for cell survival (Nakanishi et al., 2008). Chou et al. reported in 2014 that Y72 of histone H4 is phosphorylated by the epidermal growth factor receptor (EGFR) (Chou et al., 2014). Furthermore, he H4Y72 phosphorylation by EGFR was suggested to promote DNA synthesis and repair. The inhibition of the EGFR-H4 interaction using a disrupting peptide suppressed tumor growth in a breast cancer xenograft mouse model. Furthermore, Chou et al. described a differential methylation of lysine 20 of histone H4 upon phosphorylation of Y72.

The data from this study suggest that ZAP70 can directly phosphorylate histone H4 using radioactive *in vitro* kinase assays, but only when H4 was fully accessible and not forming a complex with any other nucleosomal particle. Even though the knowledge about the necessary full accessibility of the tyrosine residue (see above) as well as first mass spectrometry results hint to a phosphorylation of Y72 by ZAP70, the data were too preliminary to present them in this thesis. Hence, further studies are needed to clearly identify the ZAP70 phosphorylation site. Recombinant mutant H4 molecules lacking specific tyrosines, which can be fabricated using site-directed mutagenesis, can be used for further *in vitro* ZAP70 kinase assays to prove the site of phosphorylation. Furthermore, specific monoclonal antibodies to phosphorylated histone H4 at the tyrosine of interest have to be produced, as they are not commercially available to date, to further associate a differential H4 phosphorylation pattern with ZAP70 expression in primary CLL cells.

As the phosphorylation of histone H4 at tyrosine residue 72 has been implicated to be involved in oncogenesis and other tyrosine kinases were reported to translocate to the nucleus of leukemic cells to phosphorylate histone molecules and thereby change oncogene expression, I propose a novel function for ZAP70 in CLL cells: despite its high mobility, ZAP70 associates with chromatin components in the nucleus of CLL cells and changes gene expression by shifting the epigenetic imprint of the cell, either by directly or indirectly targeting histone modification patterns. This theory supports oncogenic implications of ZAP70 in the

pathogenesis of CLL and may be an explanation for the dismal prognosis of patients carrying a ZAP70-positive leukemia.

4.3 Conclusion

Taken together, I postulate a possible mechanism for the oncogenic drive transmitted by the overexpression of ZAP70 in CLL cells. My model supports the idea that ZAP70 translocates to the nucleus of CLL cells independently from extracellular BCR signals, where it is activated. ZAP70 also associates with several histone chaperones, which may build a scaffold for other histone-modifying enzymes like HATs and HDACs and hence facilitate the change of the epigenetic imprint at certain gene-specific sites. The modulated accessibility of transcription-regulatory sites might subsequently differentially regulate the gene expression of several genes, including tumor suppressor genes and oncogenes. Specifically, the downregulation of two genes are important for the anti-apoptotic behavior of the CLL cell - *PPP2R1B* and *GSK3B*. In the cytosol, the impaired activity of PP2A caused by the downregulation of its regulatory subunit A (*PPP2R1B*) together with the ZAP70-mediated enhanced autologous BCR signaling and possible overexpression of SET may lead to an increased activation of AKT, a subsequent inhibition of the remaining low levels of GSK3β, and finally to a stabilization of the anti-apoptotic protein Mcl-1. Its stabilization impairs the formation of the mitochondrial pores during apoptosis induction and hence mediates a higher resistance to apoptotic stimuli like chemotherapeutics.

My model falls in line with a previous publication of Longo *et al.*, who describe the AKT/GSK3β/Mcl-1 cascade to be prominently responsible for the anti-apoptotic behavior of CLL cells (Longo et al., 2008). Hence, a viable option for future therapies is to target the BH3 domain of Mcl-1 with small molecule inhibitors to release Bax and Bak and facilitate the initiation of apoptosis in ZAP70-positive CLL cells (Akgul, 2009; Balakrishnan et al., 2008; Chen et al., 2005b; Day et al., 2005). Mcl-1 antisense strategies have been reported as a new therapeutic approach for multiple myeloma, as it proved as superior strategy to Bcl-2 antagonism (Derenne et al., 2002). Researches also postulated that these new compounds might even enhance the therapeutic effects of the monoclonal anti-CD20 antibody rituximab (Hussain et al., 2007). Very recently, Leverson et al. discovered the first Mcl-1 specific small-molecule antagonists, which were able to induce the main characteristics of intrinsic apoptosis in melanoma and lung cancer cell lines (Leverson et al., 2015a; Leverson et al., 2015b). Further studies will be

needed to analyze potential toxic side effects and clinical applicability of these promising new compounds for the personalized treatment of ZAP70-positive CLL patients.

5 Summary

CLL is a very common B cell malignancy with a high incidence in western countries. The clinical course of the disease is very heterogeneous with some patients experiencing a rapid disease onset and progression, ultimately leading to bone marrow failure, whereas others have a very indolent course of the disease. The aberrant expression of the tyrosine kinase ZAP70 has been associated with a dismal prognosis, particularly in patients with unmutated IGVH genes, although the patho-biological implications of this kinase have not been understood.

This thesis addresses this issue by employing genetically modified B cell lines and primary samples from CLL patients. Rather unexpected, my data demonstrate that ZAP70 expression alters the expression of anti-apoptotic proteins, namely Mcl-1, which renders cells more resistant to cytotoxic therapies. Mechanistically, Mcl-1 expression is regulated by ZAP70 through post-translational mechanisms involving GSK3β and subsequently stabilizing of the protein.

In addition, I could demonstrate that ZAP70 directly alters gene expression independent of additional signals from the BCR. As a function of its kinase activity, ZAP70 translocates to the nucleus, where it is associated with chromatin structures. My data suggest that ZAP70 may exert a yet unknown epigenetic function by modifying histone proteins.

Conclusively, these data contribute significantly to a better understanding of the function of ZAP70 in CLL and its contribution to disease progression and treatment resistance.

6 Zusammenfassung

CLL ist eine weit verbreitete B-Zell-Erkrankung mit hoher Inzidenz in westlichen Ländern. Der klinische Verlauf der Krankheit ist sehr heterogen, wobei einige Patienten einen schnellen Krankheitsausbruch und eine schnelle Progression erfahren, die letzten Endes zu Knochenmarkversagen führt, wohingegen andere einen sehr indolenten Krankheitsverlauf haben. Die aberrante Expression der Tyrosinkinase ZAP70 wird mit einer ungünstigen Prognose assoziiert, besonders in Patienten mit unmutierten IGHV-Genen, obwohl die pathobiologischen Implikationen dieser Kinase nicht verstanden werden.

Diese Arbeit untersucht diese Fragestellung mit Hilfe von genetisch modifizierten B-Zelllinien und primären Proben von CLL-Patienten. Erstaunlicherweise zeigen meine Daten, dass die ZAP70-Expression die Expression von anti-apoptotischen Proteinen verändert, besonders von Mcl-1, das Zellen resistenter gegenüber zytotoxischen Therapien macht. Mechanistisch ist die Mcl-1-Expression von ZAP70 durch einen post-translationalen Mechanismus reguliert, der GSK3β involviert und somit das Protein stabilisiert.

Zusätzlich konnte ich zeigen, dass ZAP70 direkt die Genexpression verändert, unabhängig von zusätzlichen Signalen über den B-Zell-Rezeptor. Als Funktion seiner Kinaseaktivität transloziert ZAP70 in den Zellkern, wo es mit Chromatinstrukturen assoziiert. Meine Daten unterstützen die Hypothese, dass ZAP70 eine bisher unbekannte epigenetische Funktion durch die Modifizierung von Histonproteinen ausübt.

Zusammenfassend tragen diese Daten signifikant zu einem besseren Verständnis der Funktion von ZAP70 in der CLL und zu seinem Einfluss auf die Krankheitsprogression und die Behandlungsresistenz bei.

7 Appendices

Appendix 1 Microarray profiling heat maps showing all genes with significantly changed expression

green – downregulation; red – upregulation

All heat maps were created in collaboration with PD Dr. Ludger Klein-Hitpaß (Universitätsklinikums Essen, Germany).

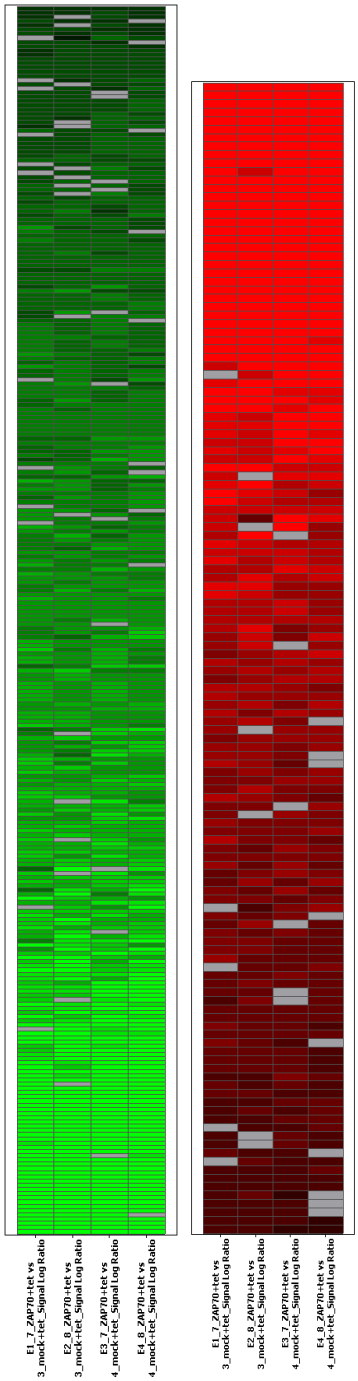

Appendix 2 Microarray profiling table showing all genes with significantly increased expression; SLR – Signal Log Ratio

Gene Symbol	E1_SLR	E1_p-value	E2_SLR	E2_p-value	E3_SLR	E3_p-value	E4_SLR	E4_p-value	Mean	Count_Increase	Count_rm Decrease
ZAP70	7,8	4,60E-05	7,9	2,00E-05	10	3,50E-05	10	2,00E-05	8,93	4	0
ZAP70	7	2,00E-05	6,9	2,00E-05	8,1	2,00E-05	8,1	2,00E-05	7,53	4	0
TBC1D8B	7,2	6,00E-05	7,1	7,80E-05	6,7	7,80E-05	6,6	7,80E-05	6,90	4	0
ENAH	6,8	2,00E-05	7	2,00E-05	5,9	2,00E-05	6,1	2,00E-05	6,45	4	0
BEND4	4,6	2,00E-05	4,6	2,00E-05	4,3	2,00E-05	4,4	2,00E-05	4,48	4	0
AJUBA	3,1	0,000189	3,5	4,00E-05	5,2	0,000492	5,6	8,80E-05	4,35	4	0
APOC2 /// APOC4 /// APOC4-APOC2	4,2	6,80E-05	4,2	3,00E-05	4,4	2,30E-05	4,6	6,80E-05	4,35	4	0
AGPAT9	4,9	3,50E-05	4,9	2,30E-05	1,8	0,000774	1,7	0,000492	3,33	4	0
FCRL4	2,7	6,00E-05	2,8	2,70E-05	3,2	2,70E-05	3,1	2,00E-05	2,95	4	0
STXBP5L	1,2	0,000189	1,1	0,000438	4,9	0,000492	4,2	0,000492	2,85	4	0
TMEM136	1	4,00E-05	0,8	0,000346	4,1	8,80E-05	4	0,001486	2,48	4	0
SMPDL3A	2,2	2,00E-05	1,9	2,30E-05	2,2	2,30E-05	2,1	2,30E-05	2,10	4	0
RUNX2	2	2,00E-05	2	2,00E-05	2	2,00E-05	2	2,00E-05	2,00	4	0
GIMAP1	1,5	2,70E-05	1,7	2,00E-05	2,1	2,00E-05	2,4	2,00E-05	1,93	4	0
NRN1	2	2,00E-05	1,8	2,00E-05	2,1	2,00E-05	1,7	3,50E-05	1,90	4	0
IPCEF1	1,8	8,80E-05	1,8	3,00E-05	1,9	2,30E-05	2,1	2,00E-05	1,90	4	0
CLEC4A	1,7	0,000147	1,8	3,00E-05	1,9	6,80E-05	2,1	2,00E-05	1,88	4	0
CLECL1	1,8	2,00E-05	1,8	2,00E-05	2,1	2,00E-05	1,7	2,00E-05	1,85	4	0
B3GALNT1	1,9	2,00E-05	1,9	2,00E-05	1,5	6,80E-05	1,7	0,000101	1,75	4	0
TRIP6	1,9	7,80E-05	1,9	0,00013	1,4	0,000492	1,4	0,000692	1,65	4	0
GIMAP8	1,4	2,00E-05	1,4	2,00E-05	1,6	2,00E-05	1,5	2,00E-05	1,48	4	0
PRDM1	1,1	2,00E-05	1,2	2,00E-05	1,6	2,00E-05	1,8	2,00E-05	1,43	4	0
KDM5B	1,3	0,000438	1,5	0,000114	1,3	0,001486	1,5	2,00E-05	1,40	4	0
MOXD1	1,2	2,00E-05	1,3	2,00E-05	1,2	2,00E-05	1,4	2,00E-05	1,28	4	0
GIMAP6	1,1	2,00E-05	1,2	2,00E-05	1,3	2,00E-05	1,4	2,00E-05	1,25	4	0
TSPAN12	1,1	2,00E-05	1,2	4,00E-05	1,2	0,000114	1,5	2,00E-05	1,25	4	0
FCRL3	1,3	2,70E-05	1,1	2,00E-05	1,3	0,000346	1,1	4,00E-05	1,20	4	0
ALOX5	1,4	2,00E-05	1,2	7,80E-05	1,2	2,00E-05	1	2,70E-05	1,20	4	0
ROR1	1,2	0,000167	1	2,00E-05	1,2	0,000167	1,3	2,00E-05	1,18	4	0
TNFRSF11A	1,2	3,50E-05	1,2	2,00E-05	1,1	0,001486	1,1	0,001336	1,15	4	0
FCRL5	1,3	2,70E-05	1,1	2,30E-05	1,1	4,00E-05	0,9	2,30E-05	1,10	4	0
YPEL2	1,2	2,00E-05	1,1	2,30E-05	1	2,00E-05	1	7,80E-05	1,08	4	0
FHOD3	1	2,00E-05	1	2,70E-05	1	0,000147	1,2	2,70E-05	1,05	4	0
TET1	0,8	0,000389	1	6,80E-05	1,3	0,000214	1,1	3,50E-05	1,05	4	0
RPP25			0,8	0,000692	1,1	0,000346	1,2	0,000167	1,03	3	0
HENMT1	0,9	2,00E-05	1,1	2,00E-05	1	2,00E-05	1	2,00E-05	1,00	4	0
PLCL1	1,1	2,00E-05	1,1	2,00E-05	0,9	2,00E-05	0,9	2,00E-05	1,00	4	0
SDC1	1,1	2,00E-05	1	0,000147	1	3,00E-05	0,9	0,000147	1,00	4	0
ITM2B	1	0,000346	1	0,000346	0,9	0,000492	1	0,000346	0,98	4	0
PTAFR	0,9	0,00013	0,8	0,000214	1,1	7,80E-05	1	0,000346	0,95	4	0
ZMAT2	0,9	2,00E-05	0,9	2,00E-05	1	2,00E-05	1	2,00E-05	0,95	4	0
RCBTB2	0,9	4,60E-05	0,8	0,000307	1,1	0,000241	0,9	3,50E-05	0,93	4	0
SCARB2	0,8	3,00E-05	0,8	2,00E-05	1	2,00E-05	1,1	2,00E-05	0,93	4	0
CRTAM	0,9	2,00E-05	0,8	2,30E-05	0,9	2,00E-05	1	2,00E-05	0,90	4	0
HTR2B	0,8	2,00E-05	0,8	2,00E-05	1,1	0,000618	0,9	0,000774	0,90	4	0
CD52	1	0	1	0	0,8	1,00E-06	0,8	1,00E-06	0,90	4	0
PIGR	0,8	0,001077			0,9	2,00E-05	0,9	4,00E-05	0,87	3	0
PYHIN1	0,9	2,00E-05	1	2,00E-05	0,7	2,00E-05	0,8	3,50E-05	0,85	4	0
CMPK2	1	2,70E-05	0,9	4,00E-05	0,8	0,000101	0,6	2,30E-05	0,83	4	0
LOC374443	1,1	2,00E-05	0,8	2,30E-05	0,7	0,000389	0,7	0,000966	0,83	4	0
ARHGAP18	0,8	2,00E-05	0,8	2,00E-05	0,8	3,00E-05	0,8	4,00E-05	0,80	4	0
COL24A1	0,8	2,70E-05	0,4	0,000147	1,1	2,00E-05	0,9	2,00E-05	0,80	4	0
MALAT1	0,8	2,00E-05			1	2,00E-05	0,6	2,00E-05	0,80	3	0
RASEF	0,7	0,000346	1,1	0,000273			0,6	0,000492	0,80	3	0
CD1D	0,9	2,00E-05	0,8	2,00E-05	0,7	2,00E-05	0,7	2,00E-05	0,78	4	0
PSMA1	0,8	2,00E-05	0,8	2,00E-05	0,8	2,00E-05	0,7	2,00E-05	0,78	4	0
TRIB2	0,9	2,00E-05	0,7	5,20E-05	0,8	2,00E-05	0,7	3,50E-05	0,78	4	0
FUCA1	0,7	2,00E-05	0,7	2,00E-05	0,9	2,00E-05	0,8	2,00E-05	0,78	4	0
GATM	0,7	2,00E-05	0,9	2,00E-05	0,7	2,00E-05	0,8	2,00E-05	0,78	4	0
OR7E14P	0,9	0,000346	0,9	0,000189	0,6	0,001486	0,6	0,000552	0,75	4	0
DNAJC12	0,9	2,00E-05	0,8	2,00E-05	0,6	2,00E-05	0,6	3,50E-05	0,73	4	0
HARS2	0,7	3,00E-05	0,7	0,000241	0,8	0,000189	0,6	0,000241	0,70	4	0
SOCS2	0,7	2,00E-05	0,7	2,00E-05	0,8	3,50E-05	0,6	0,000147	0,70	4	0
TBX21	0,7	8,80E-05	0,7	0,000101	0,7	7,80E-05	0,7	2,00E-05	0,70	4	0
AAK1	0,7	2,70E-05	0,9	2,00E-05	0,5	0,000346	0,6	4,00E-05	0,68	4	0
ARHGEF12	0,6	5,20E-05	0,8	2,00E-05	0,5	0,000101	0,8	2,00E-05	0,68	4	0
TGFBR2	0,6	0,000307	0,8	3,00E-05			0,6	4,00E-05	0,67	3	0
PRKCA	0,5	0,000307	0,6	0,000101	0,7	4,60E-05	0,8	4,60E-05	0,65	4	0
CD300A	0,7	4,00E-05	0,6	2,30E-05	0,7	0,000101	0,6	0,000214	0,65	4	0
METTL7A	0,6	2,00E-05	0,7	2,00E-05	0,6	2,00E-05	0,7	2,00E-05	0,65	4	0
CXADR	0,5	6,00E-05	0,6	0,000241	0,7	5,20E-05	0,7	0,000147	0,63	4	0
GAB1	0,7	2,00E-05	0,7	2,00E-05	0,6	2,00E-05	0,5	2,00E-05	0,63	4	0
PTPRC	0,7	2,00E-05	0,6	2,00E-05	0,6	2,00E-05	0,6	2,00E-05	0,63	4	0
RAB4A /// SPHAR	0,6	3,00E-05	0,7	2,00E-05	0,5	0,000214	0,7	2,00E-05	0,63	4	0
RNASET2	0,7	5,20E-05	0,5	4,60E-05	0,7	2,00E-05	0,6	2,00E-05	0,63	4	0
GRAMD3	0,6	2,30E-05	0,7	0,000552	0,5	0,00013			0,60	3	0
S100A13	0,6	2,00E-05			0,6	2,00E-05	0,6	0,001201	0,60	3	0
TMEM42	0,5	2,00E-05	0,6	2,00E-05	0,6	0,000389	0,6	4,00E-05	0,58	4	0
PRF1	0,6	2,00E-05	0,6	2,00E-05	0,5	2,00E-05	0,6	2,00E-05	0,58	4	0
GBP3	0,6	2,00E-05	0,6	0,000101	0,5	6,00E-05			0,57	3	0
LINC00537	0,7	2,00E-05	0,6	0,000167	0,4	0,000552			0,57	3	0
ALDH1A1	0,5	0,00013	0,6	2,00E-05	0,5	2,30E-05	0,6	2,70E-05	0,55	4	0
CREM	0,5	2,00E-05	0,5	2,00E-05	0,6	2,00E-05	0,6	2,00E-05	0,55	4	0
MCC	0,5	6,00E-05	0,7	2,00E-05	0,5	0,000692	0,5	4,60E-05	0,55	4	0
LINC00643	0,7	3,50E-05	0,6	7,80E-05	0,5	2,00E-05	0,4	5,20E-05	0,55	4	0
FDXR	0,5	0,000114	0,5	2,00E-05			0,6	0,000241	0,53	3	0
YOD1	0,5	0,00013			0,6	2,00E-05	0,5	2,70E-05	0,53	3	0
AK4 /// LOC100507855	0,6	2,00E-05	0,5	4,60E-05	0,5	2,30E-05	0,5	3,00E-05	0,53	4	0
FAM101B	0,5	0,000214	0,5	0,000189	0,5	0,000307	0,6	0,000114	0,53	4	0
NFIL3	0,7	2,00E-05	0,5	2,00E-05	0,5	2,00E-05	0,4	2,00E-05	0,53	4	0
INPP4A	0,5	2,00E-05	0,4	0,000966	0,6	3,00E-05	0,5	6,00E-05	0,50	4	0
PTCH1	0,5	2,00E-05	0,5	2,00E-05	0,5	2,00E-05	0,5	2,00E-05	0,50	4	0
RNASEH2B	0,6	2,00E-05	0,4	0,000865	0,6	2,00E-05	0,4	7,80E-05	0,50	4	0
SUB1	0,4	2,00E-05	0,5	2,00E-05	0,6	3,50E-05	0,5	0,000389	0,50	4	0
XYLT1	0,4	3,00E-05	0,6	3,50E-05	0,4	3,50E-05	0,6	2,00E-05	0,50	4	0
BHLHE40	0,5	3,50E-05	0,4	0,000189	0,6	2,00E-05	0,4	2,70E-05	0,48	4	0
KCTD12	0,5	2,00E-05	0,5	2,00E-05	0,4	2,00E-05	0,5	2,00E-05	0,48	4	0
CPOX			0,3	3,00E-05	0,5	2,00E-05	0,6	2,00E-05	0,47	3	0
ELL2	0,5	5,20E-05	0,4	0,001077	0,5	0,000241			0,47	3	0

Gene Symbol	E1_SLR	E1_p-value	E2_SLR	E2_p-value	E3_SLR	E3_p-value	E4_SLR	E4_p-value	Mean	Count_Increase	Count_rm Decrease
RAB27A	0,4	0,000114	0,6	0,000114			0,4	0,000774	0,47	3	0
CBWD1 /// CBWD2 /// CBWD3	0,5	2,00E-05	0,4	8,80E-05	0,5	3,00E-05	0,4	4,60E-05	0,45	4	0
HIST1H1C	0,5	2,00E-05	0,5	2,00E-05	0,4	3,50E-05	0,4	4,00E-05	0,45	4	0
LZTFL1	0,5	2,00E-05	0,5	2,00E-05	0,4	2,00E-05	0,4	8,80E-05	0,45	4	0
RBPMS2	0,6	0,000389	0,4	2,30E-05	0,4	0,000189	0,4	6,80E-05	0,45	4	0
HCST			0,4	0,000307	0,4	6,80E-05	0,5	3,00E-05	0,43	3	0
SIDT2	0,4	9,00E-06	0,4	2,00E-06	0,5	5,00E-05	0,4	1,00E-06	0,43	4	0
SORL1	0,4	2,00E-05	0,5	2,00E-05	0,4	2,00E-05	0,4	2,00E-05	0,43	4	0
RNF170	0,4	0,000389	0,4	2,00E-05			0,4	2,30E-05	0,40	3	0
SCIN	0,3	8,80E-05	0,5	0,000389			0,4	0,001336	0,40	3	0
DEGS1	0,4	4,00E-05	0,4	2,00E-05	0,4	6,80E-05	0,4	3,50E-05	0,40	4	0
GIMAP2	0,4	3,50E-05	0,4	7,80E-05	0,4	2,00E-05	0,4	2,00E-05	0,40	4	0
RB1	0,5	5,20E-05	0,4	0,000307	0,4	0,001336	0,3	4,60E-05	0,40	4	0
SACM1L	0,4	3,50E-05	0,4	0,000241	0,4	2,00E-05	0,4	8,80E-05	0,40	4	0
DYNLT3	0,5	2,00E-05	0,4	0,000438	0,3	0,00013			0,40	3	0
GPM6A	0,4	2,00E-05	0,4	3,00E-05	0,4	6,00E-05	0,3	4,00E-05	0,38	4	0
LMO4	0,4	2,00E-05	0,4	0,00013	0,4	2,70E-05	0,3	7,80E-05	0,38	4	0
LY86	0,4	2,00E-05	0,4	7,80E-05	0,4	2,00E-05	0,3	8,80E-05	0,38	4	0
DNAJA2	0,3	0,000114	0,3	0,000241	0,5	2,00E-05	0,4	2,00E-05	0,38	4	0
FMNL2	0,4	0,000241	0,3	0,000101	0,4	0,000241	0,3	5,20E-05	0,35	4	0
ITPR2	0,4	2,30E-05	0,4	2,00E-05	0,3	0,000101	0,3	2,00E-05	0,35	4	0
IDS	0,3	0,000618	0,3	0,000114	0,4	8,80E-05	0,4	2,00E-05	0,35	4	0
MDM2	0,3	0,001486	0,4	2,00E-05	0,3	2,70E-05	0,4	2,00E-05	0,35	4	0
NMT2	0,3	2,70E-05	0,3	4,60E-05	0,4	4,00E-05	0,4	2,00E-05	0,35	4	0
GADD45B			0,3	0,000865	0,3	0,000167	0,4	7,80E-05	0,33	3	0
MKKS	0,3	4,60E-05			0,4	0,000189	0,3	6,80E-05	0,33	3	0
MTFR1L	0,3	0,000273			0,4	0,000167	0,3	0,000241	0,33	3	0
STEAP1	0,4	2,00E-05	0,3	4,00E-05	0,3	7,80E-05			0,33	3	0
ZBTB38			0,4	0,000273	0,3	0,000273	0,3	2,70E-05	0,33	3	0
NDUFA8	0,3	0,000307	0,3	2,70E-05	0,3	5,20E-05	0,4	2,00E-05	0,33	4	0
IGKV4-1 /// IGKV4-1	0,3	2,00E-05	0,3	0,000438	0,3	2,00E-05	0,3	0,000618	0,30	4	0
SAMSN1	0,3	2,00E-05	0,3	3,50E-05	0,3	2,00E-05	0,3	7,80E-05	0,30	4	0
ATP5L	0,3	6,80E-05	0,4	0,001201	0,2	5,20E-05			0,30	3	0
SPRY2	0,3	0,000346	0,3	0,000692	0,3	0,000346			0,30	3	0
SRI	0,3	2,70E-05	0,3	0,000966	0,3	0,000214			0,30	3	0
NIPSNAP3A	0,3	4,60E-05	0,3	0,000241	0,3	0,000101	0,2	0,000692	0,28	4	0
ARL6IP5	0,3	2,30E-05	0,3	2,00E-05	0,2	7,80E-05	0,2	4,00E-05	0,25	4	0

Appendix 3 Microarray profiling table showing all genes with significantly decreased expression; SLR – Signal Log Ratio

Gene Symbol	D1_SLR	D1_p-value	D2_SLR	D2_p-value	D3_SLR	D3_p-value	D4_SLR	D4_p-value	Mean	Count_Increase	Count_rm Decrease
HLA-DPA1	-0,3	0,999308	-0,3	0,99998	-0,2	0,99996	-0,4	0,99998	-0,20	0	4
HLA-DQB1			-0,2	0,999034	-0,3	0,999135	-0,4	0,999886	-0,23	0	3
HMMR	-0,4	0,999654	-0,4	0,999911	-0,4	0,99998	-0,5	0,999973	-0,23	0	4
MCCC2	-0,2	0,999654			-0,3	0,999727	-0,3	0,999811	-0,23	0	3
PAPSS1	-0,2	0,99998	-0,4	0,999954	-0,4	0,999886	-0,6	0,999954	-0,23	0	4
CTNNA1			-0,2	0,999654	-0,4	0,99994	-0,4	0,999899	-0,25	0	3
VCL	-0,4	0,99998	-0,4	0,99998	-0,4	0,999973	-0,5	0,99996	-0,25	0	4
FAM168A	-0,6	0,998923	-0,6	0,999759	-0,6	0,999654	-0,6	0,999654	-0,27	0	4
HECW2	-0,3	0,999932	-0,3	0,99998	-0,4	0,99998	-0,4	0,99998	-0,27	0	4
CALM1 /// CALM2 /// CALM3	-0,3	0,999611	-0,2	0,999727	-0,4	0,999833	-0,3	0,999977	-0,28	0	4
CDCA7	-0,2	0,999034			-0,2	0,999448	-0,3	0,998514	-0,28	0	3
LRMP	-0,3	0,999963	-0,2	0,999954			-0,2	0,998774	-0,28	0	3
DENND5A	-0,3	0,999853	-0,3	0,999886	-0,5	0,99998	-0,5	0,99998	-0,30	0	4
DHRS7	-0,2	0,999922	-0,3	0,999562	-0,4	0,998168			-0,30	0	3
HLA-DQA1 /// HLA-DQA2 /// LOC100509457	-0,2	0,999973	-0,3	0,99998	-0,2	0,999811	-0,3	0,99998	-0,30	0	4
SNX10	-0,2	0,998349	-0,2	0,999448	-0,4	0,999811	-0,3	0,999562	-0,30	0	4
UCP2	-0,6	0,99998	-0,5	0,99998	-0,4	0,99998	-0,4	0,99998	-0,30	0	4
ALDOC	-0,4	0,999727	-0,6	0,99994	-0,4	0,999977	-0,6	0,999899	-0,30	0	4
RASGRP3	-0,4	0,999853	-0,3	0,99998	-0,4	0,999562	-0,4	0,998514	-0,30	0	4
RHOH	-0,3	0,999922	-0,3	0,999911	-0,3	0,999611	-0,3	0,999034	-0,30	0	4
TBC1D1	-0,4	0,999611	-0,4	0,99998	-0,3	0,999886	-0,3	0,99997	-0,30	0	4
TCEAL3	-0,3	0,999786	-0,2	0,998349	-0,4	0,99987	-0,3	0,99998	-0,30	0	4
ARHGEF18	-0,3	0,999922	-0,3	0,999899	-0,4	0,999922	-0,3	0,999727	-0,33	0	4
ARID5B	-0,3	0,999308	-0,3	0,998664	-0,4	0,999973	-0,4	0,999973	-0,33	0	4
QDPR	-0,3	0,999693	-0,3	0,999786	-0,3	0,999965	-0,3	0,999948	-0,33	0	4
CAST	-0,2	0,999954	-0,2	0,999611	-0,5	0,999759	-0,4	0,999448	-0,33	0	4
SLC44A1	-0,4	0,99998	-0,4	0,99998	-0,4	0,999308	-0,4	0,999922	-0,33	0	4
BARD1			-0,2	0,999693	-0,4	0,999833	-0,5	0,99998	-0,33	0	3
FADS1 /// MIR1908			-0,4	0,999811	-0,2	0,999382	-0,3	0,999911	-0,33	0	3
GNB4	-0,2	0,99997	-0,4	0,999654	-0,5	0,998923			-0,33	0	3
NR3C1	-0,3	0,999226	-0,4	0,999654	-0,3	0,99998	-0,4	0,999727	-0,33	0	4
ALOX5AP	-0,3	0,999965	-0,4	0,999973	-0,3	0,99998	-0,4	0,99998	-0,35	0	4
CCDC90B	-0,3	0,999611	-0,3	0,99998			-0,3	0,999654	-0,35	0	3
LEF1	-0,4	0,99998	-0,4	0,999977	-0,4	0,99998	-0,4	0,99998	-0,35	0	4
MMD	-0,3	0,99997	-0,3	0,999973	-0,4	0,999954	-0,4	0,99997	-0,35	0	4
PDXK	-0,4	0,99998	-0,4	0,99998	-0,4	0,99998	-0,4	0,99998	-0,35	0	4
PHF19	-0,4	0,999977	-0,3	0,99997	-0,4	0,99996	-0,4	0,999693	-0,35	0	4
CR1 /// CR1L	-0,4	0,99998	-0,5	0,999977	-0,4	0,999448	-0,4	0,999811	-0,37	0	4
ELK3	-0,5	0,999759	-0,4	0,99998	-0,5	0,998514	-0,2	0,99996	-0,37	0	4
FAM126A			-0,3	0,999948	-0,3	0,999382	-0,4	0,999899	-0,37	0	3
HSPA4L			-0,3	0,999886	-0,5	0,999562	-0,5	0,999899	-0,37	0	3
IL4R			-0,5	0,999654	-0,3	0,999965	-0,4	0,99996	-0,37	0	3
NUDT7	-0,6	0,999759	-0,8	0,999811	-0,8	0,999308	-0,7	0,999727	-0,37	0	4
TMOD1	-0,2	0,999654			-0,4	0,99998	-0,2	0,999562	-0,37	0	3
ZBTB10	-0,4	0,999853	-0,4	0,999833	-0,5	0,999886	-0,5	0,999977	-0,37	0	4
DCUN1D5	-0,3	0,999954	-0,3	0,99998	-0,3	0,99998	-0,4	0,999886	-0,38	0	4
HCP5			-0,3	0,999759	-0,4	0,998514	-0,4	0,999977	-0,38	0	3
HLA-DMA	-0,4	0,999977	-0,5	0,99998	-0,4	0,99998	-0,5	0,99998	-0,38	0	4
IGHM	-0,3	0,999135			-0,4	0,99996	-0,5	0,999899	-0,38	0	3
MIR1304 /// SNORA1 /// SNORA18	-0,3	0,999932	-0,3	0,999973	-0,3	0,998168			-0,38	0	3
KDELC2	-0,4	0,999977	-0,5	0,99998	-0,4	0,998349	-0,6	0,999034	-0,38	0	4
NDUFC2 /// NDUFC2-KCTD14	-0,3	0,99998	-0,3	0,999977	-0,3	0,99997	-0,3	0,999973	-0,38	0	4
SGCB	-0,6	0,999654	-0,5	0,999948	-0,8	0,99994	-0,6	0,999922	-0,40	0	4
GPR160	-0,5	0,99998	-0,5	0,99998	-0,6	0,99998	-0,5	0,99998	-0,40	0	4
ANXA2	-0,4	0,99998	-0,4	0,999654	-0,4	0,99998	-0,4	0,999448	-0,40	0	4
CCR10			-0,5	0,99994	-0,5	0,999786	-0,6	0,999965	-0,40	0	3
ENDOD1	-0,4	0,99996	-0,3	0,99998	-0,6	0,99998	-0,5	0,99998	-0,40	0	4
GRAMD1C	-0,4	0,99998	-0,5	0,99998	-0,6	0,999654	-0,5	0,999654	-0,40	0	4
HLA-DOA	-0,4	0,999899	-0,3	0,999759	-0,5	0,99998	-0,4	0,999977	-0,40	0	4
INPP5F	-0,4	0,999922	-0,3	0,999973	-0,3	0,999654	-0,3	0,999034	-0,40	0	4
MIPEP	-0,4	0,999998	-0,4	0,999994	-0,5	1	-0,5	1	-0,40	0	4
NREP	-0,5	0,99996	-0,5	0,999977	-0,5	0,99998	-0,4	0,999973	-0,40	0	4
PARM1	-0,2	0,999833	-0,2	0,999922	-0,4	0,99998	-0,4	0,999932	-0,40	0	4
PICALM	-0,4	0,999954	-0,4	0,999948	-0,5	0,999899	-0,4	0,999611	-0,40	0	4
PLAC8	-0,3	0,99998	-0,4	0,99998	-0,4	0,99998	-0,4	0,99998	-0,40	0	4
RAB6A /// RAB6C /// WTH3DI	-0,5	0,99998	-0,5	0,99998	-0,5	0,999965	-0,5	0,99994	-0,40	0	4
ARHGAP24	-0,6	0,99998	-0,7	0,999965	-0,6	0,999973	-0,7	0,999948	-0,43	0	4
ARAP1	-0,4	0,999993	-0,5	0,999973	-0,5	0,999999	-0,6	0,999957	-0,43	0	4
CASP4	-0,6	0,99998	-0,6	0,99998	-0,5	0,99998	-0,6	0,99998	-0,43	0	4
LAPTM4B	-0,3	0,99998	-0,3	0,99998	-0,5	0,99998	-0,5	0,99998	-0,43	0	4
RAB6A	-0,5	0,99998	-0,6	0,99997	-0,5	0,99997	-0,6	0,999932	-0,43	0	4
TMEM126B	-0,4	0,99998	-0,3	0,99998	-0,4	0,99998	-0,3	0,99998	-0,43	0	4
KLHL29	-0,3	0,999948	-0,3	0,999833	-0,3	0,999922	-0,3	0,999965	-0,43	0	4
FERMT2	-0,4	0,999954	-0,5	0,99998	-0,4	0,999977	-0,5	0,99998	-0,43	0	4
ZBED3	-0,6	0,999977	-0,6	0,999562	-0,6	0,999562	-0,6	0,998349	-0,43	0	4
COA4	-0,4	0,999853	-0,4	0,99998	-0,4	0,999508	-0,4	0,999786	-0,45	0	4
COQ2	-0,4	0,999911	-0,4	0,999911	-0,4	0,999833	-0,4	0,998514	-0,45	0	4
DPYSL2	-0,5	0,99998	-0,5	0,99998	-0,6	0,99998	-0,6	0,99998	-0,45	0	4
PITPNC1	-0,5	0,99997	-0,6	0,999977	-0,6	0,99997	-0,6	0,999977	-0,45	0	4
SCD5	-0,5	0,99996			-0,4	0,99996	-0,3	0,999811	-0,45	0	3
SPCS2	-0,4	0,99998	-0,5	0,99998	-0,5	0,99998	-0,5	0,99998	-0,45	0	4
CNR1	-0,6	0,99998	-0,6	0,99998	-0,6	0,99998	-0,7	0,99998	-0,45	0	4
GBE1	-0,4	0,99998	-0,3	0,999948	-0,5	0,99998	-0,4	0,99998	-0,45	0	4
MRPL48	-0,4	0,999135	-0,3	0,998168			-0,3	0,998799	-0,45	0	3
P2RX5	-0,5	0,999308	-0,3	0,998514	-0,5	0,999948	-0,4	0,999833	-0,45	0	4
PAK1	-0,4	0,999965	-0,5	0,999811	-0,7	0,99998	-0,8	0,999954	-0,45	0	4
PTPRCAP	-0,4	0,998923	-0,6	0,99998	-0,4	0,999886	-0,8	0,99998	-0,45	0	4
TMEM126A	-0,4	0,99998	-0,3	0,99998	-0,4	0,99998	-0,3	0,99998	-0,45	0	4
NFKBIZ	-0,4	0,999899	-0,4	0,99998	-0,4	0,999759	-0,4	0,99998	-0,47	0	4
ZNF711	-0,6	0,999308	-0,4	0,998514	-1	0,999693	-0,6	0,999727	-0,47	0	4
ACAT1	-0,5	0,99998	-0,5	0,99998	-0,5	0,99998	-0,5	0,99998	-0,48	0	4
CAND2	-0,5	0,99994	-0,5	0,999693	-0,6	0,999977	-0,6	0,999853	-0,48	0	4
HDGFRP3	-0,3	0,99994	-0,3	0,999911	-0,3	0,999611	-0,4	0,999965	-0,48	0	4
LAMTOR1	-0,4	0,999973	-0,4	0,999977	-0,5	0,999973	-0,5	0,999977	-0,48	0	4
OCLN	-0,4	0,999973	-0,5	0,99998	-0,5	0,99998	-0,6	0,99998	-0,48	0	4
SRSF8	-0,4	0,99998	-0,4	0,999977	-0,5	0,999727	-0,5	0,999727	-0,48	0	4
BCAT1	-0,3	0,999853	-0,6	0,99998	-0,4	0,999786	-0,5	0,999759	-0,50	0	4
CLNS1A	-0,5	0,99998	-0,5	0,99998	-0,5	0,99998	-0,5	0,99998	-0,50	0	4
CWC15	-0,4	0,999965	-0,4	0,99998	-0,4	0,999508	-0,4	0,999853	-0,50	0	4

Gene Symbol	D1_SLR	D1_p-value	D2_SLR	D2_p-value	D3_SLR	D3_p-value	D4_SLR	D4_p-value	Mean	Count_Increase	Count_rm Decrease
IGHG1 /// IGHG2 /// IGHM /// IGHV4-31	0,3	5,20E-05	0,3	0,001077	0,4	0,000552			-0,50	3	0
IL18R1	-0,2	0,99998	-0,5	0,999899	-0,5	0,999922	-0,6	0,99998	-0,50	0	4
KIAA1731	-0,6	0,99998	-0,6	0,99998			-0,6	0,999308	-0,50	0	3
LGALS1	-0,7	0,99998	-0,7	0,99998	-0,7	0,99998	-0,7	0,99998	-0,50	0	4
MRPL21	-0,4	0,99998	-0,4	0,99998	-0,4	0,999973	-0,4	0,99998	-0,50	0	4
MYBL1	-0,7	0,999977	-0,9	0,999932	-0,6	0,999932	-0,8	0,99998	-0,50	0	4
TAGAP	-0,5	0,999954	-0,5	0,99998	-0,3	0,999811	-0,4	0,999932	-0,50	0	4
TIAM1	-0,6	0,999965	-0,5	0,99997	-0,7	0,999973	-0,6	0,999727	-0,50	0	4
USP53	-0,6	0,99998	-0,8	0,999954	-0,7	0,99998	-0,7	0,999954	-0,50	0	4
JAM2	-0,4	0,999034	-0,5	0,999954			-0,4	0,999562	-0,50	0	3
JRKL	-0,6	0,999954	-0,5	0,998514	-0,4	0,99998			-0,50	0	3
PALLD	-0,5	0,999886	-0,4	0,999833	-0,8	0,99998	-0,7	0,99998	-0,50	0	4
AIM2	-0,4	0,99998	-0,5	0,999977	-0,4	0,99997	-0,4	0,999932	-0,53	0	4
FRMD4A	-0,5	0,999954	-0,6	0,999786	-0,6	0,99998	-0,7	0,999786	-0,53	0	4
BMP2K	-0,5	0,999901	-0,6	0,999975	-0,6	0,999954	-0,6	0,999997	-0,53	0	4
NDUFV1	-0,4	0,99997	-0,4	0,99996	-0,5	0,999973	-0,5	0,99998	-0,53	0	4
POLD4	-0,7	0,99998	-0,6	0,99998	-0,8	0,99997	-0,7	0,99996	-0,53	0	4
RNF121	-0,6	0,999899	-0,6	0,999448	-0,7	0,99996	-0,8	0,999911	-0,53	0	4
SGPP2	-0,3	0,998923			-0,4	0,99987	-0,4	0,999308	-0,53	0	3
ATM	-0,4	0,99998	-0,6	0,999727	-0,5	0,99997	-0,6	0,999654	-0,53	0	4
CCL17	-0,9	0,99998	-0,6	0,999786	-0,8	0,99987			-0,53	0	3
CLGN	-0,5	0,999135	-0,4	0,999977	-0,5	0,999833	-0,5	0,99996	-0,53	0	4
RAD9A	-0,4	0,999654	-0,5	0,999448	-0,5	0,999611	-0,5	0,998514	-0,53	0	4
RNF169	-0,7	0,999853	-0,6	0,999226	-0,6	0,99998	-0,5	0,999448	-0,53	0	4
TSPO	-0,1	0,999811	-0,1	0,999508	-0,5	0,998168	-0,6	0,999759	-0,55	0	4
ATPAF1	-0,5	0,99998	-0,6	0,99998	-0,6	0,999973	-0,7	0,99998	-0,55	0	4
CREBZF	-0,5	0,999611	-0,5	0,999932	-0,5	0,999886	-0,6	0,99994	-0,55	0	4
FAM76B	-0,6	0,99998	-0,6	0,99998	-0,7	0,999922	-0,6	0,99998	-0,55	0	4
FCHSD2	-0,7	0,99987	-0,6	0,99997	-0,8	0,999899	-0,8	0,99998	-0,55	0	4
IL13RA1	-0,3	0,999308	-0,5	0,999833	-0,5	0,999727	-0,7	0,999899	-0,55	0	4
MTMR2	-0,5	0,99998	-0,5	0,99996	-0,7	0,999973	-0,6	0,99998	-0,55	0	4
PPP1CA	-0,5	0,99998	-0,5	0,99998	-0,5	0,99998	-0,6	0,99998	-0,55	0	4
PRCP	-0,5	0,99998	-0,6	0,999973	-0,6	0,99998	-0,6	0,999948	-0,55	0	4
RSF1	-0,4	0,99998	-0,6	0,99997	-0,6	0,999611	-0,8	0,99987	-0,57	0	4
CEP78	-0,5	0,99998	-0,5	0,99998	-0,5	0,99998	-0,6	0,999965	-0,58	0	4
PPME1	-0,7	0,999965	-0,6	0,999948	-0,8	0,99996	-0,5	0,999922	-0,58	0	4
PPP6R3	-0,5	0,99998	-0,6	0,99998	-0,7	0,999948	-0,7	0,999973	-0,58	0	4
TM6SF1	-0,5	0,999922	-0,3	0,999759	-0,5	0,99987	-0,4	0,999226	-0,58	0	4
UVRAG	-0,5	0,99998	-0,6	0,99998	-0,7	0,99998	-0,8	0,99998	-0,58	0	4
ANKRD49	-0,6	0,99998	-0,5	0,99998	-0,6	0,99998	-0,5	0,99998	-0,60	0	4
DDX10	-0,6	0,99998	-0,6	0,99998	-0,7	0,99998	-0,7	0,99998	-0,60	0	4
MIR4691 /// NDUFS8	-0,6	0,99998	-0,7	0,99998	-0,6	0,999977	-0,6	0,999977	-0,60	0	4
MSANTD4	-0,6	0,99998	-0,6	0,999911	-0,6	0,99998	-0,7	0,999886	-0,60	0	4
NARS2	-0,6	0,999977	-0,6	0,99998	-0,7	0,999977	-0,7	0,999977	-0,60	0	4
NPAT	-0,6	0,99998	-0,6	0,999611	-0,7	0,99994	-0,7	0,99987	-0,60	0	4
SDHD	-0,6	0,99998	-0,6	0,99998	-0,6	0,999611	-0,6	0,999853	-0,60	0	4
TMEM135	-0,7	0,99998	-0,7	0,99998	-0,8	0,99998	-0,7	0,99998	-0,60	0	4
NUMA1	-0,7	0,998799	-0,5	0,999811	-0,7	0,999654	-0,6	0,999899	-0,60	0	4
INTS4	-0,7	0,99998	-0,6	0,999911	-0,7	0,999965	-0,6	0,999932	-0,60	0	4
KDM2A	-0,5	0,99997	-0,6	0,999911	-0,6	0,999965	-0,5	0,999759	-0,60	0	4
OGFRL1	-0,5	0,99998	-0,5	0,999886	-0,6	0,999973	-0,6	0,999886	-0,60	0	4
AAMDC	-0,5	0,999965	-0,9	0,99998	-0,6	0,999654	-0,9	0,999508	-0,63	0	4
ALG8	-0,6	0,99998	-0,5	0,99998	-0,7	0,99998	-0,6	0,99998	-0,63	0	4
ALKBH8	-0,6	0,99998	-0,8	0,99998	-0,6	0,999948	-0,8	0,99998	-0,63	0	4
CEP57	-0,6	0,99998	-0,6	0,99998	-0,7	0,99998	-0,7	0,99998	-0,63	0	4
CHKA			-0,4	0,999611	-0,7	0,999562	-0,7	0,999954	-0,63	0	3
EXPH5	-0,4	0,99998	-0,5	0,99998			-0,4	0,999973	-0,63	0	3
LINC00926	-0,4	0,99997	-0,5	0,999965	-0,4	0,999977	-0,5	0,999973	-0,63	0	4
MFI2	-0,7	0,99998	-0,6	0,99998	-0,6	0,99998	-0,5	0,99998	-0,63	0	4
POLD3	-0,6	0,99998	-0,5	0,99998	-0,7	0,99998	-0,6	0,99998	-0,63	0	4
TMEM123	-0,6	0,99998	-0,5	0,99998	-0,8	0,999922	-0,6	0,999965	-0,63	0	4
AIP	-0,6	0,99998	-0,7	0,99998	-0,6	0,999973	-0,8	0,999977	-0,65	0	4
C2CD3	-0,7	0,999997	-0,7	0,999999	-0,7	1	-0,8	0,999999	-0,65	0	4
CWF19L2	-0,6	0,99998	-0,5	0,99998	-0,7	0,99998	-0,5	0,99998	-0,65	0	4
FADD	-0,6	0,99998	-0,6	0,999911	-0,5	0,99998	-0,5	0,99998	-0,65	0	4
SMCO4	-0,6	0,99998	-0,6	0,99998	-0,6	0,99998	-0,6	0,99998	-0,65	0	4
SUV420H1	-0,7	0,999932	-0,7	0,99997	-0,7	0,999973	-0,8	0,999977	-0,65	0	4
TNFRSF19	-0,7	0,99998	-0,6	0,99998	-0,8	0,999932	-0,8	0,99998	-0,65	0	4
CCDC82	-0,8	0,99998	-0,8	0,99998	-0,6	0,999611	-0,5	0,999899	-0,65	0	4
FSD1L	-0,6	0,99994	-0,7	0,999654	-0,5	0,99994	-0,6	0,999654	-0,65	0	4
GEM	-0,8	0,999811	-0,7	0,999654	-0,6	0,999786	-0,6	0,998664	-0,65	0	4
PAAF1	-0,6	0,99998	-0,7	0,99998	-0,6	0,99998	-0,6	0,99998	-0,65	0	4
SYT17	-0,6	0,99987	-0,6	0,999922	-0,4	0,999654	-0,4	0,998664	-0,65	0	4
MARVELD2	-0,7	0,999786	-0,5	0,999308	-0,8	0,999693	-0,7	0,998514	-0,67	0	4
AASDHPPT	-0,5	0,99998	-0,6	0,99998	-0,6	0,99998	-0,6	0,99998	-0,68	0	4
DHCR7	-0,7	0,999899	-0,7	0,999911	-0,7	0,99994	-0,7	0,99996	-0,68	0	4
FAM171A1	-0,5	0,99998	-0,6	0,99998	-0,6	0,99998	-0,7	0,99998	-0,68	0	4
ICA1	-0,7	0,99998	-0,8	0,99998	-0,6	0,999965	-0,8	0,999954	-0,68	0	4
KATNAL1	-0,6	0,998349	-0,7	0,999693	-0,6	0,99998	-0,7	0,99998	-0,68	0	4
MRE11A	-0,6	0,99998	-0,7	0,99998	-0,6	0,99998	-0,8	0,999977	-0,68	0	4
PANX1	-0,6	0,999786	-0,5	0,99998	-0,7	0,999899	-0,7	0,999973	-0,68	0	4
PPFIA1	-0,9	0,99998	-0,8	0,99998	-0,8	0,999973	-0,7	0,99997	-0,68	0	4
RBMS1	-0,6	0,999759	-0,6	0,999759	-0,6	0,999853	-0,5	0,999562	-0,68	0	4
SMIM14	-0,6	0,99998	-0,7	0,99998	-0,7	0,999948	-0,8	0,999973	-0,68	0	4
MAML2	-0,8	0,99998	-0,7	0,99998	-0,8	0,99998	-0,8	0,99998	-0,70	0	4
MED17	-0,6	0,99998	-0,9	0,99998	-0,7	0,99998	-1	0,99998	-0,70	0	4
RAB30	-0,5	0,999973	-0,6	0,999965	-0,6	0,99998	-0,7	0,99998	-0,70	0	4
ARHGAP26	-0,9	0,99998	-0,5	0,999727	-0,7	0,999977	-0,5	0,999786	-0,70	0	4
CTSC	-0,6	0,99998	-0,7	0,99998	-0,6	0,99998	-0,7	0,99998	-0,70	0	4
NADSYN1			-0,5	0,999135	-0,9	0,999977	-0,9	0,99997	-0,70	0	3
PRKRIR	-0,7	0,99998	-0,7	0,99998	-0,8	0,99998	-0,8	0,99998	-0,73	0	4
TIMM8B	-0,7	0,99998	-0,6	0,99998	-0,7	0,99998	-0,6	0,99998	-0,73	0	4
KHDRBS3	-0,6	0,999811	-0,7	0,999759	-0,6	0,999973	-0,7	0,999932	-0,73	0	4
ZNF608	-0,7	0,999977	-0,5	0,999977	-0,7	0,99998	-0,9	0,999911	-0,73	0	4
ACER3	-0,6	0,99998	-0,8	0,99998	-0,6	0,99998	-0,8	0,99998	-0,73	0	4
CA8	-0,5	0,99998	-0,6	0,99998	-0,6	0,99998	-0,6	0,99998	-0,73	0	4
CUL5	-0,5	0,99998	-0,6	0,999965	-0,6	0,999973	-0,7	0,99998	-0,73	0	4
LGR4	-0,8	0,999922	-0,7	0,999886	-0,9	0,99998	-0,8	0,999954	-0,73	0	4
CCND1	-0,8	0,999922	-0,5	0,99998	-0,7	0,999611	-0,6	0,998923	-0,73	0	4
FDXACB1	-0,6	0,999977	-0,4	0,999226	-0,7	0,99998	-0,6	0,999853	-0,75	0	4

Gene Symbol	D1_SLR	D1_p-value	D2_SLR	D2_p-value	D3_SLR	D3_p-value	D4_SLR	D4_p-value	Mean	Count_Increase	Count_rm Decrease
GPR18	-0,6	0,99998	-0,8	0,999973	-0,7	0,99998	-0,7	0,99998	-0,75	0	4
INPPL1	-0,8	0,999611	-0,7	0,999786	-0,6	0,999786	-0,6	0,999853	-0,75	0	4
NOTCH2	-0,8	0,99997	-1	0,999759	-1,2	0,99998	-1,2	0,999899	-0,75	0	4
RNGTT	-0,7	0,999932	-0,7	0,999932	-1	0,999833	-0,7	0,999886	-0,75	0	4
TCIRG1	-0,8	0,99996	-0,9	0,999954	-0,8	0,99998	-1	0,999977	-0,75	0	4
EED	-1,1	0,99996	-0,7	0,999886	-1	0,999811			-0,77	0	3
ABCG2	-1,1	0,999654	-0,9	0,999508	-1,8	0,998799			-0,77	0	3
CD24	-0,8	0,999954	-0,8	0,999977	-0,8	0,999508	-0,6	0,999811	-0,78	0	4
DEPTOR	-0,8	0,99997	-0,7	0,99997	-0,7	0,99998	-0,6	0,999965	-0,78	0	4
BIRC2	-0,7	0,999965	-0,6	0,999611	-0,8	0,99998	-0,7	0,999911	-0,78	0	4
PERP	-0,8	0,999932	-0,5	0,999833	-0,5	0,999727			-0,78	0	3
PGM2L1	-0,8	0,999853	-0,6	0,999911			-0,6	0,999508	-0,78	0	3
SESN3	-0,9	0,99998	-0,9	0,99997	-0,9	0,99987	-0,7	0,999932	-0,78	0	4
TNFRSF9	-0,4	0,99998	-0,5	0,99994	-0,4	0,999973	-0,5	0,999965	-0,80	0	4
APBB2			-0,7	0,99987	-1	0,99998	-0,8	0,99997	-0,80	0	3
BIRC3	-0,7	0,999948	-0,6	0,99998	-0,7	0,999922	-0,8	0,99998	-0,80	0	4
EOMES	-0,8	0,99998	-0,6	0,99997	-0,9	0,99998	-0,8	0,999932	-0,80	0	4
LRRC1	-0,9	0,999382	-0,6	0,999932	-1,3	0,999853	-0,7	0,999508	-0,80	0	4
PTS	-0,7	0,999977	-0,8	0,999948	-0,8	0,99996	-0,9	0,999965	-0,80	0	4
TFPI2	-0,8	0,99998	-0,6	0,99996	-0,9	0,999965	-0,7	0,999853	-0,80	0	4
ACTN1	-0,9	0,99998	-0,8	0,999786	-0,9	0,999786	-0,6	0,999693	-0,80	0	4
SIK2	-1	0,99998	-1	0,99998	-1,2	0,999932	-1	0,999965	-0,83	0	4
TIMM8B	-0,8	0,99998	-0,9	0,99996	-0,6	0,999886	-0,7	0,999954	-0,83	0	4
DGAT2	-0,7	0,999911	-0,6	0,999973	-0,9	0,99996	-0,7	0,999973	-0,83	0	4
PRR18	-1	0,999948	-0,9	0,999853	-1	0,999948	-0,9	0,999899	-0,85	0	4
CD44	-0,8	0,99998	-0,7	0,99998	-0,8	0,99998	-0,9	0,999977	-0,88	0	4
CLIC6	-0,7	0,99987	-0,7	0,999965	-0,9	0,99998	-0,9	0,99997	-0,88	0	4
COL1A1	-1	0,99998	-0,9	0,99998	-0,7	0,99998	-0,5	0,99998	-0,90	0	4
SSTR2	-1,1	0,999977	-1	0,99998	-1,2	0,999833	-0,9	0,999899	-0,90	0	4
HSPA2	-1	0,999853	-0,8	0,998799	-1	0,99987	-0,7	0,998923	-0,93	0	4
IGHE /// IGHE	-1,1	0,999226	-0,9	0,999226	-0,8	0,999853	-0,6	0,99987	-0,93	0	4
JAM3	-1	0,999833	-0,8	0,999932	-0,9	0,999226	-0,8	0,999611	-0,93	0	4
NMU	-0,8	0,999977	-0,5	0,99996	-0,8	0,99998	-0,7	0,99998	-0,93	0	4
FDX1	-0,9	0,99998	-1	0,99998	-0,9	0,99998	-1	0,99998	-0,95	0	4
SCCPDH	-0,8	0,999973	-0,8	0,99998	-0,9	0,99998	-0,9	0,99998	-0,95	0	4
TRAT1	-1	0,99998	-0,9	0,99998	-0,9	0,99998	-0,8	0,99998	-0,95	0	4
SYNGR1	-1,2	0,99998	-1,4	0,999886	-1,2	0,999226			-0,97	0	3
DLAT	-1	0,99998	-0,9	0,999977	-1,2	0,99998	-1,2	0,99998	-0,98	0	4
GABRA4	-0,6	0,99998	-0,6	0,99994	-0,6	0,99998	-0,6	0,99998	-0,98	0	4
PDE5A	-1,1	0,999886	-0,9	0,99996	-0,9	0,999853	-0,8	0,999977	-0,98	0	4
RAB38	-0,8	0,999693	-0,9	0,999948	-0,7	0,999977	-0,8	0,999811	-0,98	0	4
ZC3H12C	-1,1	0,99998	-1	0,99998	-0,9	0,99998	-0,9	0,99998	-0,98	0	4
RDX	-1	0,99998	-1	0,99998	-1,1	0,99998	-1,1	0,99998	-1,00	0	4
SBF2-AS1			-0,5	0,999727	-0,8	0,999886	-0,5	0,999727	-1,00	0	3
GSTP1	-0,8	0,99998	-0,8	0,99998	-0,8	0,99998	-0,9	0,99998	-1,03	0	4
TNIP3	-1,1	0,99994	-1,1	0,99996	-1	0,999833	-1	0,999977	-1,03	0	4
ALG9	-0,9	0,99994	-0,9	0,999954	-1,1	0,99998	-1,1	0,99998	-1,05	0	4
PRTFDC1	-0,9	0,999932			-1	0,999786	-0,5	0,999226	-1,05	0	3
OTOGL	-1,1	0,99997	-1,2	0,999899	-1,2	0,99998	-1,3	0,999965	-1,08	0	4
SOX4	-1,2	0,999954	-1,1	0,999448	-1,2	0,999693	-1,3	0,999226	-1,08	0	4
KLRC1 /// KLRC2	-1,1	0,99998	-0,9	0,99998	-0,9	0,999954	-0,5	0,99998	-1,08	0	4
ANK3	-1,3	0,999954	-1,2	0,999965	-1,2	0,999508	-1	0,999654	-1,10	0	4
RASSF6	-0,9	0,999948	-1	0,99996	-1	0,99998	-1	0,99998	-1,10	0	4
TREM1	-1,2	0,999833	-1,4	0,998514	-1,3	0,999833	-1,5	0,998664	-1,10	0	4
ZNF30	-1,1	0,99998	-0,6	0,999899	-1,3	0,99998	-0,8	0,999954	-1,13	0	4
ZNF880	-0,9	0,999911	-0,8	0,99998	-0,8	0,999853	-0,8	0,999911	-1,13	0	4
CPM	-1	0,999977	-1	0,999833	-0,9	0,999954	-0,6	0,999226	-1,13	0	4
DOCK9	-1,4	0,99998	-1,2	0,99998	-1,4	0,99998	-1,2	0,99998	-1,15	0	4
CTNNA2	-2,5	0,999448	-1,4	0,999899	-1,5	0,999654	-1,1	0,99987	-1,18	0	4
PPP2R1B	-1,2	0,99994	-0,7	0,99994	-0,9	0,999954	-0,7	0,999954	-1,20	0	4
RGS1	-1,1	0,99998	-1,2	0,99998	-1	0,99998	-1,2	0,999977	-1,23	0	4
BCL6	-1	0,999965	-1,3	0,999886	-1,1	0,999932	-1,2	0,999922	-1,25	0	4
LGALS8	-1,9	0,999654	-0,8	0,999977	-1,7	0,999899	-0,7	0,999954	-1,28	0	4
TPCN2	-1,1	0,99998	-1,1	0,99998	-1,2	0,99997	-1,2	0,99997	-1,28	0	4
NTS	-1,3	0,999973	-1,2	0,99997	-1,3	0,99998	-1,2	0,999973	-1,33	0	4
CXCR4	-1,5	0,99998	-1,5	0,99998	-1,5	0,99998	-1,5	0,99998	-1,33	0	4
ROBO1	-1,2	0,99998	-1,3	0,99998	-1,4	0,99998	-1,5	0,99998	-1,35	0	4
FCER2	-1	0,99998	-2,9	0,99998	-0,9	0,99998	-1,9	0,99998	-1,40	0	4
IL1R2	-1,2	0,999932	-1,5	0,999508	-1,2	0,999811	-1,3	0,998799	-1,50	0	4
PPM1H	-1,6	0,99998	-1,2	0,99998	-1,8	0,99998	-1,4	0,99998	-1,50	0	4
TEX15	-1,8	0,99998	-1,9	0,999911	-1,7	0,99998	-1,7	0,999759	-1,53	0	4
ROBO2	-2,9	0,99998	-3,4	0,999899	-2,5	0,99997	-3,1	0,99996	-1,58	0	4
PPAP2B	-1,6	0,99998	-2,1	0,999226	-1,6	0,999508			-1,58	0	3
CTTN	-1,1	0,999654	-0,8	0,999135	-1,4	0,999833	-1,3	0,999382	-1,60	0	4
SCML1	-1,9	0,999965	-1,7	0,99997	-1,8	0,999886	-1,7	0,999965	-1,75	0	4
EMR1	-1,5	0,999899	-2,2	0,999973	-1,5	0,99998	-2,2	0,999977	-1,80	0	4
MAGI3	-1,4	0,99998	-2	0,99998	-1,6	0,99998	-2	0,99998	-1,88	0	4
LIPG	-1,8	0,99994	-2,3	0,999911	-1,6	0,99998	-2,3	0,999973	-1,90	0	4
ADAMTS3	-1,9	0,998349			-2	0,99998	-1,6	0,99997	-2,00	0	3
LRRTM4	-2	0,99997	-2,1	0,99997	-1,9	0,999973	-2	0,99998	-2,10	0	4
GABBR1 /// UBD	-2,7	0,999611	-3	0,999562	-2,8	0,999954	-2,8	0,999954	-2,55	0	4
NAP1L2	-3,1	0,99998	-2,8	0,99998	-3,3	0,99998	-2,9	0,99998	-2,80	0	4
HSPA1A /// HSPA1B	-3	0,99998	-2,8	0,99998	-3,3	0,99998	-3	0,99998	-2,90	0	4
PHGDH	-2,5	0,99998	-3,4	0,99998	-2,4	0,999977	-3,3	0,999977	-3,00	0	4
POF1B	-4,7	0,999786	-2,8	0,999965	-5,4	0,999727	-3,4	0,999965	-3,25	0	4
FHL1	-2,5	0,999508	-1,8	0,999853	-1,9	0,998923	-1,3	0,999508	-3,98	0	4
FSTL5	-3,5	0,99998	-4,3	0,99998	-3,7	0,99998	-4,3	0,99998	-4,35	0	4
NRP1	-2,9	0,999853	-5,3	0,999759	-2,6	0,99997	-5,1	0,999654	-4,43	0	4
GRM5	-5,7	0,99998	-4,9	0,99998	-5,8	0,99998	-5,2	0,99998	-5,15	0	4
NLGN4X	-5,7	0,99987	-7,1	0,99997	-5	0,99997	-6,4	0,99998	-5,35	0	4
IPW /// SNORD107 /// SNORD115-13	-4,2	0,999811	-4	0,999977	-3,8	0,99997	-4,1	0,99997	-5,50	0	4
PAR-SN /// SNORD107 /// SNRPN /// SNURF	-5,7	0,99998	-5,7	0,99998	-6	0,99998	-6,2	0,99996	-6,95	0	4

Appendix 4 Analysis of hits from microarray analysis for involvement in different cellular pathways

yellow – pathways of interest

Pathway involvement	# genes
receptor activity (GO:0004872)	515
positive regulation of CD4-positive	515
response to organic cyclic substance (GO:0014070)	275
positive regulation of programmed cell death (GO:0043068)	229
regulation of CD4-positive	208
lysosomal membrane (GO:0005765)	169
cellular developmental process (GO:0048869)	167
signaling pathway (GO:0023033)	164
lymphocyte activation (GO:0046649)	**123**
acting on ester bonds (GO:0016788)	117
electron transport chain (GO:0022900)	117
intracellular signaling pathway (GO:0023034)	117
alpha beta T cell differentiation (GO:0043370)	108
cell-matrix adhesion (GO:0007160)	104
apoptosis (GO:0006915)	**93**
inositol or phosphatidylinositol phosphatase activity (GO:0004437)	90
regulation of lymphocyte activation (GO:0051249)	90
alpha-beta T cell differentiation (GO:0046632)	88
organ development (GO:0048513)	88
cell-substrate junction (GO:0030055)	84
positive regulation of humoral immune response mediated by circulating immunoglobulin (GO:0002925)	**79**
alpha-beta T cell differentiation involved in immune response (GO:0002293)	76
tube development (GO:0035295)	75
signal transducer activity (GO:0004871)	73
cytokine binding (GO:0019955)	73
plasma membrane (GO:0005886)	69
B cell differentiation (GO:0030183)	**69**

8 Acknowledgments / Danksagung

Ich danke Herrn PD Doktor Ingo Ringshausen für die Vergabe dieses hochinteressanten Promotionsthemas und für die gute und umfangreiche Betreuung der letzten Jahre. Ich habe im Besonderen meine methodischen Fähigkeiten deutlich erweitern können, was mir für meine weitere wissenschaftliche Karriere sehr nützlich sein wird.

Herrn Professor Küster danke ich für die Betreuung meiner Promotion als Zweitgutachter. Ich danke Herrn Professor Ulrich Keller für das Mentorat dieser Arbeit. Herrn Professor Christian Peschel danke ich für die freundliche Unterstützung meiner Promotion in seiner Abteilung des Klinikums rechts der Isar.

Weiterhin möchte ich mich bei der AG Ringshausen, insbesondere bei Frau Madlen Oelsner, und der gesamten III. Medizinischen Klinik des Klinikums rechts der Isar für die gute Zusammenarbeit bedanken. Besonders erwähnen möchte ich unsere Kollaboration mit Herrn Professor Bassermann und seiner Gruppe, vor allem mit Frau Doktor Katharina Engel, Frau Doktor Bianca-Sabrina Targosz und Frau Ursula Baumann für die freundliche Bereitstellung verschiedener Reagenzien und Vektoren sowie der Vermittlung von fachlichem Know-How.

Frau PD Doktor Sandra Hake und der gesamten AG Hake der LMU München, insbesondere Herrn Doktor Sebastian Pünzeler, danke ich für die freundliche Kollaboration, die Vermittlung von komplexen Methoden und den immensen wissenschaftlichen Input für eines meiner Teilprojekte. In diesem Zusammenhang danke ich Frau Doktor Yolanda Markaki and Susanne Leidescher der AG Leonhart der LMU München für die Durchführung und Auswertung der FRAP-Analyse.

Ich danke Herrn PD Doktor Ludger Klein-Hitpaß des Universitätsklinikums Essen für die Durchführung und die umfangreiche Auswertung der Microarray-Analyse.

Zudem möchte ich mich bei Frau Doktor Stefanie Hauck vom Helmholtz Zentrum München und bei ihrer Arbeitsgruppe, insbesondere bei Frau Doktor Juliane Merl, für die massenspektrometrische Analyse meiner Proben und die umfangreiche Auswertung bedanken.

I wish to thank Doctor Arthur Weiss from the University of California, San Francisco, USA, who kindly provided us with the ZAP70 wild-type and kinase-deficient mutant constructs.

Der Deutschen Krebshilfe e.V. möchte ich für die Bereitstellung der finanziellen Mittel für dieses Forschungsprojekt danken.

Ich möchte allen meinen Freunden für deren seelische Unterstützung in der Zeit meiner Promotion danken, besonders meinen Freundinnen Franzi und Maresa.

Herrn Doktor Ulrich Zißler und seiner Frau Lisbeth danke ich für den stets guten Rat und ihr offenes Ohr. Zudem danke ich Herrn Doktor Ulrich Zißler für die neuen Perspektiven und großartigen Möglichkeiten in der Zukunft der Wissenschaft.

Herrn Doktor Adam Chaker danke ich für seinen guten Rat und seine stets aufheiternden und motivierenden Worte und Zitate, den grünen Tee und die dunkle Schokolade zur Anregung der Hirnaktivität. Das Zitat von ihm, welches mir am meisten in Erinnerung geblieben ist, lautet: „Jede Doktorarbeit muss mit Tränen begossen werden."

Nicht zuletzt möchte ich meiner Familie danken. Meinen Omas und meiner Patentante für ihre jahrelange Wegbegleitung und ihr stets offenes Ohr. Besonders meiner Oma Schwandorf, die den Abschluss dieser Arbeit leider nicht mehr miterleben durfte, möchte ich für ihre Liebe und Fürsorge in all den Jahren danken.

Meiner Schwester Carolina für ihr Vorbild der Nervenstärke und ihren guten Rat zum Abschluss meiner Promotion. Meiner Schwester Clarissa für ihre außerordentliche Hilfe in schwierigen Zeiten.

Und insbesondere meinen Eltern für ihre Liebe und Fürsorge, die mich nicht nur während der Zeit der Doktorarbeit, sondern während meines ganzen Lebens unterstützt haben und die es mir erst ermöglicht haben, meinen Traumberuf als Wissenschaftlerin einzuschlagen und auszuüben.

Mein größter Dank gilt meinem Mann Marvin, der mich durch alle Höhen und Tiefen dieser intensiven Zeit begleitet hat, mich unterstützt und aufgefangen hat und dessen Zuspruch und Liebe mich in den vielen tiefgehenden Gesprächen sehr bereichert hat. Zudem hat er mich während meiner Promotion geheiratet und so mit mir unsere neue Familie gegründet. Von daher widme ich meine Promotionsarbeit meinem Mann Marvin.

9 References

Abrahamsson, A.E., I. Geron, J. Gotlib, K.H. Dao, C.F. Barroga, I.G. Newton, F.J. Giles, J. Durocher, R.S. Creusot, M. Karimi, C. Jones, J.L. Zehnder, A. Keating, R.S. Negrin, I.L. Weissman, and C.H. Jamieson. 2009. Glycogen synthase kinase 3beta missplicing contributes to leukemia stem cell generation. *Proc Natl Acad Sci U S A* 106:3925-3929.

Adams, J.M. 2003. Ways of dying: multiple pathways to apoptosis. *Genes Dev* 17:2481-2495.

Adams, J.M., and S. Cory. 2007a. The Bcl-2 apoptotic switch in cancer development and therapy. *Oncogene* 26:1324-1337.

Adams, J.M., and S. Cory. 2007b. Bcl-2-regulated apoptosis: mechanism and therapeutic potential. *Curr Opin Immunol* 19:488-496.

Akgul, C. 2009. Mcl-1 is a potential therapeutic target in multiple types of cancer. *Cell Mol Life Sci* 66:1326-1336.

Akgul, C., D.A. Moulding, M.R. White, and S.W. Edwards. 2000. In vivo localisation and stability of human Mcl-1 using green fluorescent protein (GFP) fusion proteins. *FEBS Lett* 478:72-76.

Alberts, B., Johnson, A., Lewis, J., Raff, M., Roberts, K., Walter, P. 2008. Molecular Biology of the Cell. Garland Science, New York, USA.

Amin, S., M. Walsh, C. Wilson, A.E. Parker, D. Oscier, E. Willmore, D. Mann, and J. Mann. 2012. Cross-talk between DNA methylation and active histone modifications regulates aberrant expression of ZAP70 in CLL. *J Cell Mol Med* 16:2074-2084.

Arents, G., R.W. Burlingame, B.C. Wang, W.E. Love, and E.N. Moudrianakis. 1991. The nucleosomal core histone octamer at 3.1 A resolution: a tripartite protein assembly and a left-handed superhelix. *Proc Natl Acad Sci U S A* 88:10148-10152.

Arpaia, E., M. Shahar, H. Dadi, A. Cohen, and C.M. Roifman. 1994. Defective T cell receptor signaling and CD8+ thymic selection in humans lacking zap-70 kinase. *Cell* 76:947-958.

Attia, M., C. Rachez, A. De Pauw, P. Avner, and U.C. Rogner. 2007. Nap1l2 promotes histone acetylation activity during neuronal differentiation. *Molecular and cellular biology* 27:6093-6102.

Au-Yeung, B.B., S. Deindl, L.Y. Hsu, E.H. Palacios, S.E. Levin, J. Kuriyan, and A. Weiss. 2009. The structure, regulation, and function of ZAP-70. *Immunol Rev* 228:41-57.

Axelrod, D., D.E. Koppel, J. Schlessinger, E. Elson, and W.W. Webb. 1976. Mobility measurement by analysis of fluorescence photobleaching recovery kinetics. *Biophys J* 16:1055-1069.

Balakrishnan, K., W.G. Wierda, M.J. Keating, and V. Gandhi. 2008. Gossypol, a BH3 mimetic, induces apoptosis in chronic lymphocytic leukemia cells. *Blood* 112:1971-1980.

Balboula, A.Z., P. Stein, R.M. Schultz, and K. Schindler. 2015. RBBP4 regulates histone deacetylation and bipolar spindle assembly during oocyte maturation in the mouse. *Biol Reprod* 92:105.

Baldin, V., J. Lukas, M.J. Marcote, M. Pagano, and G. Draetta. 1993. Cyclin D1 is a nuclear protein required for cell cycle progression in G1. *Genes Dev* 7:812-821.

Baliakas, P., A. Hadzidimitriou, L.A. Sutton, D. Rossi, E. Minga, N. Villamor, M. Larrayoz, J. Kminkova, A. Agathangelidis, Z. Davis, E. Tausch, E. Stalika, B. Kantorova, L. Mansouri, L. Scarfo, D. Cortese, V. Navrkalova, M.J. Rose-Zerilli, K.E. Smedby, G. Juliusson, A. Anagnostopoulos, A.M. Makris, A. Navarro, J. Delgado, D. Oscier, C. Belessi, S. Stilgenbauer, P. Ghia, S. Pospisilova, G. Gaidano, E. Campo, J.C. Strefford, K. Stamatopoulos, R. Rosenquist, and C.L.L. European Research Initiative on. 2015. Recurrent mutations refine prognosis in chronic lymphocytic leukemia. *Leukemia* 29:329-336.

Banin, S., L. Moyal, S. Shieh, Y. Taya, C.W. Anderson, L. Chessa, N.I. Smorodinsky, C. Prives, Y. Reiss, Y. Shiloh, and Y. Ziv. 1998. Enhanced phosphorylation of p53 by ATM in response to DNA damage. *Science* 281:1674-1677.

Bechter, O.E., W. Eisterer, G. Pall, W. Hilbe, T. Kuhr, and J. Thaler. 1998. Telomere length and telomerase activity predict survival in patients with B cell chronic lymphocytic leukemia. *Cancer Res* 58:4918-4922.

Binet, J.L., A. Auquier, G. Dighiero, C. Chastang, H. Piguet, J. Goasguen, G. Vaugier, G. Potron, P. Colona, F. Oberling, M. Thomas, G. Tchernia, C. Jacquillat, P. Boivin, C. Lesty, M.T. Duault, M. Monconduit, S. Belabbes, and F. Gremy. 1981. A new prognostic classification of chronic lymphocytic leukemia derived from a multivariate survival analysis. *Cancer* 48:198-206.

Binsky-Ehrenreich, I., A. Marom, M.C. Sobotta, L. Shvidel, A. Berrebi, I. Hazan-Halevy, S. Kay, A. Aloshin, I. Sagi, D.M. Goldenberg, L. Leng, R. Bucala, Y. Herishanu, M. Haran, and I. Shachar. 2014. CD84 is a survival receptor for CLL cells. *Oncogene* 33:1006-1016.

Blanchard, N., V. Di Bartolo, and C. Hivroz. 2002. In the immune synapse, ZAP-70 controls T cell polarization and recruitment of signaling proteins but not formation of the synaptic pattern. *Immunity* 17:389-399.

Bonner, W.M. 1975. Protein migration into nuclei. II. Frog oocyte nuclei accumulate a class of microinjected oocyte nuclear proteins and exclude a class of microinjected oocyte cytoplasmic proteins. *J Cell Biol* 64:431-437.

Brdicka, T., T.A. Kadlecek, J.P. Roose, A.W. Pastuszak, and A. Weiss. 2005. Intramolecular regulatory switch in ZAP-70: analogy with receptor tyrosine kinases. *Molecular and cellular biology* 25:4924-4933.

Brownlie, R.J., and R. Zamoyska. 2013. T cell receptor signalling networks: branched, diversified and bounded. *Nat Rev Immunol* 13:257-269.

Bu, J.Y., A.S. Shaw, and A.C. Chan. 1995. Analysis of the interaction of ZAP-70 and syk protein-tyrosine kinases with the T-cell antigen receptor by plasmon resonance. *Proc Natl Acad Sci U S A* 92:5106-5110.

Buenrostro, J.D., P.G. Giresi, L.C. Zaba, H.Y. Chang, and W.J. Greenleaf. 2013. Transposition of native chromatin for fast and sensitive epigenomic profiling of open chromatin, DNA-binding proteins and nucleosome position. *Nat Methods* 10:1213-1218.

Burch, J.B., and H.G. Martinson. 1981. Iodination of nucleosomes at low ionic strength: conformational changes in H4 and stabilization by H1. *Nucleic Acids Res* 9:4367-4385.

Burger, J.A., M. Burger, and T.J. Kipps. 1999. Chronic lymphocytic leukemia B cells express functional CXCR4 chemokine receptors that mediate spontaneous migration beneath bone marrow stromal cells. *Blood* 94:3658-3667.

Burgess, R.J., and Z. Zhang. 2013. Histone chaperones in nucleosome assembly and human disease. *Nat Struct Mol Biol* 20:14-22.

Byrd, J.C., R.R. Furman, S.E. Coutre, I.W. Flinn, J.A. Burger, K.A. Blum, B. Grant, J.P. Sharman, M. Coleman, W.G. Wierda, J.A. Jones, W. Zhao, N.A. Heerema, A.J. Johnson, J. Sukbuntherng, B.Y. Chang, F. Clow, E. Hedrick, J.J. Buggy, D.F. James, and S. O'Brien. 2013. Targeting BTK with ibrutinib in relapsed chronic lymphocytic leukemia. *The New England journal of medicine* 369:32-42.

Byrd, J.C., J.J. Jones, J.A. Woyach, A.J. Johnson, and J.M. Flynn. 2014. Entering the era of targeted therapy for chronic lymphocytic leukemia: impact on the practicing clinician. *J Clin Oncol* 32:3039-3047.

Cahill, N., A.C. Bergh, M. Kanduri, H. Goransson-Kultima, L. Mansouri, A. Isaksson, F. Ryan, K.E. Smedby, G. Juliusson, C. Sundstrom, A. Rosen, and R. Rosenquist. 2013. 450K-array analysis of chronic lymphocytic leukemia cells reveals global DNA methylation to be relatively stable over time and similar in resting and proliferative compartments. *Leukemia* 27:150-158.

Calin, G.A., C.D. Dumitru, M. Shimizu, R. Bichi, S. Zupo, E. Noch, H. Aldler, S. Rattan, M. Keating, K. Rai, L. Rassenti, T. Kipps, M. Negrini, F. Bullrich, and C.M. Croce. 2002. Frequent deletions and down-regulation of micro-RNA genes miR15 and miR16 at 13q14 in chronic lymphocytic leukemia. *Proc Natl Acad Sci U S A* 99:15524-15529.

Campbell, I.G., and T. Manolitsas. 1999. Absence of PPP2R1B gene alterations in primary ovarian cancers. *Oncogene* 18:6367-6369.

Campo, E., S.H. Swerdlow, N.L. Harris, S. Pileri, H. Stein, and E.S. Jaffe. 2011. The 2008 WHO classification of lymphoid neoplasms and beyond: evolving concepts and practical applications. *Blood* 117:5019-5032.

Canman, C.E., and D.S. Lim. 1998. The role of ATM in DNA damage responses and cancer. *Oncogene* 17:3301-3308.

Caporaso, N., L. Goldin, C. Plass, G. Calin, G. Marti, S. Bauer, E. Raveche, M.L. McMaster, D. Ng, O. Landgren, and S. Slager. 2007. Chronic lymphocytic leukaemia genetics overview. *Br J Haematol* 139:630-634.

Castello, A., M. Gaya, J. Tucholski, T. Oellerich, K.H. Lu, A. Tafuri, T. Pawson, J. Wienands, M. Engelke, and F.D. Batista. 2013. Nck-mediated recruitment of BCAP to the BCR regulates the PI(3)K-Akt pathway in B cells. *Nat Immunol* 14:966-975.

Castro, J.E., C.E. Prada, O. Loria, A. Kamal, L. Chen, F.J. Burrows, and T.J. Kipps. 2005. ZAP-70 is a novel conditional heat shock protein 90 (Hsp90) client: inhibition of Hsp90 leads to ZAP-70 degradation, apoptosis, and impaired signaling in chronic lymphocytic leukemia. *Blood* 106:2506-2512.

Chan, A.C., M. Dalton, R. Johnson, G.H. Kong, T. Wang, R. Thoma, and T. Kurosaki. 1995. Activation of ZAP-70 kinase activity by phosphorylation of tyrosine 493 is required for lymphocyte antigen receptor function. *EMBO J* 14:2499-2508.

Chan, A.C., B.A. Irving, J.D. Fraser, and A. Weiss. 1991. The zeta chain is associated with a tyrosine kinase and upon T-cell antigen receptor stimulation associates with ZAP-70, a 70-kDa tyrosine phosphoprotein. *Proc Natl Acad Sci U S A* 88:9166-9170.

Chan, A.C., M. Iwashima, C.W. Turck, and A. Weiss. 1992. ZAP-70: a 70 kd protein-tyrosine kinase that associates with the TCR zeta chain. *Cell* 71:649-662.

Chan, A.C., T.A. Kadlecek, M.E. Elder, A.H. Filipovich, W.L. Kuo, M. Iwashima, T.G. Parslow, and A. Weiss. 1994. ZAP-70 deficiency in an autosomal recessive form of severe combined immunodeficiency. *Science* 264:1599-1601.

Chen, J., J. Lin, and A.J. Levine. 1995. Regulation of transcription functions of the p53 tumor suppressor by the mdm-2 oncogene. *Mol Med* 1:142-152.

Chen, L., J. Apgar, L. Huynh, F. Dicker, T. Giago-McGahan, L. Rassenti, A. Weiss, and T.J. Kipps. 2005a. ZAP-70 directly enhances IgM signaling in chronic lymphocytic leukemia. *Blood* 105:2036-2041.

Chen, L., L. Huynh, J. Apgar, L. Tang, L. Rassenti, A. Weiss, and T.J. Kipps. 2008. ZAP-70 enhances IgM signaling independent of its kinase activity in chronic lymphocytic leukemia. *Blood* 111:2685-2692.

Chen, L., G. Widhopf, L. Huynh, L. Rassenti, K.R. Rai, A. Weiss, and T.J. Kipps. 2002. Expression of ZAP-70 is associated with increased B-cell receptor signaling in chronic lymphocytic leukemia. *Blood* 100:4609-4614.

Chen, R., M.J. Keating, V. Gandhi, and W. Plunkett. 2005b. Transcription inhibition by flavopiridol: mechanism of chronic lymphocytic leukemia cell death. *Blood* 106:2513-2519.

Chiorazzi, N., and M. Ferrarini. 2003. B cell chronic lymphocytic leukemia: lessons learned from studies of the B cell antigen receptor. *Annu Rev Immunol* 21:841-894.

Chiorazzi, N., K.R. Rai, and M. Ferrarini. 2005. Chronic lymphocytic leukemia. *The New England journal of medicine* 352:804-815.

Chou, R.H., Y.N. Wang, Y.H. Hsieh, L.Y. Li, W. Xia, W.C. Chang, L.C. Chang, C.C. Cheng, C.C. Lai, J.L. Hsu, W.J. Chang, S.Y. Chiang, H.J. Lee, H.W. Liao, P.H. Chuang, H.Y. Chen, H.L. Wang, S.C. Kuo, C.H. Chen, Y.L. Yu, and M.C. Hung. 2014. EGFR modulates DNA synthesis and repair through Tyr phosphorylation of histone H4. *Dev Cell* 30:224-237.

Christensen, D.J., Y. Chen, J. Oddo, K.M. Matta, J. Neil, E.D. Davis, A.D. Volkheimer, M.C. Lanasa, D.R. Friedman, B.K. Goodman, J.P. Gockerman, L.F. Diehl, C.M. de Castro, J.O. Moore, M.P. Vitek, and J.B. Weinberg. 2011. SET oncoprotein overexpression in B-cell chronic lymphocytic leukemia and non-Hodgkin lymphoma: a predictor of aggressive disease and a new treatment target. *Blood* 118:4150-4158.

Claus, R., D.M. Lucas, A.S. Ruppert, K.E. Williams, D. Weng, K. Patterson, M. Zucknick, C.C. Oakes, L.Z. Rassenti, A.W. Greaves, S. Geyer, W.G. Wierda, J.R. Brown, J.G. Gribben, J.C. Barrientos, K.R. Rai, N.E. Kay, T.J. Kipps, P. Shields, W. Zhao, M.R. Grever, C. Plass, and J.C. Byrd. 2014. Validation of ZAP-70 methylation and its relative significance in predicting outcome in chronic lymphocytic leukemia. *Blood* 124:42-48.

Claus, R., D.M. Lucas, S. Stilgenbauer, A.S. Ruppert, L. Yu, M. Zucknick, D. Mertens, A. Buhler, C.C. Oakes, R.A. Larson, N.E. Kay, D.F. Jelinek, T.J. Kipps, L.Z. Rassenti, J.G. Gribben, H. Dohner, N.A. Heerema, G. Marcucci, C. Plass, and J.C. Byrd. 2012. Quantitative DNA methylation analysis identifies a single CpG dinucleotide important for ZAP-70 expression and predictive of prognosis in chronic lymphocytic leukemia. *J Clin Oncol* 30:2483-2491.

Clifford, R., T. Louis, P. Robbe, S. Ackroyd, A. Burns, A.T. Timbs, G. Wright Colopy, H. Dreau, F. Sigaux, J.G. Judde, M. Rotger, A. Telenti, Y.L. Lin, P. Pasero, J. Maelfait, M. Titsias, D.R. Cohen, S.J. Henderson, M.T. Ross, D. Bentley, P. Hillmen, A. Pettitt, J. Rehwinkel, S.J. Knight, J.C. Taylor, Y.J.

Crow, M. Benkirane, and A. Schuh. 2014. SAMHD1 is mutated recurrently in chronic lymphocytic leukemia and is involved in response to DNA damage. *Blood* 123:1021-1031.

Coates, P.J., R. Nenutil, A. McGregor, S.M. Picksley, D.H. Crouch, P.A. Hall, and E.G. Wright. 2001. Mammalian prohibitin proteins respond to mitochondrial stress and decrease during cellular senescence. *Exp Cell Res* 265:262-273.

Collins, R.J., L.A. Verschuer, B.V. Harmon, R.L. Prentice, J.H. Pope, and J.F. Kerr. 1989. Spontaneous programmed death (apoptosis) of B-chronic lymphocytic leukaemia cells following their culture in vitro. *Br J Haematol* 71:343-350.

Conti, E., and J. Kuriyan. 2000. Crystallographic analysis of the specific yet versatile recognition of distinct nuclear localization signals by karyopherin alpha. *Structure* 8:329-338.

Cortese, D., L.A. Sutton, N. Cahill, K.E. Smedby, C. Geisler, R. Gunnarsson, G. Juliusson, L. Mansouri, and R. Rosenquist. 2014. On the way towards a 'CLL prognostic index': focus on TP53, BIRC3, SF3B1, NOTCH1 and MYD88 in a population-based cohort. *Leukemia* 28:710-713.

Coutre, S.E., J.C. Barrientos, J.R. Brown, S. de Vos, R.R. Furman, M.J. Keating, D. Li, S.M. O'Brien, J.M. Pagel, M.H. Poleski, J.P. Sharman, N.S. Yao, and A.D. Zelenetz. 2015. Management of adverse events associated with idelalisib treatment: expert panel opinion. *Leuk Lymphoma* 1-8.

Cramer, P., P. Langerbeins, B. Eichhorst, and M. Hallek. 2015. Advances in first-line treatment of chronic lymphocytic leukemia current recommendations on management and first-line treatment by the german cll study group (gcllsg). *Eur J Haematol*

Cross, D.A., D.R. Alessi, P. Cohen, M. Andjelkovich, and B.A. Hemmings. 1995. Inhibition of glycogen synthase kinase-3 by insulin mediated by protein kinase B. *Nature* 378:785-789.

Cutrona, G., M. Colombo, S. Matis, M. Fabbi, M. Spriano, V. Callea, E. Vigna, M. Gentile, S. Zupo, N. Chiorazzi, F. Morabito, and M. Ferrarini. 2008. Clonal heterogeneity in chronic lymphocytic leukemia cells: superior response to surface IgM cross-linking in CD38, ZAP-70-positive cells. *Haematologica* 93:413-422.

Damle, R.N., F.M. Batliwalla, F. Ghiotto, A. Valetto, E. Albesiano, C. Sison, S.L. Allen, J. Kolitz, V.P. Vinciguerra, P. Kudalkar, T. Wasil, K.R. Rai, M. Ferrarini, P.K. Gregersen, and N. Chiorazzi. 2004. Telomere length and telomerase activity delineate distinctive replicative features of the B-CLL subgroups defined by immunoglobulin V gene mutations. *Blood* 103:375-382.

Damle, R.N., S. Temburni, C. Calissano, S. Yancopoulos, T. Banapour, C. Sison, S.L. Allen, K.R. Rai, and N. Chiorazzi. 2007. CD38 expression labels an activated subset within chronic lymphocytic leukemia clones enriched in proliferating B cells. *Blood* 110:3352-3359.

Dangi-Garimella, S. 2014. FDA grants accelerated approval for ibrutinib for CLL. *Am J Manag Care* 20:E10.

Danilov, A.V., A.K. Klein, H.J. Lee, D.V. Baez, and B.T. Huber. 2005. Differential control of G0 programme in chronic lymphocytic leukaemia: a novel prognostic factor. *Br J Haematol* 128:472-481.

Davanture, S., J. Leignadier, P. Milani, P. Soubeyran, B. Malissen, M. Malissen, A.M. Schmitt-Verhulst, and C. Boyer. 2005. Selective defect in antigen-

induced TCR internalization at the immune synapse of CD8 T cells bearing the ZAP-70(Y292F) mutation. *J Immunol* 175:3140-3149.

Davey, C.A., D.F. Sargent, K. Luger, A.W. Maeder, and T.J. Richmond. 2002. Solvent mediated interactions in the structure of the nucleosome core particle at 1.9 a resolution. *J Mol Biol* 319:1097-1113.

Dawson, M.A., A.J. Bannister, B. Gottgens, S.D. Foster, T. Bartke, A.R. Green, and T. Kouzarides. 2009. JAK2 phosphorylates histone H3Y41 and excludes HP1alpha from chromatin. *Nature* 461:819-822.

Day, C.L., L. Chen, S.J. Richardson, P.J. Harrison, D.C. Huang, and M.G. Hinds. 2005. Solution structure of prosurvival Mcl-1 and characterization of its binding by proapoptotic BH3-only ligands. *J Biol Chem* 280:4738-4744.

De Bondt, H.L., J. Rosenblatt, J. Jancarik, H.D. Jones, D.O. Morgan, and S.H. Kim. 1993. Crystal structure of cyclin-dependent kinase 2. *Nature* 363:595-602.

Deaglio, S., S. Aydin, M.M. Grand, T. Vaisitti, L. Bergui, G. D'Arena, G. Chiorino, and F. Malavasi. 2010. CD38/CD31 interactions activate genetic pathways leading to proliferation and migration in chronic lymphocytic leukemia cells. *Mol Med* 16:87-91.

Deglesne, P.A., N. Chevallier, R. Letestu, F. Baran-Marszak, T. Beitar, C. Salanoubat, L. Sanhes, J. Nataf, C. Roger, N. Varin-Blank, and F. Ajchenbaum-Cymbalista. 2006. Survival response to B-cell receptor ligation is restricted to progressive chronic lymphocytic leukemia cells irrespective of Zap70 expression. *Cancer Res* 66:7158-7166.

Deindl, S., T.A. Kadlecek, T. Brdicka, X. Cao, A. Weiss, and J. Kuriyan. 2007. Structural basis for the inhibition of tyrosine kinase activity of ZAP-70. *Cell* 129:735-746.

Del Porto, P., L. Bruno, M.G. Mattei, H. von Boehmer, and C. Saint-Ruf. 1995. Cloning and comparative analysis of the human pre-T-cell receptor alpha-chain gene. *Proc Natl Acad Sci U S A* 92:12105-12109.

Derenne, S., B. Monia, N.M. Dean, J.K. Taylor, M.J. Rapp, J.L. Harousseau, R. Bataille, and M. Amiot. 2002. Antisense strategy shows that Mcl-1 rather than Bcl-2 or Bcl-x(L) is an essential survival protein of human myeloma cells. *Blood* 100:194-199.

Di Bartolo, V., D. Mege, V. Germain, M. Pelosi, E. Dufour, F. Michel, G. Magistrelli, A. Isacchi, and O. Acuto. 1999. Tyrosine 319, a newly identified phosphorylation site of ZAP-70, plays a critical role in T cell antigen receptor signaling. *J Biol Chem* 274:6285-6294.

Dighiero, G., K. Maloum, B. Desablens, B. Cazin, M. Navarro, R. Leblay, M. Leporrier, J. Jaubert, G. Lepeu, B. Dreyfus, J.L. Binet, and P. Travade. 1998. Chlorambucil in indolent chronic lymphocytic leukemia. French Cooperative Group on Chronic Lymphocytic Leukemia. *The New England journal of medicine* 338:1506-1514.

Ding, Q., X. He, J.M. Hsu, W. Xia, C.T. Chen, L.Y. Li, D.F. Lee, J.C. Liu, Q. Zhong, X. Wang, and M.C. Hung. 2007. Degradation of Mcl-1 by beta-TrCP mediates glycogen synthase kinase 3-induced tumor suppression and chemosensitization. *Molecular and cellular biology* 27:4006-4017.

Dingwall, C., and R.A. Laskey. 1991. Nuclear targeting sequences--a consensus? *Trends Biochem Sci* 16:478-481.

Dohner, H., S. Stilgenbauer, A. Benner, E. Leupolt, A. Krober, L. Bullinger, K. Dohner, M. Bentz, and P. Lichter. 2000. Genomic aberrations and survival

in chronic lymphocytic leukemia. *The New England journal of medicine* 343:1910-1916.

Dolmetsch, R.E., R.S. Lewis, C.C. Goodnow, and J.I. Healy. 1997. Differential activation of transcription factors induced by Ca2+ response amplitude and duration. *Nature* 386:855-858.

Dolmetsch, R.E., K. Xu, and R.S. Lewis. 1998. Calcium oscillations increase the efficiency and specificity of gene expression. *Nature* 392:933-936.

Donahue, A.C., and D.A. Fruman. 2003. Proliferation and survival of activated B cells requires sustained antigen receptor engagement and phosphoinositide 3-kinase activation. *J Immunol* 170:5851-5860.

Dreger, P., A. Schnaiter, T. Zenz, S. Bottcher, M. Rossi, P. Paschka, A. Buhler, S. Dietrich, R. Busch, M. Ritgen, D. Bunjes, M. Zeis, M. Stadler, L. Uharek, C. Scheid, U. Hegenbart, M. Hallek, M. Kneba, N. Schmitz, H. Dohner, and S. Stilgenbauer. 2013. TP53, SF3B1, and NOTCH1 mutations and outcome of allotransplantation for chronic lymphocytic leukemia: six-year follow-up of the GCLLSG CLL3X trial. *Blood* 121:3284-3288.

Duhren-von Minden, M., R. Ubelhart, D. Schneider, T. Wossning, M.P. Bach, M. Buchner, D. Hofmann, E. Surova, M. Follo, F. Kohler, H. Wardemann, K. Zirlik, H. Veelken, and H. Jumaa. 2012. Chronic lymphocytic leukaemia is driven by antigen-independent cell-autonomous signalling. *Nature* 489:309-312.

Dumont, C., N. Blanchard, V. Di Bartolo, N. Lezot, E. Dufour, S. Jauliac, and C. Hivroz. 2002. TCR/CD3 down-modulation and zeta degradation are regulated by ZAP-70. *J Immunol* 169:1705-1712.

Egan, S.E., B.W. Giddings, M.W. Brooks, L. Buday, A.M. Sizeland, and R.A. Weinberg. 1993. Association of Sos Ras exchange protein with Grb2 is implicated in tyrosine kinase signal transduction and transformation. *Nature* 363:45-51.

Eichhorn, P.J., M.P. Creyghton, and R. Bernards. 2009. Protein phosphatase 2A regulatory subunits and cancer. *Biochim Biophys Acta* 1795:1-15.

Eichhorst, B.F., R. Busch, G. Hopfinger, R. Pasold, M. Hensel, C. Steinbrecher, S. Siehl, U. Jager, M. Bergmann, S. Stilgenbauer, C. Schweighofer, C.M. Wendtner, H. Dohner, G. Brittinger, B. Emmerich, M. Hallek, and C.L.L.S.G. German. 2006. Fludarabine plus cyclophosphamide versus fludarabine alone in first-line therapy of younger patients with chronic lymphocytic leukemia. *Blood* 107:885-891.

Eichhorst, B.F., R. Busch, S. Stilgenbauer, M. Stauch, M.A. Bergmann, M. Ritgen, N. Kranzhofer, R. Rohrberg, U. Soling, O. Burkhard, A. Westermann, V. Goede, C.D. Schweighofer, K. Fischer, A.M. Fink, C.M. Wendtner, G. Brittinger, H. Dohner, B. Emmerich, M. Hallek, and C.L.L.S.G. German. 2009. First-line therapy with fludarabine compared with chlorambucil does not result in a major benefit for elderly patients with advanced chronic lymphocytic leukemia. *Blood* 114:3382-3391.

Eickbush, T.H., and E.N. Moudrianakis. 1978. The histone core complex: an octamer assembled by two sets of protein-protein interactions. *Biochemistry* 17:4955-4964.

Elder, M.E., D. Lin, J. Clever, A.C. Chan, T.J. Hope, A. Weiss, and T.G. Parslow. 1994. Human severe combined immunodeficiency due to a defect in ZAP-70, a T cell tyrosine kinase. *Science* 264:1596-1599.

Epler, J.A., R. Liu, H. Chung, N.C. Ottoson, and Y. Shimizu. 2000. Regulation of beta 1 integrin-mediated adhesion by T cell receptor signaling involves

ZAP-70 but differs from signaling events that regulate transcriptional activity. *J Immunol* 165:4941-4949.

Erard, M.S., P. Belenguer, M. Caizergues-Ferrer, A. Pantaloni, and F. Amalric. 1988. A major nucleolar protein, nucleolin, induces chromatin decondensation by binding to histone H1. *Eur J Biochem* 175:525-530.

Fabbri, G., H. Khiabanian, A.B. Holmes, J. Wang, M. Messina, C.G. Mullighan, L. Pasqualucci, R. Rabadan, and R. Dalla-Favera. 2013. Genetic lesions associated with chronic lymphocytic leukemia transformation to Richter syndrome. *The Journal of experimental medicine* 210:2273-2288.

Fabbri, G., S. Rasi, D. Rossi, V. Trifonov, H. Khiabanian, J. Ma, A. Grunn, M. Fangazio, D. Capello, S. Monti, S. Cresta, E. Gargiulo, F. Forconi, A. Guarini, L. Arcaini, M. Paulli, L. Laurenti, L.M. Larocca, R. Marasca, V. Gattei, D. Oscier, F. Bertoni, C.G. Mullighan, R. Foa, L. Pasqualucci, R. Rabadan, R. Dalla-Favera, and G. Gaidano. 2011. Analysis of the chronic lymphocytic leukemia coding genome: role of NOTCH1 mutational activation. *The Journal of experimental medicine* 208:1389-1401.

Fais, F., F. Ghiotto, S. Hashimoto, B. Sellars, A. Valetto, S.L. Allen, P. Schulman, V.P. Vinciguerra, K. Rai, L.Z. Rassenti, T.J. Kipps, G. Dighiero, H.W. Schroeder, Jr., M. Ferrarini, and N. Chiorazzi. 1998. Chronic lymphocytic leukemia B cells express restricted sets of mutated and unmutated antigen receptors. *J Clin Invest* 102:1515-1525.

Feske, S., J. Giltnane, R. Dolmetsch, L.M. Staudt, and A. Rao. 2001. Gene regulation mediated by calcium signals in T lymphocytes. *Nat Immunol* 2:316-324.

Finco, T.S., T. Kadlecek, W. Zhang, L.E. Samelson, and A. Weiss. 1998. LAT is required for TCR-mediated activation of PLCgamma1 and the Ras pathway. *Immunity* 9:617-626.

Fischer, A., C. Picard, K. Chemin, S. Dogniaux, F. le Deist, and C. Hivroz. 2010. ZAP70: a master regulator of adaptive immunity. *Semin Immunopathol* 32:107-116.

Fontes, M.R., T. Teh, and B. Kobe. 2000. Structural basis of recognition of monopartite and bipartite nuclear localization sequences by mammalian importin-alpha. *J Mol Biol* 297:1183-1194.

Forconi, F., K.N. Potter, I. Wheatley, N. Darzentas, E. Sozzi, K. Stamatopoulos, C.I. Mockridge, G. Packham, and F.K. Stevenson. 2010. The normal IGHV1-69-derived B-cell repertoire contains stereotypic patterns characteristic of unmutated CLL. *Blood* 115:71-77.

Fraga, M.F., E. Ballestar, A. Villar-Garea, M. Boix-Chornet, J. Espada, G. Schotta, T. Bonaldi, C. Haydon, S. Ropero, K. Petrie, N.G. Iyer, A. Perez-Rosado, E. Calvo, J.A. Lopez, A. Cano, M.J. Calasanz, D. Colomer, M.A. Piris, N. Ahn, A. Imhof, C. Caldas, T. Jenuwein, and M. Esteller. 2005. Loss of acetylation at Lys16 and trimethylation at Lys20 of histone H4 is a common hallmark of human cancer. *Nat Genet* 37:391-400.

Frame, S., P. Cohen, and R.M. Biondi. 2001. A common phosphate binding site explains the unique substrate specificity of GSK3 and its inactivation by phosphorylation. *Mol Cell* 7:1321-1327.

Friedberg, J.W., J. Sharman, J. Sweetenham, P.B. Johnston, J.M. Vose, A. Lacasce, J. Schaefer-Cutillo, S. De Vos, R. Sinha, J.P. Leonard, L.D. Cripe, S.A. Gregory, M.P. Sterba, A.M. Lowe, R. Levy, and M.A. Shipp. 2010. Inhibition of Syk with fostamatinib disodium has significant clinical activity in

non-Hodgkin lymphoma and chronic lymphocytic leukemia. *Blood* 115:2578-2585.

Furman, R.R., J.P. Sharman, S.E. Coutre, B.D. Cheson, J.M. Pagel, P. Hillmen, J.C. Barrientos, A.D. Zelenetz, T.J. Kipps, I. Flinn, P. Ghia, H. Eradat, T. Ervin, N. Lamanna, B. Coiffier, A.R. Pettitt, S. Ma, S. Stilgenbauer, P. Cramer, M. Aiello, D.M. Johnson, L.L. Miller, D. Li, T.M. Jahn, R.D. Dansey, M. Hallek, and S.M. O'Brien. 2014. Idelalisib and rituximab in relapsed chronic lymphocytic leukemia. *The New England journal of medicine* 370:997-1007.

Gamble, S.C., D. Chotai, M. Odontiadis, D.A. Dart, G.N. Brooke, S.M. Powell, V. Reebye, A. Varela-Carver, Y. Kawano, J. Waxman, and C.L. Bevan. 2007. Prohibitin, a protein downregulated by androgens, represses androgen receptor activity. *Oncogene* 26:1757-1768.

Gandhi, V., K. Balakrishnan, and L.S. Chen. 2008. Mcl-1: the 1 in CLL. *Blood* 112:3538-3540.

Garcia, K.C., L. Teyton, and I.A. Wilson. 1999. Structural basis of T cell recognition. *Annu Rev Immunol* 17:369-397.

Garg, M., L.R. Perumalsamy, G.V. Shivashankar, and A. Sarin. 2014. The linker histone h1.2 is an intermediate in the apoptotic response to cytokine deprivation in T-effectors. *Int J Cell Biol* 2014:674753.

Gelkop, S., and N. Isakov. 1999. T cell activation stimulates the association of enzymatically active tyrosine-phosphorylated ZAP-70 with the Crk adapter proteins. *J Biol Chem* 274:21519-21527.

Ghia, P., N. Chiorazzi, and K. Stamatopoulos. 2008. Microenvironmental influences in chronic lymphocytic leukaemia: the role of antigen stimulation. *J Intern Med* 264:549-562.

Gobessi, S., L. Laurenti, P.G. Longo, S. Sica, G. Leone, and D.G. Efremov. 2007. ZAP-70 enhances B-cell-receptor signaling despite absent or inefficient tyrosine kinase activation in chronic lymphocytic leukemia and lymphoma B cells. *Blood* 109:2032-2039.

Goda, S., A.C. Quale, M.L. Woods, A. Felthauser, and Y. Shimizu. 2004. Control of TCR-mediated activation of beta 1 integrins by the ZAP-70 tyrosine kinase interdomain B region and the linker for activation of T cells adapter protein. *J Immunol* 172:5379-5387.

Gorlich, D., S. Kostka, R. Kraft, C. Dingwall, R.A. Laskey, E. Hartmann, and S. Prehn. 1995. Two different subunits of importin cooperate to recognize nuclear localization signals and bind them to the nuclear envelope. *Curr Biol* 5:383-392.

Guieze, R., P. Robbe, R. Clifford, S. de Guibert, B. Pereira, A. Timbs, M.S. Dilhuydy, M. Cabes, L. Ysebaert, A. Burns, F. Nguyen-Khac, F. Davi, L. Veronese, P. Combes, M. Le Garff-Tavernier, V. Leblond, H. Merle-Beral, R. Alsolami, A. Hamblin, J. Mason, A. Pettitt, P. Hillmen, J. Taylor, S.J. Knight, O. Tournilhac, and A. Schuh. 2015. Presence of multiple recurrent mutations revealed by targeted NGS confers poor trial outcome of relapsed/refractory CLL. *Blood*

Guieze, R., and C.J. Wu. 2015. Genomic and epigenomic heterogeneity in chronic lymphocytic leukemia. *Blood* 126:445-453.

Guo, B., T.T. Su, and D.J. Rawlings. 2004. Protein kinase C family functions in B-cell activation. *Curr Opin Immunol* 16:367-373.

Hake, S.B., A. Xiao, and C.D. Allis. 2004. Linking the epigenetic 'language' of covalent histone modifications to cancer. *Br J Cancer* 90:761-769.

Hallek, M. 2013. Signaling the end of chronic lymphocytic leukemia: new frontline treatment strategies. *Blood* 122:3723-3734.

Hallek, M., B.D. Cheson, D. Catovsky, F. Caligaris-Cappio, G. Dighiero, H. Dohner, P. Hillmen, M.J. Keating, E. Montserrat, K.R. Rai, T.J. Kipps, and L. International Workshop on Chronic Lymphocytic. 2008. Guidelines for the diagnosis and treatment of chronic lymphocytic leukemia: a report from the International Workshop on Chronic Lymphocytic Leukemia updating the National Cancer Institute-Working Group 1996 guidelines. *Blood* 111:5446-5456.

Hallek, M., K. Fischer, G. Fingerle-Rowson, A.M. Fink, R. Busch, J. Mayer, M. Hensel, G. Hopfinger, G. Hess, U. von Grunhagen, M. Bergmann, J. Catalano, P.L. Zinzani, F. Caligaris-Cappio, J.F. Seymour, A. Berrebi, U. Jager, B. Cazin, M. Trneny, A. Westermann, C.M. Wendtner, B.F. Eichhorst, P. Staib, A. Buhler, D. Winkler, T. Zenz, S. Bottcher, M. Ritgen, M. Mendila, M. Kneba, H. Dohner, S. Stilgenbauer, I. International Group of, and G. German Chronic Lymphocytic Leukaemia Study. 2010. Addition of rituximab to fludarabine and cyclophosphamide in patients with chronic lymphocytic leukaemia: a randomised, open-label, phase 3 trial. *Lancet* 376:1164-1174.

Happel, N., and D. Doenecke. 2009. Histone H1 and its isoforms: contribution to chromatin structure and function. *Gene* 431:1-12.

Harris, N.L., E.S. Jaffe, J. Diebold, G. Flandrin, H.K. Muller-Hermelink, J. Vardiman, T.A. Lister, and C.D. Bloomfield. 1999. World Health Organization classification of neoplastic diseases of the hematopoietic and lymphoid tissues: report of the Clinical Advisory Committee meeting-Airlie House, Virginia, November 1997. *J Clin Oncol* 17:3835-3849.

Harshman, S.W., M.E. Hoover, C. Huang, O.E. Branson, S.B. Chaney, C.M. Cheney, T.J. Rosol, C.L. Shapiro, V.H. Wysocki, K. Huebner, and M.A. Freitas. 2014. Histone H1 phosphorylation in breast cancer. *J Proteome Res* 13:2453-2467.

Hatada, M.H., X. Lu, E.R. Laird, J. Green, J.P. Morgenstern, M. Lou, C.S. Marr, T.B. Phillips, M.K. Ram, K. Theriault, and et al. 1995. Molecular basis for interaction of the protein tyrosine kinase ZAP-70 with the T-cell receptor. *Nature* 377:32-38.

Hennecke, J., and D.C. Wiley. 2001. T cell receptor-MHC interactions up close. *Cell* 104:1-4.

Herman, S.E., A.L. Gordon, A.J. Wagner, N.A. Heerema, W. Zhao, J.M. Flynn, J. Jones, L. Andritsos, K.D. Puri, B.J. Lannutti, N.A. Giese, X. Zhang, L. Wei, J.C. Byrd, and A.J. Johnson. 2010. Phosphatidylinositol 3-kinase-delta inhibitor CAL-101 shows promising preclinical activity in chronic lymphocytic leukemia by antagonizing intrinsic and extrinsic cellular survival signals. *Blood* 116:2078-2088.

Hers, I., E.E. Vincent, and J.M. Tavare. 2011. Akt signalling in health and disease. *Cell Signal* 23:1515-1527.

Hillen, W., and C. Berens. 1994. Mechanisms underlying expression of Tn10 encoded tetracycline resistance. *Annu Rev Microbiol* 48:345-369.

Hillen, W., C. Gatz, L. Altschmied, K. Schollmeier, and I. Meier. 1983. Control of expression of the Tn10-encoded tetracycline resistance genes. Equilibrium and kinetic investigation of the regulatory reactions. *J Mol Biol* 169:707-721.

Hillen, W., and K. Schollmeier. 1983. Nucleotide sequence of the Tn10 encoded tetracycline resistance gene. *Nucleic Acids Res* 11:525-539.

Hodel, A.E., M.T. Harreman, K.F. Pulliam, M.E. Harben, J.S. Holmes, M.R. Hodel, K.M. Berland, and A.H. Corbett. 2006. Nuclear localization signal receptor affinity correlates with in vivo localization in Saccharomyces cerevisiae. *J Biol Chem* 281:23545-23556.

Hodel, M.R., A.H. Corbett, and A.E. Hodel. 2001. Dissection of a nuclear localization signal. *J Biol Chem* 276:1317-1325.

Honda, R., H. Tanaka, and H. Yasuda. 1997. Oncoprotein MDM2 is a ubiquitin ligase E3 for tumor suppressor p53. *FEBS Lett* 420:25-27.

Horejsi, V., W. Zhang, and B. Schraven. 2004. Transmembrane adaptor proteins: organizers of immunoreceptor signalling. *Nat Rev Immunol* 4:603-616.

Hu, Y., M.J. Turner, J. Shields, M.S. Gale, E. Hutto, B.L. Roberts, W.M. Siders, and J.M. Kaplan. 2009. Investigation of the mechanism of action of alemtuzumab in a human CD52 transgenic mouse model. *Immunology* 128:260-270.

Hussain, S.R., C.M. Cheney, A.J. Johnson, T.S. Lin, M.R. Grever, M.A. Caligiuri, D.M. Lucas, and J.C. Byrd. 2007. Mcl-1 is a relevant therapeutic target in acute and chronic lymphoid malignancies: down-regulation enhances rituximab-mediated apoptosis and complement-dependent cytotoxicity. *Clin Cancer Res* 13:2144-2150.

Huttmann, A., L. Klein-Hitpass, J. Thomale, R. Deenen, A. Carpinteiro, H. Nuckel, P. Ebeling, A. Fuhrer, J. Edelmann, L. Sellmann, U. Duhrsen, and J. Durig. 2006. Gene expression signatures separate B-cell chronic lymphocytic leukaemia prognostic subgroups defined by ZAP-70 and CD38 expression status. *Leukemia* 20:1774-1782.

Ibrahim, S., M. Keating, K.A. Do, S. O'Brien, Y.O. Huh, I. Jilani, S. Lerner, H.M. Kantarjian, and M. Albitar. 2001. CD38 expression as an important prognostic factor in B-cell chronic lymphocytic leukemia. *Blood* 98:181-186.

Inuzuka, H., S. Shaik, I. Onoyama, D. Gao, A. Tseng, R.S. Maser, B. Zhai, L. Wan, A. Gutierrez, A.W. Lau, Y. Xiao, A.L. Christie, J. Aster, J. Settleman, S.P. Gygi, A.L. Kung, T. Look, K.I. Nakayama, R.A. DePinho, and W. Wei. 2011. SCF(FBW7) regulates cellular apoptosis by targeting MCL1 for ubiquitylation and destruction. *Nature* 471:104-109.

Irving, B.A., and A. Weiss. 1991. The cytoplasmic domain of the T cell receptor zeta chain is sufficient to couple to receptor-associated signal transduction pathways. *Cell* 64:891-901.

Ivaska, J., L. Nissinen, N. Immonen, J.E. Eriksson, V.M. Kahari, and J. Heino. 2002. Integrin alpha 2 beta 1 promotes activation of protein phosphatase 2A and dephosphorylation of Akt and glycogen synthase kinase 3 beta. *Molecular and cellular biology* 22:1352-1359.

Iwashima, M., B.A. Irving, N.S. van Oers, A.C. Chan, and A. Weiss. 1994. Sequential interactions of the TCR with two distinct cytoplasmic tyrosine kinases. *Science* 263:1136-1139.

Jackman, J.K., D.G. Motto, Q. Sun, M. Tanemoto, C.W. Turck, G.A. Peltz, G.A. Koretzky, and P.R. Findell. 1995. Molecular cloning of SLP-76, a 76-kDa tyrosine phosphoprotein associated with Grb2 in T cells. *J Biol Chem* 270:7029-7032.

Jain, P., and S. O'Brien. 2012. Richter's transformation in chronic lymphocytic leukemia. *Oncology (Williston Park)* 26:1146-1152.

Jenuwein, T., and C.D. Allis. 2001. Translating the histone code. *Science* 293:1074-1080.

Jeromin, S., S. Weissmann, C. Haferlach, F. Dicker, K. Bayer, V. Grossmann, T. Alpermann, A. Roller, A. Kohlmann, T. Haferlach, W. Kern, and S. Schnittger. 2014. SF3B1 mutations correlated to cytogenetics and mutations in NOTCH1, FBXW7, MYD88, XPO1 and TP53 in 1160 untreated CLL patients. *Leukemia* 28:108-117.

Kabak, S., B.J. Skaggs, M.R. Gold, M. Affolter, K.L. West, M.S. Foster, K. Siemasko, A.C. Chan, R. Aebersold, and M.R. Clark. 2002. The direct recruitment of BLNK to immunoglobulin alpha couples the B-cell antigen receptor to distal signaling pathways. *Molecular and cellular biology* 22:2524-2535.

Kadlecek, T.A., N.S. van Oers, L. Lefrancois, S. Olson, D. Finlay, D.H. Chu, K. Connolly, N. Killeen, and A. Weiss. 1998. Differential requirements for ZAP-70 in TCR signaling and T cell development. *J Immunol* 161:4688-4694.

Kao, S.H., W.L. Wang, C.Y. Chen, Y.L. Chang, Y.Y. Wu, Y.T. Wang, S.P. Wang, A.I. Nesvizhskii, Y.J. Chen, T.M. Hong, and P.C. Yang. 2014. GSK3beta controls epithelial-mesenchymal transition and tumor metastasis by CHIP-mediated degradation of Slug. *Oncogene* 33:3172-3182.

Katalinic, A. 2015. Gesellschaft der epidemiologischen Krebsregister in Deutschland e.V. (GEKID). In Gesellschaft epidemiologischer Krebsregister in Deutschland e.V. (GEKID e.V.).

Kim, L., and A.R. Kimmel. 2000. GSK3, a master switch regulating cell-fate specification and tumorigenesis. *Curr Opin Genet Dev* 10:508-514.

Kim, Y.J., F. Sekiya, B. Poulin, Y.S. Bae, and S.G. Rhee. 2004. Mechanism of B-cell receptor-induced phosphorylation and activation of phospholipase C-gamma2. *Molecular and cellular biology* 24:9986-9999.

Kipps, T.J. 1993. Immunoglobulin genes in chronic lymphocytic leukemia. *Blood Cells* 19:615-625; discussion 631-612.

Kitada, S., J. Andersen, S. Akar, J.M. Zapata, S. Takayama, S. Krajewski, H.G. Wang, X. Zhang, F. Bullrich, C.M. Croce, K. Rai, J. Hines, and J.C. Reed. 1998. Expression of apoptosis-regulating proteins in chronic lymphocytic leukemia: correlations with In vitro and In vivo chemoresponses. *Blood* 91:3379-3389.

Klein, U., Y. Tu, G.A. Stolovitzky, M. Mattioli, G. Cattoretti, H. Husson, A. Freedman, G. Inghirami, L. Cro, L. Baldini, A. Neri, A. Califano, and R. Dalla-Favera. 2001. Gene expression profiling of B cell chronic lymphocytic leukemia reveals a homogeneous phenotype related to memory B cells. *The Journal of experimental medicine* 194:1625-1638.

Kn, H., S. Bassal, C. Tikellis, and A. El-Osta. 2004. Expression analysis of the epigenetic methyltransferases and methyl-CpG binding protein families in the normal B-cell and B-cell chronic lymphocytic leukemia (CLL). *Cancer Biol Ther* 3:989-994.

Kong, G.H., J.Y. Bu, T. Kurosaki, A.S. Shaw, and A.C. Chan. 1995. Reconstitution of Syk function by the ZAP-70 protein tyrosine kinase. *Immunity* 2:485-492.

Kosugi, S., M. Hasebe, T. Entani, S. Takayama, M. Tomita, and H. Yanagawa. 2008. Design of peptide inhibitors for the importin alpha/beta nuclear import pathway by activity-based profiling. *Chem Biol* 15:940-949.

Kosugi, S., M. Hasebe, N. Matsumura, H. Takashima, E. Miyamoto-Sato, M. Tomita, and H. Yanagawa. 2009a. Six classes of nuclear localization signals specific to different binding grooves of importin alpha. *J Biol Chem* 284:478-485.

Kosugi, S., M. Hasebe, M. Tomita, and H. Yanagawa. 2009b. Systematic identification of cell cycle-dependent yeast nucleocytoplasmic shuttling proteins by prediction of composite motifs. *Proc Natl Acad Sci U S A* 106:10171-10176.

Kumar, V., Fausto, N., Abbas, A.K., Robbins, S.L. & Cotran, R.S. 2004. Robbins & Cotran Pathologic Basis of Disease. Elsevier Saunders, Philadelphia, USA.

Kurosaki, T., S.A. Johnson, L. Pao, K. Sada, H. Yamamura, and J.C. Cambier. 1995. Role of the Syk autophosphorylation site and SH2 domains in B cell antigen receptor signaling. *The Journal of experimental medicine* 182:1815-1823.

Landau, D.A., S.L. Carter, P. Stojanov, A. McKenna, K. Stevenson, M.S. Lawrence, C. Sougnez, C. Stewart, A. Sivachenko, L. Wang, Y. Wan, W. Zhang, S.A. Shukla, A. Vartanov, S.M. Fernandes, G. Saksena, K. Cibulskis, B. Tesar, S. Gabriel, N. Hacohen, M. Meyerson, E.S. Lander, D. Neuberg, J.R. Brown, G. Getz, and C.J. Wu. 2013. Evolution and impact of subclonal mutations in chronic lymphocytic leukemia. *Cell* 152:714-726.

Landgren, O., M. Albitar, W. Ma, F. Abbasi, R.B. Hayes, P. Ghia, G.E. Marti, and N.E. Caporaso. 2009. B-cell clones as early markers for chronic lymphocytic leukemia. *The New England journal of medicine* 360:659-667.

Lange, A., R.E. Mills, C.J. Lange, M. Stewart, S.E. Devine, and A.H. Corbett. 2007. Classical nuclear localization signals: definition, function, and interaction with importin alpha. *J Biol Chem* 282:5101-5105.

Lannutti, B.J., S.A. Meadows, S.E. Herman, A. Kashishian, B. Steiner, A.J. Johnson, J.C. Byrd, J.W. Tyner, M.M. Loriaux, M. Deininger, B.J. Druker, K.D. Puri, R.G. Ulrich, and N.A. Giese. 2011. CAL-101, a p110delta selective phosphatidylinositol-3-kinase inhibitor for the treatment of B-cell malignancies, inhibits PI3K signaling and cellular viability. *Blood* 117:591-594.

Lapeyre, B., H. Bourbon, and F. Amalric. 1987. Nucleolin, the major nucleolar protein of growing eukaryotic cells: an unusual protein structure revealed by the nucleotide sequence. *Proc Natl Acad Sci U S A* 84:1472-1476.

Ledford, H. 2015. CRISPR, the disruptor. *Nature* 522:20-24.

Lee, S.J., Y. Matsuura, S.M. Liu, and M. Stewart. 2005. Structural basis for nuclear import complex dissociation by RanGTP. *Nature* 435:693-696.

Letourneur, F., and R.D. Klausner. 1991. T-cell and basophil activation through the cytoplasmic tail of T-cell-receptor zeta family proteins. *Proc Natl Acad Sci U S A* 88:8905-8909.

Leverson, J.D., D.C. Phillips, M.J. Mitten, E.R. Boghaert, D. Diaz, S.K. Tahir, L.D. Belmont, P. Nimmer, Y. Xiao, X.M. Ma, K.N. Lowes, P. Kovar, J. Chen, S. Jin, M. Smith, J. Xue, H. Zhang, A. Oleksijew, T.J. Magoc, K.S. Vaidya, D.H. Albert, J.M. Tarrant, N. La, L. Wang, Z.F. Tao, M.D. Wendt, D. Sampath, S.H. Rosenberg, C. Tse, D.C. Huang, W.J. Fairbrother, S.W. Elmore, and A.J. Souers. 2015a. Exploiting selective BCL-2 family inhibitors to dissect cell survival dependencies and define improved strategies for cancer therapy. *Sci Transl Med* 7:279ra240.

Leverson, J.D., H. Zhang, J. Chen, S.K. Tahir, D.C. Phillips, J. Xue, P. Nimmer, S. Jin, M. Smith, Y. Xiao, P. Kovar, A. Tanaka, M. Bruncko, G.S. Sheppard, L. Wang, S. Gierke, L. Kategaya, D.J. Anderson, C. Wong, J. Eastham-Anderson, M.J. Ludlam, D. Sampath, W.J. Fairbrother, I. Wertz, S.H. Rosenberg, C. Tse, S.W. Elmore, and A.J. Souers. 2015b. Potent and selective small-molecule MCL-1 inhibitors demonstrate on-target cancer cell

killing activity as single agents and in combination with ABT-263 (navitoclax). *Cell Death Dis* 6:e1590.

Li, M., A. Makkinje, and Z. Damuni. 1996. The myeloid leukemia-associated protein SET is a potent inhibitor of protein phosphatase 2A. *J Biol Chem* 271:11059-11062.

Liu, K.Q., S.C. Bunnell, C.B. Gurniak, and L.J. Berg. 1998. T cell receptor-initiated calcium release is uncoupled from capacitative calcium entry in Itk-deficient T cells. *The Journal of experimental medicine* 187:1721-1727.

Liu, Z., F. Li, B. Zhang, S. Li, J. Wu, and Y. Shi. 2015. Structural basis of plant homeodomain finger 6 (PHF6) recognition by the retinoblastoma binding protein 4 (RBBP4) component of the nucleosome remodeling and deacetylase (NuRD) complex. *J Biol Chem* 290:6630-6638.

Livak, K.J., and T.D. Schmittgen. 2001. Analysis of relative gene expression data using real-time quantitative PCR and the 2(-Delta Delta C(T)) Method. *Methods* 25:402-408.

Longo, P.G., L. Laurenti, S. Gobessi, S. Sica, G. Leone, and D.G. Efremov. 2008. The Akt/Mcl-1 pathway plays a prominent role in mediating antiapoptotic signals downstream of the B-cell receptor in chronic lymphocytic leukemia B cells. *Blood* 111:846-855.

Lorand-Metze, I., G.B. Oliveira-Duarte, and K. Metze. 2015. Imbalance between proliferation and in vitro apoptosis rates predicts progression in chronic lymphocytic leukemia. *Cytometry. Part B, Clinical cytometry*

Lovatt, M., A. Filby, V. Parravicini, G. Werlen, E. Palmer, and R. Zamoyska. 2006. Lck regulates the threshold of activation in primary T cells, while both Lck and Fyn contribute to the magnitude of the extracellular signal-related kinase response. *Molecular and cellular biology* 26:8655-8665.

Luger, K., A.W. Mader, R.K. Richmond, D.F. Sargent, and T.J. Richmond. 1997. Crystal structure of the nucleosome core particle at 2.8 A resolution. *Nature* 389:251-260.

Lupher, M.L., Jr., Z. Songyang, S.E. Shoelson, L.C. Cantley, and H. Band. 1997. The Cbl phosphotyrosine-binding domain selects a D(N/D)XpY motif and binds to the Tyr292 negative regulatory phosphorylation site of ZAP-70. *J Biol Chem* 272:33140-33144.

Lutzny, G., T. Kocher, M. Schmidt-Supprian, M. Rudelius, L. Klein-Hitpass, A.J. Finch, J. Durig, M. Wagner, C. Haferlach, A. Kohlmann, S. Schnittger, M. Seifert, S. Wanninger, N. Zaborsky, R. Oostendorp, J. Ruland, M. Leitges, T. Kuhnt, Y. Schafer, B. Lampl, C. Peschel, A. Egle, and I. Ringshausen. 2013. Protein kinase c-beta-dependent activation of NF-kappaB in stromal cells is indispensable for the survival of chronic lymphocytic leukemia B cells in vivo. *Cancer Cell* 23:77-92.

Magnan, A., V. Di Bartolo, A.M. Mura, C. Boyer, M. Richelme, Y.L. Lin, A. Roure, A. Gillet, C. Arrieumerlou, O. Acuto, B. Malissen, and M. Malissen. 2001. T cell development and T cell responses in mice with mutations affecting tyrosines 292 or 315 of the ZAP-70 protein tyrosine kinase. *The Journal of experimental medicine* 194:491-505.

Malhotra, S., S. Kovats, W. Zhang, and K.M. Coggeshall. 2009. Vav and Rac activation in B cell antigen receptor endocytosis involves Vav recruitment to the adapter protein LAB. *J Biol Chem* 284:36202-36212.

Matutes, E., K. Owusu-Ankomah, R. Morilla, J. Garcia Marco, A. Houlihan, T.H. Que, and D. Catovsky. 1994. The immunological profile of B-cell disorders

and proposal of a scoring system for the diagnosis of CLL. *Leukemia* 8:1640-1645.

Maurer, U., C. Charvet, A.S. Wagman, E. Dejardin, and D.R. Green. 2006. Glycogen synthase kinase-3 regulates mitochondrial outer membrane permeabilization and apoptosis by destabilization of MCL-1. *Mol Cell* 21:749-760.

Meinl, E., D. Lengenfelder, N. Blank, R. Pirzer, L. Barata, and C. Hivroz. 2000. Differential requirement of ZAP-70 for CD2-mediated activation pathways of mature human T cells. *J Immunol* 165:3578-3583.

Mellacheruvu, D., Z. Wright, A.L. Couzens, J.P. Lambert, N.A. St-Denis, T. Li, Y.V. Miteva, S. Hauri, M.E. Sardiu, T.Y. Low, V.A. Halim, R.D. Bagshaw, N.C. Hubner, A. Al-Hakim, A. Bouchard, D. Faubert, D. Fermin, W.H. Dunham, M. Goudreault, Z.Y. Lin, B.G. Badillo, T. Pawson, D. Durocher, B. Coulombe, R. Aebersold, G. Superti-Furga, J. Colinge, A.J. Heck, H. Choi, M. Gstaiger, S. Mohammed, I.M. Cristea, K.L. Bennett, M.P. Washburn, B. Raught, R.M. Ewing, A.C. Gingras, and A.I. Nesvizhskii. 2013. The CRAPome: a contaminant repository for affinity purification-mass spectrometry data. *Nat Methods* 10:730-736.

Merl, J., M. Ueffing, S.M. Hauck, and C. von Toerne. 2012. Direct comparison of MS-based label-free and SILAC quantitative proteome profiling strategies in primary retinal Muller cells. *Proteomics* 12:1902-1911.

Meyvis, T.K., S.C. De Smedt, P. Van Oostveldt, and J. Demeester. 1999. Fluorescence recovery after photobleaching: a versatile tool for mobility and interaction measurements in pharmaceutical research. *Pharm Res* 16:1153-1162.

Michels, J., J.W. O'Neill, C.L. Dallman, A. Mouzakiti, F. Habens, M. Brimmell, K.Y. Zhang, R.W. Craig, E.G. Marcusson, P.W. Johnson, and G. Packham. 2004. Mcl-1 is required for Akata6 B-lymphoma cell survival and is converted to a cell death molecule by efficient caspase-mediated cleavage. *Oncogene* 23:4818-4827.

Migliazza, A., F. Bosch, H. Komatsu, E. Cayanis, S. Martinotti, E. Toniato, E. Guccione, X. Qu, M. Chien, V.V. Murty, G. Gaidano, G. Inghirami, P. Zhang, S. Fischer, S.M. Kalachikov, J. Russo, I. Edelman, A. Efstratiadis, and R. Dalla-Favera. 2001. Nucleotide sequence, transcription map, and mutation analysis of the 13q14 chromosomal region deleted in B-cell chronic lymphocytic leukemia. *Blood* 97:2098-2104.

Mikkelsen, T.S., M. Ku, D.B. Jaffe, B. Issac, E. Lieberman, G. Giannoukos, P. Alvarez, W. Brockman, T.K. Kim, R.P. Koche, W. Lee, E. Mendenhall, A. O'Donovan, A. Presser, C. Russ, X. Xie, A. Meissner, M. Wernig, R. Jaenisch, C. Nusbaum, E.S. Lander, and B.E. Bernstein. 2007. Genome-wide maps of chromatin state in pluripotent and lineage-committed cells. *Nature* 448:553-560.

Millan-Arino, L., A.B. Islam, A. Izquierdo-Bouldstridge, R. Mayor, J.M. Terme, N. Luque, M. Sancho, N. Lopez-Bigas, and A. Jordan. 2014. Mapping of six somatic linker histone H1 variants in human breast cancer cells uncovers specific features of H1.2. *Nucleic Acids Res* 42:4474-4493.

Millward, T.A., S. Zolnierowicz, and B.A. Hemmings. 1999. Regulation of protein kinase cascades by protein phosphatase 2A. *Trends Biochem Sci* 24:186-191.

Montano, M.M., K. Ekena, R. Delage-Mourroux, W. Chang, P. Martini, and B.S. Katzenellenbogen. 1999. An estrogen receptor-selective coregulator that

potentiates the effectiveness of antiestrogens and represses the activity of estrogens. *Proc Natl Acad Sci U S A* 96:6947-6952.

Motto, D.G., S.E. Ross, J. Wu, L.R. Hendricks-Taylor, and G.A. Koretzky. 1996. Implication of the GRB2-associated phosphoprotein SLP-76 in T cell receptor-mediated interleukin 2 production. *The Journal of experimental medicine* 183:1937-1943.

Nabhan, C. 2005. The emerging role of alemtuzumab in chronic lymphocytic leukemia. *Clin Lymphoma Myeloma* 6:115-121.

Nabhan, C., N. Dalal, J. Mehta, and N.E. Kay. 2011. Biologic agent activity in chronic lymphocytic leukemia: a framework for future therapies. *Leuk Lymphoma* 52:374-386.

Nabhan, C., G. Raca, and Y.L. Wang. 2015. Predicting Prognosis in Chronic Lymphocytic Leukemia in the Contemporary Era. *JAMA Oncol*

Nabhan, C., and S.T. Rosen. 2014. Chronic lymphocytic leukemia: a clinical review. *JAMA* 312:2265-2276.

Nagata, S. 2000. Apoptotic DNA fragmentation. *Exp Cell Res* 256:12-18.

Nakanishi, S., B.W. Sanderson, K.M. Delventhal, W.D. Bradford, K. Staehling-Hampton, and A. Shilatifard. 2008. A comprehensive library of histone mutants identifies nucleosomal residues required for H3K4 methylation. *Nat Struct Mol Biol* 15:881-888.

Negishi, I., N. Motoyama, K. Nakayama, K. Nakayama, S. Senju, S. Hatakeyama, Q. Zhang, A.C. Chan, and D.Y. Loh. 1995. Essential role for ZAP-70 in both positive and negative selection of thymocytes. *Nature* 376:435-438.

Neumeister, E.N., Y. Zhu, S. Richard, C. Terhorst, A.C. Chan, and A.S. Shaw. 1995. Binding of ZAP-70 to phosphorylated T-cell receptor zeta and eta enhances its autophosphorylation and generates specific binding sites for SH2 domain-containing proteins. *Molecular and cellular biology* 15:3171-3178.

Newton, A.C. 2010. Protein kinase C: poised to signal. *Am J Physiol Endocrinol Metab* 298:E395-402.

Nijhawan, D., M. Fang, E. Traer, Q. Zhong, W. Gao, F. Du, and X. Wang. 2003. Elimination of Mcl-1 is required for the initiation of apoptosis following ultraviolet irradiation. *Genes Dev* 17:1475-1486.

Noraz, N., K. Schwarz, M. Steinberg, V. Dardalhon, C. Rebouissou, R. Hipskind, W. Friedrich, H. Yssel, K. Bacon, and N. Taylor. 2000. Alternative antigen receptor (TCR) signaling in T cells derived from ZAP-70-deficient patients expressing high levels of Syk. *J Biol Chem* 275:15832-15838.

Ojha, J., C. Secreto, K. Rabe, J. Ayres-Silva, R. Tschumper, D.V. Dyke, S. Slager, R. Fonseca, T. Shanafelt, N. Kay, and E. Braggio. 2014. Monoclonal B-cell lymphocytosis is characterized by mutations in CLL putative driver genes and clonal heterogeneity many years before disease progression. *Leukemia* 28:2395-2398.

Oliner, J.D., K.W. Kinzler, P.S. Meltzer, D.L. George, and B. Vogelstein. 1992. Amplification of a gene encoding a p53-associated protein in human sarcomas. *Nature* 358:80-83.

Oscier, D.G., M.J. Rose-Zerilli, N. Winkelmann, D. Gonzalez de Castro, B. Gomez, J. Forster, H. Parker, A. Parker, A. Gardiner, A. Collins, M. Else, N.C. Cross, D. Catovsky, and J.C. Strefford. 2013. The clinical significance of NOTCH1 and SF3B1 mutations in the UK LRF CLL4 trial. *Blood* 121:468-475.

Ougolkov, A.V., N.D. Bone, M.E. Fernandez-Zapico, N.E. Kay, and D.D. Billadeau. 2007. Inhibition of glycogen synthase kinase-3 activity leads to epigenetic silencing of nuclear factor kappaB target genes and induction of apoptosis in chronic lymphocytic leukemia B cells. *Blood* 110:735-742.

Paine, P.L., L.C. Moore, and S.B. Horowitz. 1975. Nuclear envelope permeability. *Nature* 254:109-114.

Paul, J.T., E.S. Henson, S. Mai, F.J. Mushinski, M. Cheang, S.B. Gibson, and J.B. Johnston. 2005. Cyclin D expression in chronic lymphocytic leukemia. *Leuk Lymphoma* 46:1275-1285.

Pedersen, I.M., S. Kitada, L.M. Leoni, J.M. Zapata, J.G. Karras, N. Tsukada, T.J. Kipps, Y.S. Choi, F. Bennett, and J.C. Reed. 2002. Protection of CLL B cells by a follicular dendritic cell line is dependent on induction of Mcl-1. *Blood* 100:1795-1801.

Pepper, C., P. Brennan, S. Alghazal, R. Ward, G. Pratt, J. Starczynski, T. Lin, C. Rowntree, and C. Fegan. 2006. CD38+ chronic lymphocytic leukaemia cells co-express high levels of ZAP-70 and are functionally distinct from their CD38- counter-parts. *Leukemia* 20:743-744.

Pepper, C., T.T. Lin, G. Pratt, S. Hewamana, P. Brennan, L. Hiller, R. Hills, R. Ward, J. Starczynski, B. Austen, L. Hooper, T. Stankovic, and C. Fegan. 2008. Mcl-1 expression has in vitro and in vivo significance in chronic lymphocytic leukemia and is associated with other poor prognostic markers. *Blood* 112:3807-3817.

Perlmutter, R.M. 1994. Immunodeficiency. Zapping T-cell responses. *Nature* 370:249-250.

Petlickovski, A., L. Laurenti, X. Li, S. Marietti, P. Chiusolo, S. Sica, G. Leone, and D.G. Efremov. 2005. Sustained signaling through the B-cell receptor induces Mcl-1 and promotes survival of chronic lymphocytic leukemia B cells. *Blood* 105:4820-4827.

Plander, M., S. Seegers, P. Ugocsai, S. Diermeier-Daucher, J. Ivanyi, G. Schmitz, F. Hofstadter, S. Schwarz, E. Orso, R. Knuchel, and G. Brockhoff. 2009. Different proliferative and survival capacity of CLL-cells in a newly established in vitro model for pseudofollicles. *Leukemia* 23:2118-2128.

Plate, J.M. 2004. PI3-kinase regulates survival of chronic lymphocytic leukemia B-cells by preventing caspase 8 activation. *Leuk Lymphoma* 45:1519-1529.

Ponader, S., S.S. Chen, J.J. Buggy, K. Balakrishnan, V. Gandhi, W.G. Wierda, M.J. Keating, S. O'Brien, N. Chiorazzi, and J.A. Burger. 2012. The Bruton tyrosine kinase inhibitor PCI-32765 thwarts chronic lymphocytic leukemia cell survival and tissue homing in vitro and in vivo. *Blood* 119:1182-1189.

Puente, X.S., M. Pinyol, V. Quesada, L. Conde, G.R. Ordonez, N. Villamor, G. Escaramis, P. Jares, S. Bea, M. Gonzalez-Diaz, L. Bassaganyas, T. Baumann, M. Juan, M. Lopez-Guerra, D. Colomer, J.M. Tubio, C. Lopez, A. Navarro, C. Tornador, M. Aymerich, M. Rozman, J.M. Hernandez, D.A. Puente, J.M. Freije, G. Velasco, A. Gutierrez-Fernandez, D. Costa, A. Carrio, S. Guijarro, A. Enjuanes, L. Hernandez, J. Yague, P. Nicolas, C.M. Romeo-Casabona, H. Himmelbauer, E. Castillo, J.C. Dohm, S. de Sanjose, M.A. Piris, E. de Alava, J. San Miguel, R. Royo, J.L. Gelpi, D. Torrents, M. Orozco, D.G. Pisano, A. Valencia, R. Guigo, M. Bayes, S. Heath, M. Gut, P. Klatt, J. Marshall, K. Raine, L.A. Stebbings, P.A. Futreal, M.R. Stratton, P.J. Campbell, I. Gut, A. Lopez-Guillermo, X. Estivill, E. Montserrat, C. Lopez-Otin, and E. Campo. 2011. Whole-genome sequencing identifies recurrent mutations in chronic lymphocytic leukaemia. *Nature* 475:101-105.

Quesada, V., L. Conde, N. Villamor, G.R. Ordonez, P. Jares, L. Bassaganyas, A.J. Ramsay, S. Bea, M. Pinyol, A. Martinez-Trillos, M. Lopez-Guerra, D. Colomer, A. Navarro, T. Baumann, M. Aymerich, M. Rozman, J. Delgado, E. Gine, J.M. Hernandez, M. Gonzalez-Diaz, D.A. Puente, G. Velasco, J.M. Freije, J.M. Tubio, R. Royo, J.L. Gelpi, M. Orozco, D.G. Pisano, J. Zamora, M. Vazquez, A. Valencia, H. Himmelbauer, M. Bayes, S. Heath, M. Gut, I. Gut, X. Estivill, A. Lopez-Guillermo, X.S. Puente, E. Campo, and C. Lopez-Otin. 2012. Exome sequencing identifies recurrent mutations of the splicing factor SF3B1 gene in chronic lymphocytic leukemia. *Nat Genet* 44:47-52.

Rasband, W. 1997. ImageJ. In.

Rassenti, L.Z., L. Huynh, T.L. Toy, L. Chen, M.J. Keating, J.G. Gribben, D.S. Neuberg, I.W. Flinn, K.R. Rai, J.C. Byrd, N.E. Kay, A. Greaves, A. Weiss, and T.J. Kipps. 2004. ZAP-70 compared with immunoglobulin heavy-chain gene mutation status as a predictor of disease progression in chronic lymphocytic leukemia. *The New England journal of medicine* 351:893-901.

Rawstron, A.C., F.L. Bennett, S.J. O'Connor, M. Kwok, J.A. Fenton, M. Plummer, R. de Tute, R.G. Owen, S.J. Richards, A.S. Jack, and P. Hillmen. 2008. Monoclonal B-cell lymphocytosis and chronic lymphocytic leukemia. *The New England journal of medicine* 359:575-583.

Rayburn, E., R. Zhang, J. He, and H. Wang. 2005. MDM2 and human malignancies: expression, clinical pathology, prognostic markers, and implications for chemotherapy. *Curr Cancer Drug Targets* 5:27-41.

Reed, J.C., and M. Pellecchia. 2005. Apoptosis-based therapies for hematologic malignancies. *Blood* 106:408-418.

Reth, M. 1989. Antigen receptor tail clue. *Nature* 338:383-384.

Rosenfeld, J.A., Z. Wang, D.E. Schones, K. Zhao, R. DeSalle, and M.Q. Zhang. 2009. Determination of enriched histone modifications in non-genic portions of the human genome. *BMC Genomics* 10:143.

Rosenwald, A., A.A. Alizadeh, G. Widhopf, R. Simon, R.E. Davis, X. Yu, L. Yang, O.K. Pickeral, L.Z. Rassenti, J. Powell, D. Botstein, J.C. Byrd, M.R. Grever, B.D. Cheson, N. Chiorazzi, W.H. Wilson, T.J. Kipps, P.O. Brown, and L.M. Staudt. 2001. Relation of gene expression phenotype to immunoglobulin mutation genotype in B cell chronic lymphocytic leukemia. *The Journal of experimental medicine* 194:1639-1647.

Rossi, D., S. Rasi, V. Spina, A. Bruscaggin, S. Monti, C. Ciardullo, C. Deambrogi, H. Khiabanian, R. Serra, F. Bertoni, F. Forconi, L. Laurenti, R. Marasca, M. Dal-Bo, F.M. Rossi, P. Bulian, J. Nomdedeu, G. Del Poeta, V. Gattei, L. Pasqualucci, R. Rabadan, R. Foa, R. Dalla-Favera, and G. Gaidano. 2013. Integrated mutational and cytogenetic analysis identifies new prognostic subgroups in chronic lymphocytic leukemia. *Blood* 121:1403-1412.

Rossi, L., L. Bonuccelli, P. Iacopetti, M. Evangelista, C. Ghezzani, L. Tana, and A. Salvetti. 2014. Prohibitin 2 regulates cell proliferation and mitochondrial cristae morphogenesis in planarian stem cells. *Stem Cell Rev* 10:871-887.

Rowley, R.B., A.L. Burkhardt, H.G. Chao, G.R. Matsueda, and J.B. Bolen. 1995. Syk protein-tyrosine kinase is regulated by tyrosine-phosphorylated Ig alpha/Ig beta immunoreceptor tyrosine activation motif binding and autophosphorylation. *J Biol Chem* 270:11590-11594.

Saijo, K., C. Schmedt, I.H. Su, H. Karasuyama, C.A. Lowell, M. Reth, T. Adachi, A. Patke, A. Santana, and A. Tarakhovsky. 2003. Essential role of Src-family protein tyrosine kinases in NF-kappaB activation during B cell development. *Nat Immunol* 4:274-279.

Samelson, L.E. 2002. Signal transduction mediated by the T cell antigen receptor: the role of adapter proteins. *Annu Rev Immunol* 20:371-394.

Santisteban, M.S., G. Arents, E.N. Moudrianakis, and M.M. Smith. 1997. Histone octamer function in vivo: mutations in the dimer-tetramer interfaces disrupt both gene activation and repression. *EMBO J* 16:2493-2506.

Saxena, A., S. Viswanathan, O. Moshynska, P. Tandon, K. Sankaran, and D.P. Sheridan. 2004. Mcl-1 and Bcl-2/Bax ratio are associated with treatment response but not with Rai stage in B-cell chronic lymphocytic leukemia. *Am J Hematol* 75:22-33.

Schmidt-Zachmann, M.S., C. Dargemont, L.C. Kuhn, and E.A. Nigg. 1993. Nuclear export of proteins: the role of nuclear retention. *Cell* 74:493-504.

Schmidt-Zachmann, M.S., and E.A. Nigg. 1993. Protein localization to the nucleolus: a search for targeting domains in nucleolin. *J Cell Sci* 105 (Pt 3):799-806.

Schnaiter, A., P. Paschka, M. Rossi, T. Zenz, A. Buhler, D. Winkler, M. Cazzola, K. Dohner, J. Edelmann, D. Mertens, S. Kless, S. Mack, R. Busch, M. Hallek, H. Dohner, and S. Stilgenbauer. 2013. NOTCH1, SF3B1, and TP53 mutations in fludarabine-refractory CLL patients treated with alemtuzumab: results from the CLL2H trial of the GCLLSG. *Blood* 122:1266-1270.

Schneider, C.A., W.S. Rasband, and K.W. Eliceiri. 2012. NIH Image to ImageJ: 25 years of image analysis. *Nat Methods* 9:671-675.

Schneider, K., C. Fuchs, A. Dobay, A. Rottach, W. Qin, P. Wolf, J.M. Alvarez-Castro, M.M. Nalaskowski, E. Kremmer, V. Schmid, H. Leonhardt, and L. Schermelleh. 2013. Dissection of cell cycle-dependent dynamics of Dnmt1 by FRAP and diffusion-coupled modeling. *Nucleic Acids Res* 41:4860-4876.

Schonthal, A.H. 2001. Role of serine/threonine protein phosphatase 2A in cancer. *Cancer Lett* 170:1-13.

Schrader, A., W. Popal, N. Lilienthal, G. Crispatzu, P. Mayer, D. Jones, M. Hallek, and M. Herling. 2014. AKT-pathway inhibition in chronic lymphocytic leukemia reveals response relationships defined by TCL1. *Curr Cancer Drug Targets* 14:700-712.

Schulze-Luehrmann, J., and S. Ghosh. 2006. Antigen-receptor signaling to nuclear factor kappa B. *Immunity* 25:701-715.

Schwickart, M., X. Huang, J.R. Lill, J. Liu, R. Ferrando, D.M. French, H. Maecker, K. O'Rourke, F. Bazan, J. Eastham-Anderson, P. Yue, D. Dornan, D.C. Huang, and V.M. Dixit. 2010. Deubiquitinase USP9X stabilizes MCL1 and promotes tumour cell survival. *Nature* 463:103-107.

Seifert, M., L. Sellmann, J. Bloehdorn, F. Wein, S. Stilgenbauer, J. Durig, and R. Kuppers. 2012. Cellular origin and pathophysiology of chronic lymphocytic leukemia. *The Journal of experimental medicine* 209:2183-2198.

Seo, S.B., P. McNamara, S. Heo, A. Turner, W.S. Lane, and D. Chakravarti. 2001. Regulation of histone acetylation and transcription by INHAT, a human cellular complex containing the set oncoprotein. *Cell* 104:119-130.

Shi, Y. 2006. Mechanical aspects of apoptosome assembly. *Curr Opin Cell Biol* 18:677-684.

Shimura, T. 2011. Acquired radioresistance of cancer and the AKT/GSK3beta/cyclin D1 overexpression cycle. *J Radiat Res* 52:539-544.

Simon, H.U., G.B. Mills, M. Kozlowski, D. Hogg, D. Branch, Y. Ishimi, and K.A. Siminovitch. 1994. Molecular characterization of hNRP, a cDNA encoding a human nucleosome-assembly-protein-I-related gene product involved in the induction of cell proliferation. *Biochem J* 297 (Pt 2):389-397.

Singh, R.K., and A. Gunjan. 2011. Histone tyrosine phosphorylation comes of age. *Epigenetics* 6:153-160.

Skowronska, A., A. Parker, G. Ahmed, C. Oldreive, Z. Davis, S. Richards, M. Dyer, E. Matutes, D. Gonzalez, A.M. Taylor, P. Moss, P. Thomas, D. Oscier, and T. Stankovic. 2012. Biallelic ATM inactivation significantly reduces survival in patients treated on the United Kingdom Leukemia Research Fund Chronic Lymphocytic Leukemia 4 trial. *J Clin Oncol* 30:4524-4532.

Sloan-Lancaster, J., W. Zhang, J. Presley, B.L. Williams, R.T. Abraham, J. Lippincott-Schwartz, and L.E. Samelson. 1997. Regulation of ZAP-70 intracellular localization: visualization with the green fluorescent protein. *The Journal of experimental medicine* 186:1713-1724.

Slupsky, J.R. 2014. Does B cell receptor signaling in chronic lymphocytic leukaemia cells differ from that in other B cell types? *Scientifica (Cairo)* 2014:208928.

Smith, E.N., E.M. Ghia, C.M. DeBoever, L.Z. Rassenti, K. Jepsen, K.A. Yoon, H. Matsui, S. Rozenzhak, H. Alakus, P.J. Shepard, Y. Dai, M. Khosroheidari, M. Bina, K.L. Gunderson, K. Messer, L. Muthuswamy, T.J. Hudson, O. Harismendy, C.L. Barrett, C.H. Jamieson, D.A. Carson, T.J. Kipps, and K.A. Frazer. 2015. Genetic and epigenetic profiling of CLL disease progression reveals limited somatic evolution and suggests a relationship to memory-cell development. *Blood Cancer J* 5:e303.

Sprague, B.L., R.L. Pego, D.A. Stavreva, and J.G. McNally. 2004. Analysis of binding reactions by fluorescence recovery after photobleaching. *Biophys J* 86:3473-3495.

Stevenson, F.K., S. Krysov, A.J. Davies, A.J. Steele, and G. Packham. 2011. B-cell receptor signaling in chronic lymphocytic leukemia. *Blood* 118:4313-4320.

Stilgenbauer, S., C. Schaffner, A. Litterst, P. Liebisch, S. Gilad, A. Bar-Shira, M.R. James, P. Lichter, and H. Dohner. 1997. Biallelic mutations in the ATM gene in T-prolymphocytic leukemia. *Nat Med* 3:1155-1159.

Stilgenbauer, S., A. Schnaiter, P. Paschka, T. Zenz, M. Rossi, K. Dohner, A. Buhler, S. Bottcher, M. Ritgen, M. Kneba, D. Winkler, E. Tausch, P. Hoth, J. Edelmann, D. Mertens, L. Bullinger, M. Bergmann, S. Kless, S. Mack, U. Jager, N. Patten, L. Wu, M.K. Wenger, G. Fingerle-Rowson, P. Lichter, M. Cazzola, C.M. Wendtner, A.M. Fink, K. Fischer, R. Busch, M. Hallek, and H. Dohner. 2014. Gene mutations and treatment outcome in chronic lymphocytic leukemia: results from the CLL8 trial. *Blood* 123:3247-3254.

Strahl, B.D., and C.D. Allis. 2000. The language of covalent histone modifications. *Nature* 403:41-45.

Straus, D.B., and A. Weiss. 1992. Genetic evidence for the involvement of the lck tyrosine kinase in signal transduction through the T cell antigen receptor. *Cell* 70:585-593.

Swaminathan, V., A.H. Kishore, K.K. Febitha, and T.K. Kundu. 2005. Human histone chaperone nucleophosmin enhances acetylation-dependent chromatin transcription. *Molecular and cellular biology* 25:7534-7545.

Switzer, C.H., R.Y. Cheng, T.M. Vitek, D.J. Christensen, D.A. Wink, and M.P. Vitek. 2011. Targeting SET/I(2)PP2A oncoprotein functions as a multi-pathway strategy for cancer therapy. *Oncogene* 30:2504-2513.

Tam, C.S., and M.J. Keating. 2010. Chemoimmunotherapy of chronic lymphocytic leukemia. *Nature reviews. Clinical oncology* 7:521-532.

Tangye, S.G., and K.L. Good. 2007. Human IgM+CD27+ B cells: memory B cells or "memory" B cells? *J Immunol* 179:13-19.

Taniguchi, T., T. Kobayashi, J. Kondo, K. Takahashi, H. Nakamura, J. Suzuki, K. Nagai, T. Yamada, S. Nakamura, and H. Yamamura. 1991. Molecular cloning of a porcine gene syk that encodes a 72-kDa protein-tyrosine kinase showing high susceptibility to proteolysis. *J Biol Chem* 266:15790-15796.

Th'ng, J.P., R. Sung, M. Ye, and M.J. Hendzel. 2005. H1 family histones in the nucleus. Control of binding and localization by the C-terminal domain. *J Biol Chem* 280:27809-27814.

Thomas, M.P., X. Liu, J. Whangbo, G. McCrossan, K.B. Sanborn, E. Basar, M. Walch, and J. Lieberman. 2015. Apoptosis Triggers Specific, Rapid, and Global mRNA Decay with 3' Uridylated Intermediates Degraded by DIS3L2. *Cell Rep* 11:1079-1089.

Toyabe, S., A. Watanabe, W. Harada, T. Karasawa, and M. Uchiyama. 2001. Specific immunoglobulin E responses in ZAP-70-deficient patients are mediated by Syk-dependent T-cell receptor signalling. *Immunology* 103:164-171.

Turul, T., I. Tezcan, H. Artac, S. de Bruin-Versteeg, B.H. Barendregt, I. Reisli, O. Sanal, J.J. van Dongen, and M. van der Burg. 2009. Clinical heterogeneity can hamper the diagnosis of patients with ZAP70 deficiency. *Eur J Pediatr* 168:87-93.

Van Damme, M., E. Crompot, N. Meuleman, P. Mineur, B. Dessars, H. El Housni, D. Bron, L. Lagneaux, and B. Stamatopoulos. 2014. Global histone deacetylase enzymatic activity is an independent prognostic marker associated with a shorter overall survival in chronic lymphocytic leukemia patients. *Epigenetics* 9:1374-1381.

van Delft, M.F., A.H. Wei, K.D. Mason, C.J. Vandenberg, L. Chen, P.E. Czabotar, S.N. Willis, C.L. Scott, C.L. Day, S. Cory, J.M. Adams, A.W. Roberts, and D.C. Huang. 2006. The BH3 mimetic ABT-737 targets selective Bcl-2 proteins and efficiently induces apoptosis via Bak/Bax if Mcl-1 is neutralized. *Cancer Cell* 10:389-399.

Vaux, D.L. 2008. ABT-737, proving to be a great tool even before it is proven in the clinic. *Cell Death Differ* 15:807-808.

Vollbrecht, C., F.D. Mairinger, U. Koitzsch, M. Peifer, K. Koenig, L.C. Heukamp, G. Crispatzu, L. Wilden, K.A. Kreuzer, M. Hallek, M. Odenthal, C.D. Herling, and R. Buettner. 2015. Comprehensive Analysis of Disease-Related Genes in Chronic Lymphocytic Leukemia by Multiplex PCR-Based Next Generation Sequencing. *PLoS One* 10:e0129544.

Wang, H., T.A. Kadlecek, B.B. Au-Yeung, H.E. Goodfellow, L.Y. Hsu, T.S. Freedman, and A. Weiss. 2010. ZAP-70: an essential kinase in T-cell signaling. *Cold Spring Harb Perspect Biol* 2:a002279.

Wang, H.Y., Y. Altman, D. Fang, C. Elly, Y. Dai, Y. Shao, and Y.C. Liu. 2001. Cbl promotes ubiquitination of the T cell receptor zeta through an adaptor function of Zap-70. *J Biol Chem* 276:26004-26011.

Wang, J.C., M.I. Kafeel, B. Avezbakiyev, C. Chen, Y. Sun, C. Rathnasabapathy, M. Kalavar, Z. He, J. Burton, and S. Lichter. 2011a. Histone deacetylase in chronic lymphocytic leukemia. *Oncology* 81:325-329.

Wang, L., M.S. Lawrence, Y. Wan, P. Stojanov, C. Sougnez, K. Stevenson, L. Werner, A. Sivachenko, D.S. DeLuca, L. Zhang, W. Zhang, A.R. Vartanov, S.M. Fernandes, N.R. Goldstein, E.G. Folco, K. Cibulskis, B. Tesar, Q.L.

Sievers, E. Shefler, S. Gabriel, N. Hacohen, R. Reed, M. Meyerson, T.R. Golub, E.S. Lander, D. Neuberg, J.R. Brown, G. Getz, and C.J. Wu. 2011b. SF3B1 and other novel cancer genes in chronic lymphocytic leukemia. *The New England journal of medicine* 365:2497-2506.

Wang, S.S., E.D. Esplin, J.L. Li, L. Huang, A. Gazdar, J. Minna, and G.A. Evans. 1998. Alterations of the PPP2R1B gene in human lung and colon cancer. *Science* 282:284-287.

Wang, Y., J.B. Lam, K.S. Lam, J. Liu, M.C. Lam, R.L. Hoo, D. Wu, G.J. Cooper, and A. Xu. 2006. Adiponectin modulates the glycogen synthase kinase-3beta/beta-catenin signaling pathway and attenuates mammary tumorigenesis of MDA-MB-231 cells in nude mice. *Cancer Res* 66:11462-11470.

Wang, Y., R. Yang, J. Gu, X. Yin, N. Jin, S. Xie, Y. Wang, H. Chang, W. Qian, J. Shi, K. Iqbal, C.X. Gong, C. Cheng, and F. Liu. 2015. Cross talk between PI3K-AKT-GSK-3beta and PP2A pathways determines tau hyperphosphorylation. *Neurobiol Aging* 36:188-200.

Wange, R.L., R. Guitian, N. Isakov, J.D. Watts, R. Aebersold, and L.E. Samelson. 1995. Activating and inhibitory mutations in adjacent tyrosines in the kinase domain of ZAP-70. *J Biol Chem* 270:18730-18733.

Watson, R.L., A.C. Spalding, S.P. Zielske, M. Morgan, A.C. Kim, G.T. Bommer, H. Eldar-Finkelman, T. Giordano, E.R. Fearon, G.D. Hammer, T.S. Lawrence, and E. Ben-Josef. 2010. GSK3beta and beta-catenin modulate radiation cytotoxicity in pancreatic cancer. *Neoplasia* 12:357-365.

Weiss, A. 1991. Molecular and genetic insights into T cell antigen receptor structure and function. *Annu Rev Genet* 25:487-510.

Welcker, M., and B.E. Clurman. 2008. FBW7 ubiquitin ligase: a tumour suppressor at the crossroads of cell division, growth and differentiation. *Nat Rev Cancer* 8:83-93.

Wera, S., and B.A. Hemmings. 1995. Serine/threonine protein phosphatases. *Biochem J* 311 (Pt 1):17-29.

Werlen, G., B. Hausmann, and E. Palmer. 2000. A motif in the alphabeta T-cell receptor controls positive selection by modulating ERK activity. *Nature* 406:422-426.

Williams, B.L., B.J. Irvin, S.L. Sutor, C.C. Chini, E. Yacyshyn, J. Bubeck Wardenburg, M. Dalton, A.C. Chan, and R.T. Abraham. 1999. Phosphorylation of Tyr319 in ZAP-70 is required for T-cell antigen receptor-dependent phospholipase C-gamma1 and Ras activation. *EMBO J* 18:1832-1844.

Woyach, J.A., R.R. Furman, T.M. Liu, H.G. Ozer, M. Zapatka, A.S. Ruppert, L. Xue, D.H. Li, S.M. Steggerda, M. Versele, S.S. Dave, J. Zhang, A.S. Yilmaz, S.M. Jaglowski, K.A. Blum, A. Lozanski, G. Lozanski, D.F. James, J.C. Barrientos, P. Lichter, S. Stilgenbauer, J.J. Buggy, B.Y. Chang, A.J. Johnson, and J.C. Byrd. 2014. Resistance mechanisms for the Bruton's tyrosine kinase inhibitor ibrutinib. *The New England journal of medicine* 370:2286-2294.

Woyach, J.A., A.J. Johnson, and J.C. Byrd. 2012. The B-cell receptor signaling pathway as a therapeutic target in CLL. *Blood* 120:1175-1184.

Yao, X.R., H. Flaswinkel, M. Reth, and D.W. Scott. 1995. Immunoreceptor tyrosine-based activation motif is required to signal pathways of receptor-mediated growth arrest and apoptosis in murine B lymphoma cells. *J Immunol* 155:652-661.

Zenz, T., D. Mertens, R. Kuppers, H. Dohner, and S. Stilgenbauer. 2010. From pathogenesis to treatment of chronic lymphocytic leukaemia. *Nat Rev Cancer* 10:37-50.

Zhang, S., and T.J. Kipps. 2014. The pathogenesis of chronic lymphocytic leukemia. *Annu Rev Pathol* 9:103-118.

Zhang, W., B.J. Irvin, R.P. Trible, R.T. Abraham, and L.E. Samelson. 1999a. Functional analysis of LAT in TCR-mediated signaling pathways using a LAT-deficient Jurkat cell line. *Int Immunol* 11:943-950.

Zhang, W., J. Sloan-Lancaster, J. Kitchen, R.P. Trible, and L.E. Samelson. 1998. LAT: the ZAP-70 tyrosine kinase substrate that links T cell receptor to cellular activation. *Cell* 92:83-92.

Zhang, W., C.L. Sommers, D.N. Burshtyn, C.C. Stebbins, J.B. DeJarnette, R.P. Trible, A. Grinberg, H.C. Tsay, H.M. Jacobs, C.M. Kessler, E.O. Long, P.E. Love, and L.E. Samelson. 1999b. Essential role of LAT in T cell development. *Immunity* 10:323-332.

Zhang, W., R.P. Trible, M. Zhu, S.K. Liu, C.J. McGlade, and L.E. Samelson. 2000. Association of Grb2, Gads, and phospholipase C-gamma 1 with phosphorylated LAT tyrosine residues. Effect of LAT tyrosine mutations on T cell angigen receptor-mediated signaling. *J Biol Chem* 275:23355-23361.

Zhao, Q., and A. Weiss. 1996. Enhancement of lymphocyte responsiveness by a gain-of-function mutation of ZAP-70. *Molecular and cellular biology* 16:6765-6774.

Zhao, Q., B.L. Williams, R.T. Abraham, and A. Weiss. 1999. Interdomain B in ZAP-70 regulates but is not required for ZAP-70 signaling function in lymphocytes. *Molecular and cellular biology* 19:948-956.

Zhong, Q., W. Gao, F. Du, and X. Wang. 2005. Mule/ARF-BP1, a BH3-only E3 ubiquitin ligase, catalyzes the polyubiquitination of Mcl-1 and regulates apoptosis. *Cell* 121:1085-1095.

Zolnierczyk, J.D., A. Borowiak, J.Z. Blonski, B. Cebula-Obrzut, M. Rogalinska, A. Kotkowska, E. Wawrzyniak, P. Smolewski, T. Robak, and Z.M. Kilianska. 2013. In vivo and ex vivo responses of CLL cells to purine analogs combined with alkylating agent. *Pharmacol Rep* 65:460-475.

zum Buschenfelde, C.M., M. Wagner, G. Lutzny, M. Oelsner, Y. Feuerstacke, T. Decker, C. Bogner, C. Peschel, and I. Ringshausen. 2010. Recruitment of PKC-betaII to lipid rafts mediates apoptosis-resistance in chronic lymphocytic leukemia expressing ZAP-70. *Leukemia* 24:141-152.